



With the support of the
Erasmus+ Programme
of the European Union



University of Évora

ARCHMAT

ERASMUS MUNDUS MASTER IN ARCHaeological MATerials
Science

Unveiling the mural art of Almada Negreiros at the Maritime Stations of
Lisbon: *diagnosis research of paint layers as a guide for its future
conservation*

Mila Cvetković

Dr Milene Gil Duarte Casal, Universidade de Évora, Supervisor

Prof. Dr Antonio José Estêvão Grande Candeias, Universidade de Évora, Supervisor

Prof. Dr Cristina Barrocas Dias, Universidade de Évora, Supervisor



ARISTOTLE
UNIVERSITY
OF THESSALONIKI



UNIVERSIDADE
DE ÉVORA



SAPIENZA
UNIVERSITÀ DI ROMA



With the support of the
Erasmus+ Programme
of the European Union



University of Évora
ARCHMAT
ERASMUS MUNDUS MASTER IN ARCHaeological MATerials
Science

Unveiling the mural art of Almada Negreiros at the Maritime Stations of
Lisbon: *diagnosis research of paint layers as a guide for its future
conservation*

Mila Cvetković

Dr Milene Gil Duarte Casal, Universidade de Évora, Supervisor

Prof. Dr Antonio José Estêvão Grande Candeias, Universidade de Évora, Supervisor

Prof. Dr Cristina Barrocas Dias, Universidade de Évora, Supervisor



SAPIENZA
UNIVERSITÀ DI ROMA

Jury members

Presidente: Nicola Schiavon, Investigador Principal Convidado,
Universidade de Évora

Arguente: Teresa Ferreira, Professora Associada, Universidade de Évora

Orientador: Milene Gil, Investigadora, Universidade de Évora

Vogal: Donatella Magri, Professora Associada, Sapienza Università di Roma

(this page was intentionally left blank)

Table of contents

<i>Acknowledgments</i>	6
<i>Abstract</i>	8
<i>Chapter I: Introduction</i>	9
1.1. Contextualization and objectives of the research.....	9
1.2. Methodological approach.....	9
1.3. Structure of the thesis.....	10
<u>List of references</u>	
<i>Chapter II: Historical context and state of the art</i>	11
2.1. XX century art abroad and in Portugal.....	11
2.2. Almada Negreiros and his mural art production.....	14
2.2.1. The Maritime Stations of Alcântara and Rocha do Conde de óbidos.....	17
2.3. Technological approach to painting materials in the XX century.....	20
2.3.1. Causes of deterioration of mural paintings.....	21
<u>List of references</u>	
<i>Chapter III: The Case study and the Methodology</i>	26
3.1. Paintings' identification.....	26
3.2. Environmental conditions and geographic location.....	27
3.3. Experimental.....	29
3.3.1. In situ analyses.....	29
3.3.1.1. Photo documentation and technical photography (TP).....	29
3.3.1.2. Portable optical microscopy (p-OM).....	29
3.3.1.3. Colorimetry and spectrophotometry.....	29
3.3.1.4. Handled X-ray Fluorescence (XRF).....	30
3.3.2. Laboratory analyses.....	30
3.3.2.1. Optical Microscopy (OM).....	31
3.3.2.2. X-ray Diffraction (XRD).....	31
3.3.2.3. Scanning Electron Microscopy coupled with Energy Dispersive Spectroscopy (SEM-EDS).....	31
3.3.2.4. Fourier Transformed Infrared Spectroscopy (μ -FT-IR).....	31
3.3.2.5. Pyrolysis Gas Chromatography coupled with Mass Spectrometry (Py-GS-MS).....	32
<u>List of references</u>	
<i>Chapter IV: Results and discussion</i>	34
4.1. Mapping of deterioration.....	34
4.2. Salts characterization.....	41
4.3. Characterization of painting materials.....	44
<u>List of references</u>	
<i>Chapter V: Conclusion</i>	58
<i>Appendix</i>	62

(this page was intentionally left blank)

Acknowledgements

I would like to express my deepest gratitude to my supervisors Prof. Dr Antonio José Estêvão Grande Candeias, Prof. Dr Cristina Barrocas Dias and Dr Milene Gil Duarte Casal, for their patient guidance and support during my studies and research in the Hercules Laboratory. Dr Milene Gil, who was my mentor during this research, put great effort in her assistance and navigation, and I am very thankful for her encouragement.

I would like to thank the always-enthusiastic team of colleagues from Hercules Laboratory, that helped me a lot during the studies, research and thesis. Especially to Carlo Emanuele Bottaini and his help with handled X-ray Fluorescence analyses during the survey in Lisbon that took place between 1st and 6th of June, 2020; then, to Ana Margarida Andrade Cardoso for her patient guidance and help through Fourier Transformed Infrared Spectroscopy analyses and data interpretation and to Ana Manhita for her help with Pyrolysis Gas Chromatography and interpretation of the results. I would also like to express my gratitude to Mafalda Costa and her help with micro-X-ray Diffraction analyses and her help with many other data interpretations. I am grateful to Ana Fundurulić as well, for her support, many advices that she gave me, and numerous last-minute emails, discussions and talks. I would also like to thank professor José Mirão for his enthusiastic help during both, my studies and thesis.

Special thanks to the Erasmus Mundus and ArchMat programme, that allowed this amazing opportunity which I enjoyed the most. It was a pleasure to be the part of such a great collaboration programme and gain this huge learning experience. I am thankful to the programme coordinator Dr Nicola Schiavon and partners - Dr Evangelia Varela, Dr Donatella Magri; and all administrative staff of Universidade de Évora, Aristotle University and Sapienza University. I also appreciate the support of FCT contract 57/2016/CP1338, the Strategic Project funding UID/Multi/04449/2018 and APL Administração dos Portos de Lisboa.

Further, I would like to thank my ArchMat colleagues, who made this two-year experience unforgettable. I am thankful to Luka Bruketa, Athina Trebicka and Degsew Zerihun for their inspiration and support. Also, I would like to thank my housemates Berenice Baiza, Tawanda Mushweshwe and Daniele Zampierin, who were always there to give me 'a pair of fresh eyes', second opinion or cup of hot coffee. I am obliged to all my colleagues, and I will always be grateful to, and for them.

My final gratitude goes to my family and friends, who were an amazing encouragement. You are my most valuable treasure and my secret weapon.

Thank you.

(this page was intentionally left blank)

Abstract

Diagnostic research of the three mural paintings from Alcântara Maritime Station in Lisbon was conducted in order to understand the main decay phenomena and their dynamics, with respect for future conservation work. The analytical setup was composed of *in-situ* analyses by p-OM, spectro-colorimetry and h-EDXRF, followed by micro-sampling for a more profound analyses with OM, SEM-EDS, μ -XRD, FT-IR and py-GC-MS. Deterioration features identified include salts (salts efflorescence and sub efflorescence), flaking, lacunae, erosion and lack of cohesion of paint layers. Developed salts were classified as sulphates and their origin seems to be linked to polluted atmosphere and water infiltration into building materials. Greenish paint layer present in all three murals appears as the most deteriorated one, as it shows problems of severe flaking and lacunae.

Resumo

Desvelando a arte mural de Almada Negreiros nas estações marítimas de Lisboa: Diagnóstico de pesquisa de camadas de pintura como guia para sua conservação futura

Uma pesquisa diagnóstica das três pinturas murais da Estação Marítima de Alcântara, em Lisboa, foi realizada para entender os principais fenômenos de degradação e sua dinâmica com respeito a trabalhos futuros de conservação. A configuração analítica foi composta por análises *in-situ* com p-OM, espectro-colorimetria e h-EDXRF, seguida de micro-amostragem para análises mais profundas com OM, SEM-EDS, μ -XRD, FT-IR e py-GC-MS. As características de deterioração incluem sais (eflorescência e subflorescência), descamação, lacunas, erosão e falta de coesão. Os sais desenvolvidos foram classificados como sulfatos e sua origem parece estar ligada à atmosfera poluída e à infiltração de água em materiais de construção. A camada de tinta esverdeada presente nos três murais aparece como a mais deteriorada, pois apresenta severos problemas de descamação e lacunas.

Chapter I: Introduction

1.1. Contextualization and objectives of the research

Mural paintings represent important and complex part of world heritage. Old almost as human history itself, they testify of immense culture. From cave walls to modern architecture interior and exterior decorations, these paintings tell stories about technology and technique development through ages, but also the various inspirations and testimonies, coming from different sources.

Unfortunately, murals, likewise any other form of art, can be affected by ravages of time, due to different environmental conditions. This varies and depends on the technique, materials used, state of architecture that holds them and environment they are part of.

This research has a focus on collection of three murals painted by Almada Negreiros during the time period between 1943 and 1945 at the shipping halls of the Lisbon Alcântara Maritime Station [1-4]. The current research proposal is made on the framework of a wider project entitled Almada Negreiros that aims to study the painting techniques and pigments used by one of the lead Portuguese artists of the 20th century and its implications in the deterioration processes encountered by Conservators-Restorers in the past 30 years. In the aspect of future conservation works, this particular study intends to carry out the diagnosis of deteriorated paint layers.

Three main research questions are to be answered:

Primary, it is important to understand which paint layers are more deteriorated and if they are linked to a specific pigment or not. **Secondly**, which are the main decay phenomena and their dynamics and **third** - what is the role of the painting techniques when it comes to stability and deterioration of the pigments.

All the questions stated would help understand the state of the mural, the decay occurring and would stage the possible guideline for future conservation. Presence or absence of organic binders is also important as they are the materials most prone to deterioration. Furthermore, the state of the murals and environmental influences will contribute to any architectural upgrade or revitalization in future. Everything stated is therefore important as it will add to existing knowledge and literature.

1.2. Methodological approach

The first part of research is orientated towards literature review. This provides the wider picture of the time and environment in which the murals were painted. Relative data and information was collected on the artist himself in the means of style, inspirations and painting materials available at the time.

In order to answer the research questions, several analytical techniques were done. Starting with the in-situ survey and visual inspection, photographic and graphic documentation, in order to collect and map deterioration features on paint layers, differences on colour and painting textures and other technical characteristics that helped to define the subsequent analysis. The in-situ research also allowed to understand the position of the paintings inside the architecture and their relations with environmental conditions. Ultraviolet induced Fluorescence (UVF) light observations were used for preliminary detection of organic materials both original and from past interventions. Number of analysed points was unlimited, which is the biggest advantage of these techniques. They were used to get the first insight into mural paintings and they set the ground for any further analyses.

Non-invasive techniques e.g. spectro-colorimetry and portable optical microscopy (p-OM), provided insight to paint layer characterisation and pigment identification and handheld Energy Dispersive X-Ray Fluorescence (h-EDXRF) to elemental composition of deteriorated layers. This was followed by micro-sampling for a more profound stratigraphic and composition analysis, that allowed us to see the details of painting technique, materials used and deterioration

problems. These analyses were done in the HERCULES laboratory, using Optical Microscopy in Visible and Ultraviolet mode (OM-Vis-UV), Scanning Electron Microscopy with Energy Dispersive Spectroscopy (SEM-EDS), micro-X-Ray Diffraction (μ -XRD), Fourier Transform Infrared Spectroscopy (FT-IR) and Pyrolysis Gas Chromatography (Py-GC-MS).

1.3. Structure of the thesis

This thesis will be divided into 5 chapters, each containing one aspect of the research.

- ◆ *Chapter I*, the actual chapter, represents the overview of the study, e.g. the object of the research, aims, methods and structure. This chapter serves as a thesis guideline, adopting the research problems and questions.
- ◆ *Chapter II* is a historic and thematic viewpoint. Its goal is to provide introduction to the object of study itself through time and space frames in order to shape the artist environment, in which the murals were painted. Since the XX century art is a deeply complex area, likewise Portuguese situation of that period, it is important to understand the circumstances that influenced the artist. Moreover, the chapter explores the opus of Almada Negreiros, as well as his style and art versatility.
Second chapter will as well introduce the materials and techniques available at the time, with the accent on decay factors that can affect the analysed murals.
- ◆ *Chapter III* describes methodology and experimental conditions for both in-situ and laboratory analyses conducted. It also explains the environment of the murals, since it affects the decay dynamics.
- ◆ *Chapter IV* provides the results of the research, followed by the discussion. Its aim is to associate the results to the objectives of the thesis, by relating the research outcomes to the questions presented in the Chapter I. This part of the thesis also includes the perspectives of the conducted research and final remarks.
- ◆ *Chapter V* summarizes the results. Here the implementation of results is presented followed by proposition for future research and activities.

List of references

- [1] Lobo, P. R. (2010). Almada and the Maritime Stations: The portrait of Portugal that the dictatorship wanted to erase. FCSH - Universidade Nova de Lisboa, Instituto de Historia da Arte.
- [2] Monteiro, J. P. (2012, Dezembro). Dissertação para Obtenção do grau Doutor em Design: Para o projecto global - nove décadas de obra: Arte, Design e Técnica na Arquitetura do atelier Pardal Monteiro. *Para o projecto global - nove décadas de obra: Arte, Design e Técnica na Arquitetura do atelier Pardal Monteiro*. Lisboa: Universidade Técnica de Lisboa, Faculdade de Arquitetura.
- [3] Santos, M. P. (2016). On Being Modern: Possibilities of Resistance through Primitivism and Ingeniousness in Ernesto de Sousa and Almada Negreiros. *RIHA Journal* 0137.
- [4] Silva, R. H. (2014). Almada das Artes e dos ofícios. *Revista de História de arte*, n2, Instituto de História de arte, 314-321.

Chapter II: Historical context and state of the art

2.1. XX century mural art abroad and in Portugal

Beginning of the XX century set the ground for revolutionary movements. Twenties and thirties started the freedom of expression. The aesthetics prevailed over function, and became leading feature [1]. Furthermore, the echo of Second World War had a greater influence on art in general. It could be felt in the entire world: Mexican revolution in the 20s, and further in the United States, movements in postcolonial Africa, Soviet Social Realism, Neoclassicism in Mussolini's Italy and similar [2]. What was desired was a creation of new, national art, which would be independent, socially committed: avant-garde. Ideas and inspiration came from the culture and folklore itself, but even many of these artists were driven by realism and socialism, they themselves developed individualistic forms of expression [2].

According to Poulin, cofounder, design director, and principal of Poulin + Morris Inc., murals are form of visual communication:

'Our need to dedicate and consecrate places is clearly the beginning of the integration of graphic design in the built environment. Classical inscriptions, figurative murals, and ornamental surfaces have long been a part of architecture and have influenced our understanding of typographic form and graphic style and their visual representation in the built environment. Buildings and public spaces coexist with billboards and signs, patterned and textured facades, and informational and wayfinding signs to effect an overall experience with the public. Graphic design has become integrated with the built environment in shaping not only cities but also the lives of their inhabitants.' [1]

In Mexico, new movements were trying to revive the precolonial state. Some of the widely used motifs were scenes of tragedy and power, connected to native Indian population and events that occurred in history. Muralists of the period, among them Diego Maria Rivera, David Alfaro Siqueiros and José Clemente Orozco, created wall art with echo, not only in Mexico, but also abroad [2]. Diego Rivera, exhibit in New York, and so in 1929 the first book about his opus in English language was published – *The Frescoes of Diego Rivera* [2]. Orozco painted frescoes for the New School for Social Research in New York (1930-31), then, for Dartmouth College in Hanover (1932-34) and for Pomona College in Claremont (1939) [2].

It was in 1920s when communist propaganda started appearing in Mexican muralism, and involved radical politics into this form of art. Such example can be seen on the walls of Secretaría de Educación Pública where Rivera painted political cartoon about Vasconcelos, Mexican writer and politician, and so separated himself from any Vasconcelos' ideologies [3]. Tale of revolution's violence can be found in Orozco's mural "The trench" painted on the walls of National Preparatory School in Mexico (Figure 1) [2]. Mural was painted in 1926 under the influence of expressionism.

In Europe, such resistance examples could be found especially during 30s. In 1937, during the Spanish Civil War, Pablo Picasso painted one of his most famous artwork: *Guernica* (Figure 2), that represents strong political statement, and clearly comes from Picasso's involvement with Communism and Surrealism [4]. Greek muralists of the period fought traditional and strict aesthetic rules set by Byzantine church. As Ioannis Liritzis and Eliza Polychroniadou recognize in their archaeometrical analyses paper [5], such resistance could be seen, for example, in the work of Spyros Paploukas who introduces elements of post-Impressionists into his work, among them the murals of Amfissa Cathedral [5]. In Italy, during the period from 1933 – 1940, fresco technique was revived through the fifth, sixth and seventh Triennale in Malano. Mural projects were done by De Chirico, Sironi, Campigli and Archille Funi. [6]

Various artistic movements arose from difficult economic, political and social situation also known as Great Depression. The need for recovery grew hand in hand with fascism – a radical authoritarian nationalist movement, in the period of 1920s and 1930s. Thus new ideologies and influences were formed [1,2,7].

Various effects covered the painting style. Cracked lines, high contrast, clear geometrical shapes are just some of the approaches. In their book *History of Modern Art*, art historians H.H. Arnason and Elizabeth Mansfield, recognize some other influences on modern art [4]. One of them comes from Africa and investigates 'the exotic' or 'primitive' concepts. As one of the examples they give is that of Henri Matisse, the French artist of the time and his painting - *Blue Nude: Memory of Biskra* [4]. Influences of Africa on European XX century art were recognized also by Olive Jensen Theisen in her book *Walls that speak*, where she suggests that African Sculpture led Picasso and Braque towards Cubism [7].



Figure 1. José Clemente Orzco, *The trench*, mural for the National Preparatory School 1926. Source: [2]



Figure 2. Pablo Picasso, *Guernica*, 1937. mural-size canvas for the Museo Reina Sofía, Madrid, Spain (349/777). Source: [2]

As the world was fighting difficult situation caused by Second World War, in Portugal, society was facing yet another problem – dictatorship or the regime of Estado Novo, initially under Antonio de Oliveira Salazar, and subsequently with his successor Marcelo Caetano [8]. Starting from 1926 it lasted till April of 1974 [8]. Difficult times that occurred created another movement which had either orthodox or heterodox views in art, with an outset in the 30s and tendencies to fight the regime through art and literature. Numerous artists, among them Almada Negreiros himself, had a belief that art needs to be set free: *‘o artista moderno é o artista livre’*¹ [9,10]. Movement was based on the interpretation of the Soviet directions for realism, but its interpretation was somehow ‘softer’ and misunderstood version of the original [8]. During this time many artists were working under the commission of the state, and in case of mural paintings, they were usually created in partnership with architects [9,11-15].

As Mariana Pinto dos Santos recognizes in her article *On Being Modern: Possibilities of Resistance through Primitivism and Ingenuousness in Ernesto de Sousa and Almada Negreiros*, Modernism in Portugal arose with the magazine Orpheum (Figure 3), held by Fernando Pessoa, Mário de Sá Carneiro and Almada Negreiros. Since the magazine was inspired by Italian and French avant-garde movements, it attracted many young artists. Among them was a group of futurists named after it: *Orphists*. Impressionism, futurism and cubism as leading movements of the time in Portugal, were mostly founded by government, and promoted through art schools and free-expositions [11,16]. Professor José Augusto França in his book *O Modernismo na Arte Portuguesa*, writes that cubism and modernism came into Portugal in a very controversial way, and were initially moved by resistance. Many names should be mentioned with reference to this period, such as the artists Dordio Gomes, Jorge Barradas, Amadeo de Souza-Cardoso, Julio Resende, Almada Negreiros and many others [9].

In April of 1917 a *Futuristic Conference* took place in Lisbon. It was a representation of futurism and it was exactly here that Almada Negreiros launched his literary work *Ultimatum Futurista to the Portuguese generations of the century XX* [9].

The resistance movement of the time was formed in the late 30s under the influence of Soviet Writers Congress held in 1934. It was named *neo-realismo*, and intended to advance the promotion of the lower classes of the society through literature, painting and sculpture [8]. The after-war period was widely dragging inspiration from folklore. At this time many exhibitions were organized in Portugal, aiming to ‘bring back’ old motifs and landscapes [9,11].

In 1940 the ‘first historical exhibition’ took place in Lisbon, under the name *Exposição do Mundo Português*, to put order and meaning to what, in architecture and other arts, developed during 30s [9]. The exhibition was commemorating the eighth century of nationality and the third century of independence from Spain [9]. Content was divided into three main sections of display: history, ethnography, and the colonial world, and included work of many great names at the

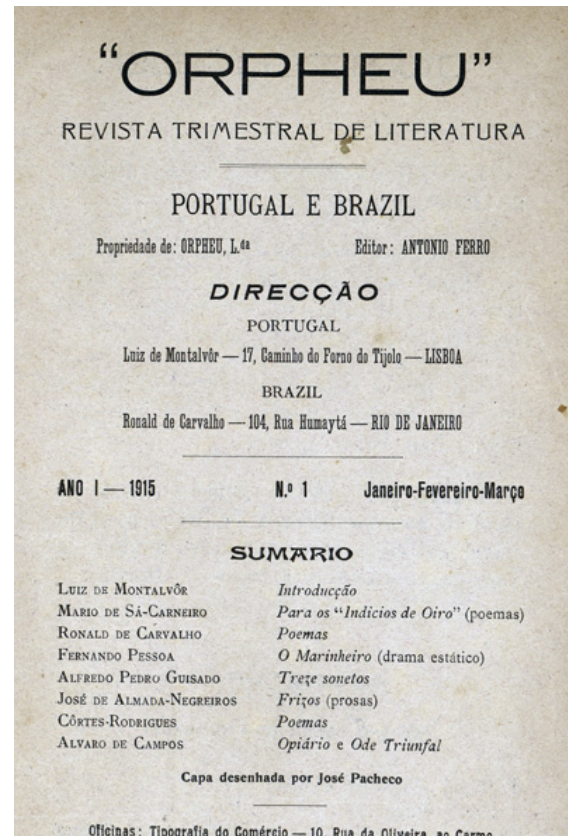


Figure 3. Orpheu magazine, poster, 1915, Source: [10]

¹ 'A modern artist is a free artist.'

time, among them architects Pardal Monteiro, Carlos Ramos, Veloso Reis, Jorge Segurado; painters and sculptors such as Bernardo Marques, Carlos Botelho, Paulo Ferreira, Almada Negreiros, Sarah Alfonso, Estrela Faria, and others [9].

Only six years after, in 1946 Ernesto de Sousa, Portuguese artist and art critic, organized an exhibition in Lisbon, named *Black Art Week*. The installations originated from Benin, African country that was controlled by Portugal till 1892 [8]. In 1969 yet another exhibition was organized by him, this time as homage to Almada: mixed-media worked named *Almada, name of war*. It included footage of 76-year old Almada Negreiros, and footage of women fish-sellers, with text slides written and read by Almada himself. Sousa sponsored these exhibitions as an artistic performance and revolutionary art. Years after that, in 1984 Ernesto organized one more tribute: *Almada, Um Nome de Guerra (Almada, A War Name)*, honoring Almada and his work through a series of footage of the artist [8].

2.2. Almada Negreiros and his mural art production

Born on the 7th of April in 1893 in São Tomé, José Sobral de Almada Negreiros lived through three quarters of XX century [9]. His name would be mentioned along with Portuguese modernism and revolutionary art of the time, and he would be recognized as painter, sculptor and writer, often connected to cinema and photography [9,11]. This versatile background, made him one of the most famous artists of the XX century Portugal. He died in Lisbon on 15th of June 1970 and left behind rich opus [9].

Along with his brother António, he started his education at Colégio dos Jesuítas de Campolide in Lisbon, but as the institution was closed in 1910, he was obliged to transfer to Liceu de Coimbra. In 1911 he started International studies in Lisbon, and remained here till 1913. Here, concurrently, he starts his artistic career, and despite the absence of art school degree, opens his first solo exhibition in 1913 presenting 90 drawings. Shortly after that, in the same year, he participates at the II Exhibition of Portuguese Humorists [9,19].

With Fernando Pessoa he was running the previously mentioned magazine *Orpheum*, published for the first time in 1915. Twenty years later he published yet another magazine: *Sudoeste*, to carry out critics about the political regime [8]. Shortly after, in 1919 he spent a year in Paris, and came back to Portugal carrying the influence of French avant-garde [9]. In the twenties he produced two novels under the impact of his travels: *Nome de Guerra*² and *De aprendizagem*³, and two easels in Café *A Brasileira do Chiado* [9]. The mentioned paintings are considered to be 'a second generation icons of Portuguese modernism [11]. They represent two female figures on the beach, and four characters sitting around a coffee table [9].

His second trip took him to Madrid where he stayed from 1927 to 1932. During his time in Spain, Almada worked with the group of Gomez de la Serna, Spanish writer and avant-garde agitator of the time [9]. This was a period of great importance for Almada, since his work had space and time to develop, gain maturity and find uniqueness [9,21].

Along with various artist of the time, among them Santa-Rita Pintor and Amadeo de Souza-Cardoso, he is identified with the creation of Portuguese avant-garde and futurism [8]. In 1934 he married the painter Sarah Alfonso, who, later represented a great support and backing for Almada and his work. Being his assistant, her 'advice' is imprinted into many of his works. The murals at the Maritime Station of Rocha de Conde de Óbidos and the famous portrait of Fernando Pessoa were two of many Almada's works that had her assistance [12].

As Rita Mendes Bispo, assistant at Superior School of Education and Social Sciences (Instituto Polytechnic of Leiria), recognises in her article *O lado sublimado do mundo: O feminine Almadiano*, after his wedding with Sarah, Almada's work gets the feminine, sensual side. His lines, with that sensuality, got clear and *Picassian*, as he paints nude female portraits, couples embracing and dancing, but also mythological figures. This can be observed in such works as

² Eng. Name of War

³ Eng. Of Learning

'*Engomadeira*', a painting from 1938 or '*Maternidade*' from 1948 [13]. Despite of their different hues, both paintings were painted with clear, cubistic lines and shapes [13].

As one of the most influential artists of XX century Portugal, Almada's opus have been an object of great attention. Starting with previously mentioned homage that Ernesto de Sousa organized in 40s and 60s of the XX century, many scholars and artists have documented and studied Almada's works. In 1974, historian José-Augusto França published two books that included the life and work of Almada Negreiros: *A Arte em Portugal no século XX* and *Almada Negreiros: o Português sem Mestre*. His opus is also a part of *Dicionário de História da I República e do Republicanismo*, a series of three books issued in Lisbon in the period between 2013-2014. Furthermore, in 2014, Instituto de História da Arte in Lisbon publishes the second issue of *Revista de História da Arte*, orientated towards Almada's life and *opus*.

As it was previously mentioned, collaboration between architects and artists was not a rare event at the time. Almada Negreiros has worked together with Portuguese architect Porfírio Pardal Monteiro several times, including the assignment on Lisbon church *Nossa Senhora de Fátima*, the former *headquarters of Diário de Notícias* [14], and of course, Maritime Stations Alcântara and Rocha de Conde de Óbidos in Lisbon.

His work on the decoration of the church *Nossa Senhora de Fátima* started in the 30s. It was a combination of modernism with neo-gothic style which he brought up to reality altogether with Monteiro's architecture design [9,15]. Beside the well-known stained-glass windows, finished in 1938, he created mosaics and mural painting with unique style and impresses with architecture and interior design, by respecting both - the iconography and the abstract [15].

During the period between 1957-1961, he has painted panels at the University of Lisbon. The panels presented can be seen in the Rectory building, Class Magna and Faculties of Law and Letters. This was another collaboration with Porfírio Pardal Monteiro, since he was the architect in charge of the building project [17,20-21]. In 1958, he decorates the walls of the Faculty of Law in Lisbon (Figure 4). Images imprinted have Greco-Roman style. Almada decorated each wall with four representations: the origins of law, it's transcendent conception, Roman construction of law and Portuguese law and its history [16].



Figure 4. Wall decoration at the Faculty of Law in Lisbon [16]

For the former headquarters of *Diário de Notícias* in Lisbon (DN building), designed also by Pardal Monteiro, he has painted five mural paintings. One of them is entitled *Mapa-Mundi* or *Planisfério*, and located on the front wall of the reception hall with most diverse motifs of four elements and twelve zodiac signs, and in a colorful palette (Figure 5), on the right wall of this painting, there is another mural, which represents the map of Portugal and the seasons [17]. On the left side, in the entrance hall for the services, stands another Almada's mural painting, being an "Allegory to the

Press" (*alegoria à Imprensa*) [17]. Two more murals are presented in the former DN headquarters building. They are telling a story of the building through 24 hours, each representing a step in the newspapers production [24].



Figure 5. *Mapa-Mundi or Planisfério* for Diário de Notícias headquarters in Lisbon, source: [17]

In the Calouste Gulbenkian Foundation Headquarters, Almada produced his final mural in 1969 and named it *Começar*. The work represented the sythesis of his art in total, geometry of his opus (Figure 6). As his career developed, his style also changed and grew. He was searching for an ancient geometrical vocabulary, with a simple and universal form. That is one of the reasons why he named his final work '*Começar*', meaning 'To begin', as he believed that all his art came from the initial geometrical language [8]. The opening point for his work '*Começar*' could be found in series of geometric abstractions he painted in 1957 and exhibited in the same year at the First Gulbenkian Exhibition [9].



Figure 6. Almada Negreiros, *Começar*, 1968-69, Source: [18]

2.2.1. Maritime Stations of Alcântara and Rocha de Conde de Óbidos

Designed in 1930s by famous Portuguese architect Pardo Monteiro, Maritime stations served as a gate and welcoming landmark for anyone who came to the Lisbon from the sea (Figure 7) [14]. Pardo Monteiro received the project in 1934 and finished its design by 1939. The importance of this construction was of national, economical and touristic significance, and its manufacture was an active debate at the time [14,17].

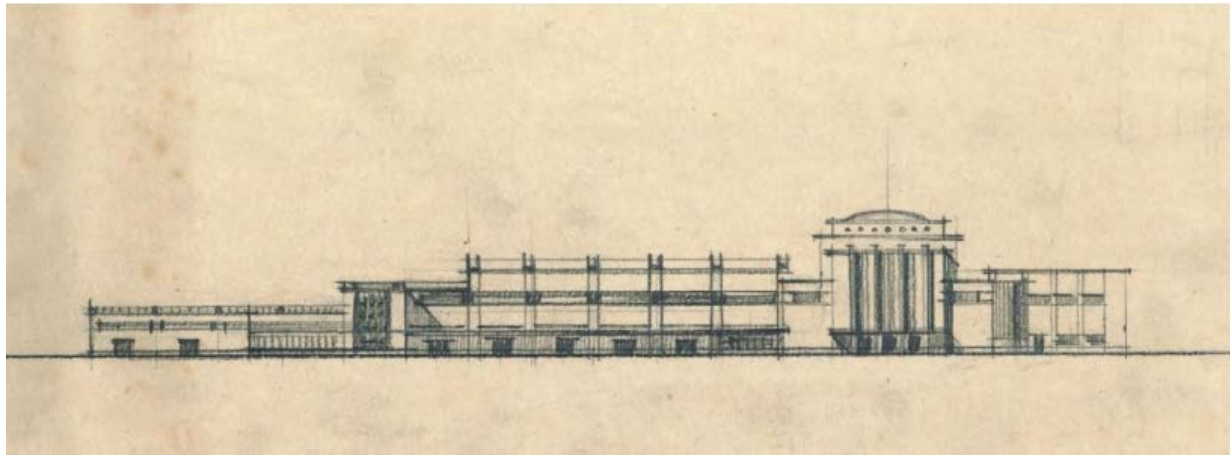


Figure 7. Plan for Alcântara station, Source: [17]

To analyse possible solutions, technical and esthetical possibilities and similar, Monteiro along with the Portuguese minister of the time, Duarte Pacheco, visited France and Italy and observed similar constructions [14,17]. The purpose of this new building, was not only functional in the means of receiving people who arrived or departed, but also to introduce the new architectural movement occurring in XX century Europe [14]. Alcântara and Rocha stations were designed in reinforced concrete, with the respect to modernistic movements in architecture. They included monumental halls and stairs which heightened the monumentality of the mural paintings painted later, by Almada during 30s and 40s [14]. Alcântara and Rocha stations were completed in 1943 and ready to receive decoration [14].

In the period between 1943 and 1949, walls of Maritime station were decorated by remarkable murals, fourteen paintings in total. Themes are representing nature of rustic Portugal, with sea and river images, originating from Lisbon and Tejo [14,17]. Unfortunately, the murals didn't meet only good critics. After the paintings of Alcântara were finished, they were immensely disapproved by minister Duarte Pacheco who named them an 'eyesore' that will welcome foreigners [14]. Fortunately they were defended by António Ferro, the director of National Propaganda, who considered them *magnificent* [14], conveying his opinion to Salazar that the murals represented a remarkable work and an appropriate welcoming to the visitors [14]. But, regardless of the debate on these panels falling silent, another one arose, related to the panes of Gare da Rocha Station. This time, paintings were even at the risk of being destroyed due to their, considered to be, political dimension. José-Augusto França suggested that the disapproval came from their '*inconvenient modernism*', while professor Rui Mário Gonçalves would add that it came from the tense moment of the Portuguese political situation, and critic Fernando Pernes stated that it was due to the artist's speculative research concerning formulation of ratio 9/10 (Almada's fascination with the composition of 15th century Nuno Gonçalves' panels and his famous essay *Mito-Alegoria-Símbolo: monólogo autodidacta na oficina de pintura*) [14]. Almada's murals were defended once more, this time by the architect Pardo Monteiro himself, engineer José Frederico do Casal Ribeiro Ulrich and João Couto. A letter was written, addressed to Museu Nacional de Arte Antiga, reaffirming the value and significance of the panels [14].

Almada painted the murals of Alcântara Station in a naturalistic way. Eight murals - two triptychs and two individual paintings are presented in the waiting hall of Alcântara. They carry names (sequentially): (P1) *Lá vem a nau*, (P2) *Catrineta que traz*, (P3) *Muito que contar*, (P4) *D. Fua Roupinho*, (P5) *O terra onde eu nasci*, (P6) *Quem não*, (P7) *Viu Lisboa não viu*, (P8) *Coisa boa* (Figure 8).

The main figures represent mostly every-day life scenes and stories of the ship *Catrineta*. Nevertheless, it must be stressed that the cost of Lisbon is painted rather empty than crowded. The reason might be found in the historical context of the panels since they were painted right after the Second World War [17,23]. On the east panels: triptych and one isolated painting the figures are related to sea and river Tagus and rustic Portugal [14,17]. On the west side, images are representing the legend of *Nau Catrineta* and the medieval miracle of D. Faus Roupinho. In this way, the artist made a contrast between themes of east and west walls by dividing them in traditional and divine motifs [14].



Figure 8. Murals of Alcântara station in their sequential order as they appear in the hall. Images are taken by Guta Carvalho (6-7th of June 2020 © all rights reserved)

After finishing the paintings of Alcântara Station in 1945, Almada started decorating Rocha de Conde de Óbidos station. In the period between 1946-1949 he painted two triptychs: *Quay* and *Coastline*, facing each other in the large waiting room of the station (Figure 9) [14,17]. Style of the murals is clearly different from his first 'Maritime Station set'. Geometric and strong lines are indicating the great influence cubism had on Almada. Another difference comes in the form of an 'new motif' – '*hardness and violence of the emigration*' and the Lisbon that remains behind. Compositions

of these panels hold images of stairs and scaffoldings, ships and pulleys, and among all figures of those who leave and those who are left behind [14,17].



Figure 9. Six murals of Rocha de Conde de Óbidos station, Source: [17]

2.3. Technical approach to painting materials in the XX century

20th century artists had the privilege of access to both natural and artificial pigments. This makes the available palette very versatile and rich, although it wouldn't be the only factor influencing their colour choice. Among the factors that we can recognise are the cost, geographical and traditional convenience or personal awareness for the materials.

Among natural pigments we can find rich palette of earth colours, which shades can vary from different hues of red and brown, up to green shades, depending on the elements present [26-29]. One example are the ochres, drawing their colour from iron oxides such as hematite $\alpha\text{-Fe}_2\text{O}_3$ and goethite $\text{FeO}(\text{OH})$. French ochres for example, also include Aluminum silicates such as Kaolinite $\text{Al}_2(\text{OH})_4\text{Si}_2\text{O}_5$ [26-28]. Similarly, Green earths draw their shades from the minerals glauconite or celadonite [26-28]. Indian yellow, rediscovered in 19th century was used only for a short time after it was banned at the beginning of 20th century due to animal cruelty caused by its production, since it is manufactured from urine of cows previously fed by mango leaves, which led to serious health problems and eventual death of these animals [29]. Another natural pigment with wide history of use is Ultramarine blue, obtained from the mineral *lapis lazuli* - $\text{Na}_7\text{Al}_6\text{Si}_6\text{O}_{24}\text{S}_3$ [27]. The earliest occurrence of lapis lazuli used as a painting pigment was noted by chemist and conservation scientist Gettens (1937-1938) in 6th and 7th century AD wall paintings in cave temples at Bliimiyyin in Afghanistan [27]. It may also be found, for example, in Titian's *Madonna and Child with Saints John the Baptist and Catherine of Alexandria*, painted in 16th century [27]. Another natural blue pigment – smalt, is a finely ground glass containing cobalt, where it gets its vibrant hue from [26-28]. Its use started in Europe during middle ages, and may be found in the oil on canvas *The Adoration of the Shepherds* painted by Bartolomé Esteban Murillo in the 17th century [26-

28]. Lead white (lead carbonate - PbCO_3), occurs naturally as the rare mineral hydrocerussite, and was the only white pigment used in European easel painting until the nineteenth century [26-29].

One example of the use of the traditional artist pigments in modern painting can be found in the palette of Greek Expressionist Spyros Paploulkas and his mural paintings at Amfisa Cathedral (1926-1932). This palette consists of ultramarine, carbon black, hematite, red and yellow ochres and lead white [5]

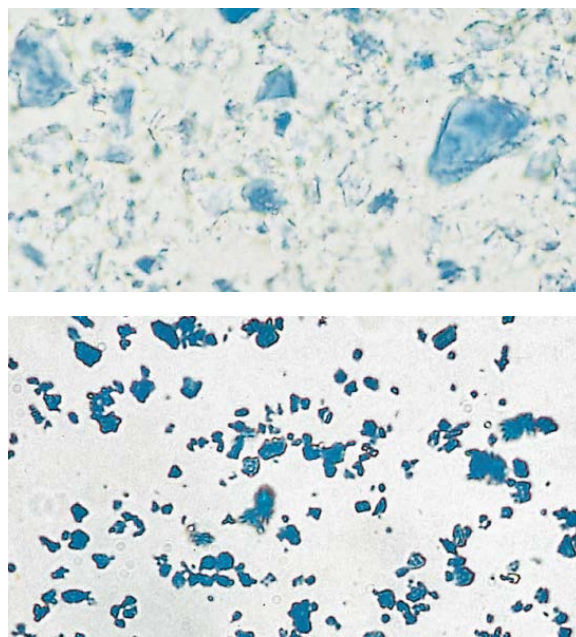
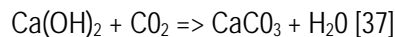


Figure 10. Up: particles of natural Ultramarine, down: particles of synthetic Ultramarine blue under transmitted light optical microscope, source [27]

The artificial ultramarine blue pigment was synthesised in 1826 [27,29], and it shortly after that widely replaced natural Ultramarine blue (Figure 10) [27]. It was a likewise deep blue pigment named French-ultramarine, and significantly less expensive than original one [27]. Use of artificial ultramarine can be found in *The Blue Room* easel painting by Pablo Picasso (20th century) [30], or in easel painting *Starry Night* painted by Van Gogh in the 19th century [31]. Smalt was mostly replaced by cobalt blue (CoAl_2O_4), in the 19th century, since this new pigment was very stable and is unaffected by heating and light, being also compatible with other pigments [26-29]. Ochres and red earths were used less after the introduction of the synthetic iron oxides - Mars colours in 19th century [27,29]. Cadmium colours were available in the early 20th century, and hues varied from lemon yellow to red colours [27]. Another group of warm hues comes from Chromium based pigments. They are formed when the chromate ion, CrO_4^{2-} , combines with several heavy metals to

form yellow to red compounds suitable for use as pigments [27]. This group includes lead chromates: chrome yellow (PbCrO_4) and ($\text{PbCrO}_4 \cdot \text{PbSO}_4$) and chrome orange ($\text{PbCrO}_4 \cdot \text{PbO}$) [27]. Lead white colours were mostly replaced by zinc-based ones, which started to be used in the 18th century [27]. Zinc-based pigments were broadly used among expressionists in Europe as well. Such examples are paintings by Alessandro Milesi, Italian artist active between the end of 19th and the beginning of 20th century [32], or the ones painted by Van Gogh, such as *Les bretonnes et le pardon de pont Aven* that shows the presence of the white Zn-based pigment [33]. Palette used by Milesi also included Titanium white, which would be used individually or in combination with Vermilion in order to achieve flesh colour hues, chrome green and cadmium red. Yet, this palette where natural pigments are used along with artificial ones, showed examples of traditional pigments such as gypsum or chalk [34]. The first attempt of introducing Zn-white as an artist pigment can be found as early as 1780, by Courtois, a demonstrator for the laboratory of the Academy of Dijon; or Guyton de Morveau, magistrate at the court of Dijon, with whom Courtois might have collaborated [27,29]. One of the most popular zinc-based colours was the Chinese white, pure pigment often used for watercolour art [27,29]. Zinc, titanium and chrome based pigments can be also find in art of Mario Sironi's Venetian fresco paintings, painted in 1930s [35]. Zinc oxides are also found in easel paintings of Yugoslavian 20th century painter Lazar Vozarević [36].

Depending on the technique of applying pigments, mural paintings could be primary divided into *secco* and *fresco*. The first one represents painting on dry plaster, by previously mixing pigments with a binding medium. In the second, pigments would be applied on fresh plaster, and fixed by the carbonization of lime. With drying of the rendering, calcium hydroxide is reaching the surface, reacting with calcium dioxide from the air and forming calcium carbonate [37]. This process can be described by following equation:



Instead of being mixed with pure water, the pigment can be mixed with lime water or lime milk. This is called lime fresco [26]. Although painting *fresco* would not initially include organic materials, their presence can sometimes indicate past interventions, retouchings, gilding, varnishing and similar [37]. On the contrary, *secco* mural paintings invariably contain organic materials, since binding medias are of organic nature. Binders used in mural painting are usually egg, casein, animal glue and certain vegetable gums [37,38].

The rendering on which the mural painting is applied can be divided into two layers – *arriccio* and *intonaco* [37]. The first one is coarser and thicker and it is applied directly on the support, while the second one is finer and thinner and it is the layer receiving the painting [37]. Another division of the painting can be found in joints in the plaster. Horizontal joints are called *pontata* and they correspond to the levels (heights) of scaffoldings [37]. Vertical joint – *giornata*, represent the amount of work performed in a day, and usually aligns with contours of figures painted [37].

2.3.1. Causes of deterioration of mural paintings

Deterioration of mural paintings is caused by various factors. This chapter identifies the most common causes of change, decay and degradation.

a) Instability of the Materials

Materials intability refers to the support, rendering and pigments used. Materials containing clays are highly sensitive to water and humidity. Water trapped within the rendering tends to expand when frozen and reduce when defrosted, which can cause cracks and fissures due to rapid change of volume [38].

Organic residues are prone do degradation and blackening [38-39]. Animal glue for exaple, in painting *secco* can be found as a medium, mixed with pigments and subsequently applied on dry plaster [40], while in painting *fresco*, it can suggest to previous retouching [39]. Frescoes on the Vault of Sistine Chapel painted by Michelangelo, showed presence of small fungus colonies that developed due to the presence of animal glues [41]. The glue was not originally part of Michelangelo's painting but was applied after a period of time—presumably during treatment by Mazzuoli in the eighteenth century [41].

Pigments can also be prone to changes, due to their different composition. It is known since antiquity that mercury sulfide pigments (α -HgS) such as cinnabar and vermilion change their hues to black, violet or even grey tones [42]. Roman fresco from Villa delle Torre, near Pompeii in Italy, shows signs of degradation of mercury chlorine compounds such as calomel and corderoite, which was identified on the surface of α -HgS model samples when exposed to light and a sodium hypochlorite solution [43]. Emerald green degrades into the white arsenic trioxide formed on the surface [44]. This can be observed on 19th century easel painting *Interior of a Restaurant* by Vincent van Gogh [44].

b) Application errors

When painting fresco, pigments are applied to wet rendering thus the humidity level can be crucial to the final quality of painting. The colours might change if pigments are applied to the rendering that is too wet, due to occurring chemical reactions [38]. This is found in Copper based pigments, since humidity and chloride ions from various sources can cause formation of black Copper oxides such as CuO, and green chlorides such as nanokite CuCl [45]. On the contrary, cohesion of paint might be reduced if the pigments are applied to dry rendering, since there is not enough water to form calcium carbonate [38].

Furthermore, application of several layers of pigment on top of each other can initiate splitting and 'falling off' of paint layers [38, 46-47]. This phenomenon can be observed in the Leonardo da Vinci's mural painting *Last Supper*, painted in the period 1494-1498 in the Refectory of Santa Maria delle Grazie in Milan, Italy. These paint layers often contain not only one but mixture of several pigments, where in some places lake pigments were identified in order to achieve a certain hue [46-47]. In some areas, azurite or ultramarine blue (or even their mixture) is placed between two layers of lead white, and covered with finishing varnish [46-47]. This quite unusual technique represents the weak point of the painting, due to physico-chemical incompatibility between the layers and the plaster or with incorrect proportions of calcium carbonate and binder [46].

c) Environmental conditions

All walls contain salts within their porous material. Under the influence of moist, pores in stone, soil, mortar or render are filled with diluted salt solutions [48]. When present in buildings, salts come not only from the material, but can come from the grounds, or arise from deposits of pollutants or due to biological colonization [49]. Continuous humidity – drying cycles can set in motion further deterioration problems, such as crystallization of salts, superficial incrustations, efflorescence, etc. Growth of salt crystals can lead to cracks and decomposition of rendering as they increase in volume. Surface evaporation in case of water rich in salts can cause external efflorescence [38]. Some pigments can also initiate salt formation. For example, in the 11th century frescoes from the church of Kostolany pod Tribečom (the oldest preserved wall paintings in Slovakia), it can be observed that lead white (hydrocerussite) slowly transforms to cerussite through the chemisorption of atmospheric CO₂ [50].

In highly polluted areas, especially big metropolis, an enemy to mural art comes from the atmosphere. Natural pollution agents such as carbon dioxide, in humid environments may create carbonic acid, that will further dissolve calcium carbonate in the murals, creating a white veil over the paintings [38]. Other pollution agents such as sulphurous anhydrides are artificial as they come from the combustion of materials containing sulphur. With the moisture they can create sulphuric acid which attacks calcareous rocks such as marble and limestone, and in case of mural paintings – the rendering [38]. Alkali sulphates such as thenarite and aphthalite salts can originate from architectural materials such as Portland cement that were originally rich in alkalis [51].

d) Biological attack

In highly humid environments there is rapid growth of fungi, algae and lichens [38,52] Presence of animal or plant fibres (added occasionally to enhance cohesion) can also have affinity towards water and may lead to biological attack [38]. The natural porosity of mural paintings makes their surfaces suitable for microbial spores and vegetative cells, transported by airborne particles to grow. [53,54] Furthermore, in case of indoor paintings, poor ventilation and non-homogeneous surface temperature, can lead to water condensation and local micro-climates. This environment is favourable to some fungi species [52,54], and thus promotes degradation. All these attacks eventually lead to chromatic

alterations, stains, formation of biofilms, cracks and detachments of fragments. In addition to that colour alterations due to pigment changes, surface modifications and salt efflorescence may occur as a result [55].

e) *Physical damage*

Environmental conditions can also cause physical damage to the mural painting (based on its location within the interior/exterior), such as erosion caused by wind, fading of colour by light, accumulation of deposits that may lead to darkening or black stains [38]. Fire can change the support structure by converting it from calcium carbonate, back to quicklime. This can initiate colour changes, cracks and detachment of layers. Such damage can be seen in churches, in areas where candles are near the paintings [38]. Due to traffic areas, public buildings also can be prone to the influence of vibrations that in some circumstances can provoke detachments of painting layers [38]. Sometimes, harm can come from everyday use of the building, due to mechanical damage, heating, dust, pollution, etc. [56].

List of references

- [1] R. Poulin, *Graphic Design + Architecture, A 20th century history*, Beverly: Rockport Publishers , 2012.
- [2] H. Foster, R. Krauss , Y.-A. Bois , B. h. Buchloh and D. Joselit, *Art Since 1900*, Third edition, London: Thames & Hudson Ltd, 2016.
- [3] L. Alvarez, *The Influence of the Mexican Muralists in the United States. From the New Deal to the Abstract Expressionism*, Faculty of Virginia Polytechnic Institute and State Universit, 2001.
- [4] H. H. Amason and E. C. Mansfield, *History of Modern Art*, Pearson Education, Inc., 2004.
- [5] I. Liritzis and E. Polychroniadou, “Archaeometrical analysis of mural paintings made by Spyros Papaloukas (1892-1957) in Amfissa Cathedral,” *Journal of Archaeometry*, 2007.
- [6] Y. Jin, *An Examination of the Place of Fresco in Contemporary Art Practice*, University of the Arts London, 2004.
- [7] O. J. Theisen, *Walls That Speak*, University of North Texas Press, 2010.
- [8] M. P. d. Santos, “On Being Modern: Possibilities of Resistance through Primitivism and Ingeniousness in Ernesto de Sousa and Almada Negreiros,” *RIHA Journal* 0137, 2016.
- [9] J. França, *História da arte em Portugal. 6. O Modernismo:(século XX)*, Presença, 2004.
- [10] *Orpheu: reedição do volume 1*, Lisboa: Edições Ática, 1915.
- [11] J. França, *GLÓRIAS DE ALMADA*, Lisbon: Instituto de História da Arte, 2014.
- [12] I. Conde, Sarah Affonso, *mulher (de) artista*, *Análise Social*, vol XXX, 459-487, 1995.
- [13] R. M. Bispo, *O Lado Sublimado do Mundo: O feminino Almadiano*, Lisbon: Instituto de História da Arte, 2014.
- [14] P. R. Lobo, *Almada and the Maritime Stations: The portrait of Portugal that the dictatorship wanted to erase*, FCSH - Universidade Nova de Lisboa, Instituto de Historia da Arte, 2010.
- [15] R. H. d. Silva, “Almada das Artes e dos Eféios,” *Revista de História da Arte* N°2, pp. 393-404, 2014.
- [16] A. M. Pascoal, *Boletim de Estudos Clássicos*, Coimbra: Associação Portuguesa de Estudos Clássicos; Instituto de Estudos, 2011.
- [17] J. P. Monteiro, *Dissertação para Obtenção do grau Doutor en Design: Para o projecto global - nove décadas de obra: Arte, Design e Técnica na Arquitetura do atelier Pardal Monteiro*, Lisboa: Universidade Técnica de Lisboa, Faculdade de Arquitetura, 2012.
- [18] L. d. Oliveira, *Os Quadrantes de Almada: Do escandalo a musealização*, *Revista de História de arte*, n°2, 2014.
- [19] E. Ferreira, *Negreiros, José de Almada*, 2014.

- [20] Revista de História da Arte N.º2, Instituto de História da Arte, 2014.
- [21] A. S. Delgado, A recepção de Almada Negreiros em Espanha, Lisbon : Instituto de História da Arte, 2014.
- [22] J. França, Glórias de Almada, Lisbon: Instituto de História da Arte, 2014.
- [23] E. W. Sapega, Almada na cidade: Encomenda ou obra?, Lisbon: Instituto de História da Arte, 2014.
- [24] A grande exposição de Almada Negreiros Os escritos de Agustina Onze histórias de esperança, (2017), Fundação Calouste Gulbenkian, #184
- [25] “266 Liberdade,” [Online]. Available: <http://www.266liberdade.pt/pt/>.
- [26] R. L. Feller, Artists' Pigments, A handbook of Their History and Characteristics, Volume 1, National Gallery of Art, Washington; Archetype Publications, London, 1986.
- [27] A. Roy, Artists' Pigments, A handbook of Their History and Characteristics, Volume 2, National Gallery of Art, Washington; Archetype Publications, London, 1993.
- [28] E. W. Fitzhugh, Artists' Pigments, A handbook of their History and Characteristics, Volume 3, National Gallery of Art, Washington; Archetype Publications, London, 1997.
- [29] J. R. Barnett, S. Miller and E. Pearce, “Colour and art: A brief history of Pigments,” Optics & Laser Technology 38, pp. 445-453, 2006.
- [30] Favero, et. al, Reflectance imaging spectroscopy and synchrotron radiation X-ray fluorescence mapping used in a technical study of The Blue Room by Pablo Picasso, Heritage Science, 5:13, 2017
- [31] Zhao, et. al., An Investigation of Multispectral Imaging for the Mapping of Pigments in Paintings, Proceedings of SPIE - The International Society for Optical Engineering, 2008
- [32] L. Giorgi, A. Nevin, D. Comelli, T. Frizzi, R. Alberti, E. Zendri, M. Oiccolo and F. C. Izzo, “In-situ technical study of modern paintings - Part 2: Imaging and spectroscopic analysis of zinc white in paintings from 1889 to 1940 by Alessandro Milesi (1856-1945),” Spectrochimica Acta Part A: Molecular and Biomolecular Spectroscopy, pp. 504-508, 2019.
- [33] D. Comelli, A. Nevin, A. Brambilla, I. Osticioli, G. Valentini, L. Toniolo, M. Fratelli and R. Cubeddu, “On the discovery of an unusual luminescent pigment in Van Gogh's painting “Les bretonnes et le pardon de pont Aven”,” Applied Physics A, Materials Science and Processing, 2011.
- [34] L. Giorgi, A. Nevin, L. Nodari, D. Comelli, R. Alberti, M. Girona, S. Mosca, E. Zendri, M. Piccolo and F. C. Izzo, “PART 1: THE EVOLUTION OF ARTISTIC MATERIALS AND PAINTING TECHNIQUES IN TEN PAINTINGS FROM 1889 TO 1940 BY ALESSANDRO MILESI (1856-1945),” Spectrochimica Acta Part A: Molecular and Biomolecular Spectroscopy, 2019.
- [35] F. C. Izzo, L. Z. Falchi and G. Biscontin, “A study of the materials and painting techniques of 1930s Italian mural paintings: Two cases by Mario Sironi and Edmondo Bacci in Venice, Italy,” in Conservation Issues in Modern and Contemporary Murals, Cambridge Scholar Publishing, 2015.
- [36] V. Jovanović, S. Erić, P. Colomban and A. Kremenović, “Identification of Lithol Red Synthetic Organic Pigment Reveals the Cause of Paint Layer Degradation on the Lazar Vozarević Painting 'Untitled' with Copper Plates,” Heritage, 2019.
- [37] P. Mora and L. Mora, Conservation of wall paintings, London, Boston: Butterworths, 1984.
- [38] P. Mora, Causes of deterioration of mural paintings, Roma: International Centre for the study of the preservation and the restoration of cultural property, 1974.
- [39] F. Casadio, I. Giangualano and F. Piqué, “Organic materials in wall paintings: the historical and analytical literature,” Studies in conservation, pp. 63-80, 2004.
- [40] F. Piqué, G. Verri, Organic Materials in Wall Paintings, The Getty Conservation Institute, Los Angeles, 2015

- [41] G. Colalucci, "The Frescoes of Michelangelo on the Vault of the Sistine Chapel: Original Technique and Conservation," in *The Conservation of Wall Paintings*, London, 1987.
- [42] M. Radepon, Understanding of chemical reactions involved in pigment discoloration, in particular in mercury sulfide (HgS) blackening, Antwerp: Université Pierre et Marie Curie - Paris, Universiteit Antwerpen, 2013.
- [43] K. Janssens et al., Non-Invasive and Non-Destructive Examination of Artistic Pigments, Paints, and Paintings by Means of X-Ray Methods, *Topics in Current Chemistry*, 2017
- [44] K. Keune et al., Analytical imaging studies of the migration of degraded orpiment, realgar, and emerald green pigments in historic paintings and related conservation issues, *Heritage Science*, 2016
- [45] A. Coccato, L. Moens, P. Vandenabeele, On the stability of mediaeval inorganic pigments: a literature review of the effect of climate, material selection, biological activity, analysis and conservation treatments, *Heritage Science*, 2017
- [46] M. Matteini, A. Moles, A preliminary investigation of the unusual technique of Leonardo's mural 'The Last Supper', *Studies in Conservation*, pp. 125-133, 1979
- [47] I. Osticioli, et al, Red lakes from Leonardo's Last Supper and other Old Masters Paintings: Micro-Raman Spectroscopy of anthraquinone pigments in paint cross-section, *Molecular and biomolecular spectroscopy*, 2019
- [48] A. Arnold and K. Zehnder, "Monitoring Wall Painting Affected by Soluble Salts," in *The Conservation of Wall Paintings*, London, 1987.
- [49] A. Arnold and K. Zehnder, "The conservation of wall paintings," in *Monitoring Wall Paintings Affected by Soluble Salts*, London, 1987.
- [50] E. Kotulanová et al., Degradation of lead-based pigments by salt solutions, *Journal of Cultural Heritage*, 2008
- [51] S. Pavia, Sulfation of a decrepit Portland cement mortar and its adjacent masonry, in *SWBSS- Salt Weathering on Buildings and Stone Sculptures*, Copenhagen, Technical University of Denmark, 2008.
- [52] K. Sterflinger, J. Ettenauer and G. Piñar, "Microbes, science, art and conservation, who wins the game?," in *THE SECOND INTERNATIONAL CONGRESS ON SCIENCE AND TECHNOLOGY FOR THE CONSERVATION OF CULTURAL HERITAGE*, Sevilla, Spain, 2014.
- [53] T. Rosado, M. Silva, L. Dias, A. Candeias, M. Gil, J. Mirão, J. Pestana and A. T. Caldeira, "Microorganisms and the integrated conservation-intervention process of Renaissance mural paintings from Casas Pintadas in Évora - Know to act, act to preserve," *Journal of King Saud University - Science*, 2017.
- [54] C. Milanesi, F. Baldi, S. Borin, L. Brusetti, F. Ciampolini, F. Iacopini and M. Cresti, "Deterioration of medieval painting in the chapel of the Holy Nail, Siena (Italy) partially treated with Paraloid B72," *International Biodeterioration & Biodegradation*, 2009.
- [55] T. Rosado, A. Candeias, A. Caldeira, J. Mirão and M. Gil, "Role of microorganisms in mural paintings decay," in *Science, Technology and Cultural Heritage*, 2014.
- [56] E. May and Jones Mark, *Conservation science, Heritage Materials*, The Royal Society of Chemistry, 2006.

Chapter III: Case study and the Methodology

3.1. Paintings' identification

In total eight murals are presented on the east and west wall of Alcântara station: two triptychs and two individual paintings (Chapter II, Figure 8, Appendices I and II). Subject of this research were murals under numbers 2,3 & 6 (Figure 12). They were chosen based on type of deterioration, since each had deteriorated features representative for all eight murals.

Panel 2: displays severe flaking of greenish blue paint layer on Angel's garment and wings (these features are presented in the Appendix III). This paint layer is also observed in the other seven panels, and it's in poor state of conservation.

Panels 3 and 6: show lacuna, lack of cohesion of pigments, formation of salts (including efflorescence and crypto-efflorescence). There is a suspicion of past consolidation and colour alterations. Panel 3 developed severe salt formation that wasn't visible in the photographs taken in the late 1990s (Figure 11). That's why it is particularly important for understanding dynamics of salts development through time. For that cause, three sets of photographic records were compared: from the late 1990s, 2013 and 2020.

Attention was on blue and green paint layers, since they are often applied a *secco* with organic binders such as egg yolk or starches [14].



Figure 11. Panel 3. On the left: photograph taken by Guta Carvalho (6-7th of June 2020), on the right: photograph taken in late 1990s (APL Archival). The area chosen for analysis of salts deterioration dynamics is indicated with interrupted line



Figure 12. From left to right: Panels 2, 3, and 6, with indicated areas of interest that were analyzed in-situ and laboratory setup (photos by Guta Carvalho 2020 © all rights reserved)

3.2. Environmental conditions and geographic location

Alcântara and Rocha do Conde de Óbidos Maritime Stations are located in Lisbon. They stretch for 1.5km along Tejo riverside and represent the main port, connecting the land of Lisbon with the Atlantic Ocean. Beside being the capital city, Lisbon is the biggest urban area of Portugal [1]. It covers the space of 952km² and it has population density of 2,794 habitants on 1km² [1].

Pollution in the city comes from traffic and peripheral industry, including textile, chemical, steel, oil and sugar refining [2]. It's location on the Atlantic coast assures that high levels of pollutants are not very common due to the regime of winds [2,3]. As a result of influences of the Ocean and Gulf Stream, Lisbon escapes extreme temperature characteristic for central Portugal [2,3], yet proximity of the ocean influences its humidity that varies between 70-80%, and is higher during winter months [2]. Relative humidity measures were also taken during the survey conducted in the period between 1st and 6th of June, 2020 by the author and Milene Gil. Measures were taken six times during the day and they gave the average results of 25.2% RH. Average temperature in Lisbon is 21.5°C during the day and 13.5°C during the night. The warmest month in year is August, where average temperature varies between 24-33°C, although there are records of recorded extremes of 44°C. The coldest month seems to be January with average temperatures between 10-19°C, and recorded extreme of -1.2°C [3]. Research conducted by Célia A. Alves, Manuel G. Scotto and Maria do Carmo Freitas, from the University of Aveiro and Technological and Nuclear Institute [2], showed that atmospheric pollutants (except for ozone), show seasonal pattern covering high winter and low summer levels. Main pollutants in Lisbon include PM10 (Particulate matter), Sulfur dioxide SO₂, Carbon Monoxide CO, Nitrogen Oxides NO and NO₂, and Ozone O₃ [2,3]. Some of them, especially CO₂, SO₂ and NO_x are recognized as ones causing the most problems in cultural heritage [4,5], as it was previously explained in the Chapter II (2.3.2).

When it comes to the position of the murals inside of the building, they are positioned on east and west walls of the great hall of Alcântara station (Figures 13-14). Location of the stations is close to railway (Alcântara), subway (Cais do Sodré) and highways (N6 and E1). This creates conditions of traffic pollution and vibrations. Along with proximity of the sea, and previously mentioned high humidity values (especially during winter), the exterior environment of these murals creates conditions favorable for development of salts (salt efflorescence and crypto-efflorescence) or cracks and fissures due to traffic activity.

The eight murals are facing each other: two triptychs and two individual ones. From south and north they are illuminated from the large windows, occupying entire wall areas, from the floor to the ceiling. Survey conducted in the period between 1st and 6th of June revealed that regardless of the size of the windows, summer light does not lay directly on these paintings.

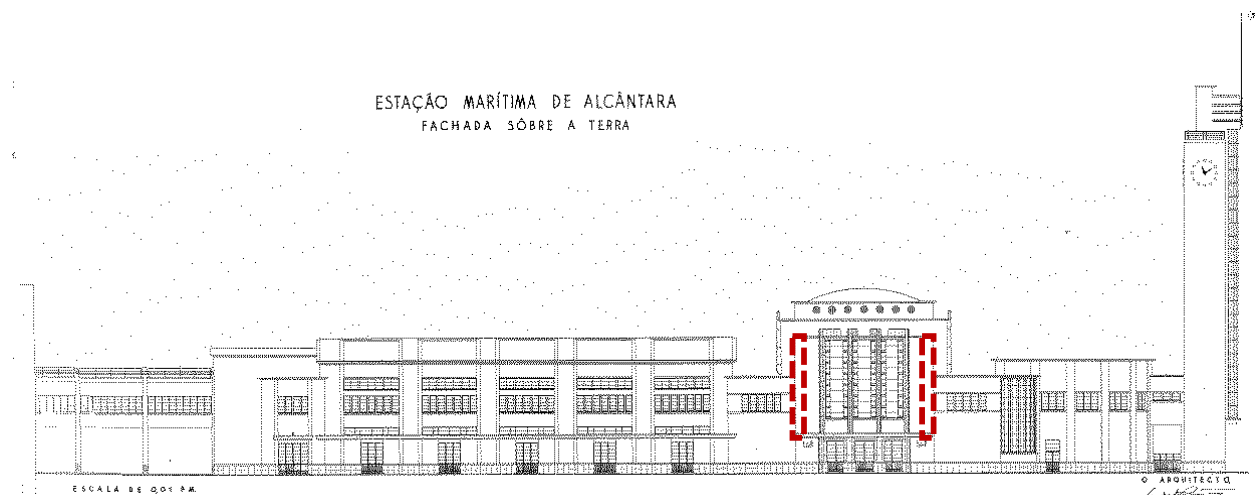


Figure 13. Cross section of Alcântara station with marked positions of murals inside of the building. Source of section: [6]

Within the main hall that holds them, the murals are located over two floor heights, which means that the floor joint is positioned right in the middle of the paintings as illustrated in the Figures 13 and 14. The most deteriorated areas, on all of the eight murals from Alcântara station, are exactly aligned with this connection (Details of deterioration features are presented in Appendix I-III). Deterioration could be explained by formation of a thermal bridge [7-8], i.e. area of heat exchange between environments (Figure 14). Thermal bridges are characteristic for all types of constructions, and are formed in the areas of joints between different materials and/or different construction elements [7-8]. They represent spots of weak insulation - heat transmittance and water evaporation, due to old and broken installations and damaged building materials. This means that exactly these parts would be prone to formation of salts, black marks or molds [7,8]. The presence of thermal bridge could be one of explanations for the alignment of salt induced deterioration or chromatic changes, present in all of the murals in the hall.

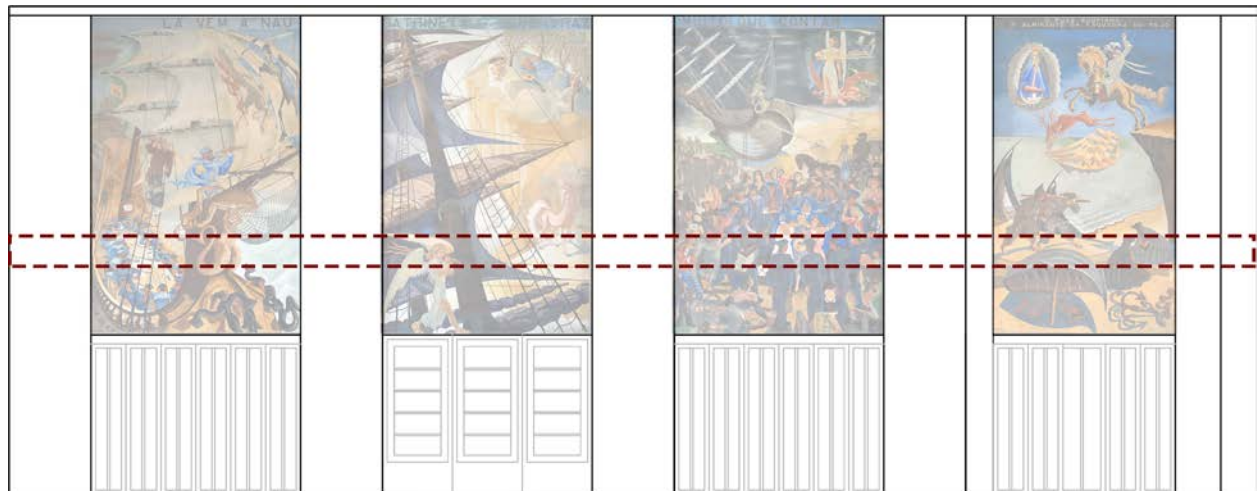


Figure 14. Scheme of the west wall of Alcântara station with display of the murals and indicated position of thermal bridge that corresponds with construction joint between two floors. Drawing by the author

3.3. Experimental

In order to understand the painting technique, pigments used and how deterioration factors are affecting these murals, set of in situ and laboratory analysis were conducted. They include both non-invasive and micro-invasive techniques, and collection of microsamples in powder and microfragments. The techniques were chosen based on their qualitative and quantitative properties, and their mutual complementarity.

3.3.1. *In situ analyses*

Diagnostic survey was conducted during the period from 1st to 6th of June by the author and Milene Gil under the auspices of Hercules Laboratory of Évora. It included photo documentation and technical photography in visible, visible raking and ultraviolet mode (Vis, Vis-RAK and UVF), portable optical microscopy (p-OM), colorimetry and spectrophotometry and handled x-ray fluorescence XRF analyses, that were used for mapping of deterioration features and preliminary identification of painting materials. These techniques were important since they are non-invasive, so they allowed screening of the entire painted surface of the areas of interest selected on each of the three panels (Figure 12). In total, 294 p-OM images, 88 EDXRF point analysis and 72 Spectro-colorimetry measures were taken, in stable and deteriorated paint layers (presented in Appendix IV-V).

Microsampling was made in deteriorated areas, such as cracks, fissures, lacunae, flaking paint layers and areas displaying formation of salts. Sixty-seven samples in total, in the form of microsamples in powder and microfragments (samples locations are presented in Appendix VI). Microsamples in powder were collected by gently scratching the surface of the painting, and microfragments with a scalpel n.10.

3.3.1.1. Photo documentation and technical photography (TP)

Visual observation and photo documentation were the first step of the survey. Photographs were acquired in visible (Vis), visible raking (Vis-RAK) and ultraviolet light (UV), and taken with a Nikon D3200 camera, with 24Mpx, and objective Nikkor 18-55mm f:3.5-5.6 GII. In total 202 photographs were taken from the three analysed panels. Photo documentation was important for further mapping of deterioration zones and other zones of interest.

Raking light (RAK) was used to reveal flaking, detachments, tool marks, incisions and similar. *Giornata*¹ and *pontata*² were not evident. Photographs were obtained under the angle of 15-20° from the painting surface, from three different sides. UV induced fluorescence in visible (UVF) photography was used to discover previous interventions or presence of organic binder. It was taken with the same Nikon D3200 camera and Labino® MPXL UV PS135 light (35W PS135 UV Midlight 230V) with UV filter included (310-400nm and a peak at 365nm), a midlight distribution angle of 20° and a start-up time full power after 5-15sec.

3.3.1.2. Portable optical microscopy (p-OM)

For documentation of details of painting technique, pigment composition and deterioration features, two series of portable microscopes were used, Dinolite PRO AM13T-FVW and DinoLite Premier AD3713TB, with 20 and 434 x magnifications. First magnification was primary used for mapping and imaging of deterioration of painting materials, while the second one was used for the first image record of pigments particles.

3.3.1.3. Colorimetry and spectrophotometry

Colorimetry is the technique that is used to quantify and describe colours, while spectrophotometry represents a method used to calculate colorimetric values by reflectance/transmittance properties of an object of interest [9].

¹ *Giornata* – “a day’s work”, is amount of work done per day by the artist. It is a form of vertical joint, often corresponding to edges of the painted figures. [12]

² *Pontata* is also a form of a joint, but corresponding to the height of a scaffoldings. [12]

Spectrophotometer is used to measure the amount of radiation at each wavelength [9]. To locate the colour hues in space, CIELab system uses a , b and L coordinates (Figure 15) [10]. When a colour is expressed in CIELAB, L^* coordinate defines lightness, a^* coordinate represents the red/green hues (positive values correspond to red and negative values green colours) and b^* coordinate the yellow/blue hues (positive values correspond to yellow and negative to blue colours) [10].

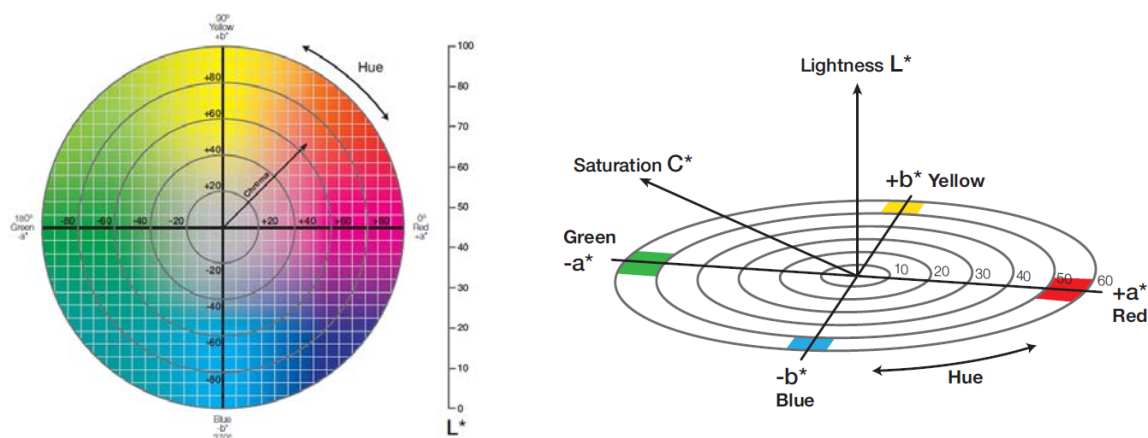


Figure 15. CIELAB colour chart in two (left) and three (right) coordinate system. Source: [10]

This study used spectro-colorimetry for pigment characterization and evaluation of colour value of paint layers in degraded and non-degraded areas. Data Colour Check Plus II colorimeter was used, equipped with integrating sphere. Measures were performed using following parameters: diffuse illumination 8 viewing (in accordance with the CIE standard No 15.2. colorimetry), SCE and Standard Illuminant/Observer D65/10. The aperture size was USAV (Ø5mm). Wavelengths were analysed in the range of 360-750nm.

3.3.1.4. Handled X-ray fluorescence (h-EDXRF)

Handled X-Ray Fluorescence h-EDXRF allowed first in situ non-invasive inspection of elemental composition of painting materials. In total 88 point analyses were collected on areas of different paint layers. Being simple to use, this technique allowed us to, in a short time, collect preliminary elemental composition data, although it is important to indicate that the X-ray beam penetrates a few millimetres into the surface and thus gives the information not only for the paint layer but for the intonaco³ layer as well.

A handheld X-ray fluorescence analyser Bruker tracer III SD (Bruker, Germany) was used, equipped with an X-ray tube with rhodium target and a silicon drift detector. Results were organized using corresponding Artrax 7 software.

3.3.2. Laboratory analyses

After in situ non-invasive techniques, collected samples were inspected in Hercules Laboratory in Évora, Portugal. Micro-invasive techniques were conducted for more profound analyses on the deterioration features, painting technique and materials.

The analyses team, beside the author and research supervisors, included Mafalda Costa, geologist and current PhD student at University of Evora, who helped with μ -XRD analyses and data interpretation, researcher Ana Margarida Cardoso, who guided through FTIR analyses and data interpretation, and post-doctoral researchers Carlo Bottaini and Ana Mahnita who helped with h-EDXRF and py-GC-MS analyses and data interpretation.

³ Intonaco is a thin layer of mortar in fresco paintings, prior to the layer of paint. [12]

3.3.2.1. Optical Microscopy (OM)

First step in laboratory analysis was optical microscopic documentation of samples. It allowed understanding the stratigraphy of paint layers and the description of pigments and mortar characteristics (Appendix VII).

Cross sections were embedded in epoxy fix resin and studied using Leica DM2500M reflected light optical microscope in dark field illumination mode. Observations were carried in 100x, 200x and 500x magnification (images are presented in Appendix VI). Photographs of cross sections were obtained with Leica MC 170HD digital camera attachment equipped with corresponding Leica software. UV mode was used to spot the presence of organic materials. Also stereomicroscope Leica M205 C was used, for obtaining the images of both powder samples and cross sections in magnifications 7.8x - 160x. Microscope is equipped with Leica DFC295 camera and external illumination.

3.3.2.2. μ -X-ray Diffraction (μ -XRD)

In order to understand the mineralogical composition and crystalline structure of samples, micro X-ray Diffractometer was used. The analyses included five samples from the areas affected by salts and salt efflorescence (Appendix VIII).

This research used Bruker AXS-D8 Advance diffractometer with Cu K α radiation. The samples were mounted as powder on standard plastic sample holders. A step of 0.02°/s and counting time of 1 s was used for collecting 2–70° 2 θ diffractograms and The EVA code was used for the identification of the peaks and phase analysis.

3.3.2.3. Scanning Electron Microscopy coupled with Energy Dispersive Spectroscopy SEM-EDS

After examination under optical microscopes and analyses of elemental composition, Scanning Electron Microscope (SEM) coupled with Energy Dispersive Spectrometer (EDS) were used. This allowed more profound stratigraphic analyses. High resolution pictures of the samples were obtained in 20x-30 000x magnification mode (images are presented in Appendix IX).

SEM microscope can be used in two modes: backscattering and secondary electron mode. For this study backscattering mode was used, which allowed observation of micro-morphology of paint layers.

Variable pressure Scanning Electron Microscope HITACHI S-3700N operator was used, with an accelerating voltage of 20kV and chamber pressure of 40Pa. Variable pressure mode is convenient for studies of non-conductive samples, since it allows analysis without sample coating. Pressure would be added to the chamber in order to remove electron charging effect.

SEM was coupled with Bruker XFlash 5010 Silicon Frift Detector (SDD) with resolution of 129eV at Mn K α .

3.3.2.4. Fourier Transformed Infrared Spectroscopy μ -FT-IR

For detection of organic compounds, Fourier Transformed Infrared Spectroscopy μ -FT-IR was used. Study was performed in order to identify possible presence of binders and/or previous intervention products. Twenty-two samples in powder were analysed using a Bruker Tensor 27 Mid-IR (MIR) spectrometer, coupled with HYPERION 3000 microscope and controlled by OPUS 7.2 software with corresponding OPUS library (copyright© 2012 Bruker Optics and Microanalysis GmbH, Berlin, Germany). Detector used is MCT (Mercury Cadmium Telluride) cooled with liquid nitrogen that allows spectra acquisition at different points of the sample.

Analyses were done in transmission mode using a 15x objective and an EX'Press 1,6mm diamond compression microcell, STJ-0169. Spectra were plotted in region of 4000-600 cm^{-1} , with 64 scans and 4 cm^{-1} resolution.

3.3.2.5. Pyrolysis Gas Chromatography coupled with Mass Spectrometry Py-GS-MS

For identification of organic residues, Pyrolysis Gas Chromatography coupled with Mass Spectrometry Py-GS-MS were used.

System utilized was Frontier Lab PY-3030D double-shot pyrolyser coupled to a Shimadzu GC2010 gas chromatographer, and a Shimadzu GCMS-QP2010 Plus mass spectrometer. The interface was maintained at a temperature of 280 °C. A capillary column Phenomenex Zebron-ZB-5HT (30-m length, 0.25-mm internal diameter, 0.50- μm film thickness) was used for separation, with helium as carrier gas, adjusted to a flow rate of 1.5 ml min⁻¹. The split injector (15:1 ratio) operated at a temperature of 250 °C. GC temperature programme was as follows: 35 °C during 1 min, followed by a series of temperature ramps: until 110 °C at 60 °C min⁻¹, until 240 °C at 14 °C min⁻¹, up to 280 °C at 6 °C min⁻¹, until 320 °C at 30 °C min⁻¹, and then an isothermal period of 6 min. Source temperature was placed at 240 °C, and the interface temperature was maintained at 280 °C. The mass spectrometer was programmed to acquire data between 40 and 1090 m/z. The sample (<200 μg) was previously derivatized with 3 μL of tetramethylammonium hydroxide (2.5% in methanol, v/v) in a 50- μL Eco-cup capsule and pyrolysed at 500 °C. Compound identification was performed using AMDIS software integrated with NIST-Wiley database.

List of references

- [1] D. W. U. Areas, *Demographia World Urban Areas (Built-Up Urban Areas or Urban Agglomerations)*, 16th annual edition, 2020.
- [2] C. A. Alves, M. G. Scotto and M. do Carmo Freitas, "AIR POLLUTION AND EMERGENCY ADMISSIONS FOR CARDIORESPIRATORY DISEASES IN LISBON," *Quim. Nova*, Vol. 33, pp. 337-344, 2010.
- [3] J. Monjardino, N. Barros, F. Ferreira, H. Tente, T. Fontes, P. Pereira and C. Manso, "Improving Air Quality in Lisbon: modelling emission abatement scenarios," *IFAC PapersOnLine* 51-5, pp. 61-66, 2018.
- [4] A. Arnold and K. Zehnder, "Monitoring Wall Paintings Affected by Soluble Salts," in *The Conservation of Wall Paintings*, Courtauld Institute of Art and the Getty Conservation Institute, London, 1987.
- [5] H. M. Mahmoud, N. Kantiranis and J. Stratis, "Salt damage on the wall paintings of the festival temple of Thutmosis III, Karnak Temples Complex, Upper Egypt. A case study," *International Journal of Conservation Science*, vol. Volume 1, no. Issue 3, pp. 133-142, 2010.
- [6] J. P. Monteiro, *Dissertação para Obtenção do grau Doutor en Design: Para o projecto global - nove décadas de obra: Arte, Design e Técnica na Arquitetura do atelier Pardal Monteiro*, Lisbon: Universidade Técnica de Lisboa, Faculdade de Arquitetura, 2012.
- [7] M. Jedidi and O. Benjeddou, "Effect of Thermal Bridges on the Heat Balance of Buildings," *International Journal of Scientific Research in Civil Engineering*, vol. Volume 2, no. Issue 5, pp. 41-49, 2018.
- [8] M. F. Zedan, S. Al-Sanea, A. Al-Mujahid and Z. Al-Suhaibani, "Effect of Thermal Bridges in Insulated Walls on Air-Conditioning Loads Using Whole Building Energy Analysis," *Sustainability*, vol. 8, no. 560, 2016.

-
- [9] N. Ohta and A. R. Robertson, *Colorimetry, Fundamentals and Applications*, England: John Wiley & Sons, Ltd, 2005.
- [10] *A guide to understanding colour*, US: X-rite Pantone, 2016.
- [11] A. V. Girão, G. Caputo and M. C. Ferro, “Application of Scanning Electron Microscopy-Energy Dispersive X-ray Spectroscopy (SEM-EDS),” in *Characterization and Analysis of Microplastics*, Elsevier, 2017.
- [12] P. Mora, L. Mora and P. Philippot, *Conservation of Wall Paintings*, London: Butterworths, 1984.

Chapter IV: Results and discussion

4.1. Mapping of deterioration

Initial insight into the deterioration and the painting materials was obtained after *in-situ* analyses. The first step was to identify and locate the main deteriorated areas of all eight murals, with later focus on three of them: murals 2,3 and 6 (Figure 11 of previous chapter). As it was explained in *Chapter III*, these murals were chosen based on their representability regarding decay phenomena which are affecting all paintings of Alcântara station. Photographic documentation in visible (Vis), visible raking (Vis-RAK) and UV induced fluorescence (UVF) light allowed us to detect, mark and record all areas of interest. Visible raking light (RAK) highlighted the extent and severity of flaking and lack of cohesion of paint layers, and ultraviolet induced fluorescence (UVF) light showed presence of areas that potentially underwent previous treatments (Figure 16).



Figure 16. Area of the basket with fruits from the panel 3, Photo-documentation taken in Vis, RAK and UVF light during the survey (1st-6th June, 2020)

An overall identification of the main areas observed during the survey as the ones severely affected by lacuna, flaking and formation of salts (including salt efflorescence and sub-efflorescence), are displayed in the Figure 17. It is apparent in the photographs that many of these areas are corresponding to previously defined thermal bridge and horizontal building joints (please see Chapter II: 3.2.). Detailed mapping documentation of deterioration features is presented in the Appendix I and II.

Beside the photo documentation survey of eight panels taken in 2020 (Figure 8 of the chapter II), two other sets of images were part of this research. The photographs from APL Archival coming from the late 1990s and the set photographed by José Vicente on 16th of July 2013 (Photographs are presented in the Appendix I). Decay dynamics are evident when photographs of the panel 3 are compared (Figure 18). Many of salt induced phenomena developed in the 30 years that elapsed between the first and last set of photos analysed. Since Almada completed the murals of Alcântara station in 1943, this would mean that main decay phenomena rapidly evolved during the last third of their existence. One of the deteriorated spots affected by salts sub-efflorescence and salt efflorescence is marked in red in the three photographs from 1990, 2013 and 2020 (Figure 18). White veil covering paint layer is clearly visible in last two photographs and yet we can notice that it didn't exist in the first one, taken in late 1990s. Based on the location of the area affected as presented in the figures 12 and 13 of the previous chapter, this white veil can be a consequence of poor isolation and concentration of water vapour formed by installations (pipes) for hot water or heating.

Photo documentation was combined with Portable optical microscopy (p-OM). Two series of portable optical microscopes were used, for more detailed images of the area of interest. The first one - in 20x gave insight into deterioration such as flaking, lacunae and loss of pigment, while the second one - in 434x revealed subtler details of the paint surface linked to pigments' particles, salts' veils and salt efflorescence.



Figure 17. Images of eight panels of Alcântara station. Areas that display deterioration problems such as flaking, lacuna and formation of salts are marked in white



Figure 18. Three images of panel 3 of Alcântara station. From left to right: APL Archival (late 1990s), José Vicente (16th of July 2013), Guta Carvalho (6-7th of June 2020). Deteriorated area marked in red illustrating decay dynamics

For easier mapping of deterioration features, panels were divided in two zones of interest each. These zones are presented in following figures: Fig. 18 for the display of zones in panel 2, Fig. 21 for the display of zones in panel 3, and Fig. 24 and 25, displaying zones of panel 6. More detailed presentation can be found in Appendices I - III, and it includes presentation of examined deteriorated areas for each of the panels, photographed in Vis, Vis-RAK and UVF light, accompanied with detailed images of deterioration features taken with two series of portable optical microscopes (p-OM), one in magnification 20x and another in 434x.

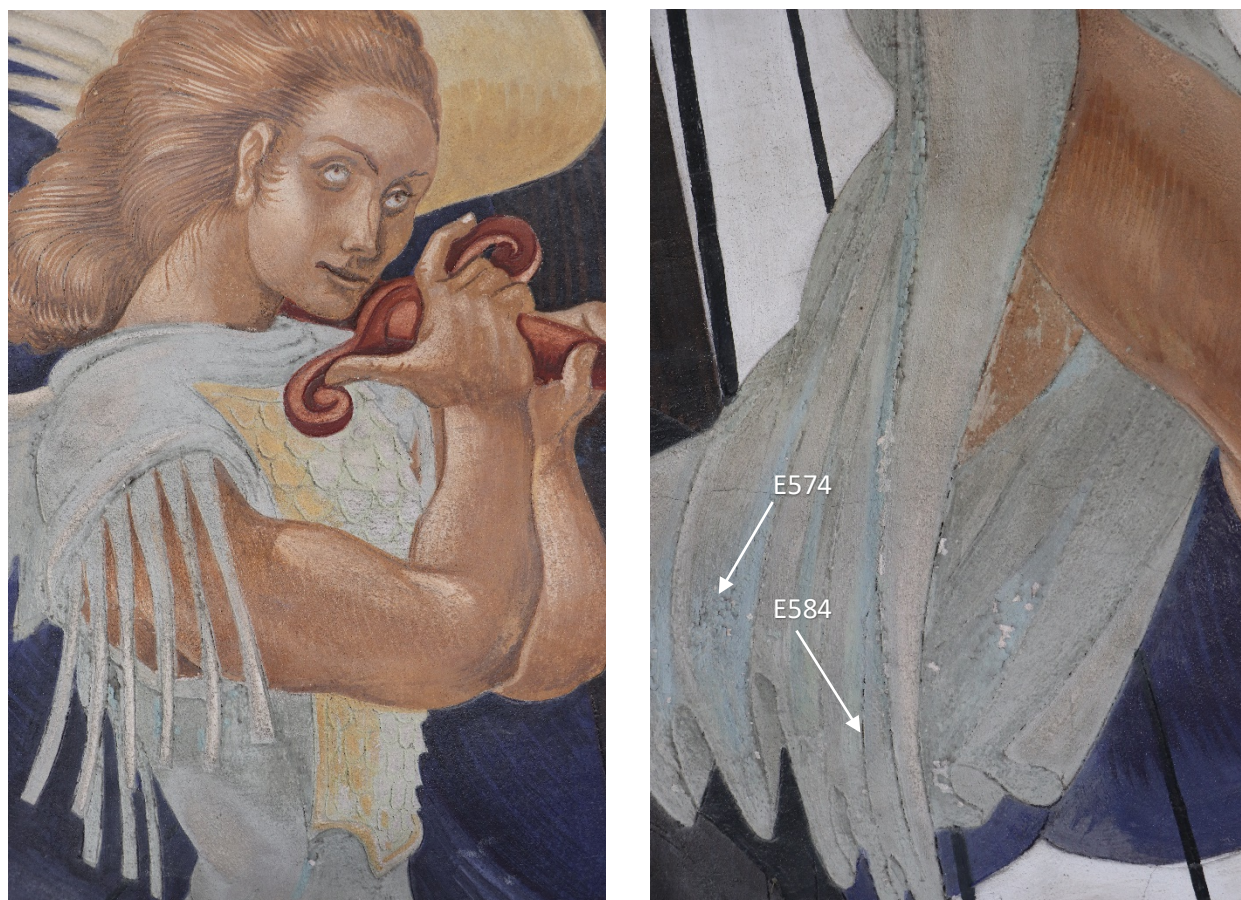


Figure 18. Two zones of interest in Vis light of panel 2 displaying image of Angel and his garment

Panel 2 was divided into upper and lower zones of interest as presented in the Figure 18 above. They illustrate the image of the Angel, and they are mostly composed of a severe flaking of the greenish paint layer, used at Angel's garment. This characteristic paint layer is also present in other two panels.

Ultraviolet induced fluorescence (UVF) photography in visible revealed the spots of possible previous interventions (adhesion/consolidation areas - Appendix III). Samples were collected in these areas for further analyses in HERCULES laboratory to look for the evidence of organic materials. All sampling locations are presented in the Appendix VI.

Regarding deterioration features, panel 2 is showing appearance of cracks and fissures, as well as significant lacunae, flaking and pigment loss, particularly in the previously mentioned greenish paint layer. Cracks were mapped with photo-documentation in visible and visible-raking light, and fissures were identified by DinoLite optical microscope (p-OM) in 434x magnification (Figure 19). They most likely occurred during the drying of the paint layer and plaster underneath [1]. One more possibility is that they appeared due to the induced stress caused by strength in compression, tension or shear of building elements over the years [2].

Lacunae and flaking are documented using portable optical microscope (p-OM) in 20x magnification as presented in the Figure 20. At first sight, these areas do not seem to be linked to salts, but to the paint layer itself. Samples were collected on the edges of lacuna in order to conduct more profound analyses of this decay phenomena, later in the HERCULES laboratory (micro-sampling locations are presented in the Appendix VI).

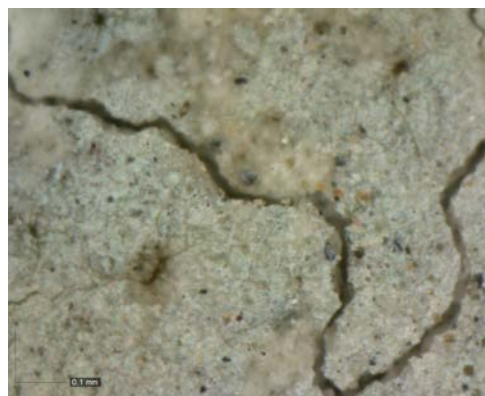


Figure 19. Portable optical microscope image E584 of a fissure in the greenish layer of Angel's garment, mag. 434x



Figure 19. Portable optical microscope image E574 of a flaking greenish layer of Angel's garment, mag. 20x



Figure 21. Two zones of interest of panel 3. First one, on the left, displaying the basket with fruits, second one, near the right edge of the panel, presenting figures of sailors

Panel 3 was divided into two zones of interest as presented in the Figure 21 above. They are displayed in Appendices I and II in more detail. The first one is a basket with fruits, that held the largest amount of different colour hues, while the second one, on the right, near the edge of the panel, was previously described as the area displaying severe salts formation in the last 30 years (Figure 18). Regarding the first zone - basket with fruits, the main issue seems to be the lack of cohesion of the paint layers, which caused erosion and lacunae (Figure 22).

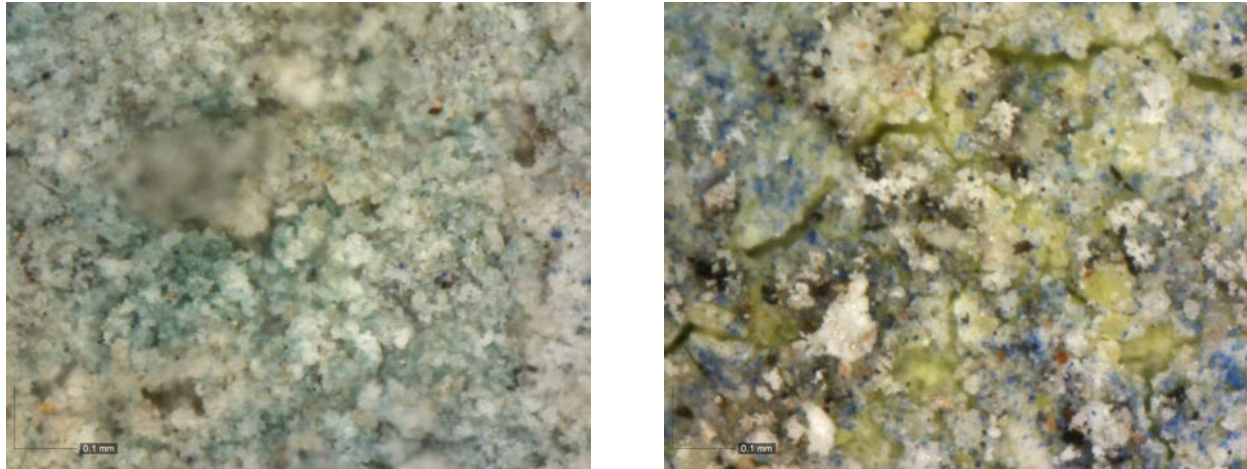


Figure 22. Two portable optical microscope (p-OM) images E658 (on the left) and E630 (on the right) in magnification 434x from the area in the basket of fruits, panel 3. Images are displaying paint layers affected by lack of cohesion

The second area of interest seems to have developed some more dangerous deterioration phenomena: salt efflorescence and sub-efflorescence. A white veil is clearly visible in some parts, as it completely covers paint layers. This phenomenon initiated further deterioration features such as flaking, loss of pigments' cohesion and lacunae (Figure 23). From detailed observation of the three sets of photographs from the late 1990s, 2013 and 2020 (Figure 18) it is possible to conclude that this issue is ongoing and thus requires immediate attention. The deterioration is not affecting any pigment or paint layer in particular, and it is rather linked to the location itself. In this case salts would be formed due to the thermal differences between the wall, the pipe installations and the environment [3-4]. It is not unusual for heritage buildings to have these types of issues, generally caused by condensation and infiltration of water into the building material, due to old and damaged installations and leaking pipes [3-4].

Beside the flaking and lacuna that were formed in this area, formation of a white veil and accumulation of superficial dirt are causing chromatic changes of the paint layer. The most affected pigment seems to be the dark blue shade and its hues as visible in the Figure 23.

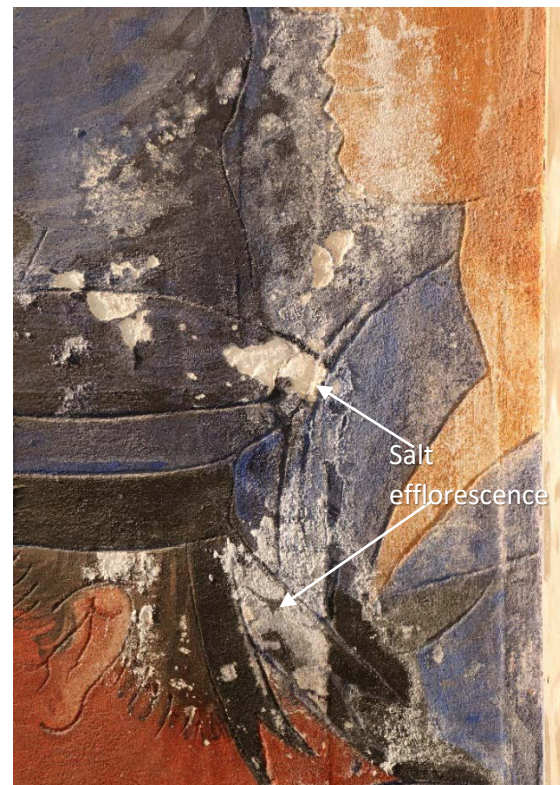


Figure 23. Vis-RAK image of deterioration features on the second area of panel 3, affected severely by salts, salt efflorescence and sub-efflorescence

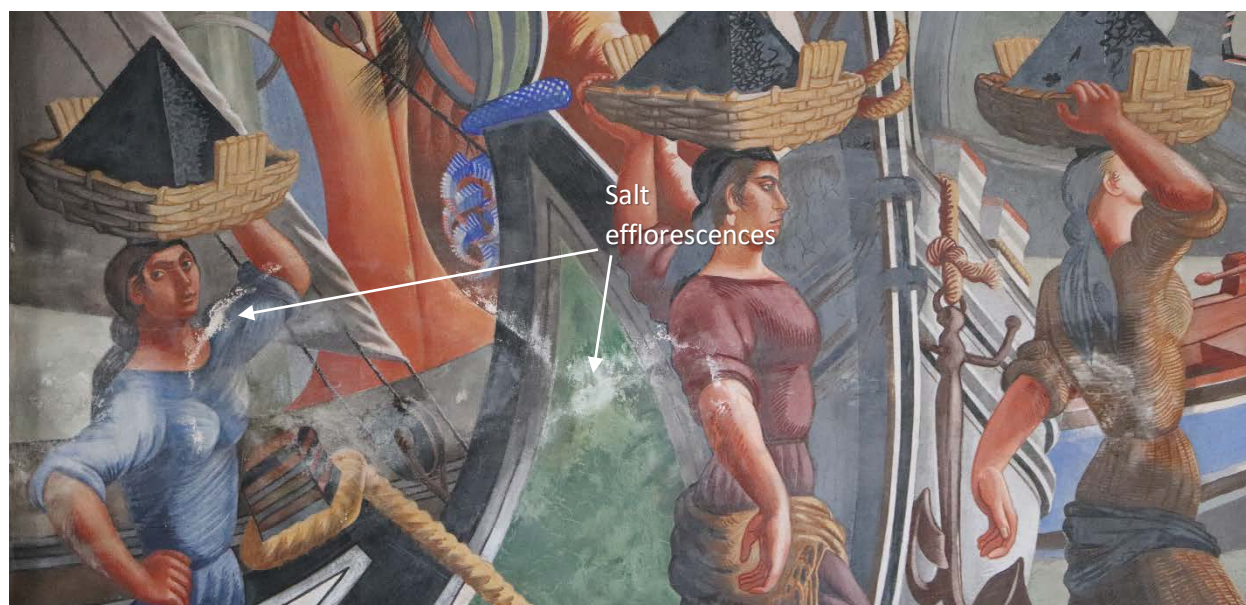


Figure 24. Zone 1 of panel 6, displaying three female figures

Panel 6 was the most complex one. Similarly to the first two panels it was divided into two deterioration zones. Zone 1, an extremely large zone, covering three female figures in the lower part of the panel, starting from the left edge and spreading almost to the right one (Figure 24). Zone 2, is located below Zone 1, and covers the greenish background at large (Figure 25). The main decay phenomena in this panel follows the pattern of the two previous ones: formation of salts, salt efflorescence and sub-efflorescence, flaking, erosion and lacunae. Salts' formation doesn't seem to be linked to a specific pigment. It rather aligns with architectural joints of the hall (similar as in the second area of panel 3) and, based on the photo documentation from last 30 years, it has been actively growing (sets of photographs of panel 6 are presented in the Appendix I). In some places, an opaque white veil is present, covering paint layers (Figure 24).

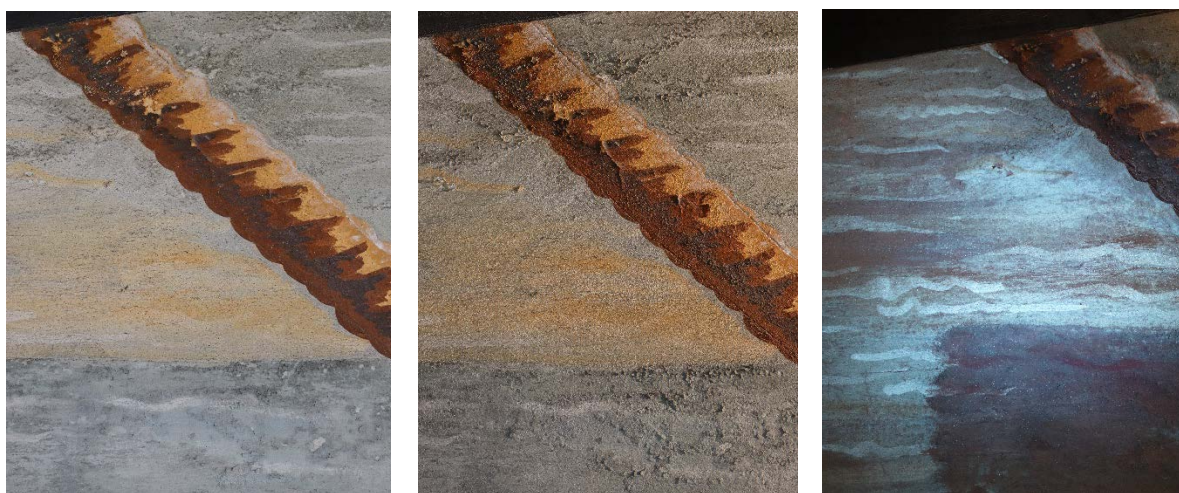


Figure 25. Vis, Vis-RAM and UVF images of flaking area with greenish background, Zone 2 of panel 6

Salts created yet further problems. In some areas, similarly to the previous two panels, this activity triggered flaking and lacunae, and loss of the paint layers is evident. Example of this can be clearly observed in the reddish area on the arm of one of the female figures (Figure 26). In this part, the layer of the paint is flaking off, revealing the under-layer beneath.

Another problem occurring from the formation of salts might be seen in the Figures 27 and 28 of the green paint layer from the figures of the boats in the middle of the Zone 1. Portable optical microscope (p-OM) images taken in 20x magnification, show differences in the paint layer, as in some parts it is being covered with an opaque white veil of salts, and in others darkening of green hue is seen, most likely caused by moisture stains.

Similarly to the previous two panels, the most degraded layer seems to be greenish blue one, present in the background and displayed in Figure 25 above. Flaking of the paint layer is clearly observed under vis-raking light (RAK) and under portable optical microscope (p-OM) in magnification 20x (Figure 29).

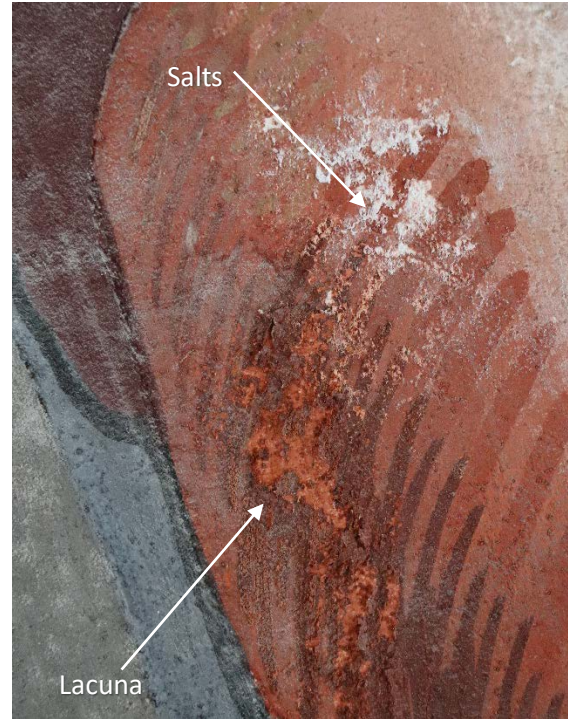


Figure 26. Flaking of the top reddish brushstrokes. The underneath pinkish background is also affected by pigments' lack of cohesion (detail of the female arm, panel 6)

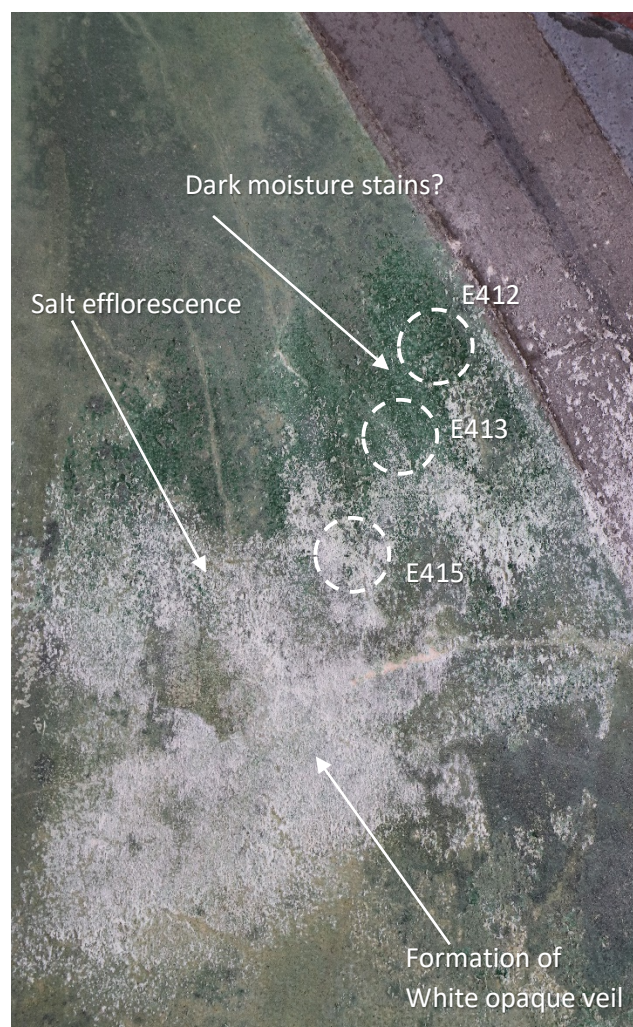


Figure 27. Details in visible of the green paint layer, figure of the boat, panel 6, with marked locations of p-OM images presented on the right

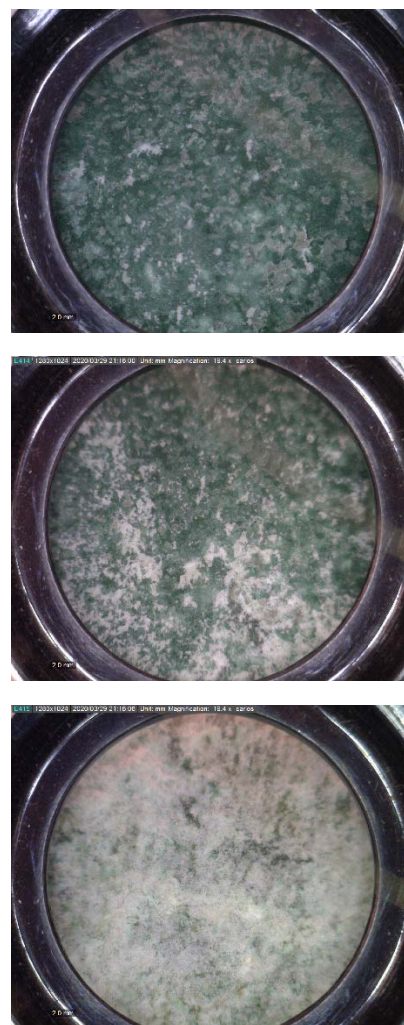


Figure 28. OM images E412, E413 and E415 (upper to lower) of different stages in the formation of white veil caused by salts mechanism. Magnification: 20x

4.2. Salts characterization

Most of deterioration features identified in chapter 4.1. were caused by the presence of salts. That's why their identification was the first step of the laboratory research. For these analyses, panels 3 and 6 were chosen, based on appearance of salts and salt efflorescence that was representative for all panels of the Alcântara Station. Five salt powder samples were collected and analysed using micro-X-ray diffraction (μ -XRD), for mineralogical phase identification (Appendix VIII). This included two samples from the panel number 3 (P3B_5 and P3B_6) and three samples from panel number 6 (P6A_2, P6A_15 and P6A_18). Locations of micro-sampling are presented in Appendix VI.

In panel 3, two samples were collected from the blue paint layers, heavily affected by salts' sub-efflorescence and efflorescence (Figures 23 and 30). The phases identified in both samples were thenardite (Na_2SO_4), syngenite ($\text{K}_2\text{Ca}(\text{SO}_4)_2 \times \text{H}_2\text{O}$) and aphthitalite ($\text{K}_3\text{Na}(\text{SO}_4)_2$). Gypsum ($\text{CaSO}_4 \times 2\text{H}_2\text{O}$) was found only in sample P3B_5 (Table 1).

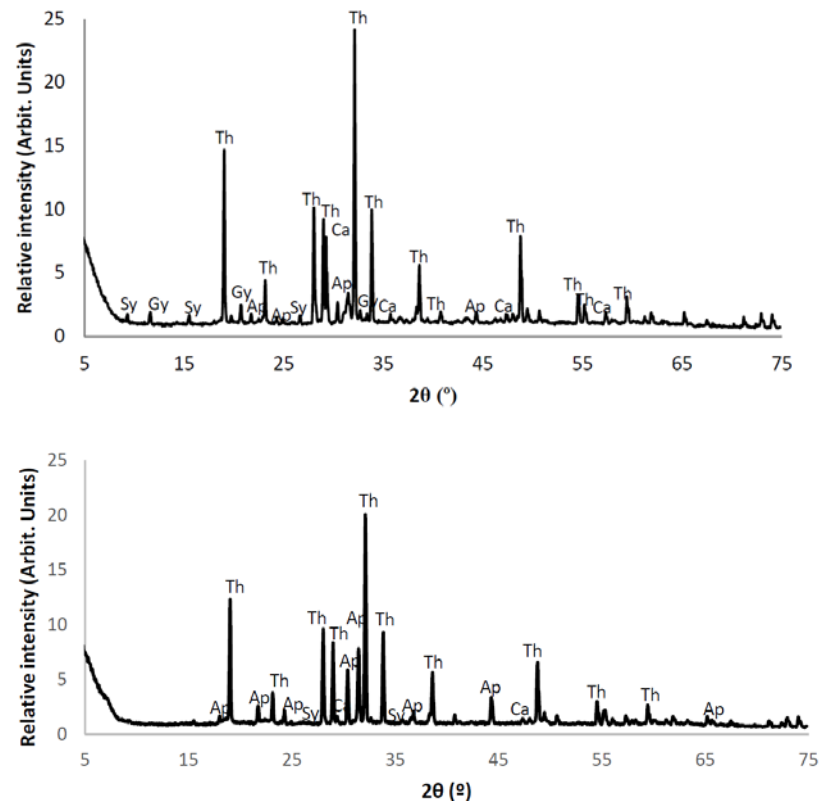
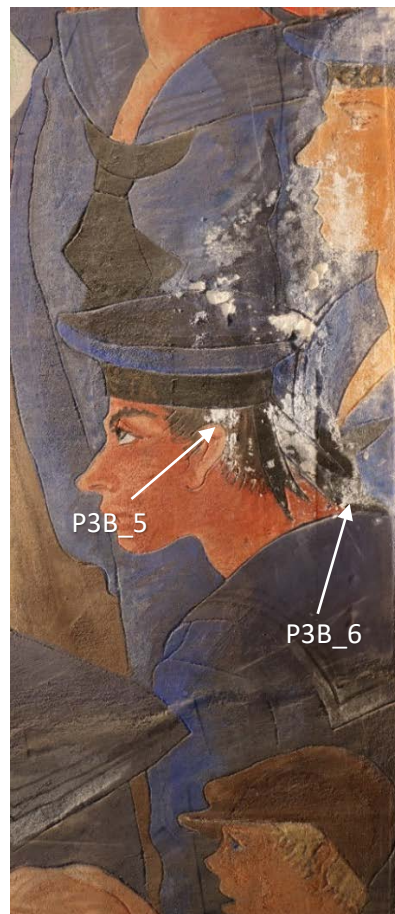


Figure 30. Left: locations of sample extraction, panel 3. Right top: μ -XRD diffractogram of sample P3B_5, right bottom: μ -XRD diffractogram of sample P3B_6. (Ca – Calcite, Th – Thenardite, Sy – Syngenite, Ap – Aphthitalite, Gy – Gypsum)

In panel 6, samples were collected from green (P6A_2 and P6A_15) and red paint layers (P6A_18). They display similar results as the ones from panel 3. Thenardite and gypsum were identified in all three samples, syngenite in samples P6A_2 and P6A_15 (Table 1). Sample P6A_2 also showed the presence of anhydrite (CaSO_4). Minerals calcite (CaCO_3) and barite (BaSO_4) were also identified (Table 1). Calcite is present in both samples from panel 3, as well as in samples P6A_15 and P6A_18 from panel 6. Barite is found in sample P6A_15.

Table 1. Crystalline phases identified by μ -XRD analyses in five powder samples from panels 3 and 6

Samples	Salts					Minerals	
	Thenardite	Gypsum	Syngenite	Aphthitalite	Anhydrite	Calcite	Barite
P3B_5	♦	♦	♦	♦		♦	♦
P3B_6	♦		♦	♦		♦	
P6A_2	♦	♦	♦		♦		
P6A_15	♦	♦	♦			♦	♦
P6A_18	♦	♦				♦	

Sulphates are common in nature as they are found in all soils. They can also come from the atmosphere or sea spray as it includes sea-water drops, brine drops and salt drops [5-6]. Alkali sulphates such as thenardite and aphthitalite can originate from architectural materials such as cement that were originally rich in alkalis [5]. Presence of thenardite is often connected to underground water or air pollution. It can be formed when calcite reacts with different oxides in the presence of moisture sources [7]. NO_2 from the atmosphere acts as a catalyst as the yields increase in its presence [7]. Furthermore, sodium sulphates (among them thenardite) are the main component of efflorescence and subefflorescence in calcite surfaces, thus becoming the most efficient factor in their disintegration [7,8].

Similarly, apththalite shows complex crystallization behaviour and can be extremely damaging for architectural materials [5,9]. Presence of calcite identified by micro-X-Ray Diffraction (Table 3), combined with the coastal location of the building might have influenced the formation of these salts on the surface of the Maritime Stations' murals.

Furthermore, gypsum dehydrates and transforms into anhydrite (CaSO_4) at relatively high temperatures or high brine salinities (e.g. 45°C at $a_{\text{H}_2\text{O}}^1$ 0.88) [10-12]. Therefore, the presence of anhydrite can originate from gypsum itself. Previously mentioned temperatures in Lisbon's summer period that can reach up to 40° and proximity of the sea as the source of salts (please see Chapter III: 3.2.) might in a way contribute to the formation of salts. Regarding the formation of syngenite ($\text{K}_2\text{Ca}(\text{SO}_4)_2 \times \text{H}_2\text{O}$), the source of potassium ions is still being resolved by many scholars. Some research showed that syngenite can develop from Portland cement as well, since this type of material can release certain amounts of potassium hydroxides, sulphates and carbonates [11,13]. After its first appearance in the 19th century, Portland cement quickly found its wide use in architecture in Europe. It was also used in Portugal as the period between 19th and 20th century can be perceived as a transitional period between the use of lime-based binders and the general use of the modern Portland cement [14]. There are no exact records of use of Portland cement during the construction of Maritime Stations, although this possibility has to be considered as a hypothesis. Potassium can also originate from the atmospheric water [15], which would in the case of Maritime Stations only be explained by situations of leakage in the past. The possibility of the potassium ions originating from the pigment is less probable since samples were collected from variously coloured areas. Barium sulphate identified in the sample P6A_15 from panel 6, is most likely a filler added by the pigment manufacturer. There are cases of barite used as filler especially in case of titanium pigments [16,17].

Crosslinking the images in backscattering mode with the EDS analyses and elemental mapping, it was possible to differentiate between different salts phases (Appendix IX). In Figure 31 below, the presence of sodium and potassium can be linked to the previously detected salts thenardite and syngenite. Accordingly, EDS analyses of the same sample confirm the presence of potassium, sodium and sulphur, as the Table 2 displays. SEM-EDS analyses of sample P6A_2 (Figure 32) shows the presence of elongated crystals that are enriched in Na, S, and Ca, likely corresponding to gypsum and anhydrite, previously identified by μ -XRD. EDS displays significant amounts of calcium and sulphur as a confirmation, but also potassium, possibly coming from syngenite.

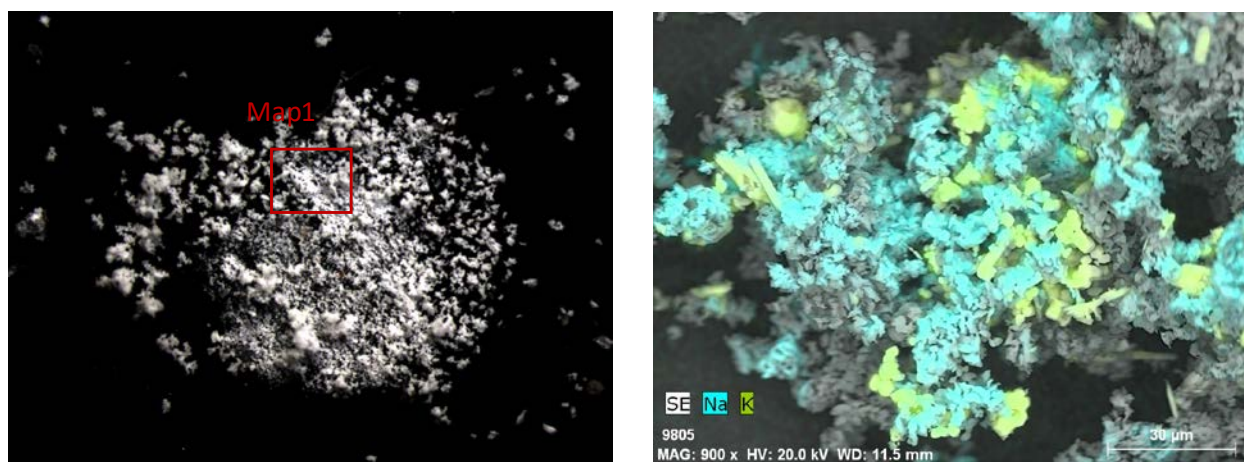


Figure 31. Powder sample P3B_5, panel 3. On the left: stereo microscope image of the sample in magnification 25x; on the right: Map1, SEM-EDS elemental distribution of Na and K, magnification 900x

¹ $a_{\text{H}_2\text{O}}$ - water activity, ratio between pressure of the water in a substance and one of a pure water.

Table 2. EDS elemental analyses of powder samples. Weight and atomic percentage (wt%, at%)

EL	P3B_5		P3B_6		P6A_2		P6A_15		P6A_18	
	wt%	at%	wt%	at%	wt%	at%	wt%	at%	wt%	at%
Carbon	8,30	13,24	1,78	2,97	25,03	37,47	11,91	28,44	10,28	16,41
Oxygen	44,88	53,74	47,68	59,66	38,00	42,70	26,29	47,11	45,06	53,98
Sodium	24,09	20,07	25,98	22,63	4,53	3,54	2,42	3,02	20,27	16,90
Aluminium	0,28	0,20					0,39	0,41	0,26	0,18
Silicon	1,68	1,41	0,19	0,13	0,52	0,33			0,55	0,38
Sulphur	14,79	8,84	19,26	12,02	14,29	8,09	11,06	9,86	9,18	5,49
Potassium	2,87	1,41	2,48	1,27	11,3	5,07				
Calcium	2,15	1,03	2,64	1,32	6,07	2,72	1,93	1,38	12,72	6,09
Iron	0,98	0,34							1,68	0,58
Copper					0,54	0,15				
Strontium							1,23	0,40		
Barium							44,76	9,35		

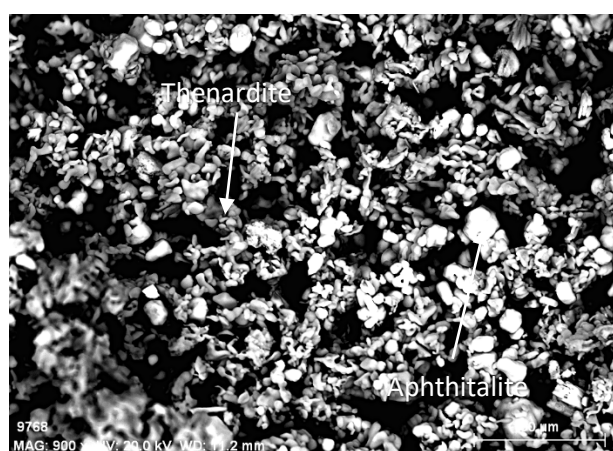
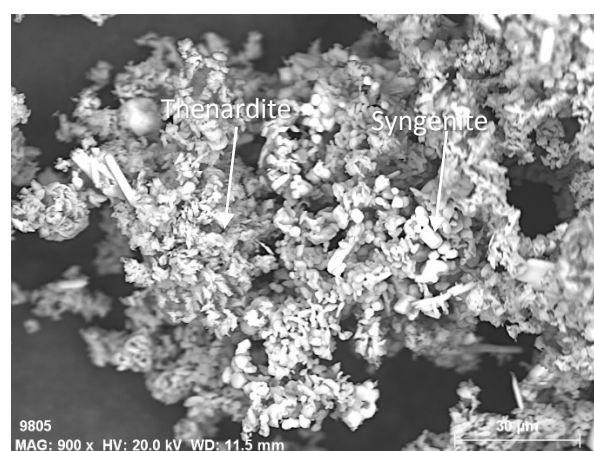
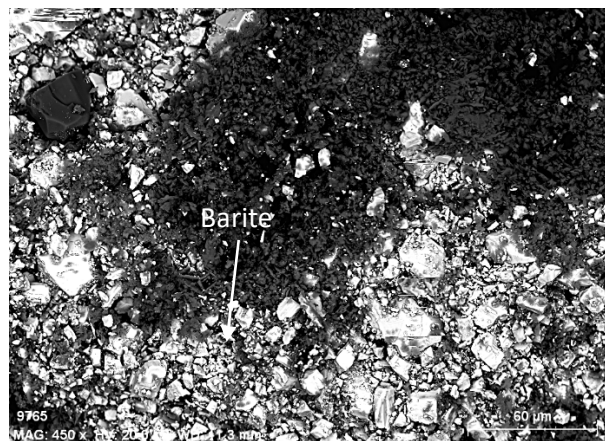
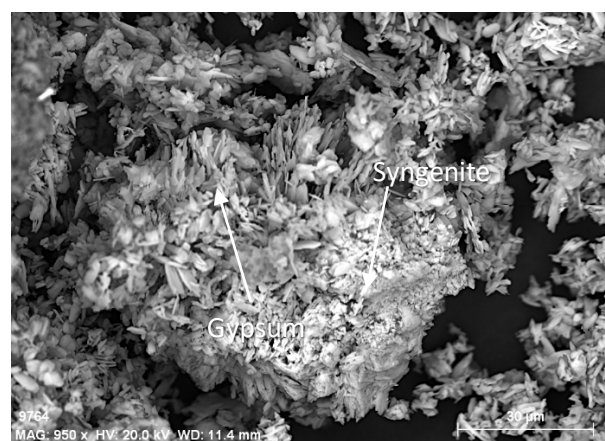


Figure 32. Left top image: sample P6A_2 and distribution of gypsum and syngenite, right top image: sample P6A_15 and distribution of barite, left bottom image: sample P3B_5 and distribution of thenardite and syngenite, right bottom image: sample P3B_6 and distribution of thenardite and apthitalite

4.3. Characterization of painting materials

First step in characterization of painting materials was done in-situ using handheld X-Ray fluorescence (h-EDXF) to collect information on elemental composition; and Data Colour Check Plus II colorimeter for evaluation of colour values (Appendices IV-V). It was important to recognise and understand not only elemental differences between colours, but also differences between hues within the same colour.

Handled EDXRF analyses were done on 6 red, 17 brown, 3 yellow, 10 blue, 7 green, 2 purple and 7 black hues, while spectro-colorimetry analyses included 4 red, 22 brown, 5 yellow, 9 blue, 4 green, 2 purple and 3 black hues. Greenish paint layer that was recognized as the most deteriorated one, was also analysed. Analyses included 21 XRF analyses and 17 spectro-colorimetry measurements. The spots' locations are displayed in the Appendix IV and V.

Table 3. Combined analyses results of representative samples from panels 2,3 and 6

Description				Elemental analysis		Chemical analysis
Sample	Location	Colour	Stratigraphy	h-EDXRF main elements	SEM-EDS (at%)	FTIR
<i>Panel 2</i>						
P2_4 cs	Angel's dress (salts)	Area of greenish blue	Layer of white pigment (27-72 μm) over the mortar	E576: Al, Ba, Ca, Cl, Cr, Cu, Fe, K, Mn, S, Si, Ti	White pigment: Na (338), Mg (4,51), Al (8,46), Si (14,05), S(10,79), Cl (1,42), Ca (21,81)Ti (30,16), Fe (4,86)	Calcite, Gypsum, Barite, Oxaltes
P2_8 cs	Bottom of the panel	Brownish with blue details	Layer of blue over the layer of brownish pigment (275-375 μm), and mortar underneath	No XRF (fragment collected from the bottom of the panel)	Blue layer: Na (11,08), Al (6,53), Si (7,12), S (3,36), Cl (0,91), K (1,33), Ca (14,89), Ti (38,65), Cr (12,69), Fe (2,15), As (1,29) Brownish pigment: Na (3,77), Mg (2,54), Al (3,15), Si (5,73), S (1,53), Cl (2,64), K (1,11), Ca (76,51), Fe (3,02)	Gypsum, Calcite, Calcium Oxalate
<i>Panel 3</i>						
P3B_2 cs	Sailor's beret	Dark blue	Dark blue layer (39-104 μm) over mortar	E700: Al, Ba, Ca, Cl, Cr, Cu, Fe, K, Na, Ni, P, Pb, S, Si, Sr, Ti	Grains: CaCo_3 Layer of pigment: Na (3,96), Al (29,09), Si (25,82), S (3,47), K (2,71), Ca (32,67), Fe (2,27) Mortar: Na (2,01), Mg (0,83), Al (0,73), Si (0,78), S (0,79), Cl (1,40), Ca (93,46)	/
P3B_5	Sailor's hair (salts)	Black	/	Area was too degraded for EDXRF	C (3,74), O (56,84) Na (20,23), Al (0,21), Si (0,19), S (10,59), K (1,67), Ca (0,53)	/
P3B_6	Ribbon (salts)	Black	/	Area was too degraded for EDXRF	C (2,97), O (59,66), Na (22,63), Si (0,13), S (12,02), K (1,27), Ca (1,32)	/
<i>Panel 6</i>						
P6A_2	Background (salts)	Green	/	E361: Al, Ba, Ca, Cl, Co, Cu, Fe, K, Mg, Mn, Ni, Pb, S, Si, Sr, Ti, Zn	C (8,40), O (57,73), Na (17,32), Si (0,25), S (11,21), K (1,24), Ca (3,86)	/
P6A_3	Background (salts)	Green	/	E361: Al, Ba, Ca, Cl, Cu, Fe, K,	C (20,80), O (59,66), Na (0,66), Mg (0,43), Al (0,58), Si (0,78), S	/

				Mg, Mn, Ni, Pb, S, Si, Sr, Ti	(2,99), K (0,38), Ca (4,45), Ti (5,98), Fe (3,28)	
P6A_3 cs	Background	Green	White pigment layer (10 – 23 µm) framing the matrix	E361: Al, Ba, Ca, Cl, Cu, Fe, K, Mg, Mn, Ni, Pb, S, Si, Sr, Ti	White layer: Na (2,78), Mg (1,87), Al (1,99), Si (2,49), S (1,15), Cl (1,48), K (0,93), Ca (12,51), Ti (71,72), Cr (0,79), Fe (2,28) Matrix: Na (3,00), Mg (14,02), Al (1,68), Si (16,57), S (3,20), Cl (3,00), K (3,11), Ca (55,42)	/
P6A_6rep	Shoulder sleeve	Red	Sample of red pigment	Similar as E433: Al, Ba, Ca, Cd, Cl, Co, Cr, Cu, Fe, K, Ni, P, S, Si, Sr, Ti	Na (0,43), Al (0,17), Si (0,39), S (6,89), Cl (0,18), K (3,21), Ca (7,99), Ti (0,32), Fe (0,61)	Aluminum silicates, Calcite, Gypsum, Calcium Oxalate, Barite
P6A_7	Shoulder sleeve (salts)	Blue	/	E365/66/67: Al, Ba, Ca, Cl, Cr, Cu, Fe, K, Ni, Pb, S, Si, Sr, Ti	C (17,16), O (58,87), Na (0,17), Al (0,09), Si (0,23), S (6,79), K (7,23), Ca (9,45)	/
P6A_7 cs	Shoulder sleeve	Blue	Blue pigment layer (10-61 µm), intonaco and arriccio.	E365/66/67: Al, Ba, Ca, Cl, Cr, Cu, Fe, K, Ni, Pb, S, Si, Sr, Ti	Blue layer: Na (13,30), Mg (0,68), Al (14,36), Si (16,19), P (0,80), S (26,51), K (1,91), Ca (26,25)	/
P6A_10 cs	Grey green with moist	Grey green	Layer of green pigment over mortar	E380: Al, Ba, Ca, Cl, Cu, Fe, K, Mg, Mn, Ni, Pb, S, Si, Sr, Ti, Zn	Mg (0,29), Al (0,77), Si (2,43), S (37,68), K (1,51), Ca (55,96), Fe (1,36)	Calcite, Gypsum, Calcium Oxalate, Barite
P6A_14	Boat (salts)	Green	/	E412: Al, Ba, Ca, Cu, Fe, K, Mn, Ni, Pb, S, Si, Sr, Zn, As	C (33,73), O (40,87), Na (16,32), Si (0,07), S (6,82), Ca (1,00), Ba (1,19)	Gypsum, Calcite, Calcium Oxalate, Barite
P6A_14 cs	Boat	Green	Layer of green pigment (73-277 µm)	E412: Al, Ba, Ca, Cu, Fe, K, Mn, Ni, S, Si, Sr, Zn, As	Na (1,83), Al (2,51), S (36,49), Cl (1,79), K (0,64), Ca (17,35), Fe (3,10), As (2,80), Sr (2,79), Ba (30,68)	Gypsum, Calcite, Calcium Oxalate, Barite
P6A_15	Boat (salts)	Green	/	E415: Al, Ba, Ca, Cu, Fe, K, Mn, Ni, S, Si, Sr, Zn, As	C (24,41), O (50,80), Na (8,30), Mg (0,60), Al (0,68), S (8,33), Ca (0,61), Sr (0,61), Ba (5,65)	/
P6A_17 cs	Sleeve	Brownish red	Layer of red pigment over layer of black pigment	E427: Ba, Ca, Cl, Co, Cr, Cu, Fe, K, Ni, S, Si, Sr, Ti, Zn	Red layer: Na (2,21), Mg (1,17), Al (2,69), Si (2,95), S (30,80), K (1,03), Ca (54,73), Fe (4,43) Black layer: Na (2,34), Mg (0,93), Al (0,93), Si (0,67), P (2,47), S (3,99), Cl (1,57), Ca (87,10)	Gypsum, Calcite, Bone black
P6A_18	Sleeve (salts)	Brownish red	/	E426: Ba, Ca, Cl, Co, Cr, Cu, Fe, K, Ni, S, Si, Sr, Ti, Zn	C (6,41), O (53,98), Na (16,90), Al (0,18), Si (0,38), S (5,49), Ca (6,09), Fe (0,58)	/
P6A_20 cs	Arm	Brown	Layer of red over the layer of black	Similar as E433: Al, Ba, Ca, Cd, Cl, Cr, Cu, Fe, K, Ni, P, S, Si, Sr, Ti	Red layer: Na (4,73), Mg (2,87), Al (3,95), Si (1,70), S (9,42), Cl (2,87), Ca (64,60), Fe (9,86) Dark layer: Na (1,96), Mg (0,95), Al (0,79), Si (0,68), S (12,74), Cl	Gypsum, Calcium Oxalate

					(2,33), K (0,83), Ca (79,71)	
P6A_23 cs	Background	Green	/	E478: Al, Ba, Ca, Cl, Cu, Fe, K, Mg, Mn, Ni, Pb, S, Si, Sr, Ti, Zn	Mg (10,24), Al (8,57), Si (16,87), S (5,16), Cl (1,16), K (0,59), Ca (4,95), Fe (50,15), Ba (2,31)	Gypsum, Calcite, Calcium Oxalate, Vinyl Polymer
P6C_2 cs	Brownish rope	White/brownish area	Layer of white (19-38 µm) over the layer of orange	E527: Ba, Ca, Cl, Co, Cr, Cu, Fe, K, Mn, I, Pb, S, Si, Sr, Ti, Zn	White layer: Na (3,14), Mg (2,18), Al (3,19), Si (3,07), P (0,75), S (2,46), Cl (0,94), Ca (7,95), Ti (71,72), Fe (2,59), Cd (2,00) Layer of orange: Na (3,65), Mg (3,27), Al (15,47), Si (27,52), P (1,68), S (4,34), Cl (1,62), Ca (16,83), Fe (20,93), Cd (2,62)	Aluminum Silicates, Kaolinite, Gypsum, Calcite, Calcium Oxalate
P6C_4	Greenish blue/yellow	Greenish blue/yellow	/	E527: Ba, Ca, Cl, Cr, Cu, Fe, K, Mn, I, Pb, S, Si, Sr, Ti, Zn	C (38,63), O (51,95), Na (0,40), Mg (0,38), Al (0,32), S (1,74), Cl (0,08), Ca (6,26), Fe (0,25)	Gypsum, Calcite, Oxalate, Vinyl Polymer
P6C_5	Greenish blue	Greenish blue	/	E527: Ba, Ca, Cl, Co, Cr, Cu, Fe, K, Mn, I, Pb, S, Si, Sr, Ti, Zn	C (22,2), O (57,57), Na (0,43), Al (0,17), Si (0,39), S (6,69), K (3,21), Ca (7,99), Ti (0,32), Fe (0,6)	Gypsum, Calcite, Calcium Oxalate, Vinyl Polymer
P6C_5 cs	Greenish blue	Greenish blue	Layer of greenish bleu pigment	E527: Ba, Ca, Cl, Co, Cr, Cu, Fe, K, Mn, I, Pb, S, Si, Sr, Ti, Zn	Mg (2,55), Al (2,12), Si (4,83), S (32,02), Ca (55,79), Fe (2,69)	Gypsum, Calcite, Calcium Oxalate, Vinyl Polymer

CIE a^*b^* plot graph representing colour hues is quite homogenous for the areas analysed on the three murals (Figure 33a). This indicates that the artist was using the same pigments in all of the murals and, therefore, the same palette of colour hues. Most used pigments in murals of Alcântara station are, in that same order of representation: red, green and blue shades. Warm colours are the most represented ones and they include red, brown and flesh hues, but also orange and yellow ones, although in lesser amount. When it comes to 'cold shades', it is important to point out the previously mentioned greenish paint layer is present in the backgrounds of panels and the Angel's garment of panel 2. Areas covered with this particular paint layer, seem to be the most complex ones as they cover hues from light blue and green, up to yellowish shades. This can be observed in the Figure 33 (b), as analysed colours vary between first and second coordinate quadrants of CIE a^*b^* chromatic palette.

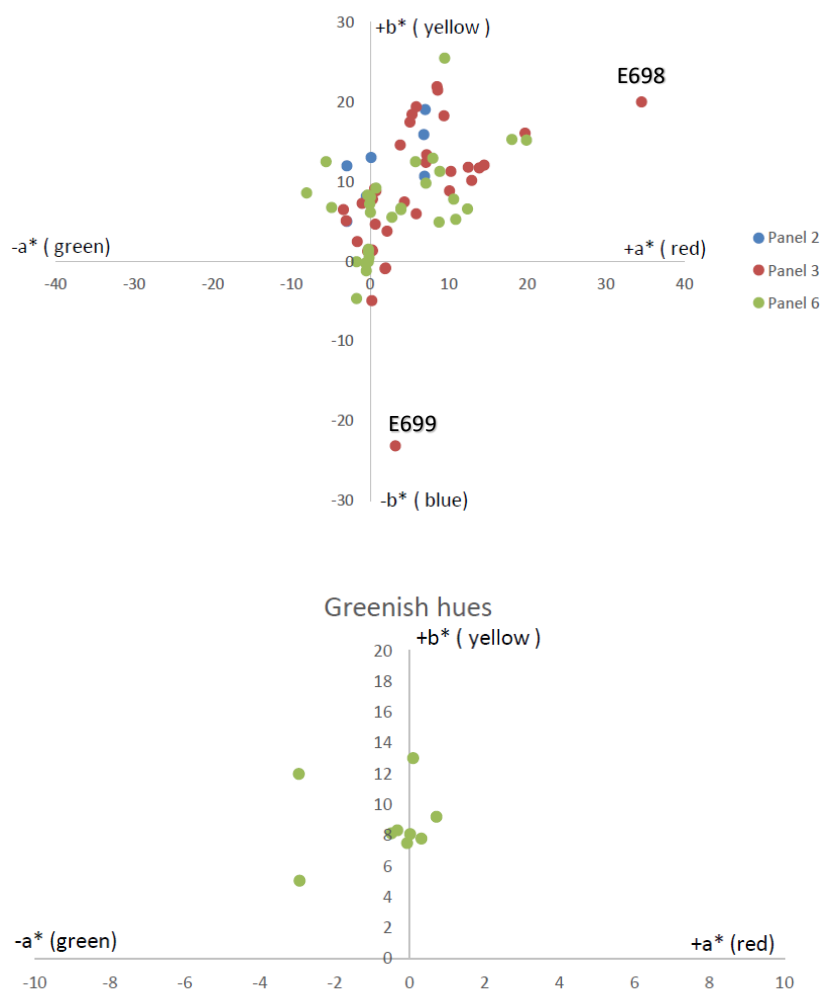


Figure 33. Up image (a): chromatic palette (CIE a^*b^*) off all hues of panels 2,3 and 6 showing the variety of colours and shades. Down image (b): chromatic palette (CIE a^*b^*) of Greenish hues showing the complexity of hues in the areas of this paint layer

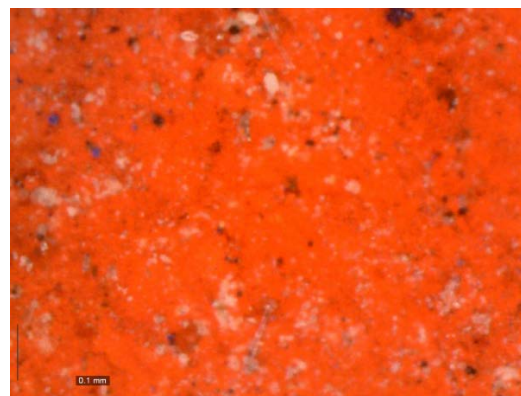
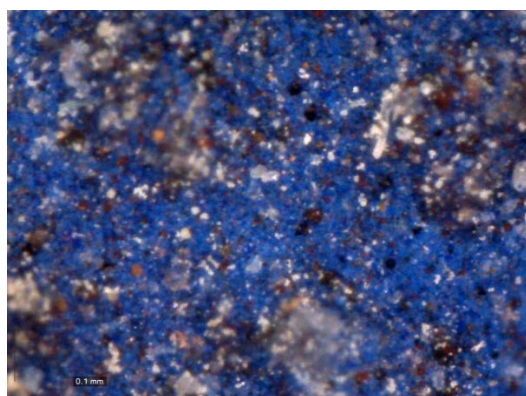


Figure 34. Portable optical microscope (p-OM) images of pigment particles from two specific paint layer in the panel 3. On the left, measurement E699, on the right, measurement E698

There are two measurements which hues seem to be out of the balanced group presented in the Fig. 33. These measurements, E689 and E699, are both coming from panel 3. Measurement E698 comes from the heavy red area behind one of the figures of the sailors, and measurement E699 is the heavy blue colour of sailor's beret (locations are presented in Appendix IV). As it is apparent, these areas are characteristic for their vibrant hues (Figure 34), that are distinguishable among all others, which are softer. For this reason, it was important to understand the chemical difference between these hues. Micro-samples were collected from these two paint layers for perform more analyses in the HERCULES laboratory. Sampling locations are presented in the Appendix VI.

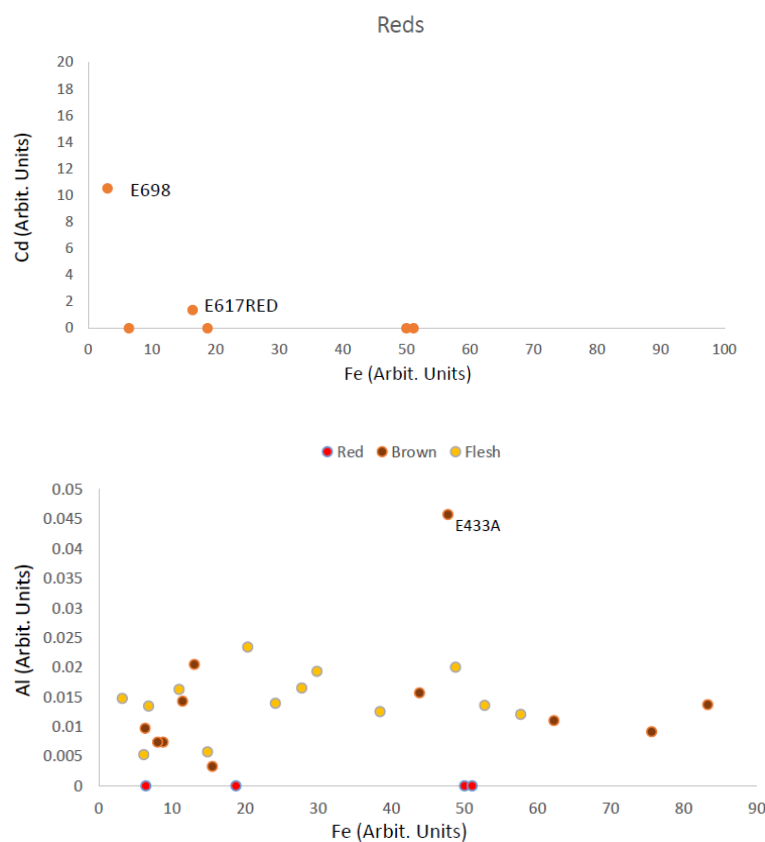


Figure 35. Graph (a) h-EDXRF plot of red hues, cadmium versus iron, graph (b) h-EDXRF plot of red, brown and flesh hues, aluminum versus iron



Figures 36 and 37. Area of sample E617RED, rose hue, panel 3 (on the left), area of the sample E698, vibrant red hue, panel 3 (on the right)

Handled X-ray fluorescence analyses of red, brown and flesh coloured hues, showed two types of reddish pigments. First group of point analyses seem to be enriched in iron and aluminium (Figure 35), which suggests the use of ochre-based pigments. The other one – a group of two samples from panel 3, E698 and E617RED, likely corresponds to the use of artificial cadmium pigments (Figure 35). However, it is important to note that the measurement E698 appears to have a higher amount of cadmium than measurement E617RED. Given the rose-coloured hue of measurement E617RED (Figures 36 and 37), it is possible that the cadmium pigment was mixed with lighter hue pigment in order to achieve the desired shade. One hypothesis is that E617RED might have been obtained with the mixture of cadmium and ochre pigments.

Furthermore, both green and blue hues seem to show the presence of cobalt, as displayed in the Figures 38 and 39. There are two h-EDXRF measurements that deviate from this pattern. These are the measurements E699 and E700 both coming from the heavy blue paint layer in the panel 3

Samples extracted from the greenish paint layer seem to have a rather homogeneous elemental pattern. This is quite interesting, given the complexity of this particular paint layer, considering the hue variations it includes. All h-EDXRF measurements show similar composition except for three of them indicated in the figure 43: E553, E554 and E55 (Figure 38). They come from the area of Angle's armour in panel 2, that shows mixture of green, blue and yellow shades. The show higher amounts of both iron and cobalt.

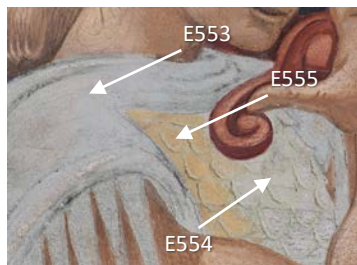


Figure 38. Location of samples E553, E554 and E555, Angel's armor, panel 2

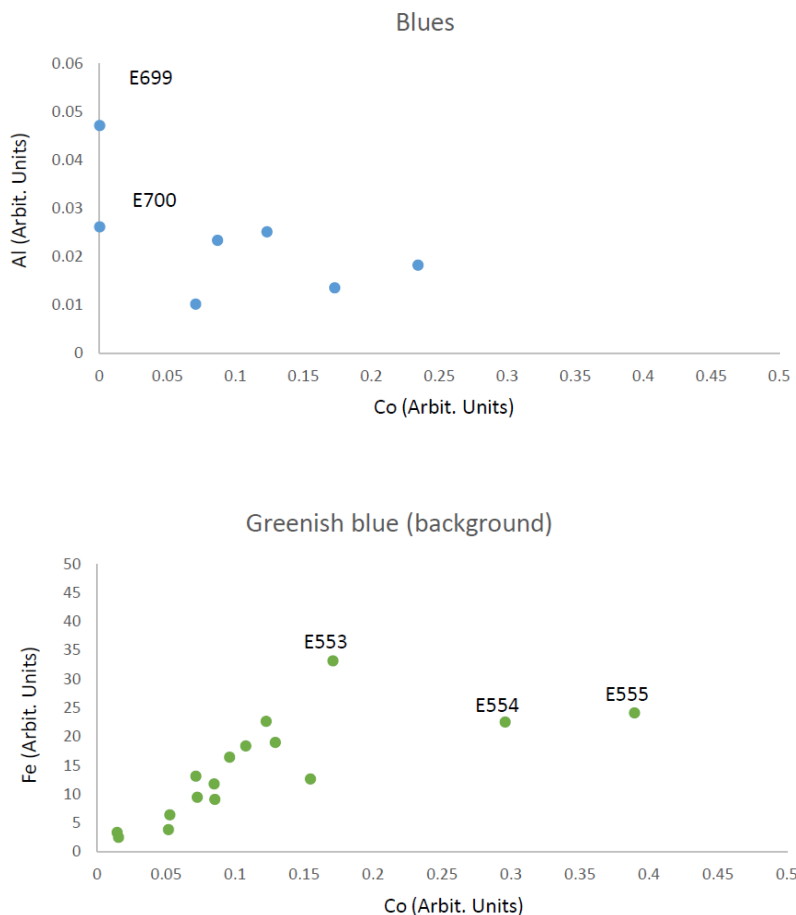


Figure 39. Graph(a): Handled EDXRF plot of blue hues (aluminium versus cobalt), graph(b) handled EDXRF plot of greenish hues (iron versus cobalt)

Twelve cross section samples from all three panels were subsequently analysed by SEM-EDS in the HERCULES laboratory. Analyses were done on samples P2_4 and P2_8 collected from the panel 2, sample P3B_2 collected from the panel 3 and samples P6A_3, P6A_7, P6A_10, P6A_14, P6A_17, P6A_20, P6A_23, P6C_2 and P6C_5 collected from the panel 6. The total sampling locations are presented in the Appendix V. Handled XRF, SEM-EDS and FT-IR analyses of selected cross section samples are presented in the Table 3.

Regarding the micro-samples collected from the greenish paint layer in the background of panel 6 and from the Angel's garment in panel 2 (samples P2_4, P6A_3, P6A_10, P6A_23 and P6C_5), SEM-EDS analyses revealed presence of iron, magnesium and aluminium (Table 3), which might indicate to the use of Green Earth, a natural pigment containing the minerals glauconite or celadonite, that was widely used in medieval painting as the under-layer for flesh colours [18]. These samples also showed presence of titanium, that could have been used to achieve the lighter shade (Figure 40). Another green hue was analysed within the sample P6A_14, coming from panel 6 as well. EDS analyses yet pointed out to another pigment – Emerald green, that was confirmed by presence of arsenic and copper previously identified with handled EDXRF (Table 3). This type of green, also known as Paris green is Copper acetoarsenite. It was introduced between 1800 and 1814 and has been available until recently [19]. Emerald green was very popular among French impressionists and post-impressionists [19], which might have influenced Almada during his time spent in Paris. This pigment was also confirmed by μ -FT-IR analyses, by characteristic bands at 1558, 145 818, 765, 640 cm^{-1} and main bands at 1558 and 640 cm^{-1} [20-21] (Figure 41).

Blue hues that were analysed, included micro-sample P3B_2 (Figure 42) coming from vibrant blue area in panel 3, and micro-sample P6A_7 that was extracted from the blue dress of one of the female figures in panel 6 (Appendix VI). These two colours seem to share same pigment, since SEM-EDS analyses revealed considerable amounts of sodium, aluminium and sulphur in both of the samples, indicating synthetic Ultramarine blue (Table 3) [22]. The essential elements for its synthesis are sodium, aluminum, sulfur and silicon, and the raw materials for manufacture include carbonates, china clay, quartz and sulphur [22]. The artificial pigment has rounded particles with regular size and shape, and this is how it is distinguished from the natural one which is coarse [22] (please see chapter 2.3.) Micro-sample P3B_2 also shows presence of phosphorus (Table 3), that might indicate that the artist was mixing ultramarine blue with bone black in order to achieve darker hues. Bone Black was confirmed in micro-samples P3B_2 and P6A_17 by μ -FT-IR analyses. Confirmation was based on characteristic sharp band around

2014 cm^{-1} (please see Appendix XII).

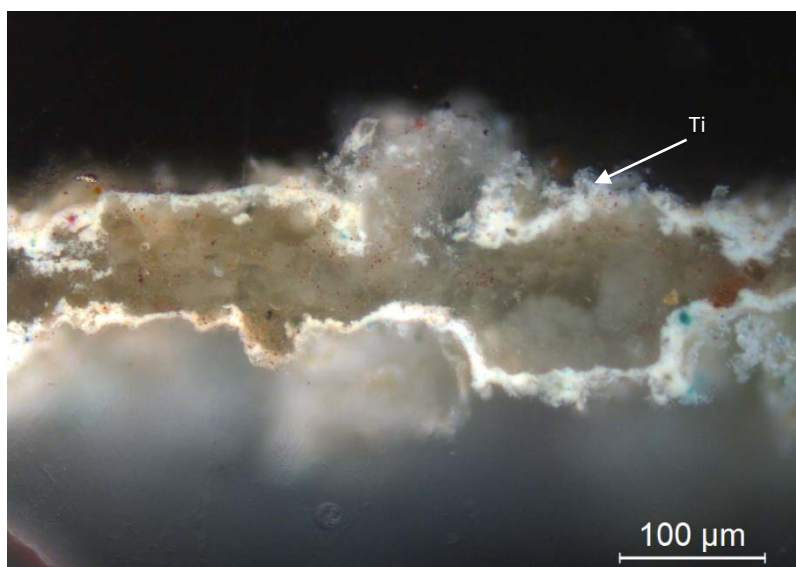


Figure 40. Microscope image of sample P6A_3 in magnification 200x. White layer covering the edges is titanium based which is identified by SEM-EDS analyses

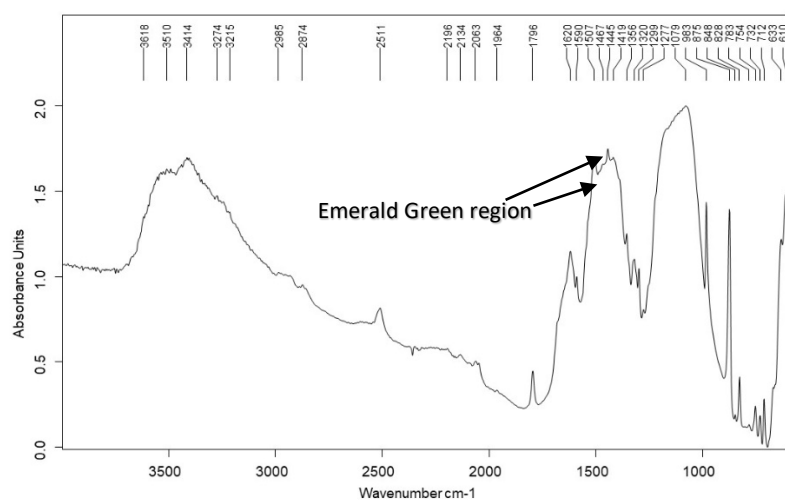


Figure 41. μ -FT-IR spectra of sample P6A_14, with indication of Emerald Green characteristic band

The painting method used by Almada was probably the same for both pigments, as they might have been mixed with bone black to achieve darker hue – in the case of micro-sample P3B_2 a shade of blue, and in the case of P6A_17 a shade of red. In the micro-sample P3B_2 it is possible to identify the painting technique as fresco since there is an absence of carbonization crust in the interface of the paint layer with the underneath mortar substrate (Figures 42 and 43). By the thickness of the blue paint layer it can be deduced that Almada mixed the pigments with the lime before applying them onto the fresh mortar. In this technique, known as *lime-fresco*, pigment-bearing layer is thicker than in *buon fresco* technique [23].

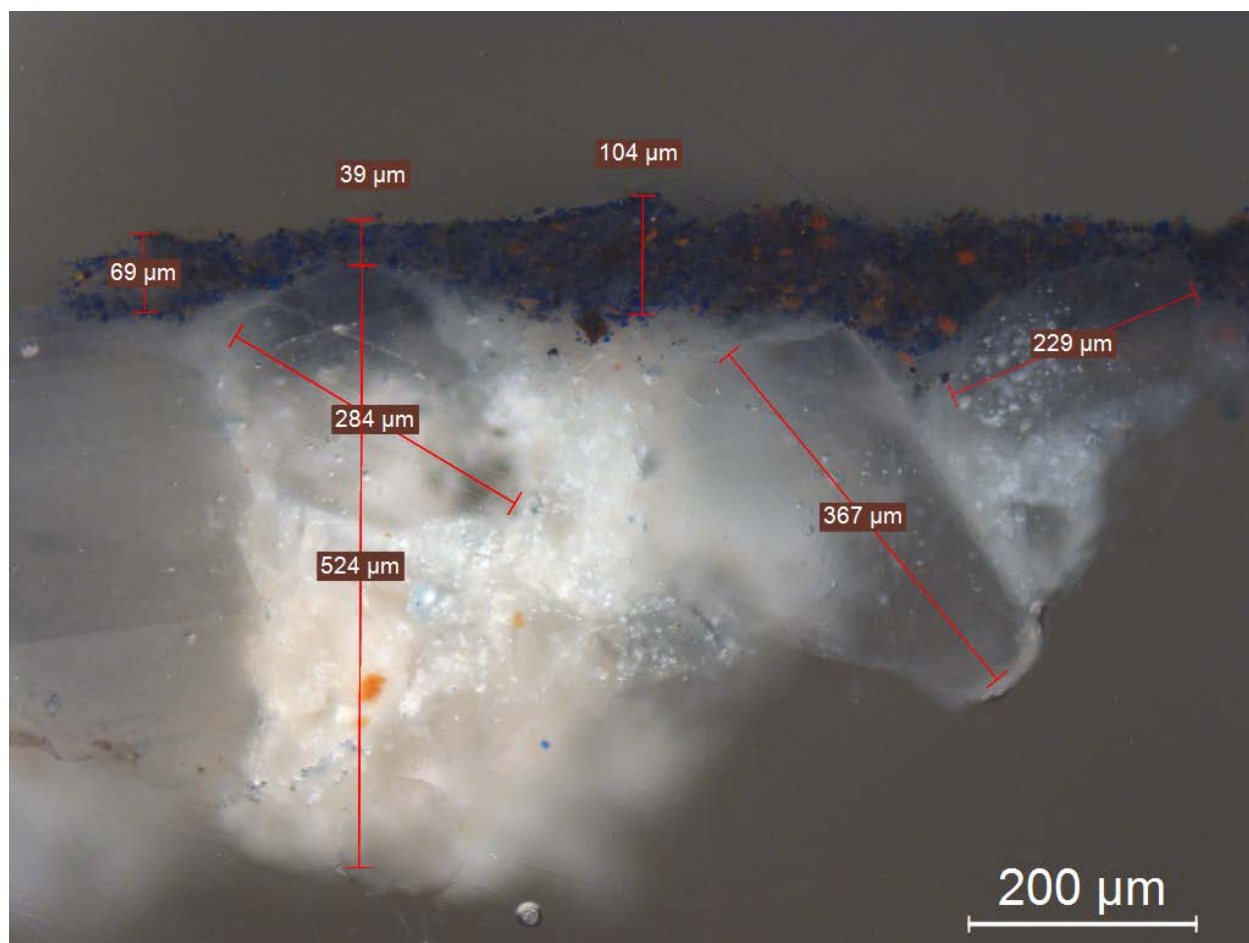


Figure 42. Microscope image of sample P3B_2 in magnification 100x showing admixture of pigments' particles in the paint layer and a lower layer of intonaco with large grains of aggregate identified as CaCO_3 by SEM-EDS

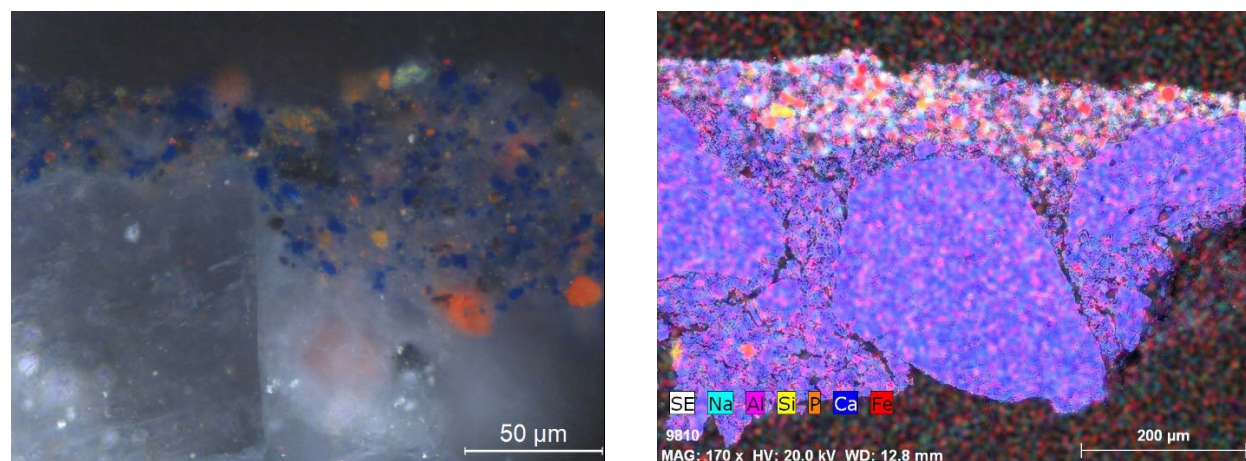


Figure 43. On the left: microscope image of sample P3B_2 in magnification 500x, on the right: SEM-EDS image of the elemental distribution of sodium, aluminum, silicon, phosphorous, calcium and iron, magnification 170x

Cross sections of reddish hues from micro- samples P6A_17 and P6A_20 were collected from panel 6. First one comes from the previously mentioned area of red dress of one of the female figures, while the other is taken from the edge of

lacuna of the reddish layer in the arm of the same figure (micro-sampling locations in the Appendix VI). As SEM-EDS and handled EDXRF analyses revealed, both pigments seem to be iron based (Table 3). SEM-EDS analyses of these samples revealed the presence of aluminium and silicates, which were confirmed by characteristic bands at 780cm^{-1} appearing in $\mu\text{-FT-IR}$ spectra. Aluminium silicates, or more precisely Kaolinite $\text{Al}_2(\text{OH})_4\text{Si}_2\text{O}_5$ are often found in French ochres, sometimes along with illite and quartz [24]. This suggests the use of ochres, natural earth colorants widely used as artist pigments. Their colour comes from iron oxides such as hematite $\alpha\text{-Fe}_2\text{O}_3$ and goethite $\text{FeO}(\text{OH})$ [23]. When the hematite is the main iron oxide, pigment has red colour, and the goethite dominates, pigment has yellowish colour [26].

Another warm shade micro-sample was analysed, collected from panel 6 as well. Micro-sample P6C_2 comes from the area of the rope painted in brown, yellow and white hues (Figure 44). Handled X-ray fluorescence analyses pointed out that the yellowish brown hue might be Iron based, and SEM-EDS analyses showed a considerable amount of cadmium (Table 3). This information suggests that red ochres, previously identified in red shades are also present here, were mixed with cadmium based pigments in order to achieve a desired hue. In this case, based on the colour, this pigment might be Cadmium red ($\text{CdS} + \text{CdSe}$), introduced in the 19th century [18]. This hypothesis should be studied further, since no Se was identified by SEM-EDS analyses.

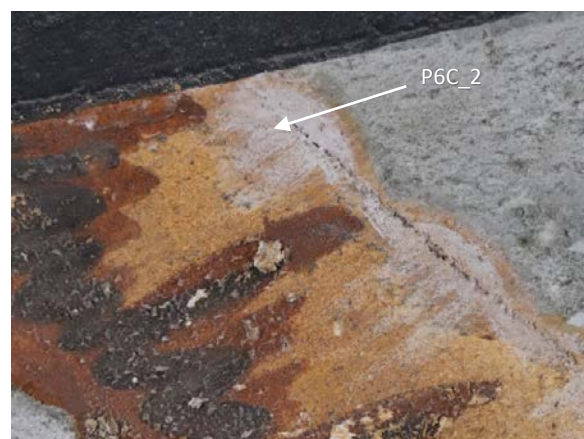


Figure 44. Area of the rope in panel 6 with marked extraction point of sample P6C_2

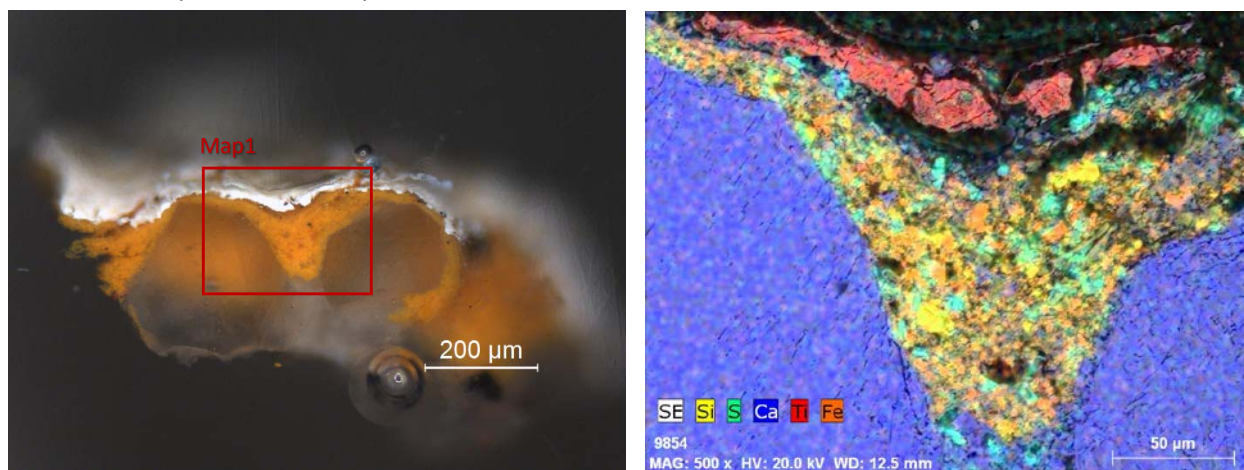


Figure 45. On the left: Microscope image of sample P6C_2 in magnification 100x with representation of paint layers and marked area of the Map, on the right: SEM image – Map1 in backscattering more in magnification 500x with representation of distribution of chemical elements within painting layers

As it is evident in the optical microscope image of the sample in magnification 100x (Figure 45-left), the brownish shade is covered with a thinner, white paint layer. SEM-EDS analyses revealed that this coat is Titanium based (Figure 45-right). Titanium oxide (TiO_2) white pigments were introduced in 20th century, and they rapidly replaced the traditional white pigments [19]. They are synthetic products, and can be manufactured either as pure titanium dioxide or with a base of barium or calcium sulphate into which a coating of titanium dioxide has been precipitated [19].

Further examination was done using μ -FT-IR and py-GC-MS of some samples (Appendices XII-XIII). Micro-samples were collected from paint layers of panels 2 and 6 that suggested the presence of organic materials in the means of binders used the artist, or treatment materials used by conservators (Table 4). μ -FT-IR analyses of the samples P2_2 and P2_5 from the greenish paint layer in panel 2, and samples P6A_23, P6A_24, P6C_4 and P6C_5 coming from the same paint layer in panel 6, all showed presence of vinyl polymer when analysed by μ -FT-IR. Samples P6A_17 and P6C_1a coming from reddish paint layers in the panel 6 displayed characteristic vibration in the area of 1700cm^{-1} that might indicate the presence of organic compounds (please see Appendix XI). Polymer was identified by characteristic bands at $2939, 1735, 1572, 1430, 1374, 1250, 942, 848, 797, 608\text{ cm}^{-1}$ and main bands at 1735 and 1250 cm^{-1} (Figure 46).

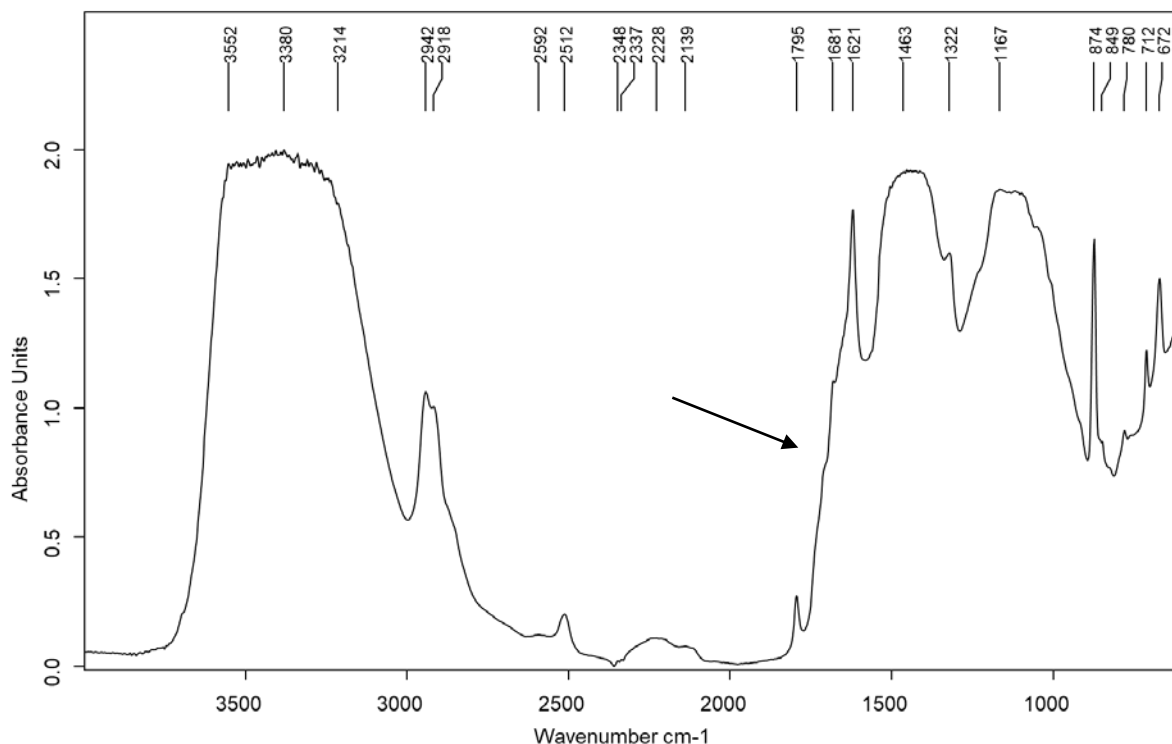


Figure 46. FT-IR spectra of the sample P6C_4 extracted from the greenish background in the panel 6. Characteristic band at 1735cm^{-1} is corresponded to vinyl polymer

Samples that showed possible presence of organic compounds were analysed further by py-GC-MS. Eight pyrolyzed samples from panels 2 and 6 displayed appearance of compounds of vinyl and aromatic origin such as styrene, fluorine, indene, naphthalene, toluene, or additives, in this case plasticizers. No sign of the use of any binder was detected on the samples. Results are displayed in Table 4 below.

Aromatic compounds with fused benzene rings such as Indene or Naphthalene, may origin from the layer of soot covering the paint layer [25]. They can form due to the different combustion processes and can arise from traffic, biomass combustion and charcoal soot [25].

Calcium oxalates identified by FT-IR analyses (Table 3), may originate from lichen or algal activity [26], but since no such activity was found on the analysed samples other possibilities should be considered in the further analyses as well, such as reaction of calcium monoxide from the air with calcium carbonate from the painting surface [26].

Table 4. Compounds identified by py-GC-MS analyses in eight samples from panels 3 and 6

RT (min)	Compound	Sample							
		P2_4	P2_5	P2_7	P6A_6	P6A_17	P6A_23	P6C_1a	P6C_5
1.55	Phthalic anhydride	♦							
1.90	PVA hexadienal	♦					♦	♦	♦
5.23	Nonanal	♦							
4.26	Phenolics: phenol and phenol-3-methyl	♦			♦		♦	♦	
4.85									
4.39	Benzonitrile	♦							
9.70	Plasticizers: phthalates, dibutyl and diethyl phthalate	♦		♦		♦			
6.02	Fluorene	♦							♦
2.81	Toulene						♦		♦
3.67	Styrene		♦	♦	♦	♦	♦	♦	
4.03	Alpha-methylstyrene							♦	
17.57	Styrene trimer	♦	♦	♦	♦	♦			♦
3.41	Ethylbenzene		♦	♦					
1.56	Epoxy activator: methylamine, N, N-dimehyl		♦						
5.26	Benzolc acid				♦	♦			
4.19	Benzaldehyde				♦	♦	♦	♦	♦
5.02	O-xylene						♦		
4.70	Naphthalene						♦	♦	
4.91	Indene	♦					♦	♦	♦
5.04	Acetophenone						♦	♦	♦
4.50	Ether: benzofuran						♦	♦	
4.08	Benzene, cyclopropyl							♦	♦
3.37	Dimethyl sulphate					♦			

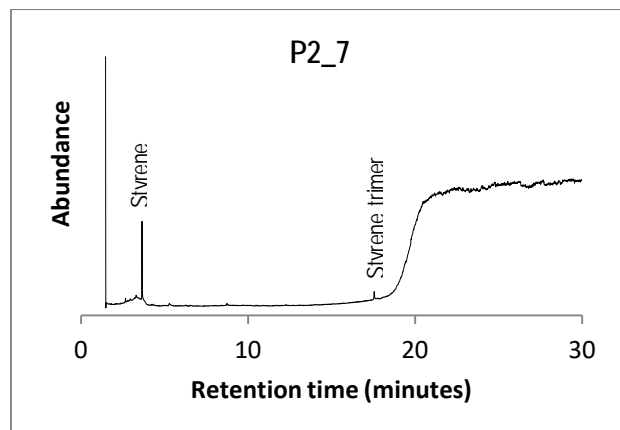


Figure 51. Py-GC-MS chromatogram of sample P2_7 with identified Styrene and Styrene trimer with characteristic molecular ions 91 and 104 m/z

Furthermore, the unpublished data on previous conservation work of panels from Gare Marítima de Alcântara, implied that the treatment of paintings included mixture of various compounds.

Many acrylic and vinyl compounds are used in art and art conservation field as binding media, paint additives or varnishes, coatings and consolidants [27-28]. Styrene identified by py-GC-MS analyses can thus be attributed to previous treatment, although this hypothesis cannot be confirmed with certainty, since there are no official records of the used material. Styrene was identified by intense molecular ion at 104 m/z and confirmed by Styrene trimer at molecular ion 91 m/z (Figure 51) [28].

The unpublished conservation reports Conservation Institute *José de Figueiredo (IJF)* suggested the treatment with various products including Calaton. This was confirmed by the personal communication with conservator. Calaton, also as 'soluble nylon', primarily used for consolidation of textiles, ivory or stone surfaces [29]. Nevertheless, despite the fact that soluble nylon has attributes such as elasticity and flexibility, it seems to lose them with time [29]. Materials such as stone or ivory, that have good pressure resistance, may not display serious changes as the consolidant changes with time. Unfortunately, lime based paintings materials are more likely to be prone to degradation by flaking as Calaton loses its elasticity, since the forces occurring can cause pressure to material itself. This seems to be probable phenomena affecting the greenish paint layer identified in all three studied murals.

List of references

- [1] P. Mora, Causes of deterioration of mural paintings, Rome: INTERNATIONAL CENTRE FOR THE STUDY OF THE PRESERVATION AND THE RESTORATION OF CULTURAL PROPERTY, 1974.
- [2] C. T. Grimm, "Masonry Cracks: A review of the Literature," in *Masonry: Materials. Design. Construction and Maintenance*, Philadelphia, American Society for Testing and Materials, 1988, pp. 257-280.
- [3] M. H. Hanafi, M. U. Umar, A. A. Razak, Z. Z. A. Rashid, N. Z. Noriman and O. S. Dahham, "An Introduction to Thermal Bridge Assessment and Mould Risk at Dampness Surface for Heritage Building," in *IOP International Conference on Materials Engineering and Science*, 2018.
- [4] D. Young, Salt attack and rising damp: A guide to salt damp in historic and older buildings, Heritage Council of NSW, Heritage Victoria, South Australian Department for Environment and Heritage, Adelaide City Council, 2008.
- [5] S. Pavia, "Sulfation of a decrepit Portland cement mortar and its adjacent masonry," in *SWBSS- Salt Weathering on Buildings and Stone Sculptures*, Copenhagen, Technical University of Denmark, 2008.
- [6] F. Zezza, "The E. C. Project "Marine spray and polluted atmosphere as factors of damage to monuments in the Mediterranean coastal environment": objectives and results," *Origin, Mechanisms and effects of salts on degradation of monuments in marine and continental environments* Protection and Conservation of the European Cultural Heritage Research Report n° 4, Bari, Italy, pp. 3-19, 1996.
- [7] M. El-Gohary, "Chemical deterioration of Egyptian limestone affected by saline water," *International Journal of Conservation Science*, vol. 2, no. 1, pp. 17-28, 2011.
- [8] M. El-Gohary, "Air Pollution and Aspects of Stone Degradation "Umayyed Liwân - Amman Citadel as a Case Study", " *Journal of Applied Science Research*, vol. 4, no. 6, pp. 669-682, 2008.
- [9] M. Marszałek, K. Dudek and A. Gawęł, "Cement Render and Mortar and Their Damages Due to Salt Crystallization in the Holy Trinity Church, Dominicans Monastery in Cracow, Poland," *Minerals*, vol. 10, no. 641, 2020.
- [10] F. Mees and M. De Dapper, "Vertical variations in bassanite distribution patterns in near-surface sediments, southern Egypt," *Sedimentary Geology*, no. 181, pp. 225-229, 2005.
- [11] H. M. Mahmoud, N. Kantiranis and J. Stratis, "Salt damage of the wall paintings of the Festival Temple of Thutmosis III, Karnak Temples Complex, Upper Egypt. A case study," *International Journal of Conservation Science*, vol. 1, no. 3, pp. 133-142, 2010.
- [12] L. A. Hardie, "The gypsum - anhydrite equilibrium at one atmosphere pressure," *The American Mineralogist*, vol. 52, 1967.

- [13] A. E. Charola and C. Bläuer, "Salts in Masonry: An Overview of the Problem," *Restoration of Buildings and Monuments*, pp. 119-135, 2015.
- [14] C. Figueiredo, C. Pimenta do Vale, M. R. Veiga, A. S. Silva, M. Vieira, A. Tavares and A. L. Velosa, "Natural cement in Portuguese heritage buildings," in *Materials for a better life*, Lisbon, 2019.
- [15] V. Matović, S. Erić, A. Kremenović, P. Colomban, D. Srečković-Batočanin and N. Matović, "The origin of syngenite in black crusts on the limestone monument King's Gate (Belgrade Fortress, Serbia) – the role of agriculture fertiliser," *Journal of Cultural Heritage*, 2011.
- [16] L. Lähteenmäki, *COMBINATIONS OF TITANIUM DIOXIDE AND FILLERS IN PAINTS*, Degree Programme in Chemical Engineering, 2009.
- [17] B. A. v. Driel, K. J. van den Berg, J. Gerretzen and J. Dik, "The white of the 20th century: an explorative survey into Dutch modern art collections," *Heritage Science*, vol. 6, no. 16, 2016.
- [18] Robert L. Feller, *Artists' Pigments: A Handbook of their History and Characteristics, Volume 1*, National Gallery of Art, Washington, Archetype Publications, London, 1986.
- [19] b. W. FitzHugh, *Artists' Pigments: A Handbook of Their History and Characteristics, Volume 3*, National Gallery of Art, Washington; Archetype Publications, London, 1997.
- [20] I. M. Cortea, L. Ghervase, L. Ratoiu, M. Dinu and R. Rădvan, "Uncovering hidden jewels: an investigation of the pictorial layers of an 18th-century Taskin harpsichord," *Heritage Science*, vol. 8, no. 55, 2020.
- [21] D. Buti, F. Rosi, B. G. Brunetti and C. Miliani, "In-situ identification of copper-based green pigments on paintings and manuscripts by reflection FTIR," *Analytical and Bioanalytical Chemistry*, no. 405, pp. 2699-2711, 2013.
- [22] A. Roy, *Artists' Pigments: A Handbook of Their History and Characteristics, Volume 2*, National Gallery of Art, Washington, Archetype Publications, London, 1993.
- [23] M. Gil, M. L. Carvalho, A. Seruya, A. E. Candeias, J. Mirao and I. Queralt, "Yellow and red ochre pigments from southern Portugal: Elemental composition and characterization by WDXRF and XRD," *Nuclear Instruments and Methods in Physics Research A*, no. 580, pp. 728-731, 2007.
- [24] D. Hradil, J. Hradilova and B. Hřebíčkova, "Clay minerals in pigments of mediaval and baroque paintings," *Geologica Carpathica*, vol. 53, no. 2, pp. 123-126, 2002.
- [25] J. Song and P. Peng, "Characterisation of black carbon materials by pyrolysis–gas chromatography–mass spectrometry," *Journal of Analytical and Applied Pyrolysis*, no. 87, pp. 129-137, 2010.
- [26] G. Chiari, N. Gabrielli, G. Torracca, "Calcium oxalates on mural paintings in internal exposure Sistine Chapel and others", II International Symposium The Oxalate films in the conservation of works of arts, p. 179-188, 1996
- [27] J. Peris-Vicente, U. Baumer, H. Stege, K. Lutzenberger and J. V. Gimeno Adelantado, "Characterization of Commercial Synthetic Resins by Pyrolysis-Gas Chromatography/Mass Spectrometry: Application to Modern Art and Conservation," *Analytical Chemistry*, vol. 81, p. 3180–3187, 2009.
- [28] P. Schossler, I. Fortes, J. Cura D'Ars de Figueiredo Júnior, F. Carazza and L. Antônio Cruz Souza, "Acrylic and Vinyl Resins Identification by Pyrolysis-Gas Chromatography/Mass Spectrometry: A Study of Cases in Modern Art Conservation," *Analytical Letters*, vol. 46, no. 12, pp. 1869-1884, 2013.
- [29] E. D. Witte, "SOLUBLE NYLON AS CONSOLIDATION AGENT FOR STONE," *Studies in Conservation*, vol. 20, no. 1, pp. 30-34, 1975.
- [30] R. Poulin, *Graphic Design + Architecture, A 20th century history*, Beverly: Rockport Publishers, 2012.

- [31] H. Foster, R. Krauss, Y.-A. Bois, B. h. Buchloh and D. Joselit, *Art Since 1900*, Third edition, London: Thames & Hudson Ltd, 2016.
- [32] L. Pereira-Pardo, B. Prieto and B. Silva, "Assessing the risk of salt decay for wall paintings in historic buildings, thermo-dynamic modelling and transition cycles count," *International Journal of Conservation Science*, vol. 8, no. 3, pp. 351-364, 2017.
- [33] S. Švarcová, P. Bezdička, D. Hradil, J. Hradilová and I. Žižak, "Clay pigment structure characterisation as a guide for provenance determination - a comparison between laboratory powder micro-XRD and synchrotron radiation XRD," *Analytical and Bioanalytical Chemistry*, no. 399, pp. 331-336, 2011.
- [34] K. Hu, C. Bai, L. Ma, K. Bai, D. Liu and B. Fan, "A study on the painting techniques and materials of the murals in the Five Northern Provinces' Assembly Hall, Ziyang, China," *Heritage Science*, vol. 1, no. 18, 2013.

Chapter V: Conclusion

Three panels of Alcântara Maritime Lisbon Station have been analysed *in-situ* and micro-samples have been collected from the areas of interest for more detailed analyses which took place in HERCULES laboratory in Évora, Portugal. The objective of the research was to identify the main decay phenomena and their dynamics, and to determine if there is a link to a specific pigment and what's the role of painting technique when it comes to stability and deterioration of the pigments.

It seems that the large deterioration areas appear in the region of architectural joints, e.g. connections of horizontal and vertical building elements and presence of installations (water or heating pipes). The most affected parts of the paintings seem to be aligned with floor construction of the building and installation system. The main decay phenomena include salts, with following efflorescence and sub-efflorescence, flaking, lacunae and possible chromatic changes. Salts that were identified are sulphates thenardite, gypsum, syngenite, aphthitalite and anhydrite. Their origin seems to be linked to polluted atmosphere and water infiltration into building materials, but they also can originate from architectural materials such as cement, or from sea spray or atmospheric water.

The majority of deterioration doesn't seem to be linked to a specific pigments or paint layer. It rather forms in the weak areas of the murals. Nevertheless, greenish paint layer, present in the background and in the Angel's garment, seems to deviate from this 'pattern'. This particular paint layer displayed presence of vinyl polymer when analysed by μ -FT-IR. Eight samples analysed by py-GC-MS displayed appearance of compounds of vinyl and aromatic origin such as styrene, fluorine, indene, naphthalene, toluene, or additives, in this case plasticizers. Aromatic compounds with fused benzene rings may form due to the different combustion processes or can be linked to traffic pollution. They can also origin from the layer of soot covering the paint layers.

Both natural and artificial pigments have been identified. Natural ochres have been used for warm hues, as well as artificial pigment cadmium red. Blues are composed of synthetic Ultramarine blue pigment, and green colours are painted using artificial pigment Emerald Green or natural one - Green Earth. To achieve certain lighter or darker hue, artist was mixing pigments with Titanium White or Bone Black.

Painting technique was confirmed to be *fresco*. No sign of the use of any binder was detected on the samples. Nevertheless, the possibility of some areas being painted *secco* is not yet excluded, and this matter is still to be examined in the future.

In conclusion, it is to be hoped that the analyses done within this thesis will contribute to the future conservation/restoration activities on the murals of Maritime Stations in Lisbon, and that they will find their use in conservation/restoration science at large.



Appendices

Table of contents

<i>Appendix I:</i> Photo-documentation.....	65
<i>Appendix II:</i> Display of deterioration features.....	74
<i>Appendix III:</i> Photo-documentation in UVF light.....	83
<i>Appendix IV:</i> Handled X-Ray Fluorescence Analyses, locations.....	84
<i>Appendix V:</i> Spectro-colorimetry measures, locations.....	89
<i>Appendix VI:</i> Micro-sampling locations.....	92
<i>Appendix VII:</i> Optical microscope images.....	99
<i>Appendix VIII:</i> μ -XRD Analyses.....	104
<i>Appendix IX:</i> SEM-EDS Analyses of powder samples.....	108
<i>Appendix X:</i> Combined analyses of cross-section samples.....	118
<i>Appendix XI:</i> Combined analyses of micro-fragments and powder samples.....	124
<i>Appendix XII:</i> μ -FT-IR Analyses.....	131
<i>Appendix XIII:</i> py-GC-MS Analyses.....	149
<i>Appendix XIV:</i> Combined Data.....	152
<i>Appendix V:</i> Presentation for the third ICP congress.....	155

Appendix I: Photo-documentation

Photo-documentation of the panels 2,3 and 6 taken in the late 1990s by APL Archival:



Photo-documentation of the panels 2,3 and 6 taken by José Vicente on the 16th of July 2013:



Photo-documentation of the panels 2,3 and 6 taken by Guta Carvalho on the 6th and 7th of June 2020:



Individual presentation of panel 1, areas that display deterioration are marked in white. Photograph is taken by Guta Carvalho (6-7th of June 2020 © all rights reserved):



Individual presentation of panel 1, areas that display deterioration are marked in white. Photograph is taken by Guta Carvalho (6-7th of June 2020 © all rights reserved):



Individual presentation of panel 3, areas that display deterioration are marked in white. Photograph is taken by Guta Carvalho (6-7th of June 2020 © all rights reserved):



Individual presentation of panel 4, areas that display deterioration are marked in white. Photograph is taken by Guta Carvalho (6-7th of June 2020 © all rights reserved):



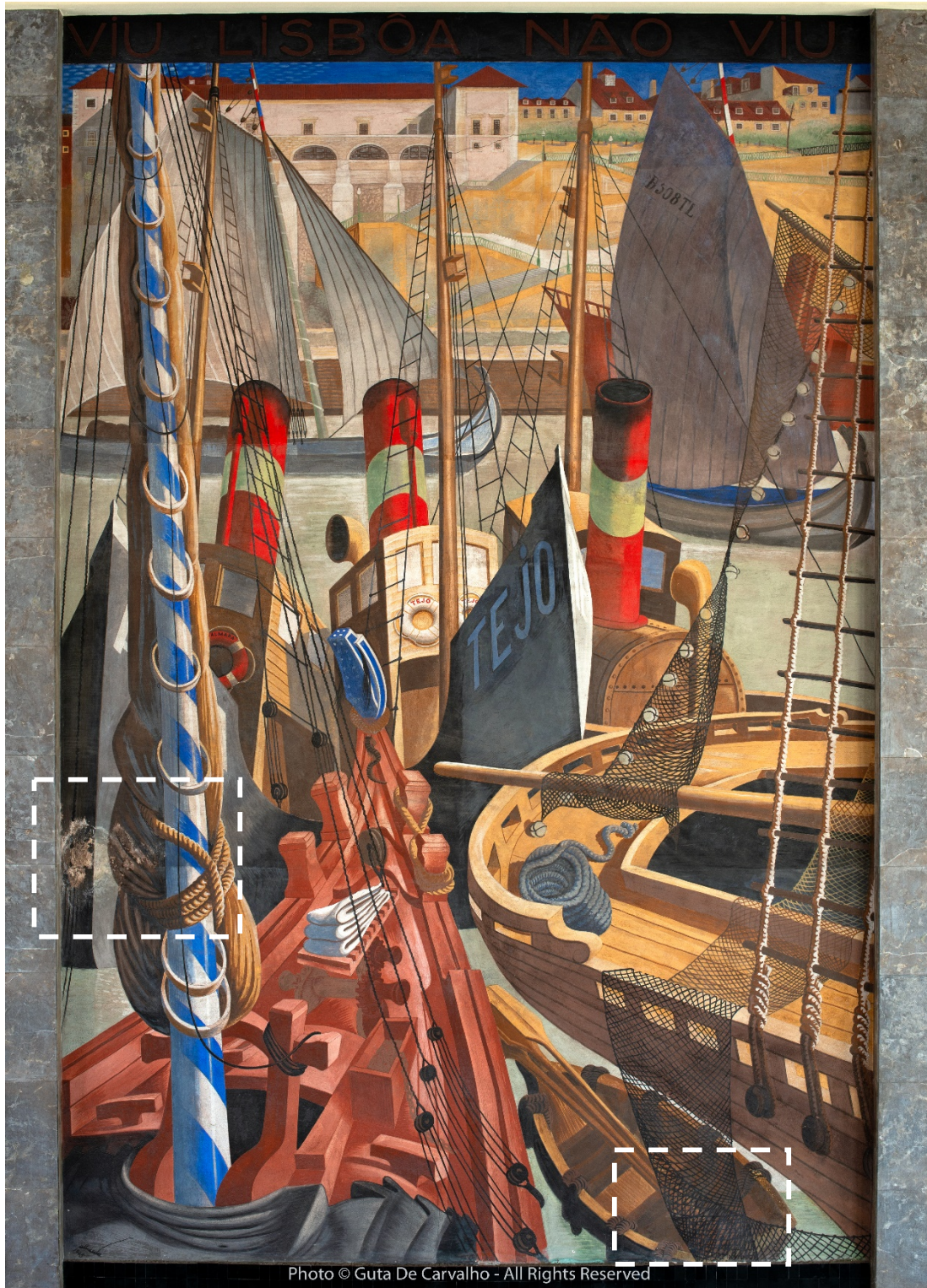
Individual presentation of panel 5, areas that display deterioration are marked in white. Photograph is taken by Guta Carvalho (6-7th of June 2020 © all rights reserved):



Individual presentation of panel 6, areas that display deterioration are marked in white. Photograph is taken by Guta Carvalho (6-7th of June 2020 © all rights reserved):



Individual presentation of panel 7, areas that display deterioration are marked in white. Photograph is taken by Guta Carvalho (6-7th of June 2020 © all rights reserved):

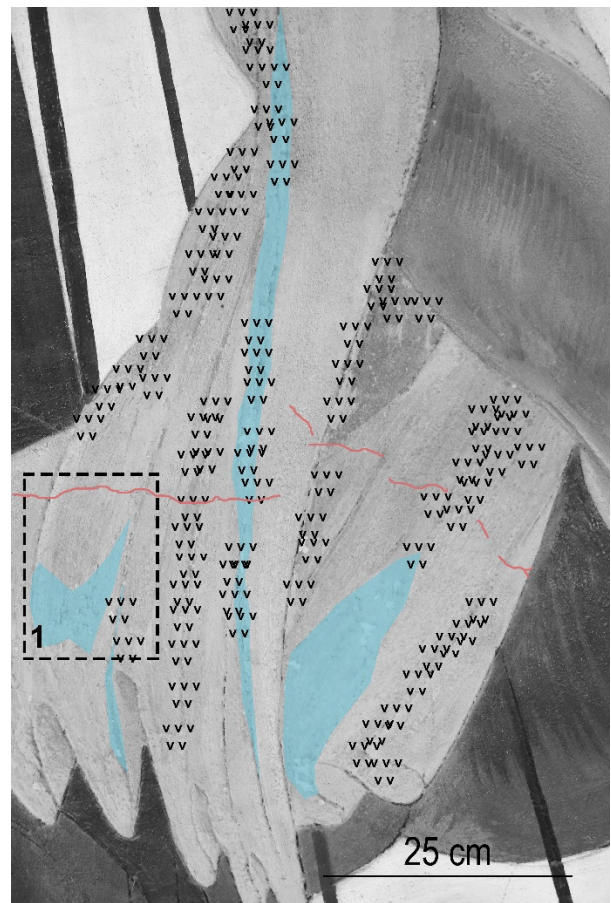
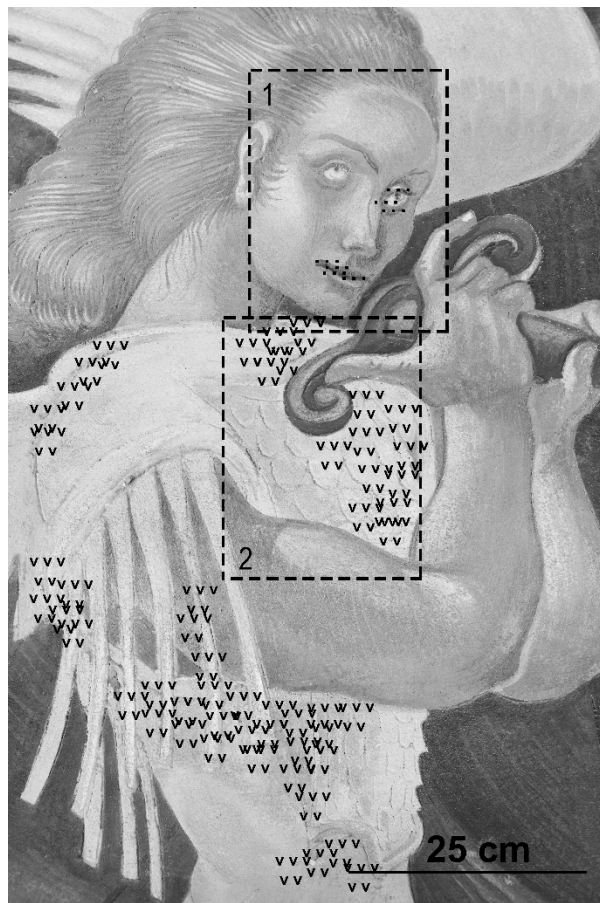






Individual presentation of panel 8, areas that display deterioration are marked in white. Photograph is taken by Guta Carvalho (6-7th of June 2020 © all rights reserved):

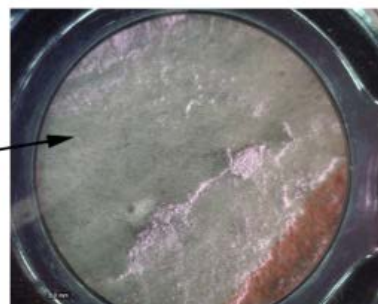


Appendix II: Display of deterioration features

Analysed zones of panel 2 with the display of deterioration features:

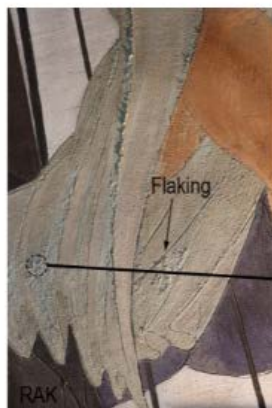


- | | |
|---|---------------------------|
| ▽▽▽
▽▽ | Flaking |
| ■ ■ ■ | Lack of cohesion |
| ▲▲▲
▲▲ | Salts' efflorescence |
| ≡ ≡ ≡ | Erosion |
|  | Fissure |
|  | Detachment of paint layer |
|  | Salts' veils |
|  | Lacunae |



Zone 1
Areas 1&2

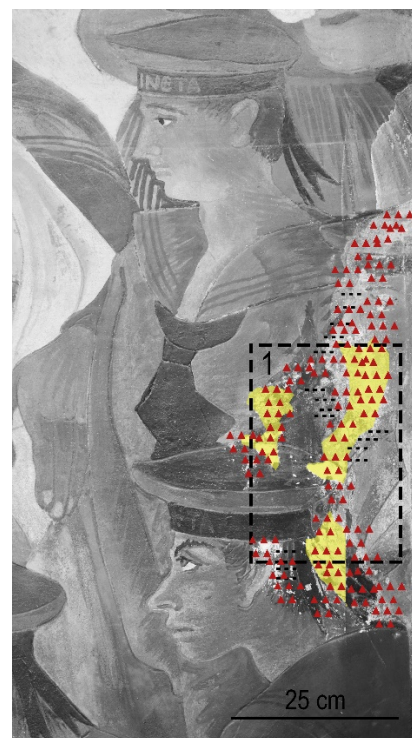
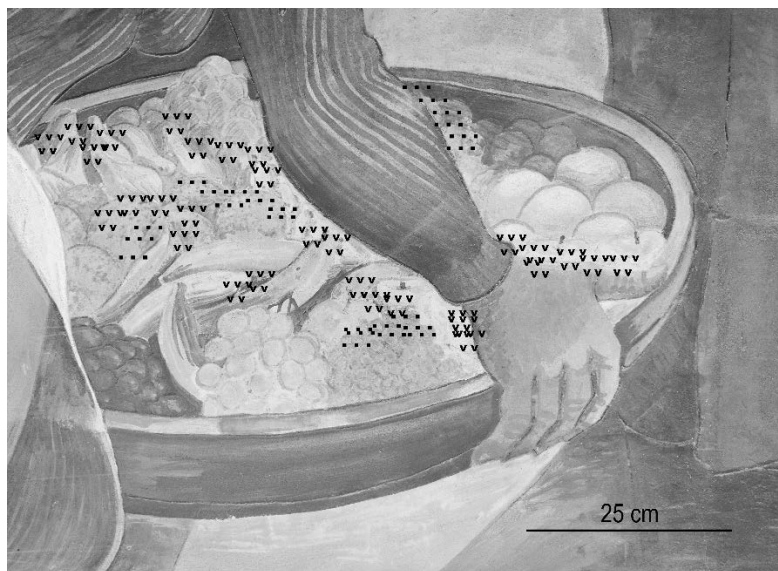
Portable optical microscope image E550
displaying lacuna of greenish paint layer
magnification 20x








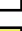


Zone 2

Portable optical microscope image E574
displaying formation of lacunae
magnification 20x

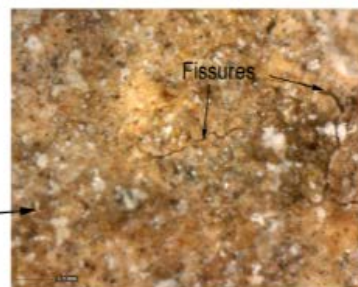
Analysed zones of panel 3 with the display of deterioration features:



- | | |
|---|---------------------------|
|  | Flaking |
|  | Lack of cohesion |
|  | Salts' efflorescence |
|  | Erosion |
|  | Fissure |
|  | Detachment of paint layer |
|  | Salts' veils |
|  | Lacunae |



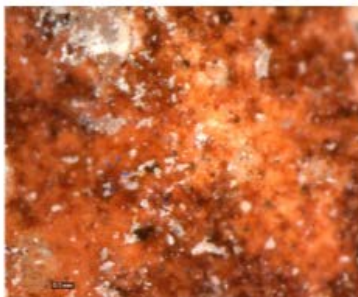
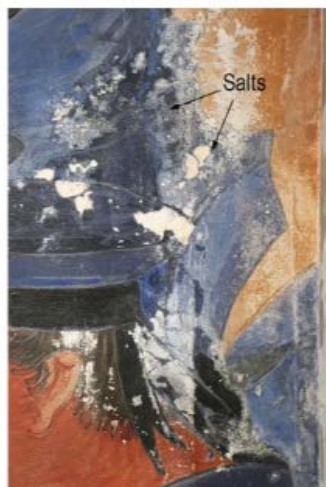
Zone 1



Portable optical microscope image E675 displaying brownish paint layer affected by the lack of cohesion and fissures, magnification 434x

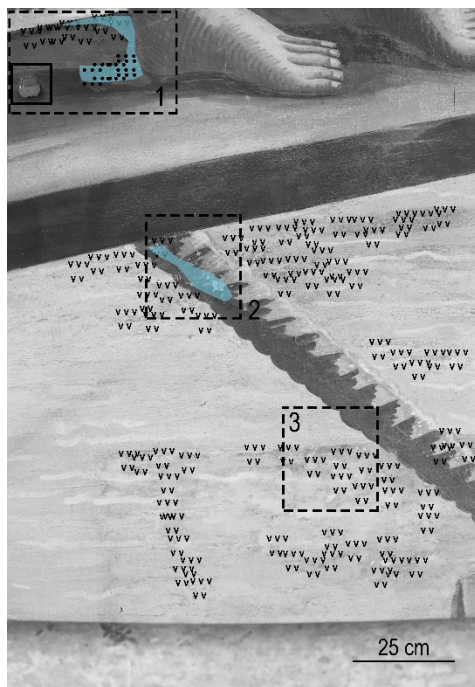


Zone 2



Portable optical microscope image E713 displaying brownish paint layer from the area of sailor's nose, affected by the lack of cohesion magnification 434x

Analysed zones of panel 6 with the display of deterioration features:

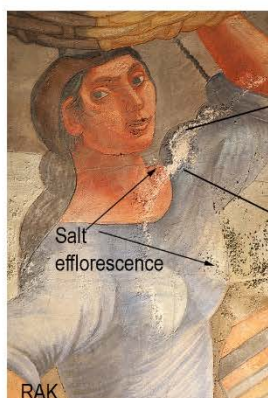


- | | |
|-------|---------------------------|
| v v v | Flaking |
| v v | |
| ... | Lack of cohesion |
| ▲ ▲ ▲ | Salts' efflorescence |
| ≡ ≡ ≡ | Erosion |
| — | Fissure |
| □ | Detachment of paint layer |
| ■ | Salts' veils |
| ■ | Lacunae |
| ■ | Possible moisture stains |



Portable optical microscope image E735 of greenish paintlayer in the background affected by flaking and salts, magnification 434x

Zone 1, Area 1



Portable optical microscope images E367 (on the left) and E365 (on the right) displaying different stages of salts' formation, magnification 20x

Zone 1, Area 2



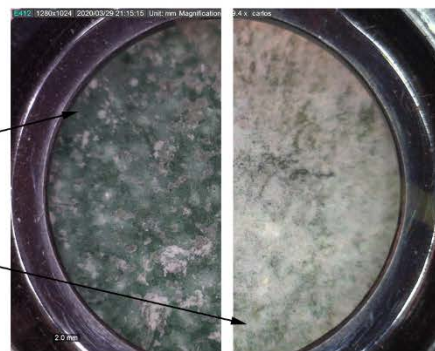
Portable optical microscope image E378 displaying green paint layer affected by salts' formation, magnification 20x

Zone 1
Areaa 3&4



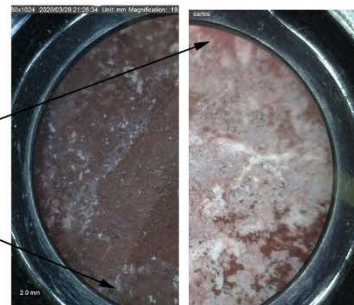
Portable optical microscope image E3418 displaying black paint layer affected by salts' efflorescence, magnification 20x

Zone 1, Area 5



Zone 1, Area 6

Portable optical microscope images E412 (left) and E415 (right) displaying different stages of salts' efflorescence magnification 20x



Zone 1
Areas 7&8

Portable optical microscope images E427 (left) and E426 (right) displaying different stages of salts' efflorescence, magnification 20x



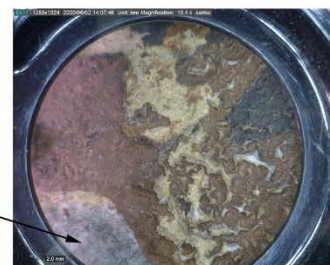
Zone 1, Area 9

Portable optical microscope image E450 displaying brownish paint layer affected by salts' efflorescence magnification 20x



Portable optical microscope image E496
displaying the flaking brownish paint layer
magnification 20x

Zone 2, Area 1



Portable optical microscope image E517
displaying the brownish paint layer affected
by lacunae, magnification 20x

Zone 2, Areas 2&3

Appendix III: Photo-documentation in ultraviolet light (UVF)

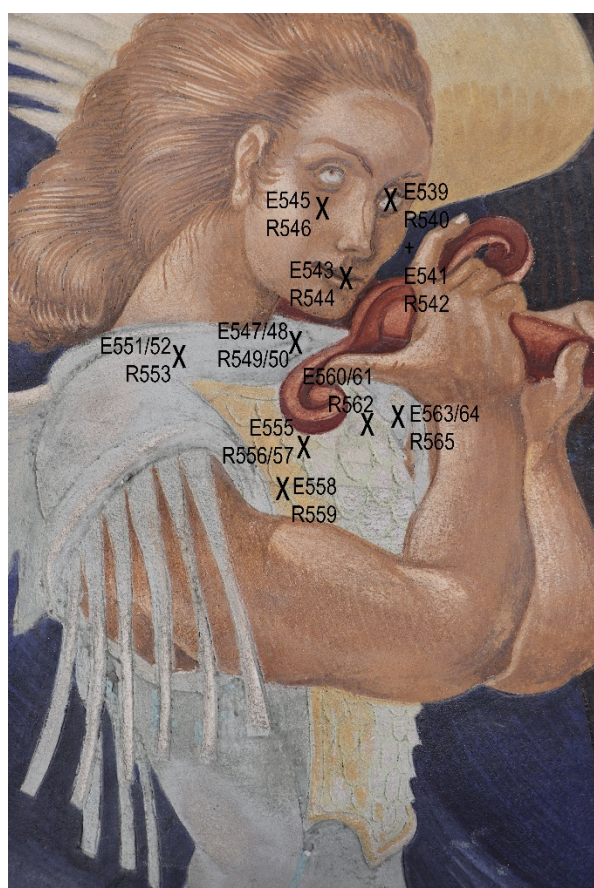
Photo-documentation in ultraviolet light (UVF), in following order:

Angel's garment from panel 2, two images of basket with fruits from panel 3 and area of the background in the panel 6:



Appendix IV: Handled X-Ray Fluorescence analyses

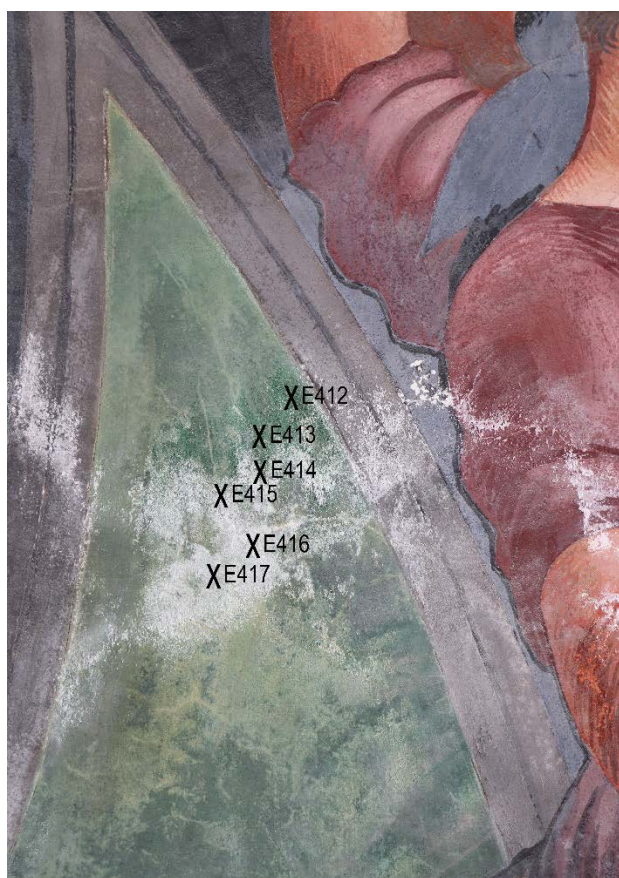
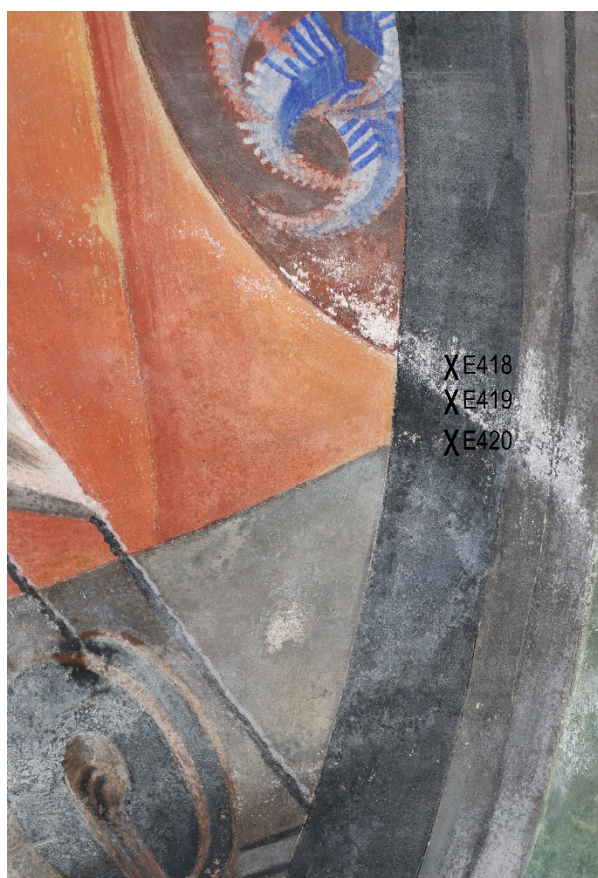
Locations of handled X-ray fluorescence analyses (h-EDXRF), panel 2:

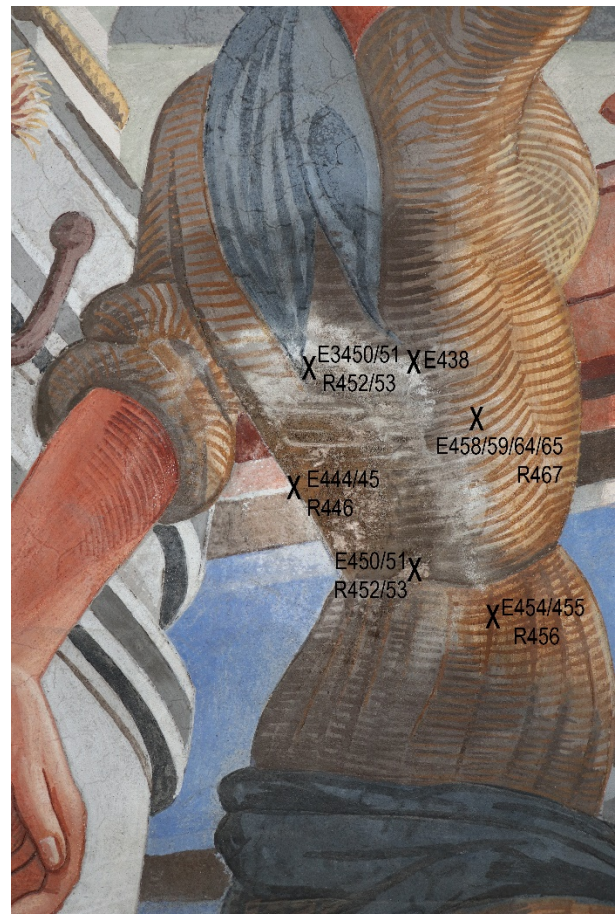
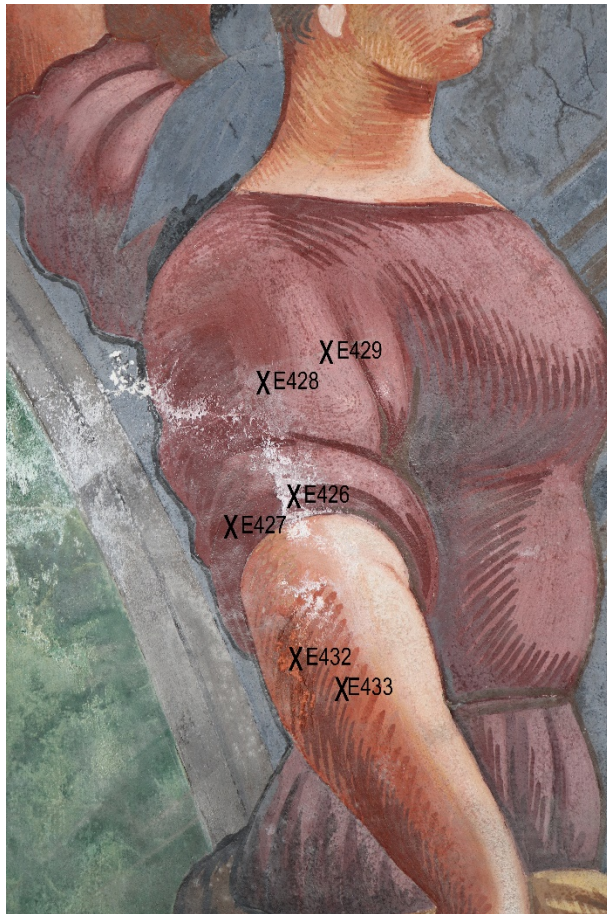


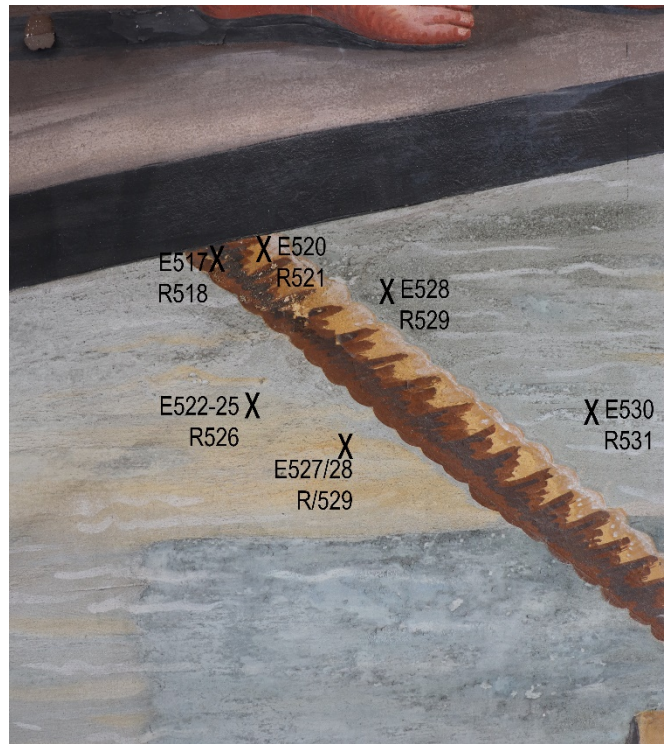
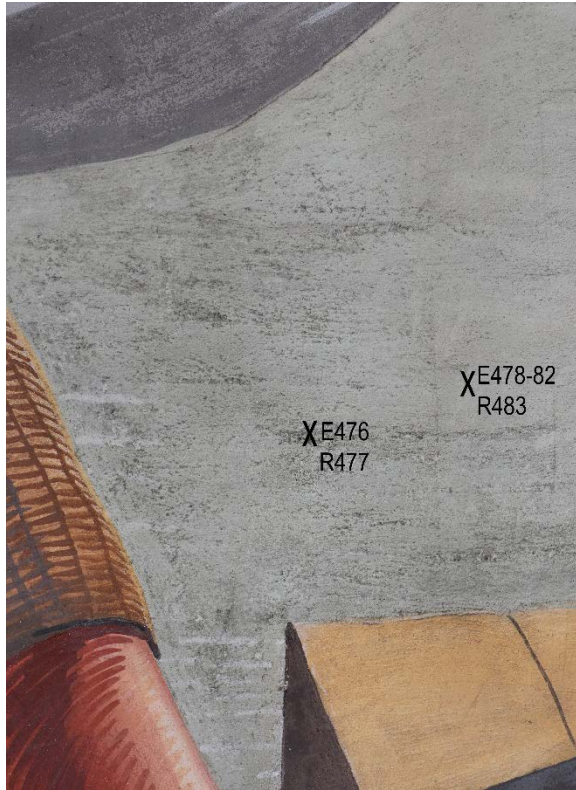
Locations of handled X-ray fluorescence analyses (h-EDXRF), panel 3:



Locations of handled X-ray fluorescence analyses (h-EDXRF), panel 6:







Correspondence between h-EDXRF analyses and spectro-colorimetry measures:

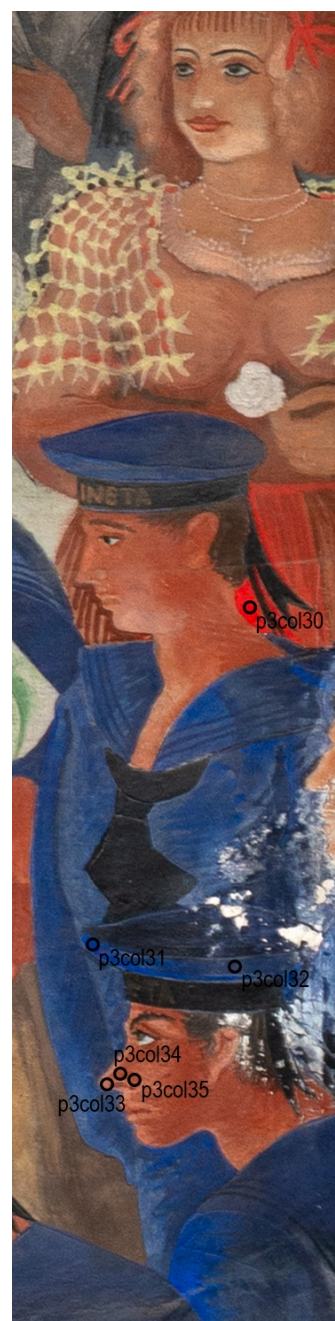
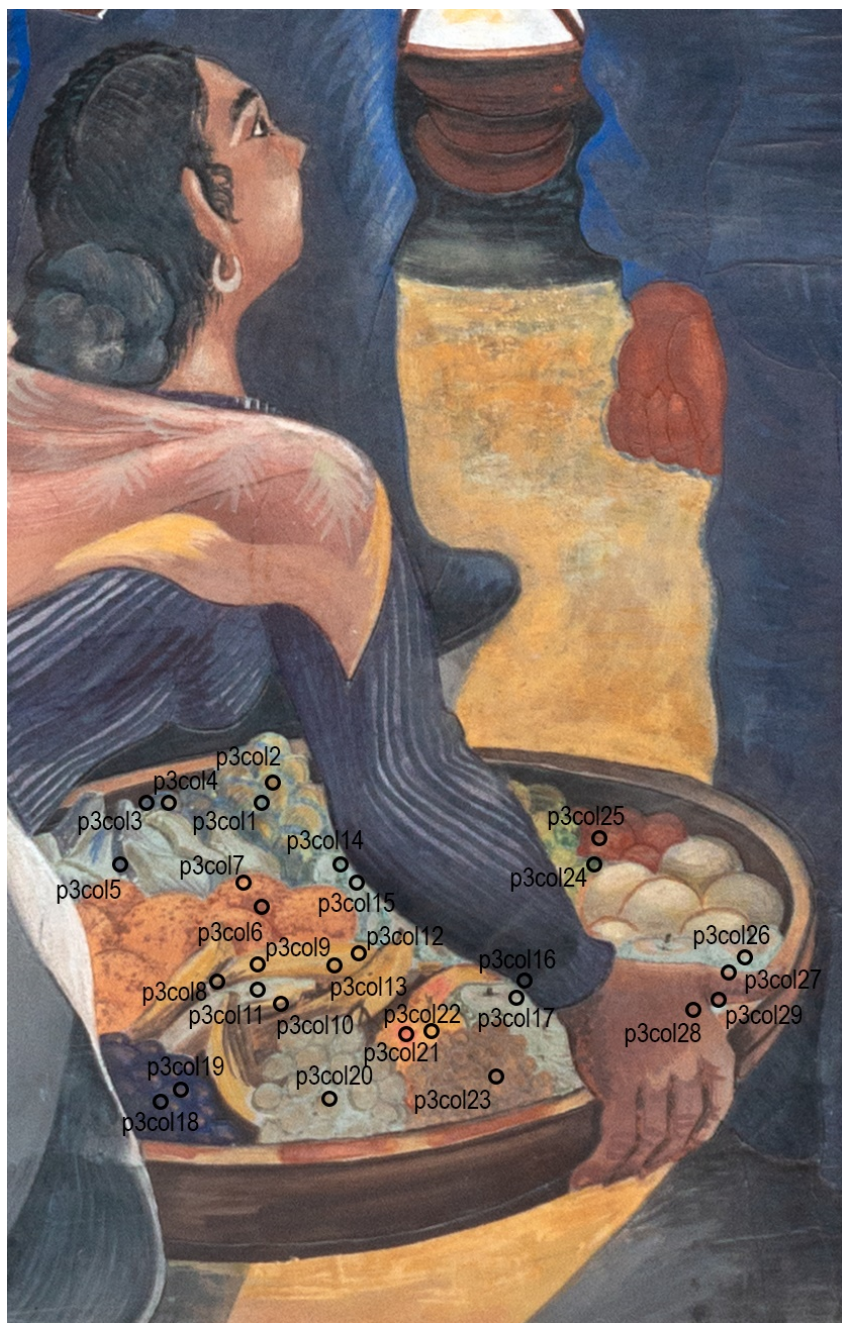
Panel 2					
<i>Spectro-colorimetry</i>	<i>h-EDXRF</i>		E617RED (red)	p1col7	E415
p2col1 (dark)	E545A (dark)	p3col23	E613	p1col8	E416
p2col2 (light)	E545B (light)	p3col24 (green)	E679GREEN_A (dark)	/	E417
/	E539FLASH E539WHITE	p3col25 (red)	E679GREEN_B (light) E679RED	p1col9	E428
p2col3	E551	p3col26 (green)	/	p1col10	E429
/	E555	p3col27 (brown)	/	/	/
p2col4	E558	p3col28 (dark)	E684A (dark)	p1col11 (dark)	E433A (dark)
p2col5	E560	p3col29 (light)	E684B (middle) E684C (light)	p1col12 (middle)	E433B (middle)
p2col6	E563	p3col30	E698	p1col13 (light)	E433C (light)
p2col7 (green)	E576BLUE	p3col31	E699	/	E426
p2col8 (blue)	E576GREEN	p3col32	E700	p1col32	E427
Panel 3				/	E438
<i>Spectro-colorimetry</i>	<i>h-EDXRF</i>			/	E444
p3col1 (blue)	E586A (blue)	p3col33 (light)	E701A (dark)	p1col14 (dark)	E466/68 (dark)
p3col2 (yellow)	E586B (yellow)	p3col34 (middle)	E701B (middle)	p1col15 (middle)	E458A (middle)
p3col3 (purple)	E589ORANGE	p3col35 (dark)	E701C (light)	p1col16 (light)	E458B (light)
p3col4 (brown)	E589PURPLE	Panel 6		/	E454
p3col5	E591	<i>Spectro-colorimetry</i>	<i>h-EDXRF</i>	p1col17 (dark)	/
p3col6 (dark)	E593A (dark)	p1col1	E361	p1col18 (light)	/
p3col7 (light)	E593B (light)	p1col2	E365	p1col25	E485
p3col8 (dark)	E595A (dark)	p1col3	E366	/	E490A (dark tone) E490B (light tone)
p3col9 (light)	E595B (light)	p1col4	E367	p1col19	/
p3col12 (dark)	E600	/	E375	p1col20	E513
p3col13 (light)	/	/	E378	p1col23 (yellow)	/
p3col10 (yellow)	E598 (blue)	p1col5	E380	p1col24 (brown)	/
p3col11 (blue)	/	p1col30	E385	p1col21	/
p3col14 (dark)	E603	/	E386	/	E527
p3col15 (light)	/	/	E388	p1col26 (dark)	RO1 (dark)
p3col16 (blue)	E605A (blue)	/	E418	p1col27 (middle)	RO2 (middle)
p3col17 (greenish)	E605B (greenish)	/	E419	p1col28 (light)	RO3 (light)
p3col18 (dark)	E607A (dark)	p1col31	E420		
p3col19 (light)	E607B (light)	p1col6	E412		
p3col20	E609A (dark) E609B (light)	/	E413		
p3col21 (red)	E617ORANGE	/	E414		
p3col22 (yellow)	E (yellow)				

Appendix V: Spectro-colorimetry measures:

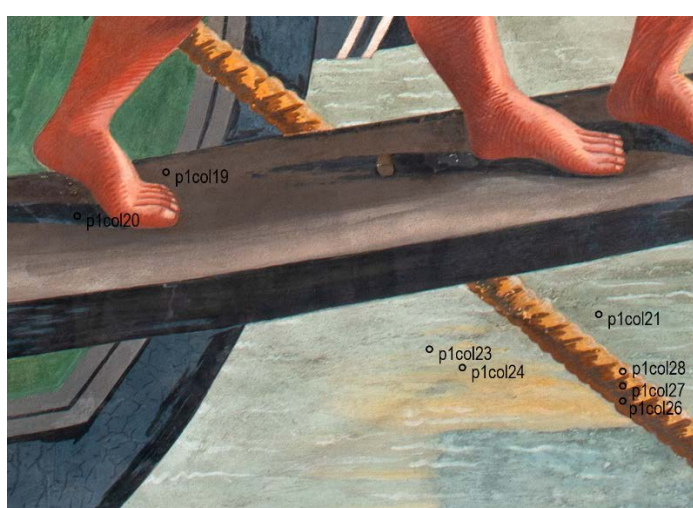
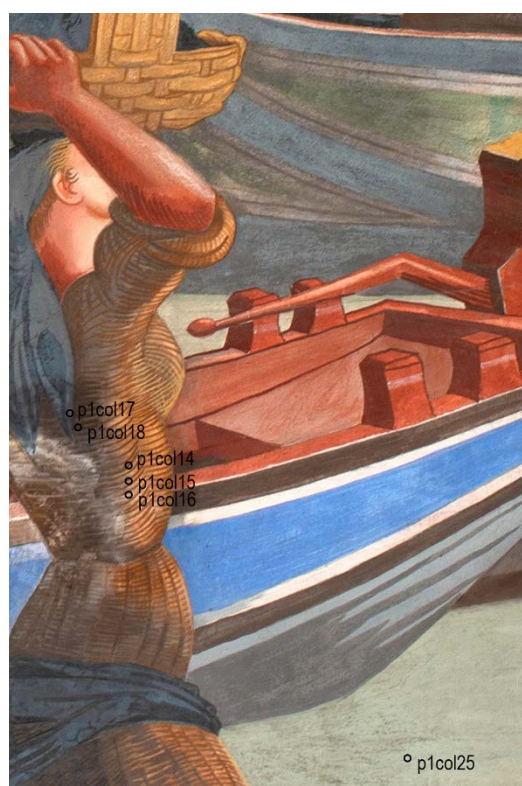
Locations of spectro-colorimetry measures in the panel 2:



Locations of spectro-colorimetry measures in the panel 3:








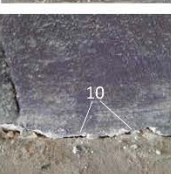
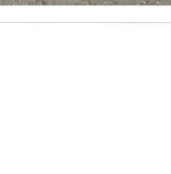

Locations of spectro-colorimetry measures in the panel 6:



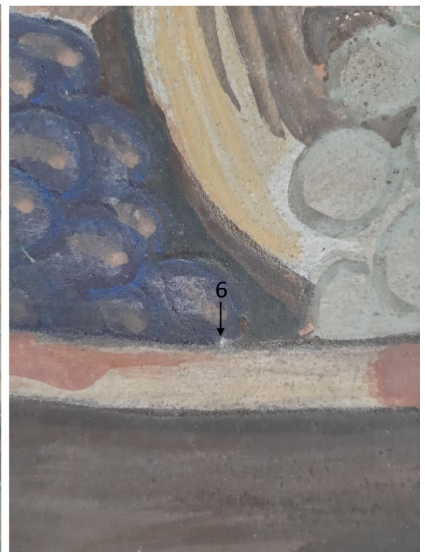
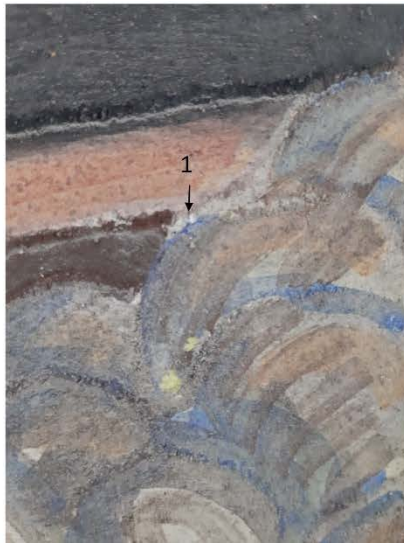
Appendix VI: Micro-sampling locations

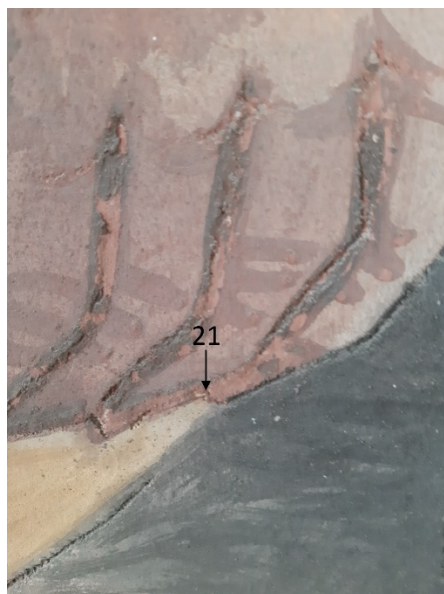
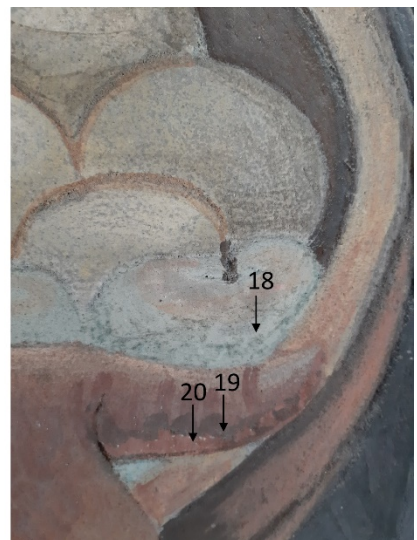
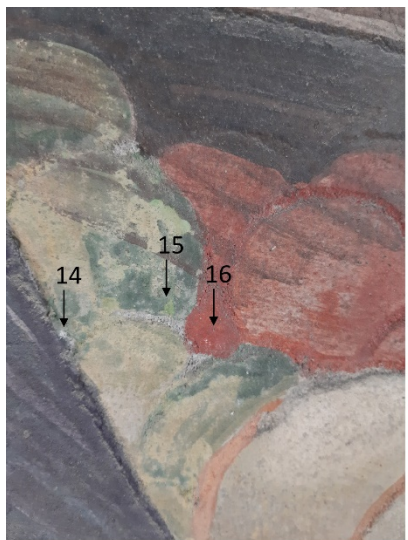
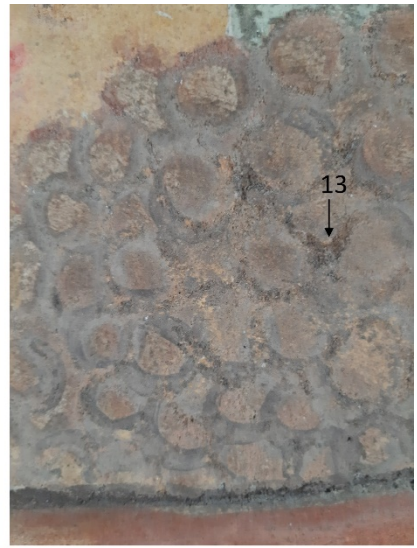
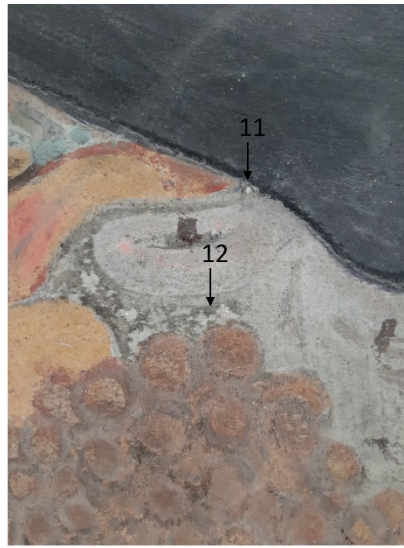
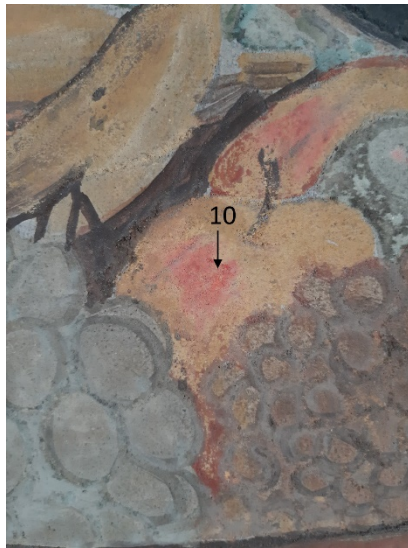
Micro-sampling locations in panel number 2:

MICROSAMPLING LOCATION - PANEL 2	Detail	Description	Goal
  <p>Building: Shipping station of Alcântara Painting. Ref. Guardian angel protects the 'nau' Painting author: Almada Negreiros Date of the paintings: 1943-1945 Dimensions: 6.20x3.50m Date of the microsampling: 5 June 2020 Collector: Milene Gil</p>		1-angel's neck (flesh tone-brown shadow)	1-identify painting technique/pigment
		2-angel's dress (flaking light greenish blue)	2-identify painting technique/pigment
		3- angel's dress (traces of yellowish green)	3 -identify painting technique/pigment
		4- angel's dress (flaking light greenish blue)	4-identify painting technique/pigment






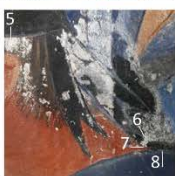
MICROSAMPLING LOCATION - PANEL 2	Detail	Description	Goal
  <p>Building: Shipping station of Alcântara Painting. Ref. Guardian angel protects the 'nau' Painting author: Almada Negreiros Date of the paintings: 1943-1945 Dimensions: 6.20x3.50m Date of the microsampling: 5 June 2020 Collector: Milene Gil</p>		5-angel's dress (flaking light green)	5 to7-identify painting technique/pigment
		6-angel's dress (flaking light green/blue)	
		7-angel's dress (brownish white)- under UV, it fluorescence	
		8- angel's sandal (brownish white)	8-identify painting technique/pigment
		9- mastro base (bluish black)	9 -identify painting technique/pigment
		10- velas (pink)	10-identify painting technique/pigment

Micro-sampling locations in panel number 3, sampling zone A – basket with fruits:












Micro-sampling locations in panel number 3, sampling zone B – sailors:

MICROSAMPLING LOCATION - PANEL 3	Detail	Description	Goal
  <p>Building: Shipping station of Alcântara Painting. Ref.: Arrival of the 'nau' (ship) with the Captain embracing his three daughters, surrounded by sailors Painting author: Almada Negreiros Date of the paintings: 1943-1945 Dimensions: 6.20x3.50m Date of the microsampling: 5 June 2020 Collector: Milene Gil</p>		1/1a-apron (red) – verificar se não apanhou tb azul	1/1a-identify painting technique/pigment
		2-sailor's beret (flacking dark blue) 3-shirt (blue)	2-identify painting technique/pigment 3-identify painting technique/pigment
		4- sailor neck (flesh tone affected by salts)	4 -identify painting technique/pigment
		5- sailor hair (salt efflorescence) 6-sailor's beret ribbon (salt efflorescence) 7- sailor neck (flesh tone –shadow tone) 8- sailor's shirt (dark blue)	5 and 6- Identify salt efflorescence 7 and 8 -identify painting technique/pigment

Micro-sampling locations in panel number 6, sampling zone A – female figures:

MICROSAMPLING LOCATION - PANEL 6	Detail	Description	Goal
  <p>Building: Shipping station of Alcântara Painting. Ref.: Barefoot fishwives at the offloading of the coal Painting author: Almada Negreiros Date of the paintings: 1943-1945 Dimensions: 6.20x3.50 m Date of the microsampling: 5 June 2020 Collector: Milene Gil</p>		1-Background (flacking greyish green) 2-Background (salt efflorescence)	1-identify painting technique/pigment 2-Identify salt efflorescence
		3-Background (green)	3-identify painting technique/pigment
		4-shoulder sleeve (flacking greyish blue) 5-flesh tone (dark brown shadow) 6-flesh tone (greysh shadow) 6rep-flesh tone (greysh shadow) 7- shoulder sleeve (flacking light blue)	4 to 7-identify painting technique/pigment
		6rep-flesh tone (greysh shadow)	

MICROSAMPLING LOCATION - PANEL 6



Building: Shipping station of Alcântara
 Painting. Ref.: Barefoot fishwives at the offloading of the coal
 Painting author: Almada Negreiros
 Date of the paintings: 1943-1945
 Dimensions: 6.20x3.50 m
 Date of the microsampling: 5 June 2020
 Collector: Milene Gil

Detail

Description

Goal



8-Dress (flaking blue)

8-identify painting technique/pigment



9-mast (flaking dark greyish green)
 10-mast (flaking light greyish green)
 11- mast (powdering blue)

9 to 10-identify painting technique/pigment



12- roldana (flaking dark grey)


12 -identify painting technique/pigment



13-boat (flaking black)

13 -identify painting technique/pigment

MICROSAMPLING LOCATION - PANEL 6



Building: Shipping station of Alcântara
 Painting. Ref.: Barefoot fishwives at the offloading of the coal
 Painting author: Almada Negreiros
 Date of the paintings: 1943-1945
 Dimensions: 6.20x3.50 m
 Date of the microsampling: 5 June 2020
 Collector: Milene Gil

Detail

Description

Goal



14/14a-boat (flaking and powdering green-original? retouching?)
 15-boat (salt efflorescences)

14/14a-identify painting technique/pigment
 15- identify salt efflorescences



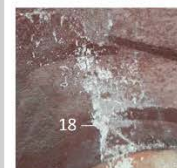
16-boat (flaking and powdering light green-original? retouching?)

16-identify painting technique/pigment



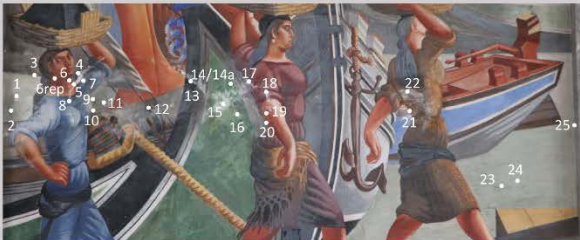
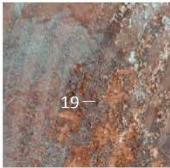



17- sleeve (dark brownish red)





17 -identify painting technique/pigment




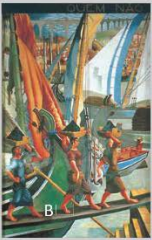
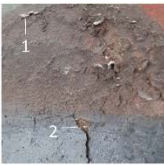

18-sleeve (salt efflorescences)

18 - identify salt efflorescences

MICROSAMPLING LOCATION - PANEL 6	Detail	Description	Goal
 <p>Building: Shipping station of Alcântara Painting. Ref.: Barefoot fishwives at the offloading of the coal Painting author: Almada Negreiros Date of the paintings: 1943-1945 Dimensions: 6.20x3.50 m Date of the microsampling: 5 June 2020 Collector: Milene Gil</p>		19-sleeve (flaking and powdering dark red)	19-identify painting technique/pigment
		20- arm (flesh tone, shadow)	20-identify painting technique/pigment
		21- dress (dark flaking brown)	21 -identify painting technique/pigment
		22- lenço (dark flaking bluish black)	22 - identify painting technique/pigment

MICROSAMPLING LOCATION - PANEL 6	Detail	Description	Goal
 <p>Building: Shipping station of Alcântara Painting. Ref.: Barefoot fishwives at the offloading of the coal Painting author: Almada Negreiros Date of the paintings: 1943-1945 Dimensions: 6.20x3.50 m Date of the microsampling: 5 June 2020 Collector: Milene Gil</p>		23-background (flaking greenish white-darker tone)	23-identify painting technique/pigment
		24-background (greenish white, slightly powdering)	24-identify painting technique/pigment
		25-background (greenish white)	25 -identify painting technique/pigment

Micro-sampling locations in panel number 6, sampling zone B – bottom of the panel:

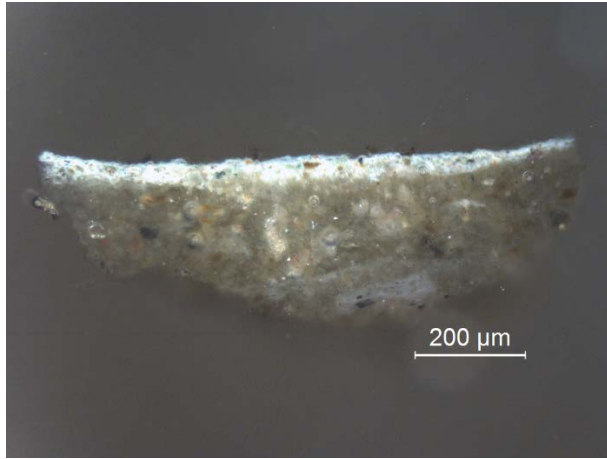
MICROSAMPLING LOCATION - PANEL 6	Detail	Description	Goal
  <p>Building: Shipping station of Alcântara Painting. Ref.: Barefoot fishwives at the offloading of the coal Painting author: Almada Negreiros Date of the paintings: 1943-1945 Dimensions: 6.20x3.50 m Date of the microsampling: 5 June 2020 Collector: Milene Gil</p>		1-platform (flaking brown)	23-identify painting technique/pigment
		2-platform (flaking glossy black/what is the glossing material?)	24-identify painting technique/pigment / intervention material?

Micro-sampling locations in panel number 6, sampling zone C – bottom of the panel:

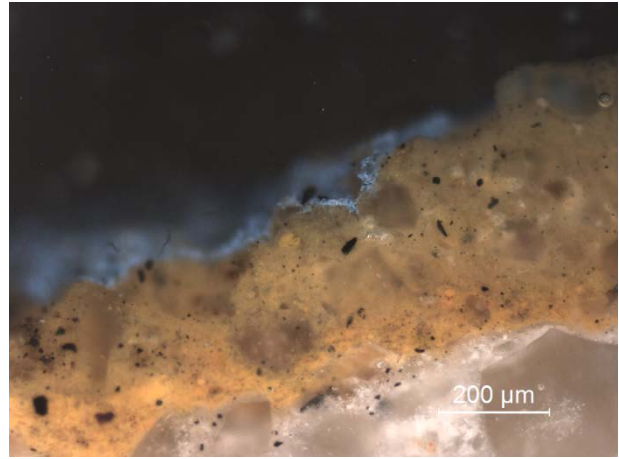


Appendix VII: Optical microscope images

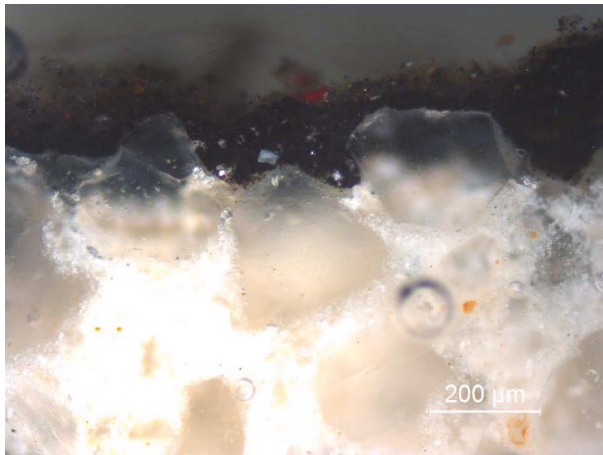
Images of cross section samples with using Leica DM2500M reflected light optical microscope in dark field illumination mode, magnification 100,200 and 500x:



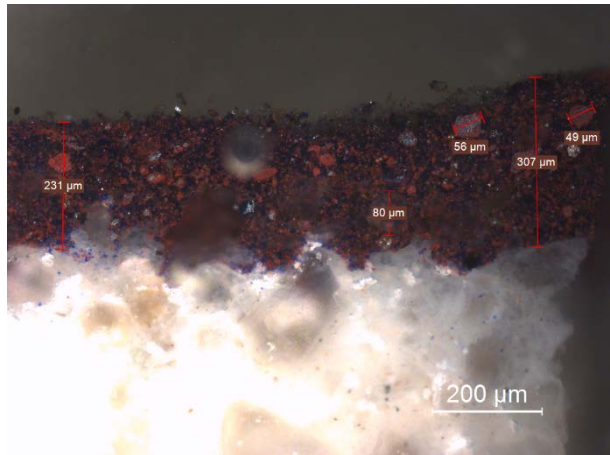
P2_4. Magnification 100x



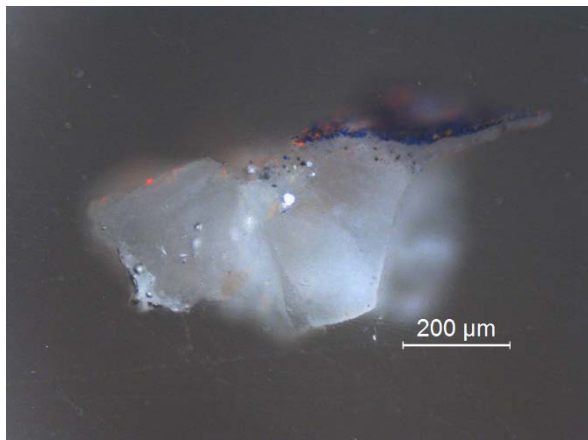
P2_8. Magnification 500x



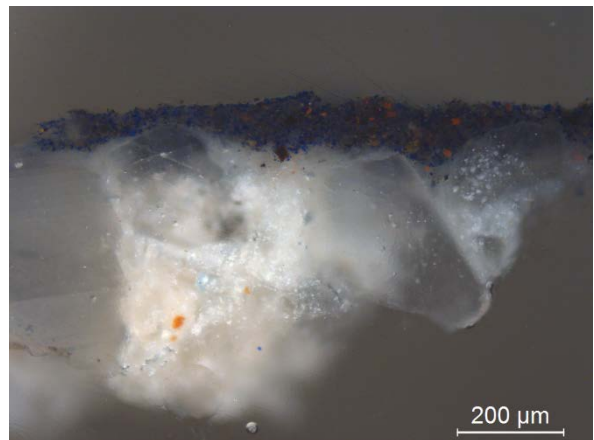
P2_9. Magnification 100x



P2_10. Magnification 200x



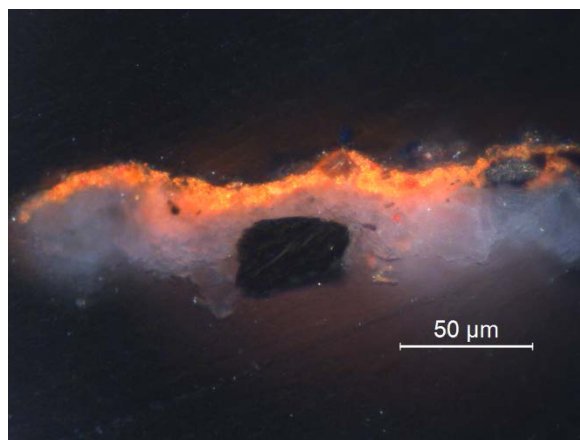
P3B_1. Magnification 100x



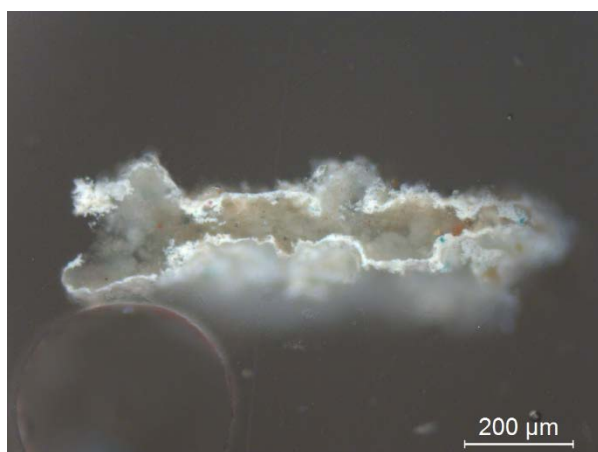
P3B_2. Magnification 100x



P3B_4. Magnification 100x



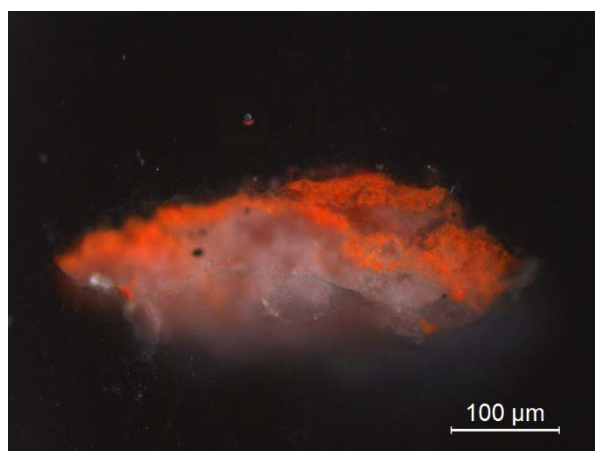
P3B_7. Magnification 500x



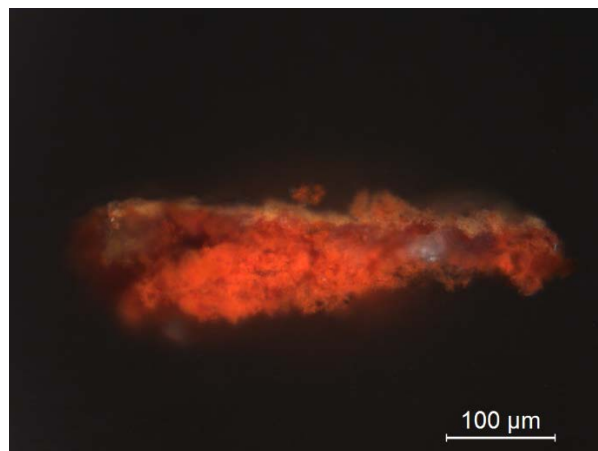
P6A_3. Magnification 100x



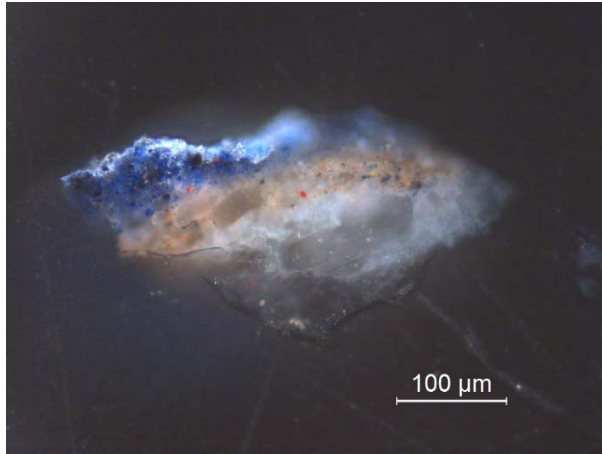
P6A_4. Magnification 100x



P6A_5. Magnification 200x



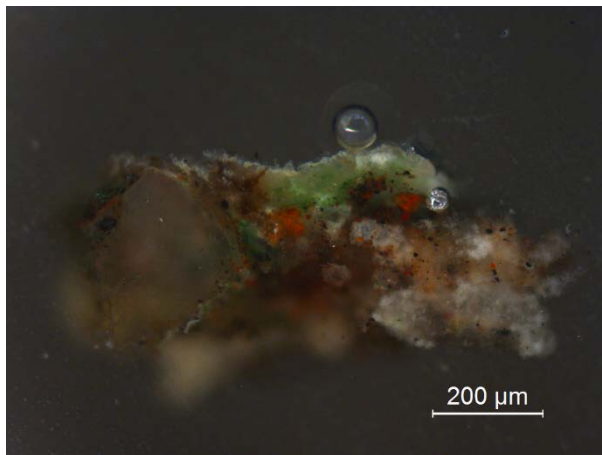
P6A_6rep. Magnification 200x



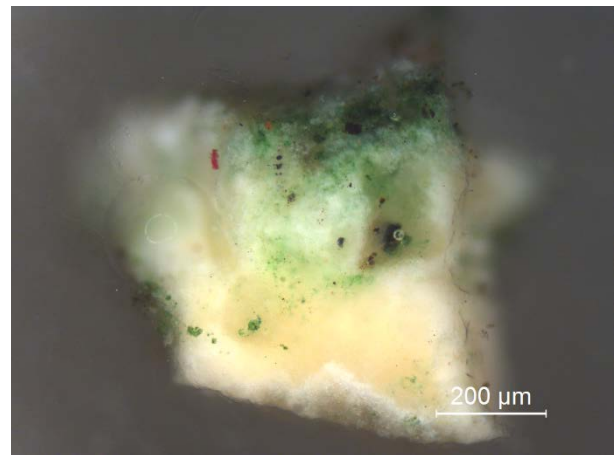
P6A_7. Magnification 200x



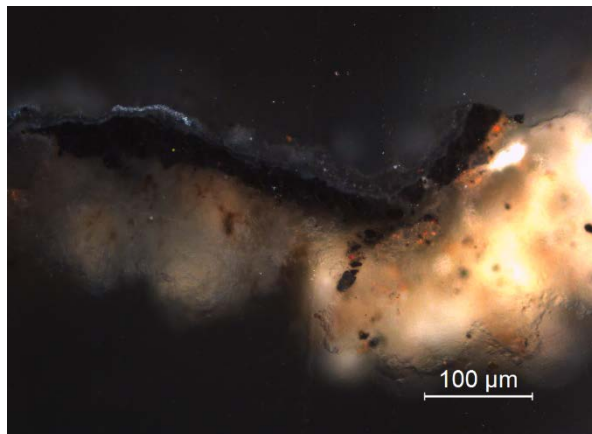
P6A_9. Magnification 100x



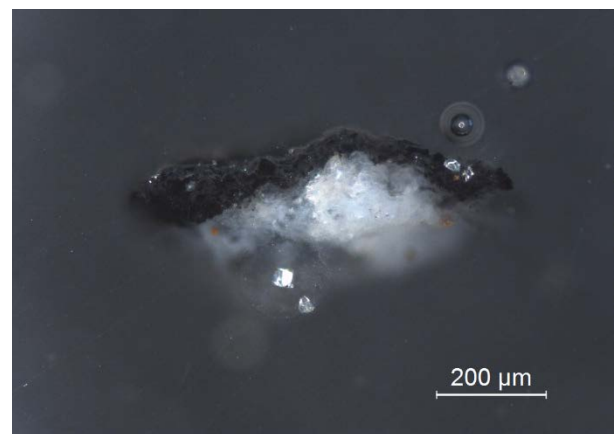
P6A_10. Magnification 100x



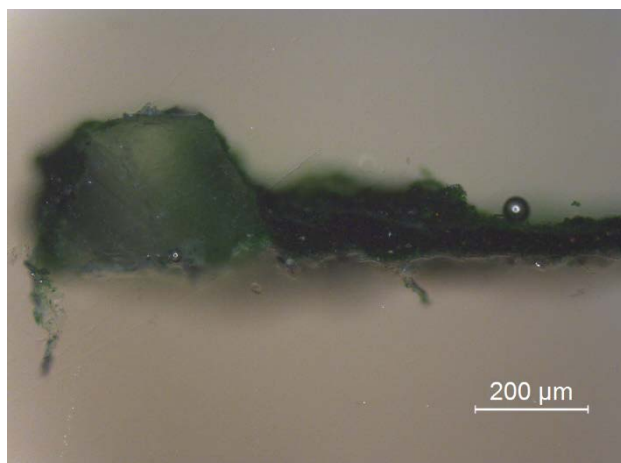
P6A_11. Magnification 100x



P6A_12. Magnification 200x



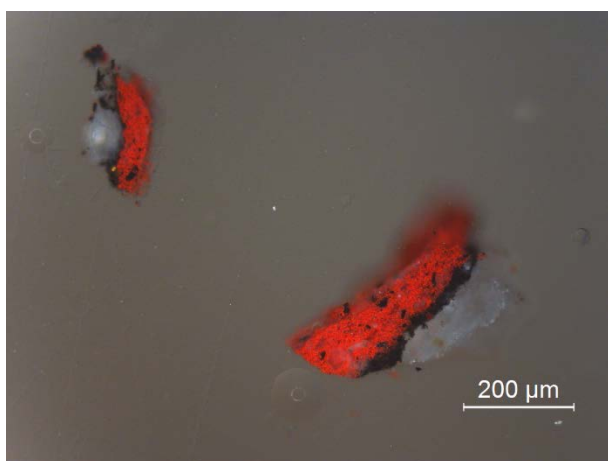
P6A_13. Magnification 100x



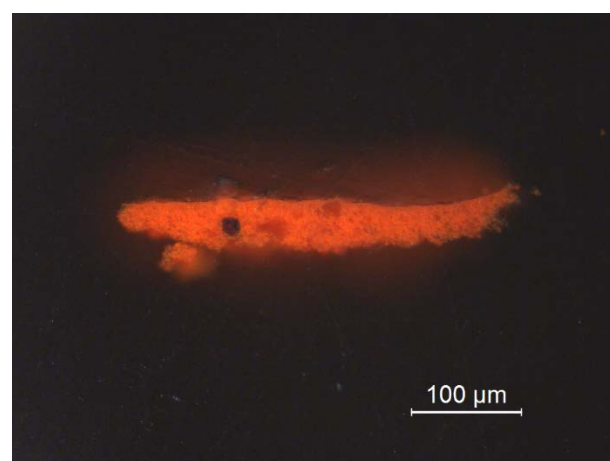
P6A_14. Magnification 100x



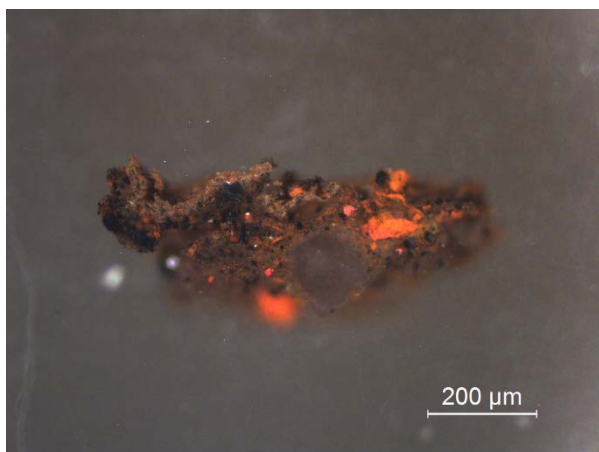
P6A_16. Magnification 100x



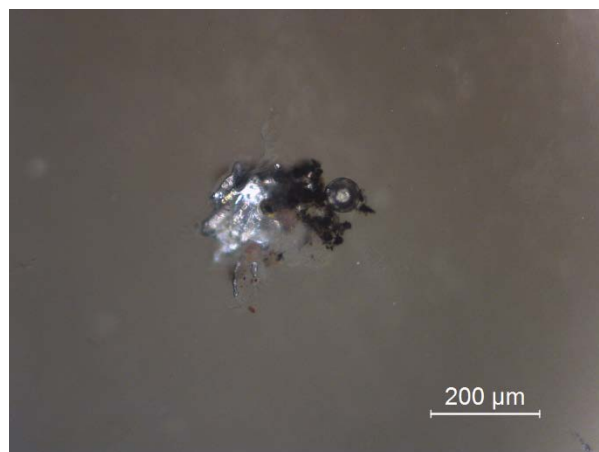
P6A_17. Magnification 100x



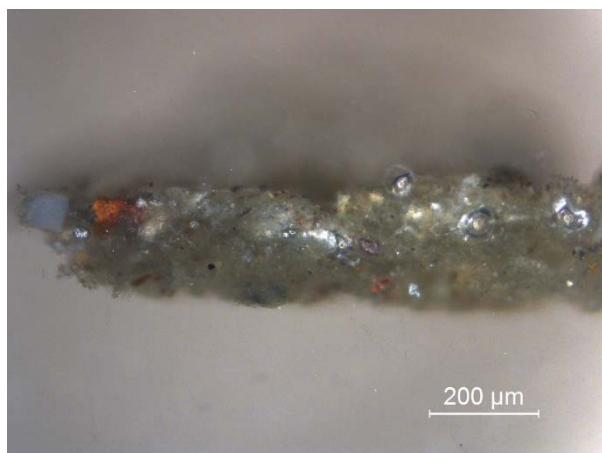
P6A_20. Magnification 200x



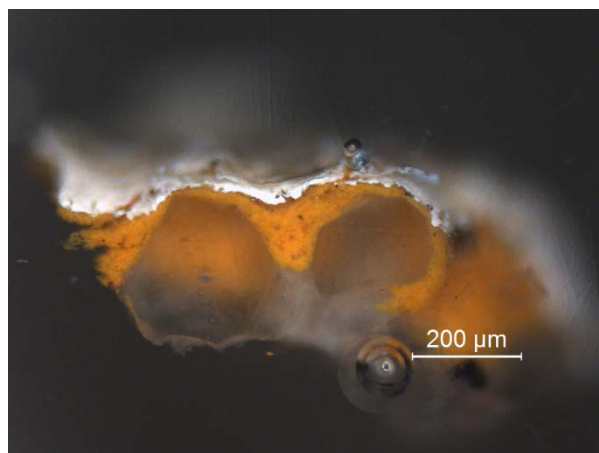
P6A_21. Magnification 100x



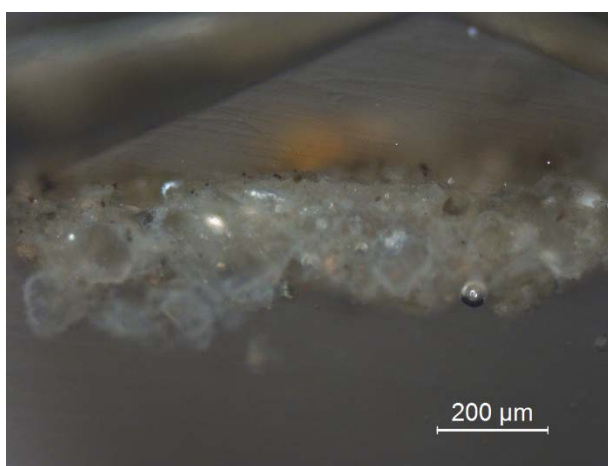
P6A_22. Magnification 100x



P6A_23. Magnification 100x



P6C_2. Magnification 100x



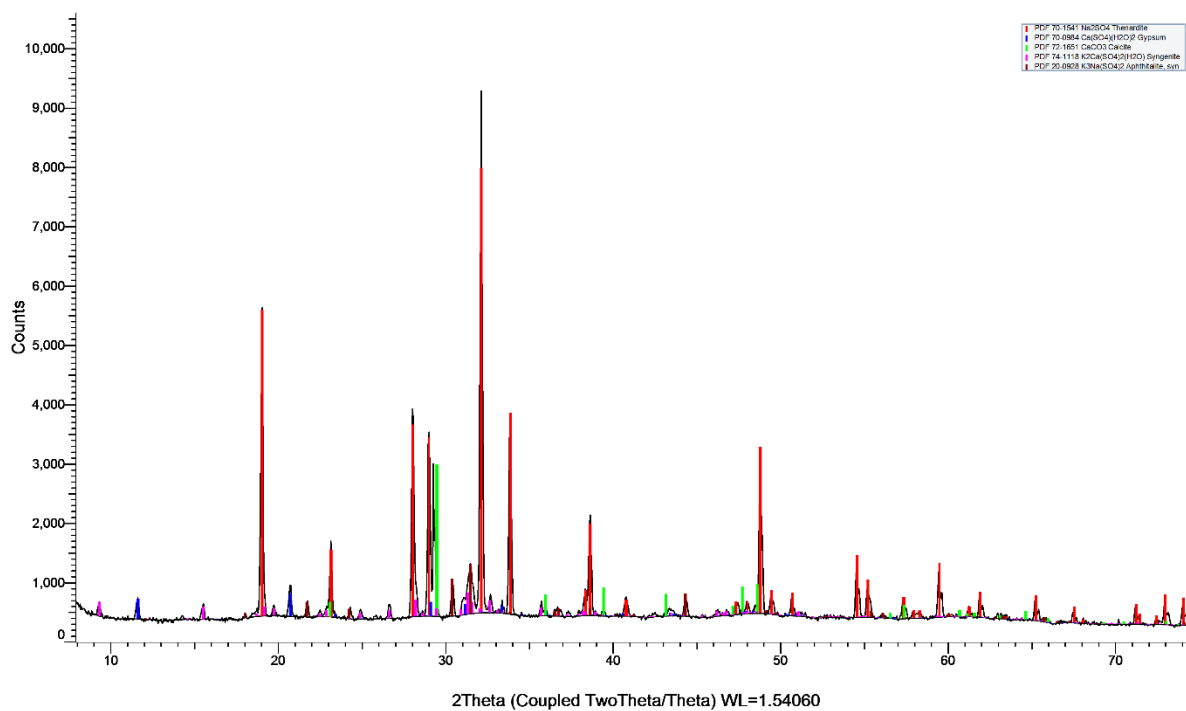
P6C_5. Magnification 100x

Appendix VIII: μ -XRD analyses

Diffractogram images of samples analysed with micro-X-ray diffractometer, displaying the presence of salts.

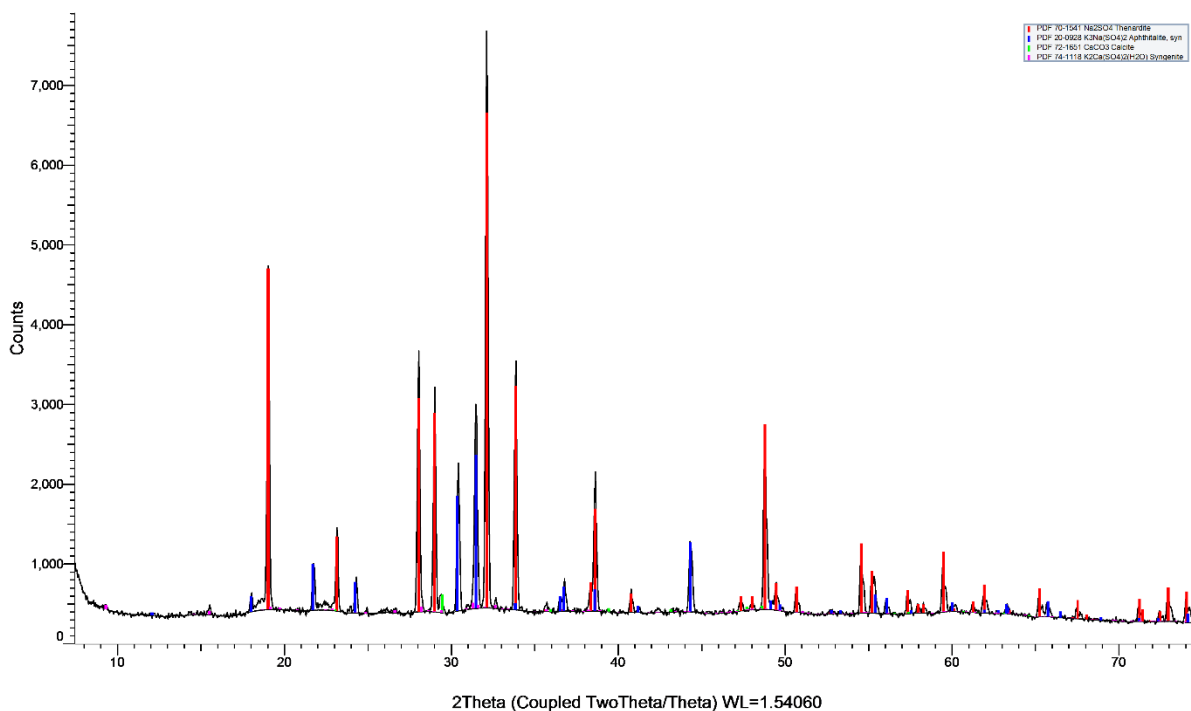
1. P3B_5

Commander Sample ID (Coupled TwoTheta/Theta)



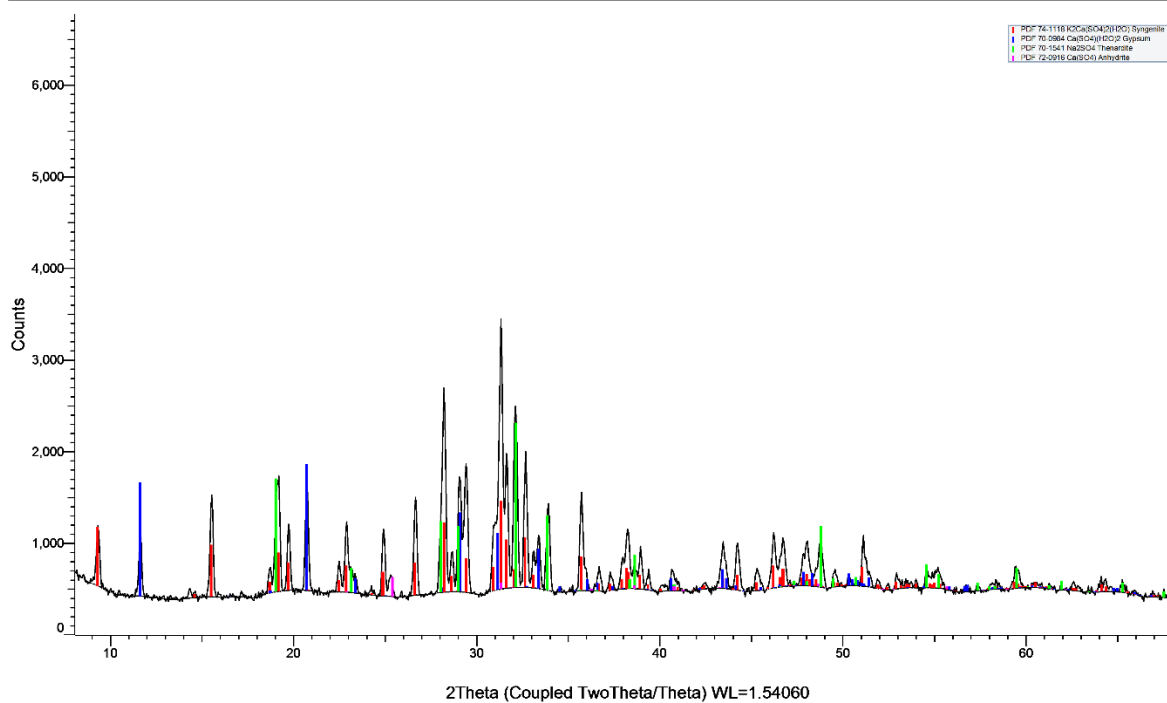
2. P3B_6

Commander Sample ID (Coupled TwoTheta/Theta)



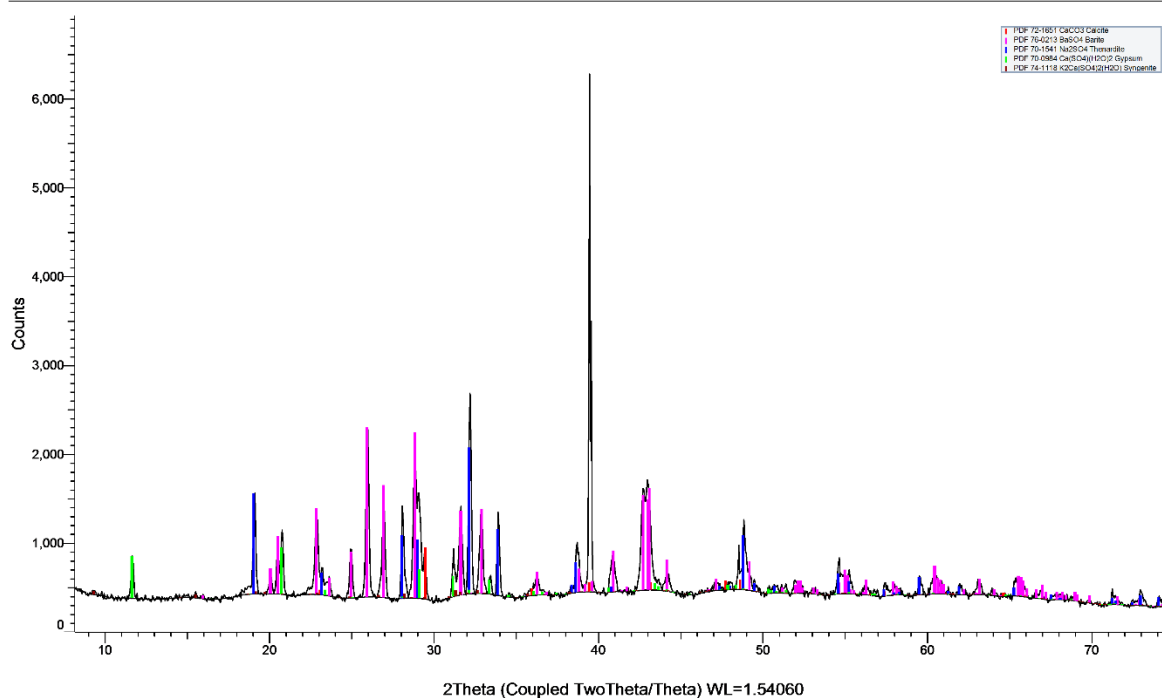
3. P6A_2

Commander Sample ID (Coupled TwoTheta/Theta)



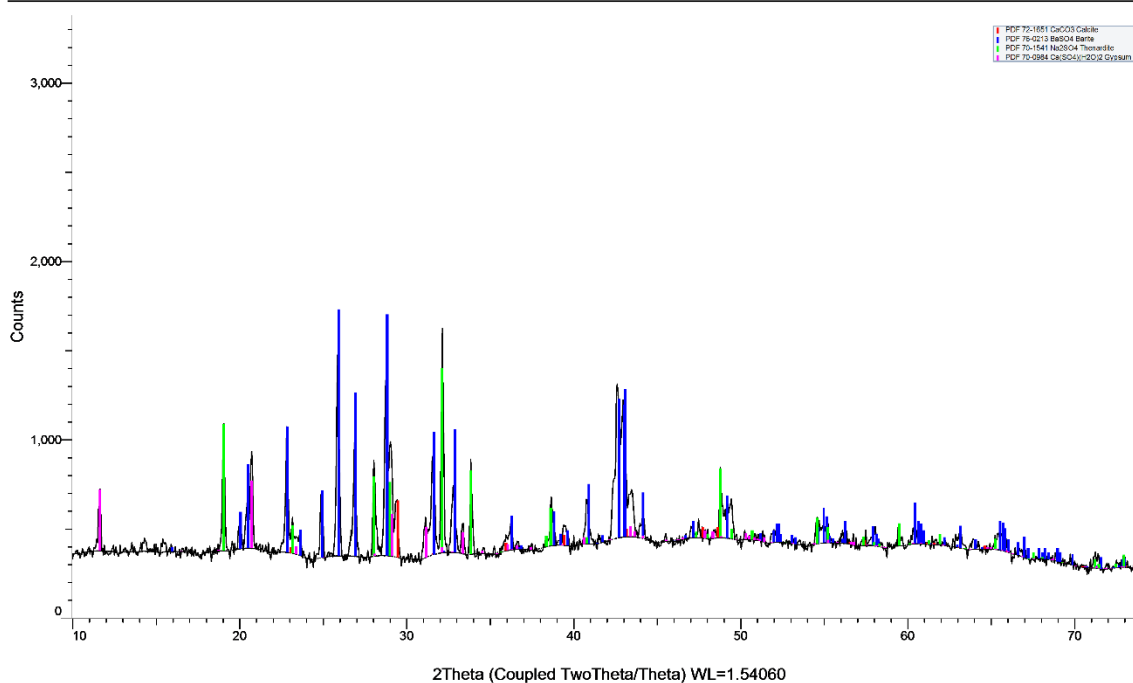
4. P6A_15

Commander Sample ID (Coupled TwoTheta/Theta)



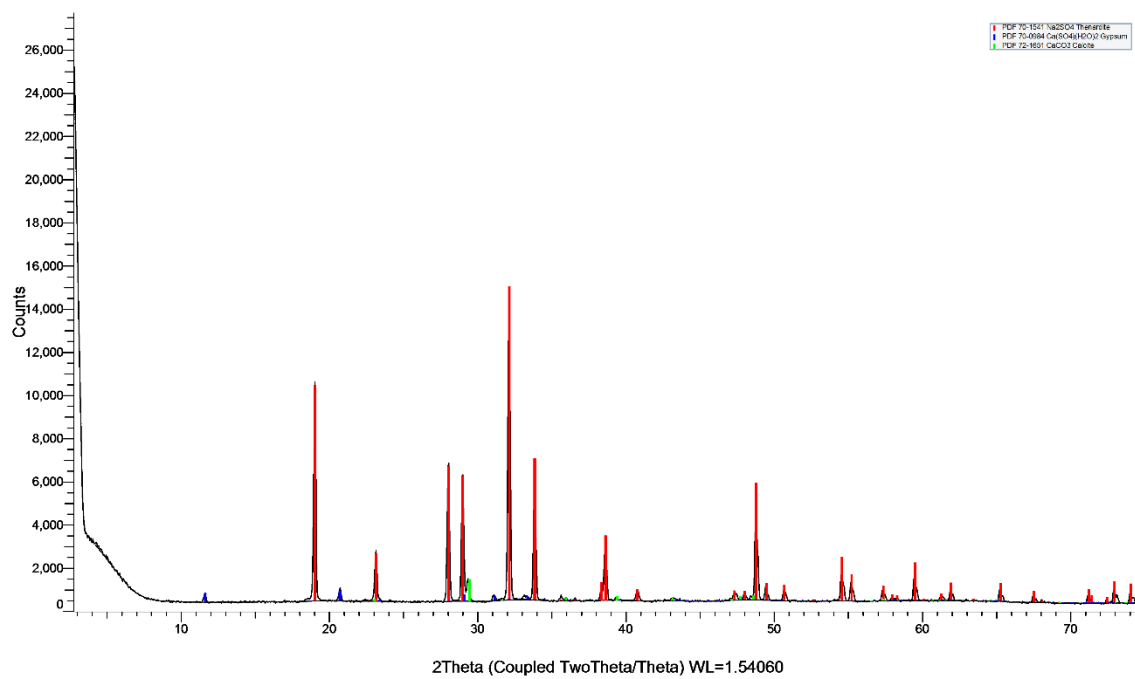
5. P6A_15rep

Commander Sample ID (Coupled TwoTheta/Theta)



6. P6A_18

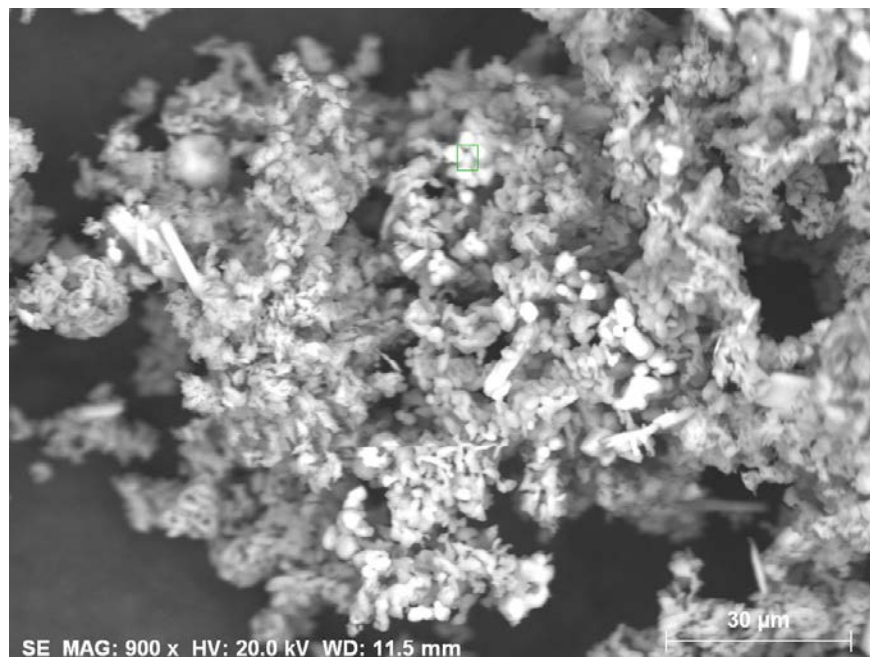
Commander Sample ID (Coupled TwoTheta/Theta)



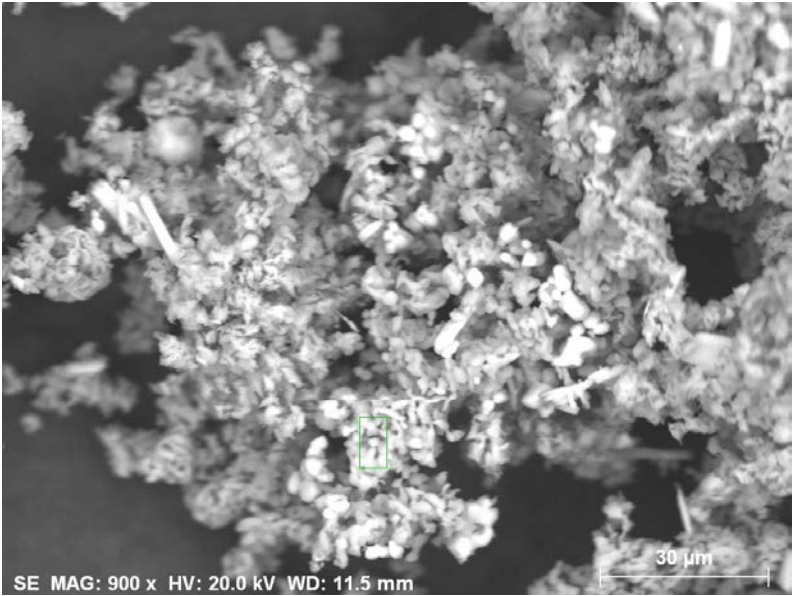
Appendix IX: SEM-EDS analyses of powder samples

SEM-EDS analyses of micro-powder samples collected from panels 3 and 6.

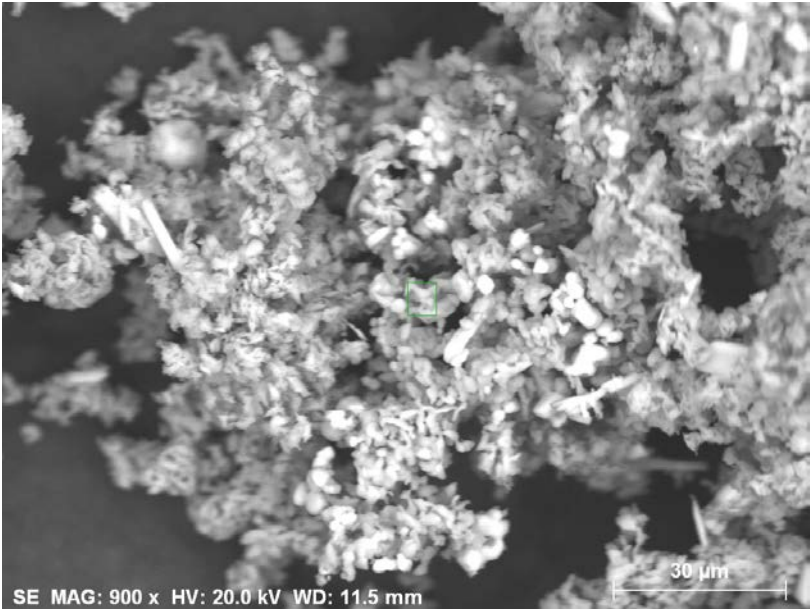
Sample P3B_5



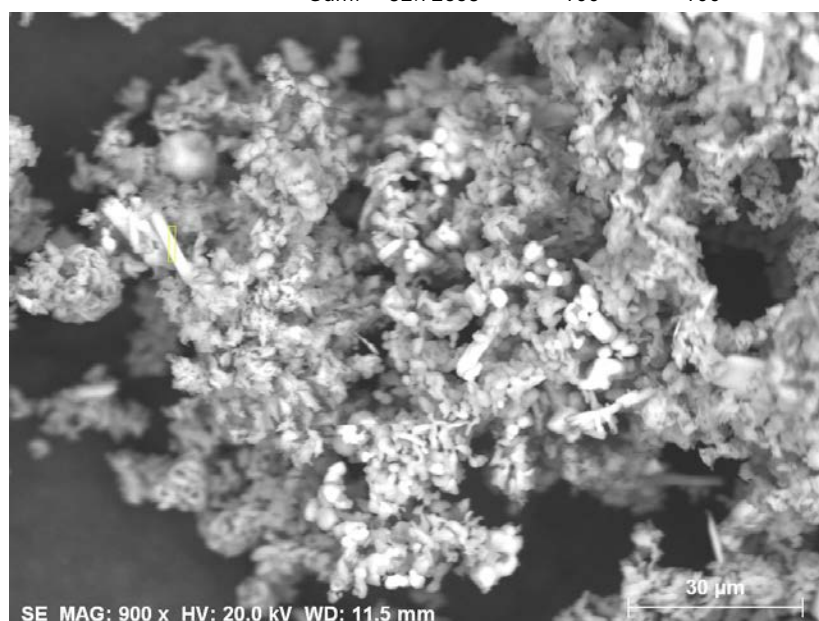
Element	AN	series	[wt.%]	[norm. wt.%]	[norm. at.%]	Error in wt.% (1 Sigma)	K fact.	Z corr.	A corr.	F corr.
Carbon	6	K-series	3.743113	4.241853	7.428062	2.262135	0.193577	0.21913	1	1
Oxygen	8	K-series	39.53782	44.80591	58.9021	5.086011	1.23342	0.363266	1	1
Sodium	11	K-series	10.08408	11.4277	10.45499	0.683675	0.103209	1.104233	1	1.002724
Aluminium	13	K-series	0.158361	0.179461	0.139895	0.037498	0.001252	1.420357	1	1.00931
Silicon	14	K-series	0.184241	0.208789	0.15636	0.037076	0.001075	1.909848	1	1.016688
Sulfur	16	K-series	13.95162	15.81056	10.37055	0.528907	0.080635	1.9236	1	1.019322
Potassium	19	K-series	20.58318	23.32572	12.54805	0.655268	0.105034	2.200034	1	1.009434
Sum:			88.24242	100	100					



Element	AN	series	[wt.%]	[norm. wt.%]	[norm. at.%]	Error in wt.% (1 Sigma)	K fact.	Z corr.	A corr.	F corr.
Carbon	6	K-series	7.617038	8.30178	13.24236	3.38957	0.190993	0.434664	1	1
Oxygen	8	K-series	41.17812	44.87987	53.74291	5.045294	0.689537	0.650869	1	1
Sodium	11	K-series	22.0992	24.08583	20.07244	1.455795	0.206882	1.16169	1	1.002185
Aluminium	13	K-series	0.253242	0.276007	0.195987	0.042364	0.001832	1.496549	1	1.00692
Silicon	14	K-series	1.539178	1.677543	1.144366	0.096102	0.008241	2.013723	1	1.010924
Sulfur	16	K-series	13.56817	14.7879	8.835578	0.514968	0.072258	2.030936	1	1.007683
Potassium	19	K-series	2.630739	2.867232	1.405006	0.112595	0.012116	2.327099	1	1.016966
Calcium	20	K-series	1.969049	2.146058	1.025909	0.091483	0.009471	2.228454	1	1.016786
Iron	26	K-series	0.897136	0.977785	0.335442	0.062793	0.004008	2.276272	1	1.071853
Sum:			91.75188	100	100					

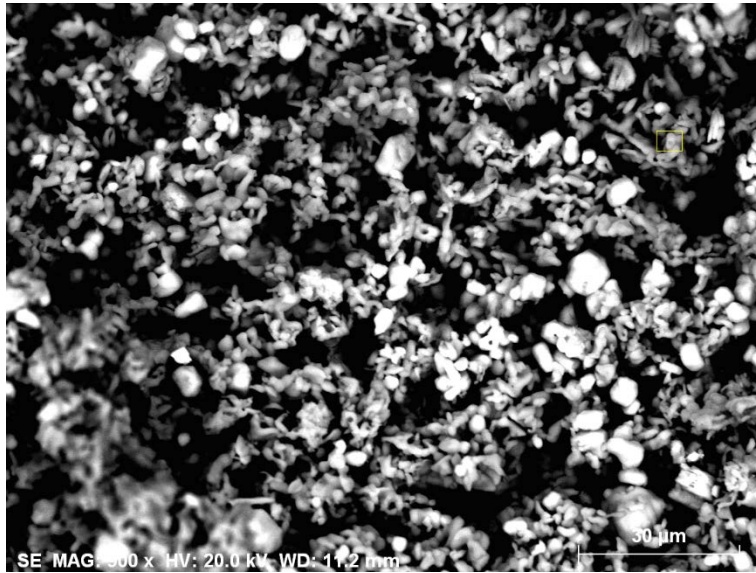


Element	AN	series	[wt.%]	[norm. wt.%]	[norm. at.%]	Error in wt.% (1 Sigma)	K fact.	Z corr.	A corr.	F corr.
Carbon	6	K-series	5.016565	6.064023	9.737154	2.538635	0.180823	0.335357	1	1
Oxygen	8	K-series	39.00708	47.15175	56.83875	4.729577	0.956308	0.493061	1	1
Sodium	11	K-series	19.94992	24.11547	20.23072	1.315865	0.163844	1.468602	1	1.002214
Aluminium	13	K-series	0.244256	0.295257	0.211049	0.042779	0.001549	1.89234	1	1.007056
Silicon	14	K-series	0.234252	0.283163	0.194449	0.039709	0.001098	2.546544	1	1.012391
Sulfur	16	K-series	14.5635	17.60435	10.58829	0.550738	0.068039	2.568793	1	1.007242
Potassium	19	K-series	2.801801	3.386817	1.670645	0.118358	0.011343	2.944143	1	1.014169
Calcium	20	K-series	0.909303	1.099165	0.528941	0.060205	0.003837	2.819572	1	1.015943
Sum:			82.72668	100	100					

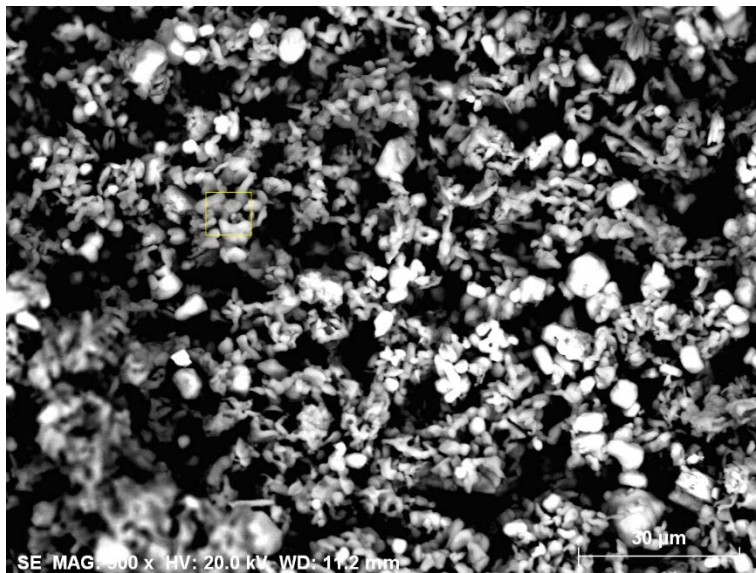


Element	AN	series	[wt.%]	[norm. wt.%]	[norm. at.%]	Error in wt.% (1 Sigma)	K fact.	Z corr.	A corr.	F corr.
Carbon	6	K-series	8.677501	9.045906	15.10295	2.997826	0.425228	0.212731	1	1
Oxygen	8	K-series	43.15182	44.98384	56.38216	5.53756	1.227345	0.366513	1	1
Sodium	11	K-series	9.164486	9.553566	8.333352	0.625726	0.087807	1.085308	1	1.002503
Aluminium	13	K-series	0.087466	0.091179	0.067767	0.03316	0.000648	1.396047	1	1.008542
Silicon	14	K-series	0.124599	0.129888	0.092742	0.033938	0.000682	1.877188	1	1.0153
Sulfur	16	K-series	13.39284	13.96144	8.731206	0.508633	0.072558	1.890765	1	1.017675
Potassium	19	K-series	12.60362	13.13871	6.738816	0.413699	0.059241	2.162598	1	1.025551
Calcium	20	K-series	8.725049	9.095472	4.551013	0.289159	0.043405	2.069738	1	1.01244
Sum:			95.92739	100	100					

Sample P3B_6



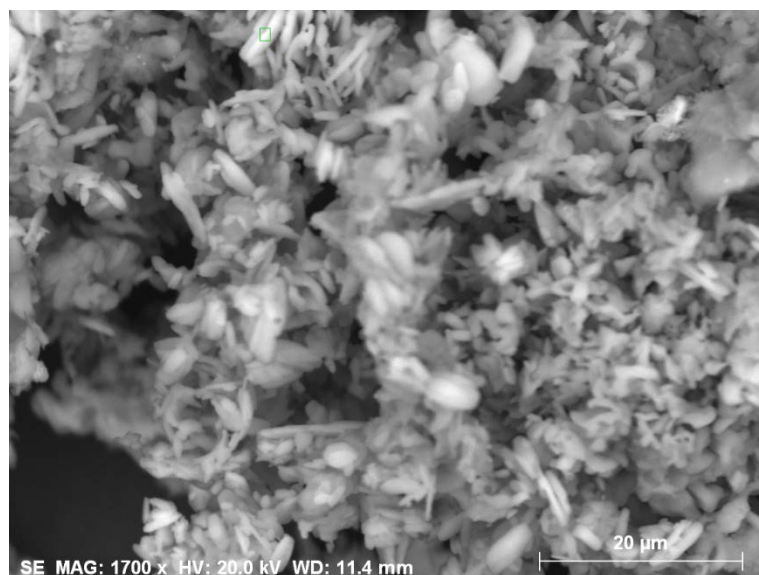
Element	AN	series	[wt.%]	[norm. wt.%]	[norm. at.%]	Error in wt.% (1 Sigma)	K fact.	Z corr.	A corr.	F corr.
Carbon	6	K-series	8.401519	11.20782	18.25159	3.415894	0.222969	0.502663	1	1
Oxygen	8	K-series	26.84577	35.81288	43.78188	3.599158	0.550589	0.650446	1	1
Sodium	11	K-series	18.94333	25.27084	21.50026	1.258644	0.181275	1.390385	1	1.002646
Sulfur	16	K-series	17.79655	23.74101	14.48149	0.665339	0.097054	2.430013	1	1.006646
Potassium	19	K-series	2.974052	3.967455	1.984782	0.12121	0.014091	2.783925	1	1.011369
Sum:			74.96122	100	100					



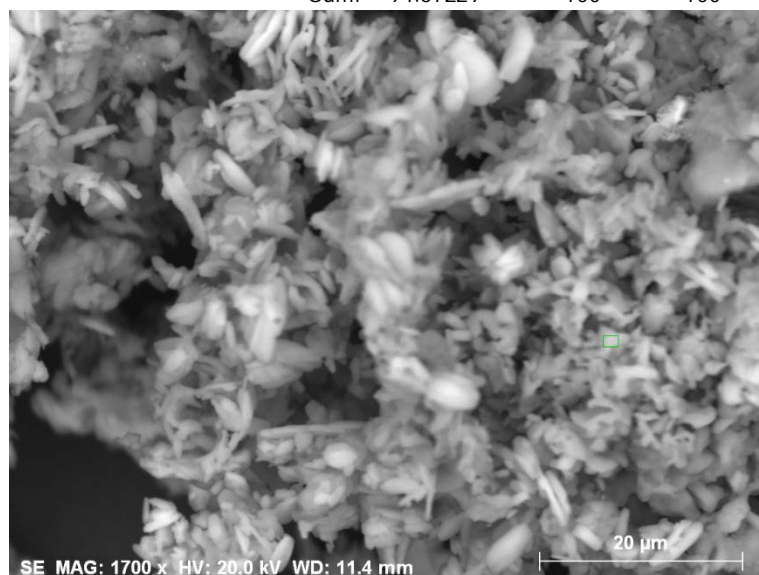
Element	AN	series	[wt.%]	[norm. wt.%]	[norm. at.%]	Error in wt.% (1 Sigma)	K fact.	Z corr.	A corr.	F corr.
Carbon	6	K-series	1.421637	1.779827	2.966845	1.782506	0.050383	0.35326	1	1
Oxygen	8	K-series	38.08084	47.67553	59.66065	4.59258	0.906481	0.525941	1	1
Sodium	11	K-series	20.75372	25.98275	22.62802	1.366933	0.183602	1.411992	1	1.002249

Silicon	14	K-series	0.148321	0.185691	0.132375	0.035328	0.000749	2.447524	1	1.012979
Sulfur	16	K-series	15.38132	19.25673	12.02358	0.580309	0.077457	2.468378	1	1.007194
Potassium	19	K-series	1.980016	2.478893	1.269393	0.094425	0.008623	2.828202	1	1.016489
Calcium	20	K-series	2.109164	2.640581	1.319136	0.097545	0.009603	2.708273	1	1.015295
Sum:			79.87501	100	100					

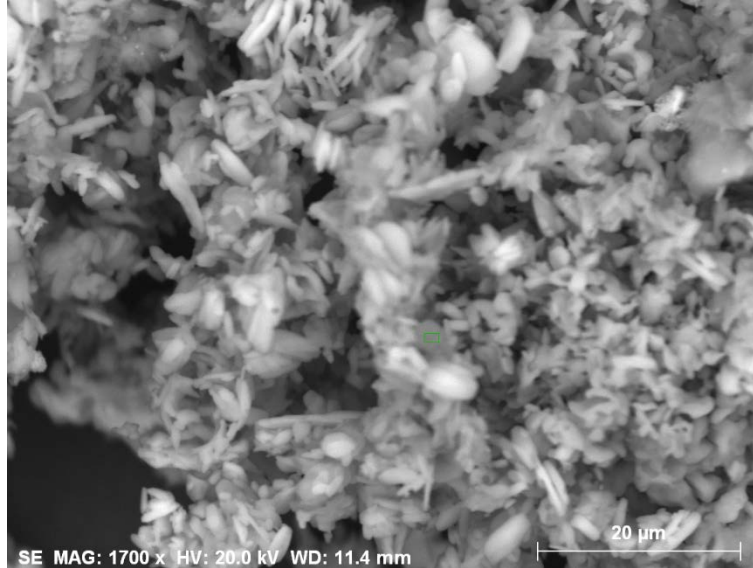
Sample P6A_2



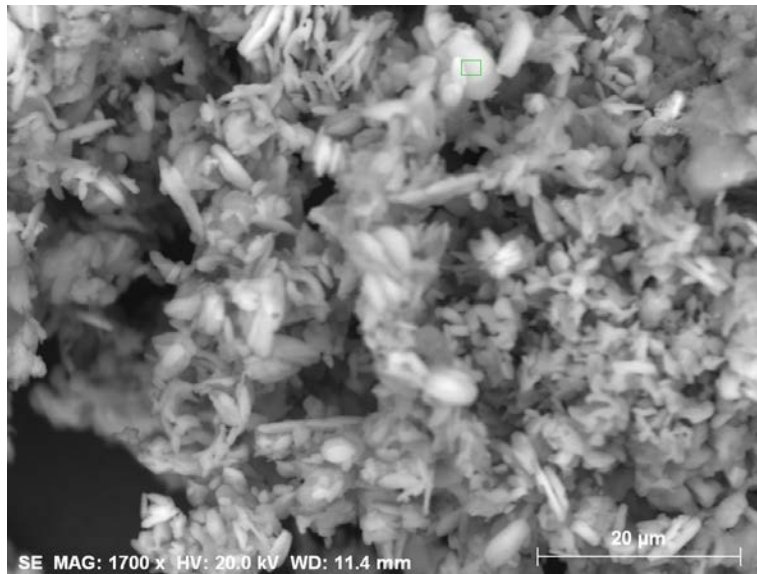
Element	AN	series	[wt.%]	[norm. wt.%]	[norm. at.%]	Error in wt.% (1 Sigma)	K fact.	Z corr.	A corr.	F corr.
Carbon	6	K-series	2.544739	2.687945	4.651707	2.552406	0.156971	0.171238	1	1
Oxygen	8	K-series	48.06392	50.76873	65.95743	6.029261	1.693908	0.299714	1	1
Sodium	11	K-series	7.477323	7.898111	7.141012	0.514947	0.071479	1.102117	1	1.00258
Silicon	14	K-series	0.200586	0.211874	0.156807	0.03751	0.001094	1.905933	1	1.016028
Sulfur	16	K-series	14.4487	15.2618	9.893095	0.546707	0.07812	1.919507	1	1.017774
Potassium	19	K-series	13.27932	14.02661	7.457033	0.434605	0.062356	2.195126	1	1.024744
Calcium	20	K-series	8.657709	9.144924	4.742913	0.288269	0.043006	2.100761	1	1.012211
Sum:			94.67229	100	100					



Element	AN	series	[wt.%]	[norm. wt.%]	[norm. at.%]	Error in wt.% (1 Sigma)	K fact.	Z corr.	A corr.	F corr.
Carbon	6	K-series	4.321371	5.061542	8.395135	2.506557	0.162347	0.311773	1	1
Oxygen	8	K-series	39.58665	46.36711	57.73382	4.882957	0.934327	0.496262	1	1
Sodium	11	K-series	17.06072	19.98291	17.31602	1.130554	0.156206	1.276267	1	1.002353
Silicon	14	K-series	0.29704	0.347917	0.246784	0.042261	0.001553	2.210487	1	1.013761
Sulfur	16	K-series	15.40098	18.03888	11.20699	0.580448	0.080178	2.228268	1	1.009683
Potassium	19	K-series	2.078367	2.434353	1.240366	0.096231	0.009302	2.55144	1	1.025728
Calcium	20	K-series	6.631442	7.767285	3.860888	0.228627	0.031355	2.442744	1	1.014103
Sum:			85.37658	100	100					

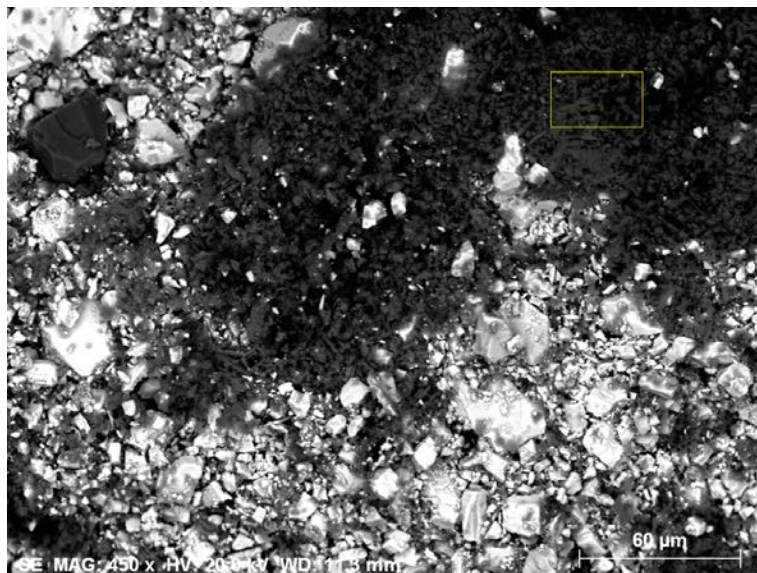


Element	AN	series	[wt.%]	[norm. wt.%]	[norm. at.%]	Error in wt.% (1 Sigma)	K fact.	Z corr.	A corr.	F corr.
Carbon	6	K-series	3.981417	4.223521	7.171626	2.819513	0.199495	0.21171	1	1
Oxygen	8	K-series	45.68374	48.46171	61.77562	5.713434	1.358962	0.356608	1	1
Sodium	11	K-series	11.89634	12.61974	11.19536	0.799836	0.112104	1.122943	1	1.002473
Sulfur	16	K-series	15.24295	16.16985	10.2845	0.575087	0.081383	1.957594	1	1.014956
Potassium	19	K-series	10.77765	11.43303	5.963832	0.359268	0.049945	2.239755	1	1.022038
Calcium	20	K-series	6.68561	7.092153	3.60906	0.230525	0.032662	2.1438	1	1.012856
Sum:			94.26771	100	100					



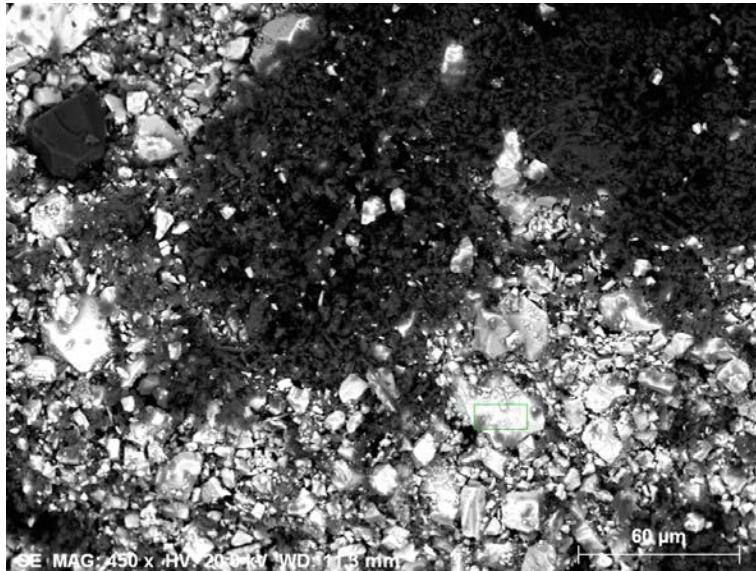
Element	AN	series	[wt.%]	[norm. wt.%]	[norm. at.%]	Error in wt.% (1 Sigma)	K fact.	Z corr.	A corr.	F corr.
Carbon	6	K-series	1.533127	1.624482	2.892703	2.392605	0.096651	0.168077	1	1
Oxygen	8	K-series	47.10135	49.90799	66.71669	6.038547	1.788071	0.279116	1	1
Sodium	11	K-series	5.154963	5.462133	5.081544	0.367312	0.052088	1.04578	1	1.002731
Sulfur	16	K-series	15.15157	16.05441	10.70823	0.572125	0.086514	1.819779	1	1.01974
Potassium	19	K-series	15.40414	16.32203	8.928622	0.498596	0.076481	2.080119	1	1.025968
Calcium	20	K-series	10.03122	10.62895	5.672211	0.328128	0.052787	1.990403	1	1.011639
Sum:			94.37637	100	100					

Sample P6A_15

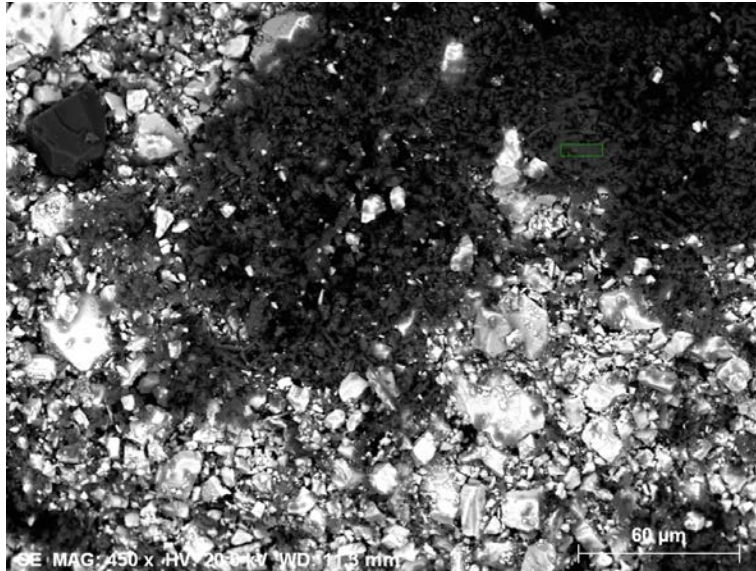


Element	AN	series	[wt.%]	[norm. wt.%]	[norm. at.%]	Error in wt.% (1 Sigma)	K fact.	Z corr.	A corr.	F corr.
Carbon	6	K-series	20.16405	16.07491	24.07154	3.202475	0.466203	0.344805	1	1
Oxygen	8	K-series	58.72536	46.81624	52.62926	7.122241	0.853377	0.5486	1	1

Sodium	11	K-series	21.669	17.27467	13.5148	1.856524	0.187565	0.919238	1	1.001915
Aluminium	13	K-series	0.604279	0.481735	0.321126	0.060596	0.00405	1.182551	1	1.00586
Silicon	14	K-series	0.242674	0.193461	0.123893	0.039593	0.001204	1.590168	1	1.010143
Sulfur	16	K-series	13.45086	10.72311	6.014653	0.510793	0.066295	1.601742	1	1.009831
Calcium	20	K-series	8.761953	6.985085	3.13473	0.288768	0.039065	1.753382	1	1.019787
Barium	56	L-series	1.819838	1.450787	0.190008	0.091449	0.011277	1.255524	1	1.024682
Sum:			125.438	100	100					

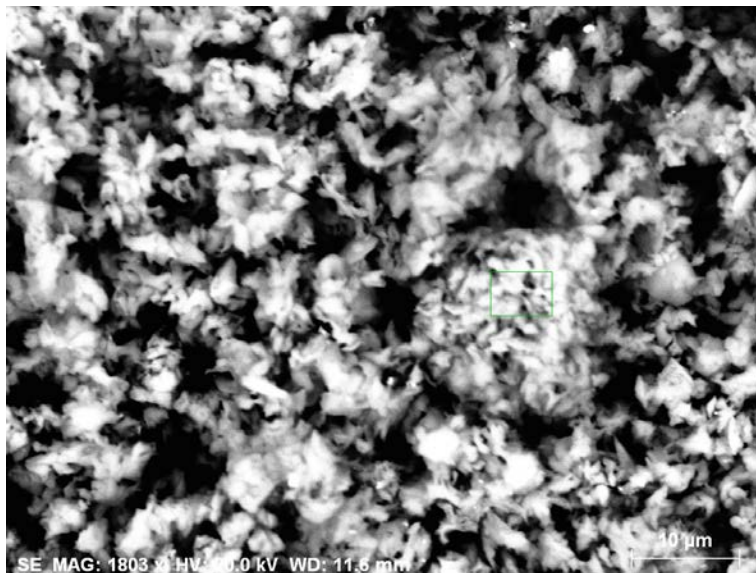


Element	AN	series	[wt.%]	[norm. wt.%]	[norm. at.%]	Error in wt.% (1 Sigma)	K fact.	Z corr.	A corr.	F corr.
Carbon	6	K-series	12.29826	11.91496	28.44031	2.047376	0.280745	0.424406	1	1
Oxygen	8	K-series	27.13551	26.28978	47.109	3.494203	0.447984	0.586847	1	1
Sodium	11	K-series	2.502681	2.42468	3.023713	0.472412	0.025604	0.944155	1	1.003001
Aluminium	13	K-series	0.398486	0.386067	0.410219	0.052323	0.003243	1.181025	1	1.007947
Sulfur	16	K-series	11.41255	11.05685	9.885701	0.441107	0.070426	1.540729	1	1.019002
Calcium	20	K-series	1.996413	1.934191	1.383611	0.093174	0.011008	1.612619	1	1.089547
Strontium	38	L-series	1.26949	1.229924	0.402435	0.091398	0.015926	0.764139	1	1.010669
Barium	56	L-series	46.20357	44.76355	9.34501	1.305444	0.385823	1.131178	1	1.025665
Sum:			103.217	100	100					



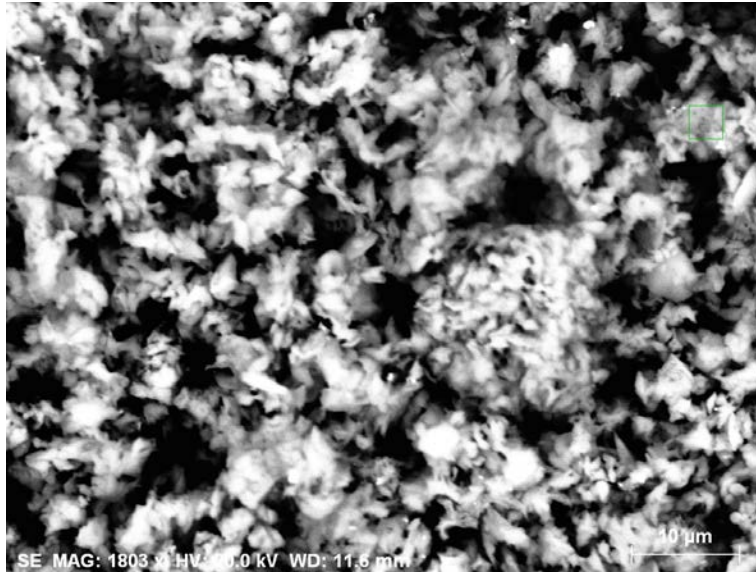
Element	AN	series	[wt.%]	[norm. wt.%]	[norm. at.%]	Error in wt.% (1 Sigma)	K fact.	Z corr.	A corr.	F corr.
Carbon	6	K-series	16.66415	15.3383	23.50764	2.651927	0.49978	0.306901	1	1
Oxygen	8	K-series	56.05526	51.59533	59.36325	6.904899	0.977743	0.527698	1	1
Sodium	11	K-series	3.388563	3.118959	2.497388	0.458527	0.029943	1.039254	1	1.002287
Aluminium	13	K-series	0.313788	0.288822	0.197049	0.044614	0.002147	1.335163	1	1.007614
Sulfur	16	K-series	12.90506	11.87829	6.818992	0.490968	0.064797	1.805254	1	1.015456
Calcium	20	K-series	17.47691	16.0864	7.388627	0.542107	0.080215	1.972023	1	1.016925
Barium	56	L-series	1.84033	1.693907	0.227057	0.095335	0.01177	1.410714	1	1.020172
Sum:			108.6441	100	100					

Sample P6A_18



Element	AN	series	[wt.%]	[norm. wt.%]	[norm. at.%]	Error in wt.% (1 Sigma)	K fact.	Z corr.	A corr.	F corr.
Carbon	6	K-series	11.36582	10.2822	16.40963	2.018446	0.281878	0.364774	1	1

Oxygen	8	K-series	49.80542	45.05699	53.98216	6.175393	0.80613	0.55893	1	1
Sodium	11	K-series	22.40119	20.26547	16.89716	1.478231	0.216978	0.932257	1	1.001858
Aluminium	13	K-series	0.285385	0.258176	0.183418	0.044478	0.002139	1.199957	1	1.00579
Silicon	14	K-series	0.608532	0.550515	0.375733	0.056026	0.003378	1.614002	1	1.009752
Sulfur	16	K-series	10.15237	9.184447	5.490349	0.393073	0.055783	1.626601	1	1.012214
Calcium	20	K-series	14.06374	12.72291	6.085161	0.442095	0.070272	1.782424	1	1.015759
Iron	26	K-series	1.856269	1.679293	0.576392	0.089475	0.008708	1.817322	1	1.061089
Sum:			110.5387	100	100					

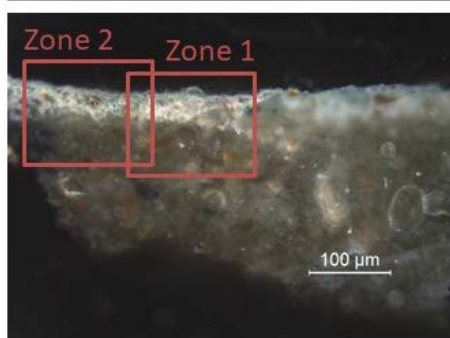
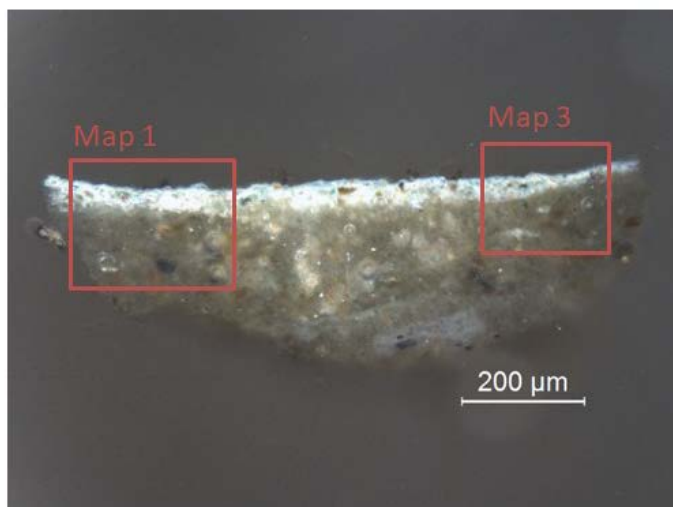


Element	AN	series	[wt.%]	[norm. wt.%]	[norm. at.%]	Error in wt.% (1 Sigma)	K fact.	Z corr.	A corr.	F corr.
Carbon	6	K-series	29.84212	24.11812	34.72851	4.739473	0.558146	0.432111	1	1
Oxygen	8	K-series	45.23003	36.55448	39.51472	5.79265	0.565077	0.646894	1	1
Sodium	11	K-series	27.83	22.49194	16.92054	1.832205	0.252615	0.88859	1	1.001996
Sulfur	16	K-series	18.89494	15.27071	8.236383	0.705425	0.09756	1.556255	1	1.005791
Calcium	20	K-series	1.170453	0.945949	0.40821	0.064625	0.00543	1.709742	1	1.018853
Iron	26	K-series	0.765664	0.618802	0.191635	0.052837	0.003262	1.749499	1	1.084347
Sum:			123.7332	100	100					

Appendix IX: Combined analyses of cross sections

Analyses of 12 cross section from murals 2,3 and 6.

P2_4



SEM-EDS analysis:

Map 1:

Area 1 (grain in the upper layer): Na, Mg, Al, Si, S, K, Ca, Ti

Area 2 (Orange grain in down layer): Na, Mg, Al, Si, S, Cl, K, Ca, Ti, Fe

Area 3 (matrix in upper layer): Mg, Al, Si, S, Cl, K, Ca, Ti, Fe

Area 4 (matrix): Na, Mg, Al, Si, S, Cl, K, Ca, Ti, Fe

Area 5 (matrix upper layer): Mg, Al, Si, S, Cl, K, Ca, Ti, Fe

Point 1 (point in upper layer): Na, Mg, Al, Si, S, Cl, K, Ca, Ti, Fe

Map 2:

Point 1 (blue particle): Na, Mg, Al, Si, S, Cl, Ca, Ti, Cr, Fe, Cd

Point 2 (particle in upper layer): Na, Mg, Al, Si, P, S, Cl, Ca, Ti, Fe, Cd

Area 1 (matrix in upper layer): Na, Mg, Al, Si, S, Cl, K, Ca, Ti, Cr, Fe

Area 2 (matrix in the upper part): Na, Mg, Al, Si, S, Cl, K, Ca, Ti, Fe

Observations:

Sample comes from Angel's dress, greenish blue.

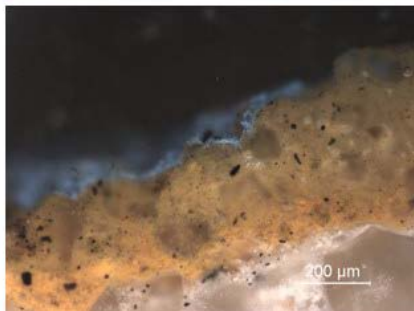
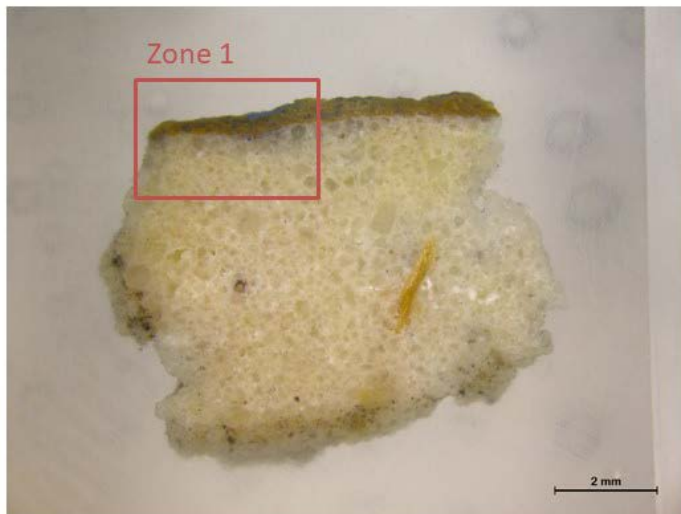
Flaking area.

Upper layer is Ti based.

Cr and Cd might indicate bluish pigment.

Sample for FTIR

P2_8



SEM-EDS analysis:

Point 1 (point in blue part of upper layer): Na, Mg, Al, Si, P, S, Cl, K, Ca, Ti, Fe

Point 2 (same as previous): Na, Mg, Al, Si, P, S, Cl, Ca, Ti, Fe

Point 3 (another point in blue): Na, Mg, Al, Si, S, Cl, K, Ca, Ti, Cr, Fe

Point 4 (same as previous): Na, Mg, Al, Si, Cl, K, Ca, Ti, Cr, Fe

Area 1 (grain in upper layer): Na, Mg, Al, Si, S, Cl, Ca

Area 2 (matrix of brownish layer): Na, Mg, Al, Si, S, Cl, K, Ca, Fe

Area 3 (grain in the upper layer): Na, Mg, Al, Si, P, S, Cl, Ca, Fe

Area 4 (matrix of upper brown layer): Na, Mg, Al, Si, S, Cl, K, Ca, Fe

Area 5 (matrix of mortar): Na, Mg, Al, Si, S, Cl, Ca

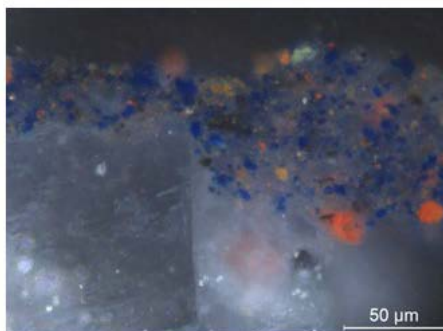
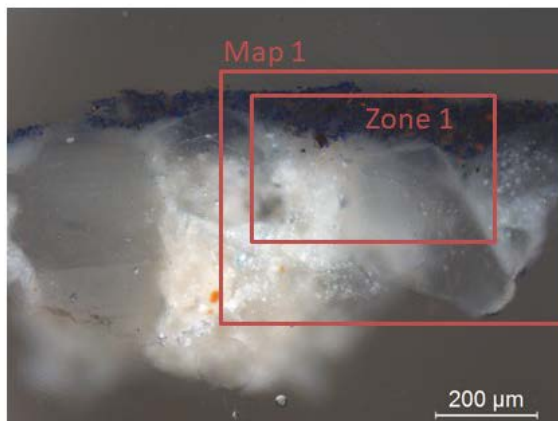
Area 6 (grain in mortar): Mg, Al, Si, Ca

Observations:

Sample comes from the bottom of Angel's foot.
Homogeneous area.

Bluish part is Ti white mixed with Ultramarine blue
Brownish part is Fe based.

P3B_2 (Close to P3B_5 and P3B_6)



SEM-EDS analysis:

Map 1 (zone 1):

Area 1 (big grain): Na, Mg, Al, Si, S, Cl, Ca

Area 2 (white matrix): Na, Mg, Al, Si, S, Cl, Ca

Area 3 (blue pigment): Na, Al, Si, S, K, Ca, Fe

Area 4 (black grain in pigment area): Na, Mg, Al, Si, P, S, Cl, K, Ca

Area 5 (grain in pigment layer): Na, Mg, Al, Si, P, S, Cl, K, Ca, Ti, Fe

Area 6 (matrix, blue): Na, Mg, Al, Si, S, Cl, K, Ca

Observations:

Sample comes from the sailor's baret, dark blue colour.

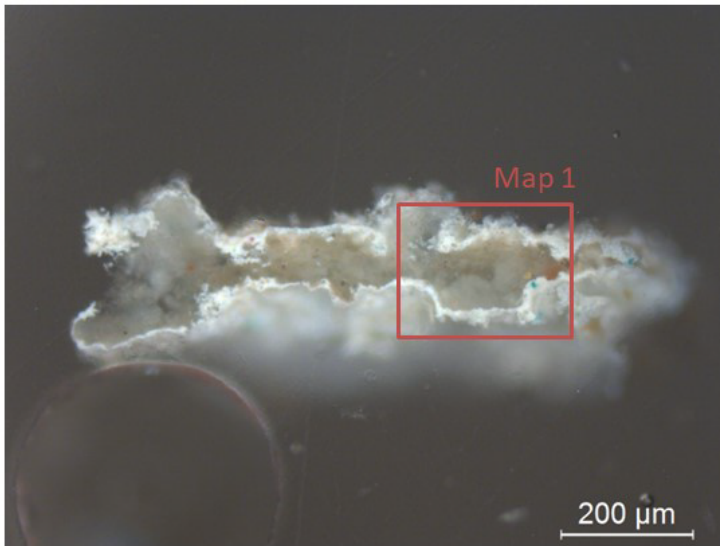
Grains of CaCO_3 present. Used as aggregate?

Blue pigment might be ultramarine blue (presence of Al, S, Si..)

Here we can recognize that technique was fresco painting, probably lime fresco because in case of buon fresco the pigment layer would be thinner.

Presence of P, probably to make blue pigment darker.

P6A_3 (close to P6A_2)



SEM-EDS analysis:

Map 1:

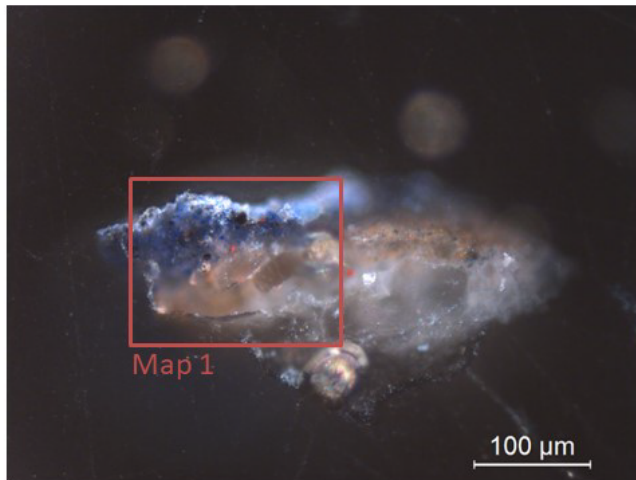
Area 1 (white frame): Na, Mg, Al, Si, S, Cl, K, Ca, Ti, Cr, Fe
 Area 2 (matrix): Na, Mg, Al, Si, S, Cl, K, Ca
 Area 3 (matrix): Na, Mg, Al, Si, S, Cl, K, Ca, Te
 Area 4 (matrix): Na, Mg, Al, Si, S, Cl, Ca, Te
 Area 5 (brownish grain): Na, Mg, Al, Si, S, Cl, K, Ca, Ti, Fe
 Area 6 (whitish veil): Na, Mg, Al, Si, S, Ca, Ti, Te
 Point1 (blue in white): Na, Mg, Al, Si, S, Cl, K, Ca, Ti, Cr

Observations:

Sample is taken from the area of greenish background.
 Presence of Ti, probably to achieve the lighter hue of green.
 White 'frame' around the sample is thin layer of Ti.
 Presence of salts (NaCl in particular) is also detected in this area.
 Te present in spectrum (in relation to Ca)

Yellow particles Fe based
 Blue particles S based

P6A_7



SEM-EDS analysis:

Point 1 (blue pigment): Na, Mg, Al, Si, P, S, K, Ca
 Point 2 (black grain): Na, Mg, Al, Si, P, S, Cl, K, Ca
 Point 3 (grain in mortar): Na, Mg, Al, Si, S, Cl, K, Ca, Fe, Ba
 Point 4 (grains in mortar): Na, Mg, Al, Si, S, K, Ca, Ba
 Point 5 (grain in pigment): Na, Mg, Al, Si, S, K, Ca, Ba
 Area 1 (matrix of pigment): Mg, Al, Si, S, Cl, K, Ca, Fe, Ba
 Area 2 (aggregate grains): Mg, Al, Si, S, Cl, Ca
 Area 3 (matrix): Mg, Al, Si, S, Cl, K, Ca, Fe, Ba
 Area 4 (matrix in pigment): Na, Mg, Al, Si, P, S, Cl, K, Ca
 Area 5 (matrix in pigment): Na, Mg, Al, Si, P, S, K, Ca

Observations:

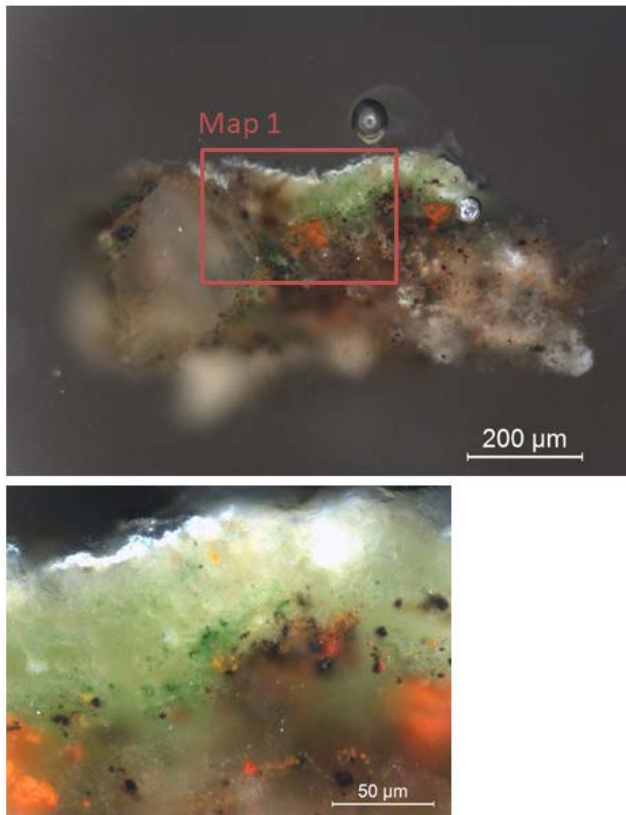
Sample is coming from shoulder sleeve of blue pigment. Flaking.

Large concentration of S and Ca in upper (blue) layer, also presence of Na, where S and Na might indicate pigment. EDS confirmed that blue comes from Ultramarine blue (p1).

CaCO₃ is used as aggregate, and intonaccho is also made with it. There is presence of gypsum in the upper layer but because its spread evenly, probably it was mixed with pigment and doesn't come from salt formation.

It is not possible to say if this area was painted fresco since layers in the sample are well separated.

P6A_10



SEM-EDS analysis:

Area 1 (big gran on the left): Na, Si, S, Cl, Ca
 Area 2 (matrix): Mg, Al, Si, S, K, Ca, Fe
 Area 3 (grain in matrix): Na, Mg, Al, Si, S, Cl, K, Ca, Ti, Fe
 Area 4 (matrix in pigment layer): Na, Mg, Al, Si, S, Cl, K, Ca, Fe, Ba
 Point 1 (grain in the matrix): Al, Si, P, S, K, Ca, Fe, Ba

Observations:

Sample is coming from green background affected by flaking in panel 6.

Orange areas are Fe based. Big grains of CaCO_3 present, and gypsum as well, probably previously mixed with pigment.

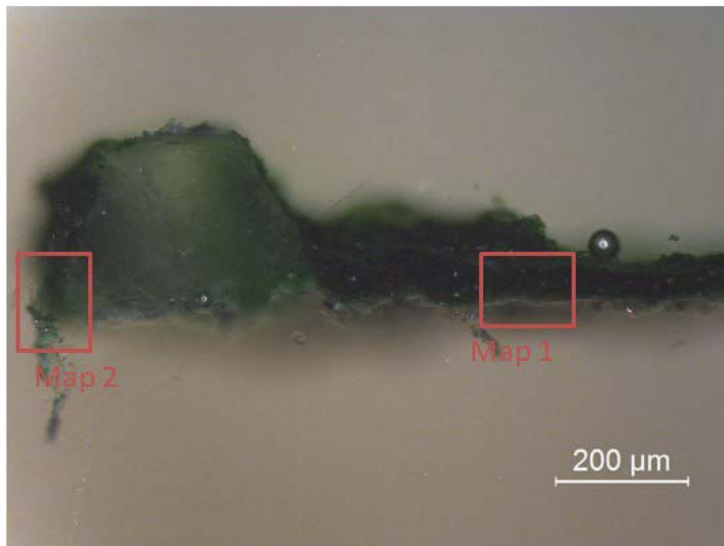
Fe, Mg, Al, K might indicate red ochre.

Hipotesis 1: green pigment is green earth.

Hipotesis 2: green pigment is Cobalt titanate green (Co_2TiO_4)

Sample for FTIR! (origin of green might be organic)

P6A_14 (Close to P6A_15)



SEM-EDS analysis:

Map 1:

Area 1 (grain): S, Ca, Sr, Ba
 Area 2 (down edge matrix): Na, Al, S, Cl, K, Ca, Fe, As, Sr, Ba
 Area 3 (matrix): Na, Mg, Al, S, Cl, K, Ca, Fe, Sr, Ba
 Area 4 (matrix upper layer): Na, Mg, Al, S, Cl, Ca, Fe, Sr, Ba
 Area 5 (grain upper layer): Na, Mg, S, Cl, Ca, Fe, Sr, Ba
 Area 6 (batch, matrix with grains): Na, Mg, S, Cl, K, Ca, Fe, Sr, Ba

Map 2:

S, Ca, Ba

Observations:

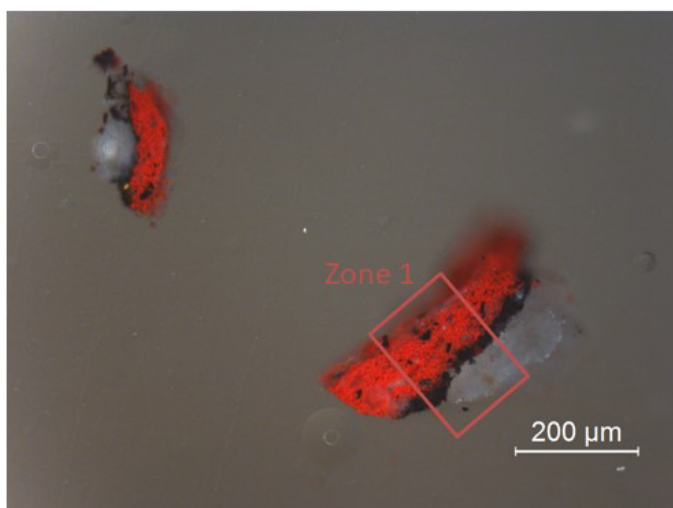
Sample comes from green ship in the panel 6.

Preceence of barium sulphate, big grain on the left is CaCO_3 (visible in the SEM image of Map 2).

Could the green pigment be Emerald green ($\text{Cu}(\text{AsO}_2)_2 \cdot \text{Cu}(\text{CH}_3\text{COO})_2$) since EDXRF shows presence of Cu? As can be related to Emerald green as well.

Check again under UV for organic binder

P6A_17 (Close to P6A_18)



SEM-EDS analysis:

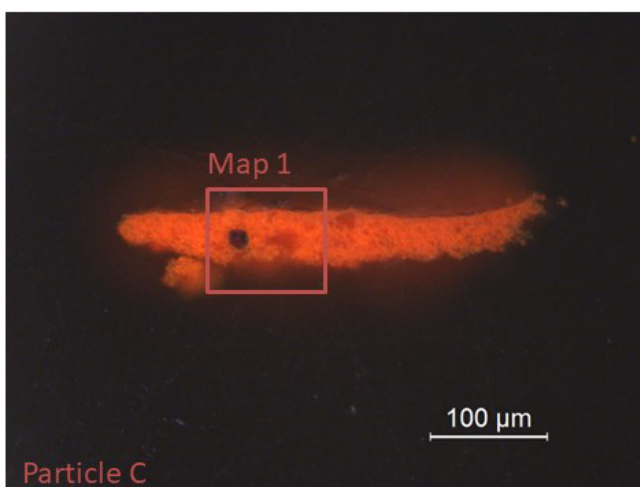
Fragment A (bigger)

Area 1 (grain): S, Ca
 Area 2 (matrix black layer): Na, Mg, Al, Si, P, S, Cl, Ca
 Area 3 (grain): Na, Mg, Al, Si, P, S, Cl, Ca, Fe, Te
 Area 4 (grain in red layer): Na, Mg, Al, Si, P, S, Cl, Ca, Fe
 Area 5 (grain): Na, Mg, Al, P, S, Cl, K, Ca, Fe, Zr
 Area 6 (matrix in red): Na, Mg, Al, Si, S, K, Ca, Fe
 Area 7 (matrix between red and black): Na, Mg, Al, Si, P, S, Cl, Ca
 Area 8 (matrix in red): Na, Si, P, S, Cl, K, Ca, Fe
Fragment B (smaller)

Observations:

Sample comes from dark red sleeve (panel 6).
 Black pigment might be bone black (based on concentration of Ca and P).
 Red pigment might be ochre: due to the presence of Al in relation to Fe.
 Grains of CaCO₃ across the matrix as an aggregate.

P6A_20



SEM-EDS analysis:

Fragment A:

Area 1 (matrix): Na, Mg, Al, Si, S, Cl, K, Ca
 Area 2 (grains in the matrix): Al, Si, S, Cl, Ca
 Area 3 (matrix): Na, Mg, Al, Si, S, Cl, Ca
 Area 4 (matrix): Na, Mg, Al, Si, S, Cl, Ca
 Area 5 (matrix): Mg, Al, Si, P, S, Cl, Ca
 Area 6 (grain in matrix): Mg, Al, Si, S, Cl, Ca, Fe, As
 Point 1 (grain in upper layer): Mg, Al, Si, S, Cl, Ca, Fe, Zn

Fragment B:

Area 1 (matrix): Na, Mg, Al, Si, S, Cl, K, Ca
 Area 2 (grain in matrix): Si, S, Cl, Ca
 Area 3 (matrix of red pigment): Na, Mg, Si, S, Cl, Ca, Fe
 Area 4 (red grain in layer of red pigment): Al, S, Cl, Ca, Fe, Sr, Ba
 Area 5 (matrix in red layer): Al, Si, S, Cl, Ca, Fe
 Area 6 (grain in layer of pigment): Mg, Al, Si, S, Cl, K, Ca, Fe, Zn

Fragment C:

SEM image: Si, S, Ca, Fe, Ba

Observations:

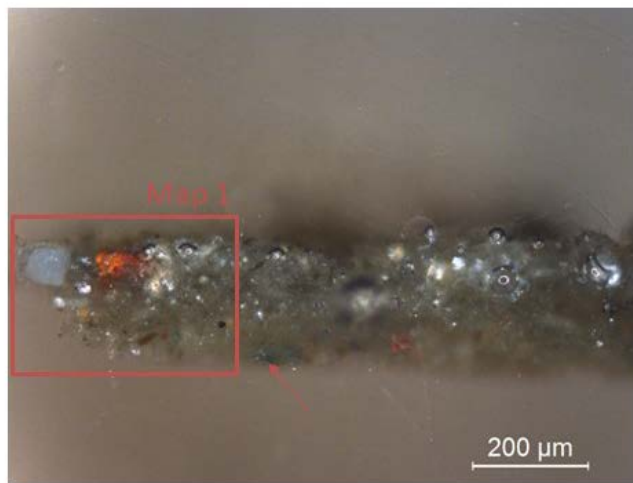
Sample is coming from the arm of figure 2 in panel 6, red pigment.

Pigment is Fe based, probably red ochre due to the presence of K, Al, Fe.
 Barium sulphate is used as filler.

Sample for FTIR!



P6A_23

**SEM-EDS analysis:**

Area 1 (light blue grain on the left): Na, Mg, Al, Si, S, Cl, Ca

Area 2 (redish grain on the left): Na, Mg, Al, Si, S, Cl, K, Ca, Fe, Ba

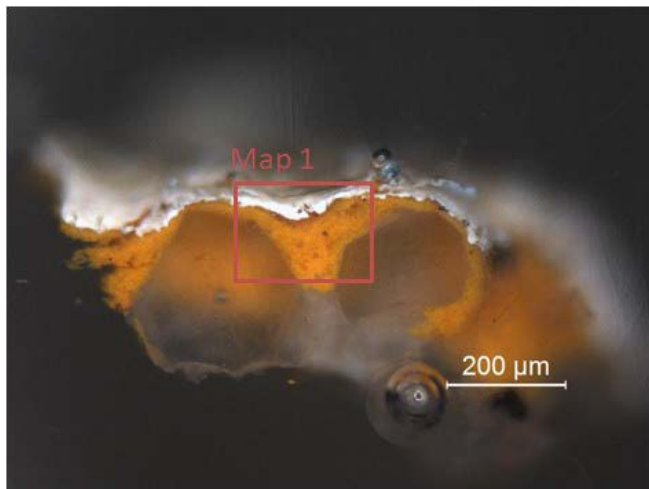
Area 3 (grain in green matrix): Na, Mg, Al, Si, S, Cl, K, Ca, Fe

Observations:

Sample is coming from green background of panel 6.
Area is flaking.

Whitish - bluish grain: calcium sulphate
Red grains: Fe based

P6C_2

**SEM-EDS analysis:**

Area 1 (matrix in white layer): Na, Mg, Al, Si, P, S, Cl, Ca, Ti, Fe, Cd

Area 2 (matrix of orange pigment): Na, Mg, Al, Si, P, S, Cl, Ca, Fe, Cd, Te

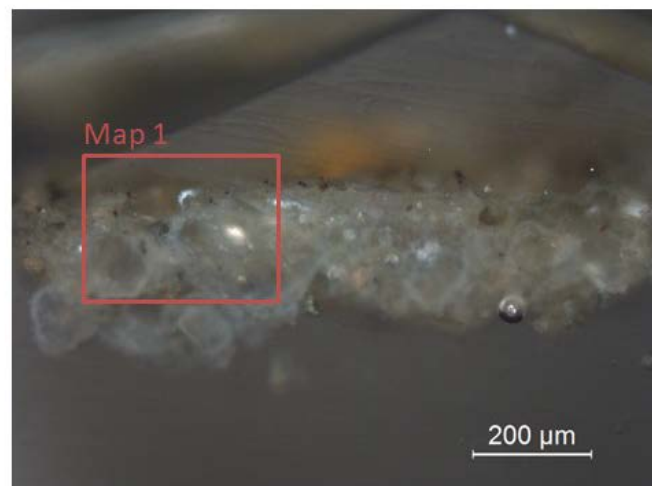
SEM image: S, Ca, Ti, Fe

Observations:

Sample comes from the whitish part of rope in the panel 6.
Based on EDS white layer is Ti based. Orange pigment is Fe based.
Based on SEM image, large grains are CaCO_3 .

Pigment might be Cadmium (mixed with ochre).

P6C_5

**SEM-EDS analysis:**

Area 1 (grain in the upper layer): Na, Mg, Al, Si, S, Ca, Fe

Area 2 (matrix in upper layer): Mg, Al, Si, S, Ca, Fe

Area 3 (matrix in upper layer): Mg, Al, Si, S, Ca, Fe

Observations:

Sample comes from bluish green background in the down part of panel 6.

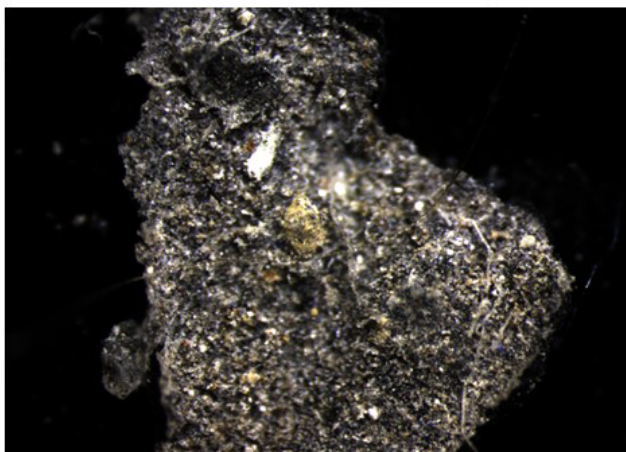
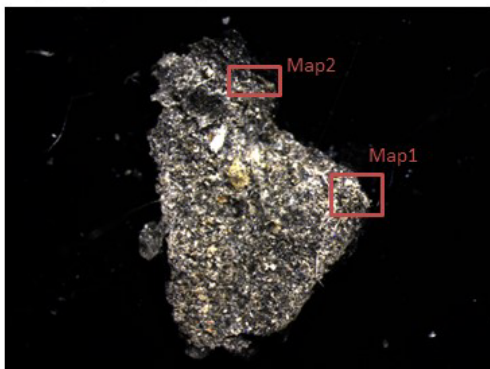
Does gypsum comes from neo-formation or is it from the origin?

Sample for FTIR

Appendix X: Combined analyses of micro-fragments and powder samples

Analyses of 12 cross section from murals 2,3 and 6.

P2_9 –paint layer and fibres on the surface



SEM-EDS analysis:

Map 1:

Area 1 (fibre): C, O, Na, Mg, Al, Si, P, S, Cl, K, Ca
 Area 2 (matrix): C, O, Na, Mg, Al, Si, P, S, Cl, K, Ca, Fe
 Area 3 (matrix): C, O, Na, Mg, Al, Si, P, S, Cl, K, Ca, Ti, Fe
 Area 4 (matrix): C, O, Na, Mg, Al, Si, P, S, Cl, K, Ca, Ti, Fe
 Area 5 (grain in the matrix): C, O, Na, Mg, Al, Si, S, Cl, K, Ca, Fe, Ba
 Point 1 (grain in the matrix): C, O, Na, Al, Si, P, S, Cl, K, Ca, Fe

Map 2:

Area 1 (matrix): C, O, Na, Mg, Al, Si, P, S, Cl, K, Ca, Fe
 Area 2 (grain in the matrix): C, O, Na, Mg, Al, Si, P, S, Cl, K, Ca, Ti, Fe

Observations:

P2A_9 is one of the fragments that comes from the base of the panel two.

Areas 1 and 2 differ in the amount of Cl (higher in area 1), Si is higher in area 2, both show presence of Na, Mg and Al, although the amount of Al is significantly higher in the area 2.

Phosphorus present might indicate that the pigment was mixed with black in order to achieve darker hue.

P3B_5 –salt efflorescence



SEM-EDS analysis:

Area 1 (matrix): C, O, Na, Al, Si, S, K
 Area 2 (matrix): C, O, Na, Al, Si, S, K, Ca, Fe
 Area 3 (matrix): C, O, Na, Al, Si, S, K, Ca
 Area 4 (elongated grain): C, O, Na, Al, Si, S, K, Ca

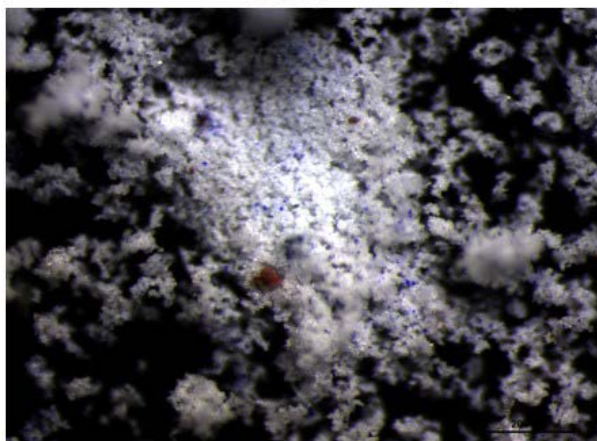
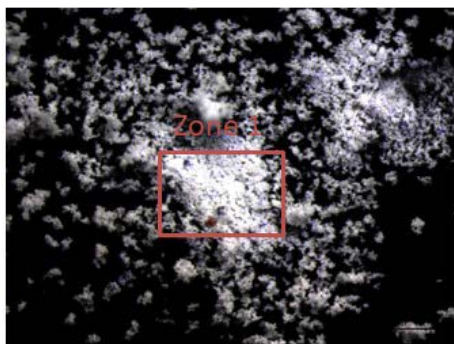
Observations:

Sample comes from sailor's hair, area of dark pigment affected by salts.

No indications of pigment.

Areas differ in the presence of Fe, that is detected only in the area 2. Furthermore, area 1 shows significantly higher amount of K, while the amount of Na is higher in the area 2.

P3B_6 –salt efflorescence



SEM-EDS analysis:

Area 1: C, O, Na, Si, S, K

Area 2: C, O, Na, S, K

Area 3: C, O, Na, Si, S, K, Ca

Observations:

Sample comes from sailor's beret ribbon, which is the area of strong blue pigment.

Presence of salts detected, including K and Na. It might be Aphthalite ($(K, Na)_3Na(SO_4)_2$)

P6A_2f –salt efflorescence



SEM-EDS analysis:

Zone1:

Area 1 : C, O, Na, Si, S, K, Ca

Area 2: C, O, Na, Si, S, K, Ca

Area 3: C, O, Na, S, K, Ca

Area 4: C, O, Na, S, K, Ca

Zone2:

Area 1: C, O, Na, S, K, Ca

Area 2: C, O, Na, S, K, Ca, Cu

Area 3: C, O, Na, Al, Si, S, K, Ca

Area 4: C, O, Na, Si, S, K, Ca, Cu

Observations:

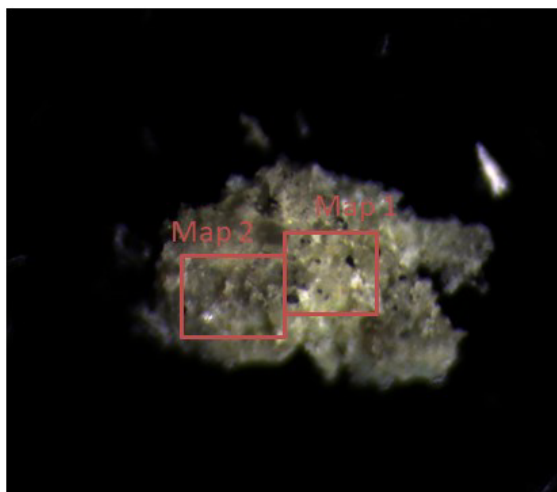
Sample comes from green flaking background of panel 6.

Presence of mineral with both K and Na, in different amounts. Possibility: Aphthalite ($(K, Na)_3Na(SO_4)_2$).

Higher presence of Na in the zone 2, and on the opposite to that, presence of K is higher within the zone 1.

This might also be confirmed by the shape of the grains, where zone 1 shows presence of more round shaped grains while zone 2 has more elongated grains.

P6A_3 (green background)

**SEM-EDS analysis:****Map 1:**

Point 1: C, O, Na, Mg, Al, Si, S, K, Ca, Ti, Fe
 Point 2: C, O, Al, Si, S, K, Ca, Ba
 Point 3: C, O, Mg, Al, Si, S, K, Ca, Ti, Cr, Fe, Zn
 Point 4: C, O, Na, Mg, Al, Si, S, Cl, K
 Area 1: C, O, Al, Si, S, K, Ca, Ti, Fe
 Area 2: C, O, Na, Mg, Al, Si, S, Cl, K, Ca, Ti, Fe
 Area 3: C, O, Na, Mg, Al, Si, S, K, Ca, Fe

Map 2:

Area 1: C, O, Si, S, K, Ca, Ti, Fe
 C, O, Al, Si, S, K, Ca, Ti

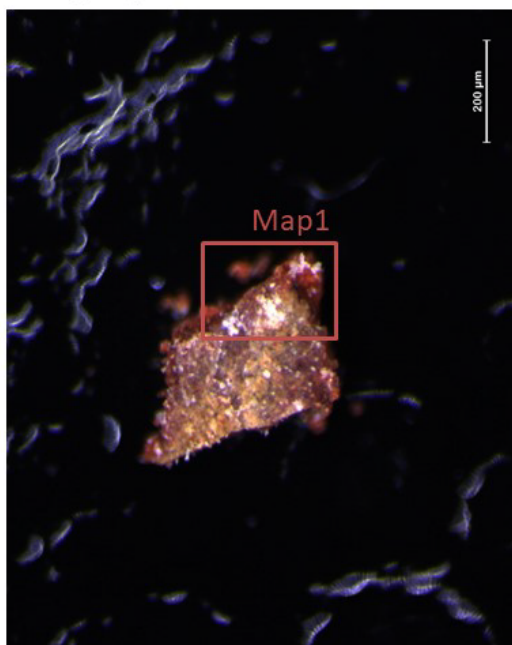
Observations:

Sample comes from the area of greenish background of panel 6.

Ti was detected in the zone 1, barium in zone 2. Both zones show presence of Al, S and K. Amount of S is higher in zone 2.

Ti might have been used for achieving the lighter hue of green.

P6A_6rep

**SEM-EDS analysis:**

Area 1 (red pigment affected by salts): C, O, Na, Al, Si, S, Cl, K, Ca, Ti, Fe
 Area 2 (matrix of red pigment): C, O, Na, Mg, Al, Si, S, Cl, K, Ca, Ti, Fe
 Area 3 (grain in the matrix): C, O, Al, Si, S, K, Ca, Mn, Fe

Observations:

Sample comes from red flesh tone, neck of the figure in the panel 6.

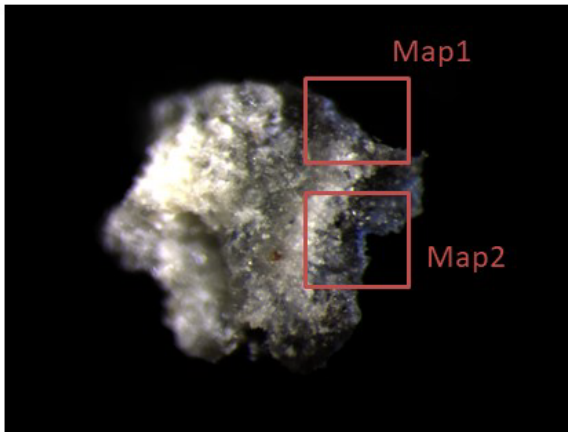
Presence of Calcium Sulphate (in cross section check for presence of salts, or the gypsum comes from origin).

Pigment is Fe based – red ochre.

Area shows greyish brown layer over the layer of pigment. Cross section will show better what it might be.

Sample for FTIR

P6A_7 (flaking shoulder sleeve)



SEM-EDS analysis:

Map 1:

Area 1 (grain in matrix): C, O, Na, Mg, Si, S, K, Ca

Area 2 (matrix): C, O, Na, Al, Si, S, K, Ca

Area 3 (matrix): C, O, Al, Si, S, K, Ca

Area 4 (grain in the matrix): C, O, Si, S, K, Ca, Ba

Area 5: C, O, Si, S, K, Ca

Point 1: C, O, Na, Al, Si, S, K, Ca, Fe

Point 2: C, O, Na, Mg, Al, Si, S, K, Ca, Fe

Map 2:

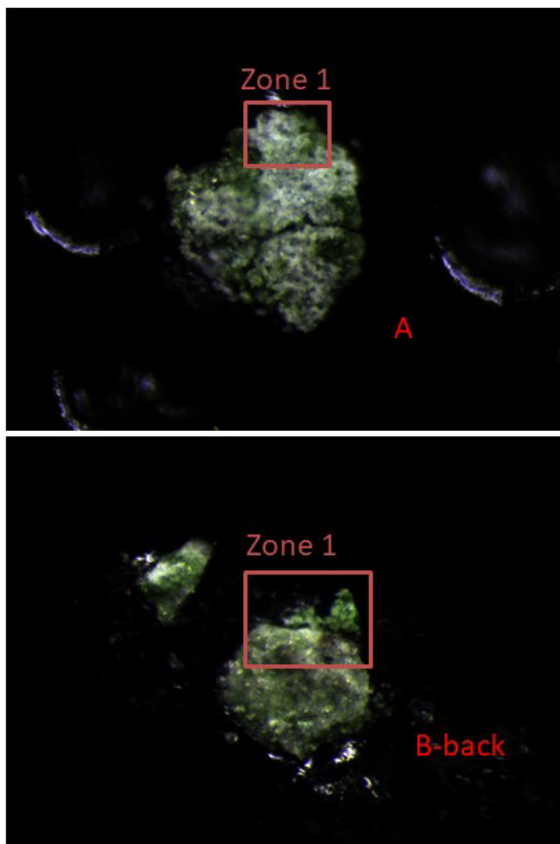
SEM image: Si, K, Ca, Fe

Observations:

Sample comes from flaking shoulder sleeve in the panel 6. (blue pigment)

Areas 1 and 2 differ in the presence of Al and Mg. Pigment was not identified. Mostly salts were detected.

P6A_14f A and B



SEM-EDS analysis:

Part A:

Area 1 (matrix of green pigment affected by salts): C, O, Na, Si, S, Ca, Ba

Area 2 (grain in the matrix): C, O, Na, S, Ca, Sr, Ba

Part B:

Area 1 (matrix): C, O, Na, Al, Si, S, Ca, Ba

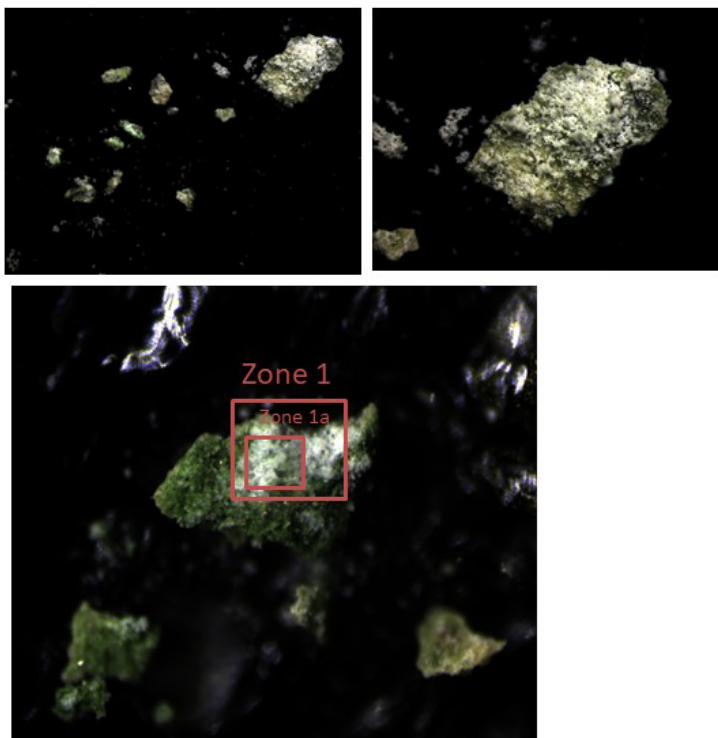
Area 2 (grains in the matrix of pigment): C, O, Na, S, Ca, Fe, Sr, Ba

Area 3 (matrix): C, O, Na, S, Ca, Ba

Observations:

A and B belonged initially to the same microfragment. It was broken to see in A the paint layer and the white particles; in B the back of the microfragment.

P6A_15f –salt efflorescence + green paint layer



SEM-EDS analysis:

Zone 1:

Area 1 (green pigment covered by salts): C, O, Na, Al, Si, S, Ca, Ba

Area 2 (grain in matrix of salts): C, O, Na, Al, S, Ca, Sr, Ba

Area 3 (matrix): C, O, Na, Al, S, Ca, Ba

Zone 1a:

Area 1 (grain in the matrix): C, O, Na, Mg, Al, S, Ca, Sr, Ba

Observations:

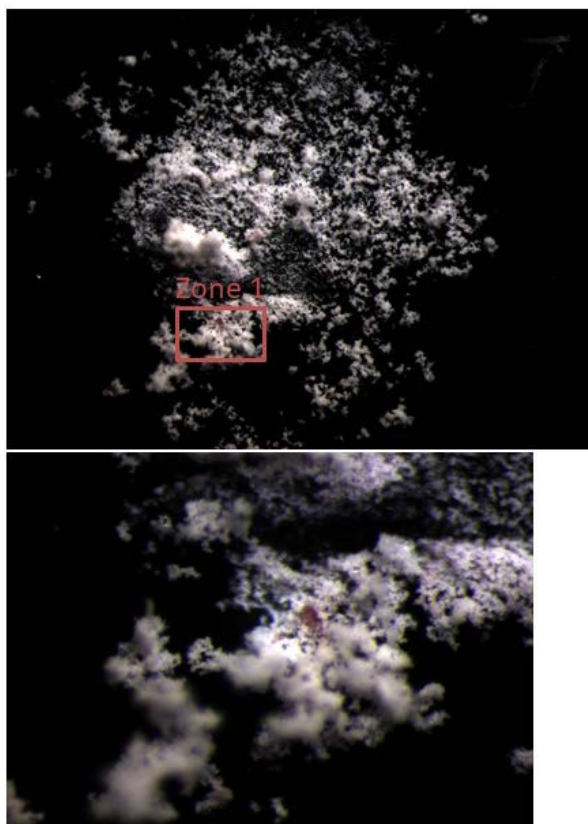
The analysis was made in a microfragment near the edge and not in the bigger microfragment.

Grains of barium sulfate in the green part-pigment filler.

The green pigment is most likely *vert à la chaux*. The XRD analysis on the pigment in powder found at Almada studio has shown barite (barium sulphate). In what concerns the chromophorous, the pigment *vert à la chaux* was apparently prepared with a copper phthalocyanine.

White zone (black in SEM image) is rich in Na (coming from the formation of salts)

P6A_18f –salt efflorescence



SEM-EDS analysis:

Zone 1:

Area 1: C, O, Na, Al, Si, S, Ca, Fe

Area 2: C, O, Na, S, Ca, Fe

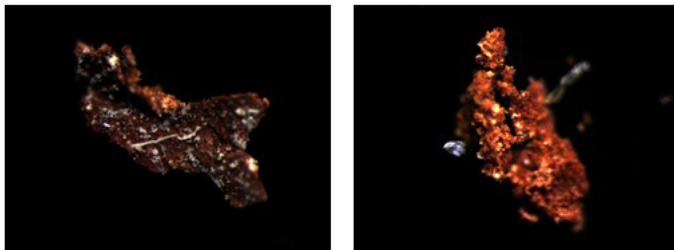
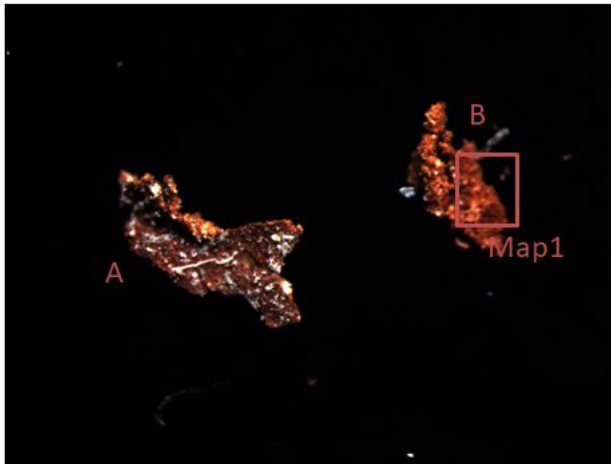
Observations:

Sample comes from dark red sleeve area of panel 6.

Presence of Na might indicate to the formation of Thenardite Na_2SO_4

Pigment is red ochre Fe_2O_3 .

P6A_19 (flaking dark red sleeve)



SEM-EDS analysis:

Fragment A: not done yet

Fragment B:

Area 1 (grain in the matrix of pigment): C, O, Na, Mg, Al, Si, P, S, Cl, K, Ca, Fe, Cd

Area 2 (matrix of pigment): C, O, Na, Mg, Al, Si, S, Cl, K, Ca, Fe

Area 3 (grain in the matrix of pigment): C, O, Na, Al, Si, S, K, Ca, Fe

Area 4 (matrix): C, O, Na, Mg, Al, Si, S, Cl, K, Ca, Fe

Observations:

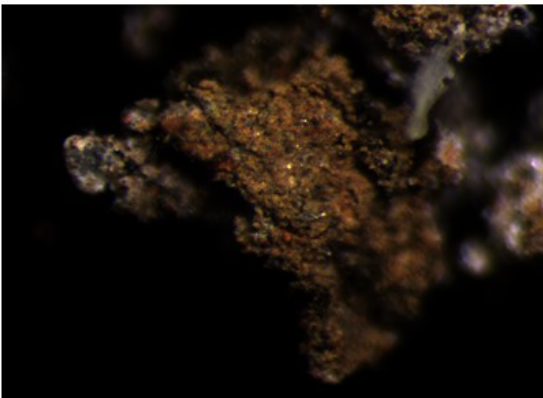
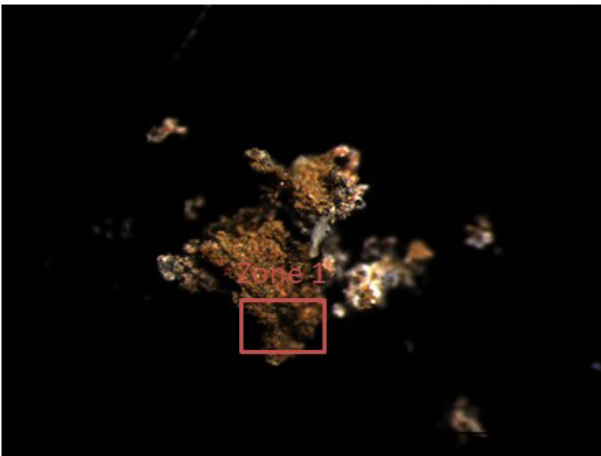
Sample is coming from the area of flaking dark red sleeve in panel 6.

Different orientation of fragments A and B was suitable for analysis of both pigment (fragment B) and deterioration (fragment A).

It is visible in the SEM images of fragment A that pigment has lack of cohesion (presence of cracks and pores)

Pigment is definitely Fe based, probably ochre due to the presence of Al and K. Bone black added for darker hue (was it identified only through the amount of Ca and P)

P6A_21 – pigment lack of cohesion?



SEM-EDS analysis:

SEM image: Ca, Cr, Fe, Si

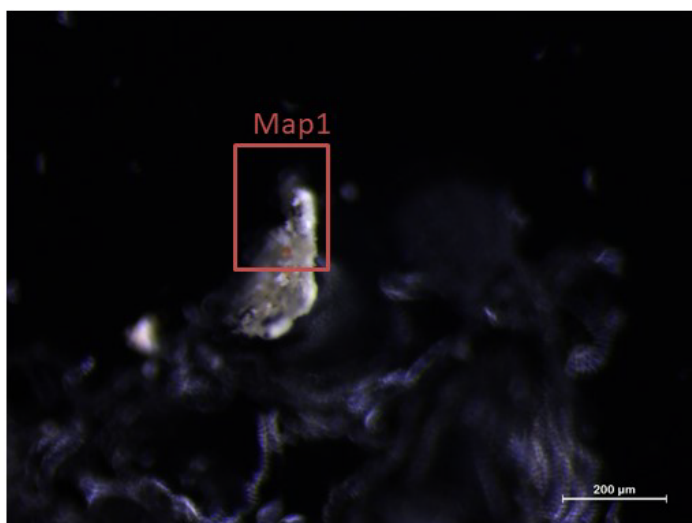
Observations:

Sample comes from the area of dark flaking brown colour.

Similar to the sample P6A_18, Fe might be explained by pigment, probably red ochre Fe_2O_3 . We need others elements to confirm if it is an ochre or not.

One of the salts that can cause flaking and detachment is **gypsum** because due to its low solubility it crystallizes below the surface (ICCROM).

P6C_4

**SEM-EDS analysis:**

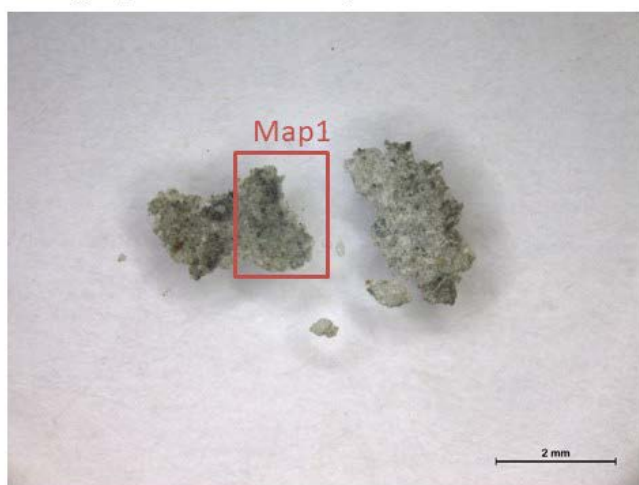
Area 1 (blurred grey layer): C, O, Na, Mg, Al, Si, S, Cl, Ca
 Area 2 (matrix): C, O, Na, Mg, Al, S, Cl, Ca, Fe

Observations:

Sample comes from greenish-yellow background area. Affected by flaking.
 Presence of calcium sulphate.

Hipotesis: Gypsum might have been mixed with pigment – it comes from origin not from formation of salts.

P6C_5 (place that shines)

**SEM-EDS analysis:**

Area 1: C, O, Na, Al, Si, S, Cl, K, Ca, Ti, Fe
 Area 2: C, O, Na, Mg, Al, Si, S, Cl, K, Ca, Ti, Fe
 Area 3: C, O, Al, Si, S, K, Ca, Mn, Fe

Observations:

Sample comes from the area of green flaking background of panel 6.
 Sample seems to have organic fibres.
 Shiny surface might be result of consolidant (fixative), probably put to treat the flaking.

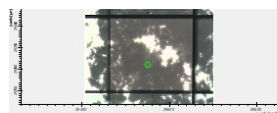
Hipotesis: pigment is Ultramarine blue (due to the presence of Al, Na, S)

Sample for FTIR

Appendix XI: μ -FT-IR Analyses

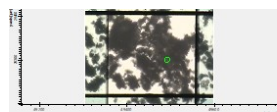
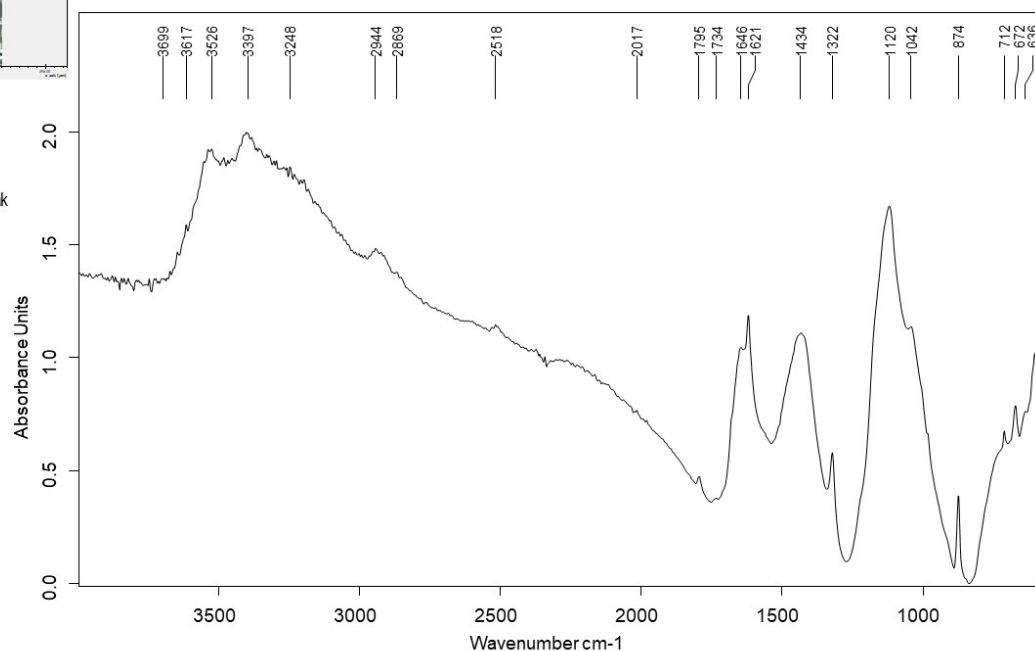
Analyses of 22 using Fourier Transformed Infrared Spectroscopy μ -FT-IR.

Compound	Description	Chemical Formula	Vibrations
Calcite	Calcium carbonate	CaCO_3	2512, 1793, 874, 712 cm^{-1} main peak (carbonate band) 1423 cm^{-1}
Gypsum	Calcium sulfate dihydrate	$\text{CaSO}_4 \cdot 2\text{H}_2\text{O}$	3536, 1682, 1620 cm^{-1} main peak (sulphate band) 1168 cm^{-1}
Oxalate of lime	Calcium oxalate	$\text{CaC}_2\text{O}_4 \cdot (\text{H}_2\text{O})_x$	1620, 1320, -780 cm^{-1}
Barite	Barium sulfate	BaSO_4	1086, 983, 634, 610 cm^{-1} main peak (sulphate band) 1079 cm^{-1}
Kaolinite	Aluminum silicate	$\text{Al}_2(\text{OH})_4\text{Si}_2\text{O}_5$	3689, 3662, 3646, 3615, 1117, 1006, 914, 797, 755, 693 cm^{-1} main peak (silicate band) 1034 cm^{-1}
Bone black	Calcium phosphate	$\text{Ca}_5(\text{OH})(\text{PO}_4)_3$	Broad peak around 3355 cm^{-1} 2917, 2846, 2360, 2334, 2013, 1590, 1462, 1411, 962, 878 cm^{-1} main peak (phosphate band) 1042 cm^{-1}
Quartz	Silicon oxide	SiO_2	1164, 801, 778, 693 cm^{-1} main peak (silicate band) 1079 cm^{-1}
Emerald green	Copper (II)-acetoarsenite	$3\text{Cu}(\text{AsO}_2)_2 \cdot \text{Cu}(\text{CH}_3\text{COO})_2$	1558, 145-818, 765, 640 cm^{-1} main peaks 1558 and 640 cm^{-1}
Polyvinyl	Polymer (acetate)	$\text{CH}_2=\text{CHR}$	-2939, 1735, 1572, 1430, 1374, 1250, 942, 848, 797, 608 cm^{-1} main peaks 1735 and 1250 cm^{-1}

**P2_4**

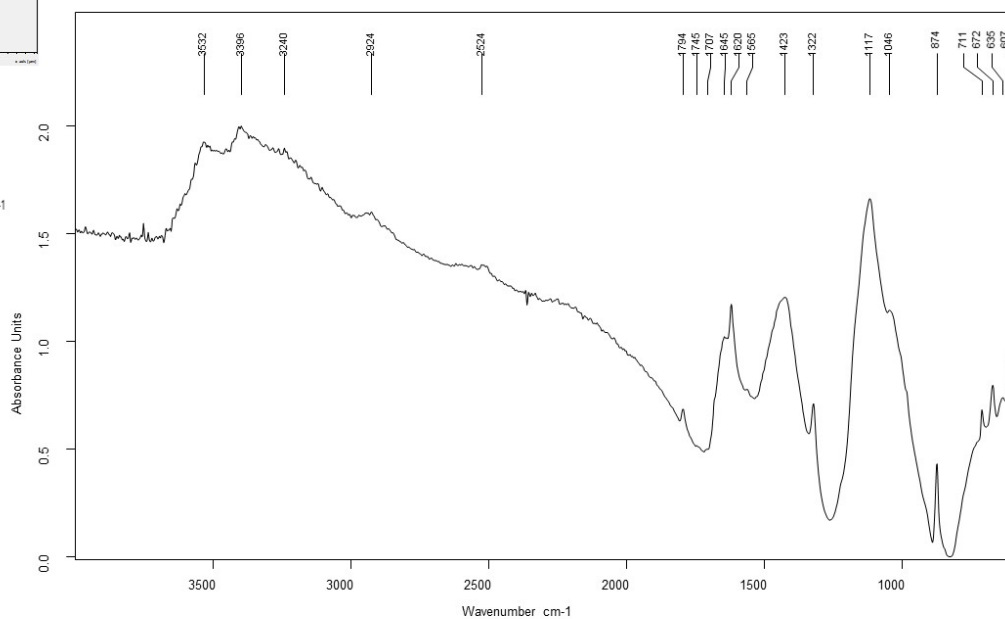
(Angel's shoulder)

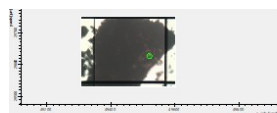
- Possible organic residue due to the peak around 1734 cm^{-1}
- Calcite
- Gypsum
- Barite (984 cm^{-1})
- Oxalates

**P2_4 rep**

(Angel's shoulder)

- Possible organic residue (oil) due to the peaks around 2924 and 1707 cm^{-1}
- Calcite
- Gypsum
- Barite (984 cm^{-1})
- Oxalates

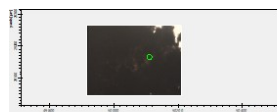
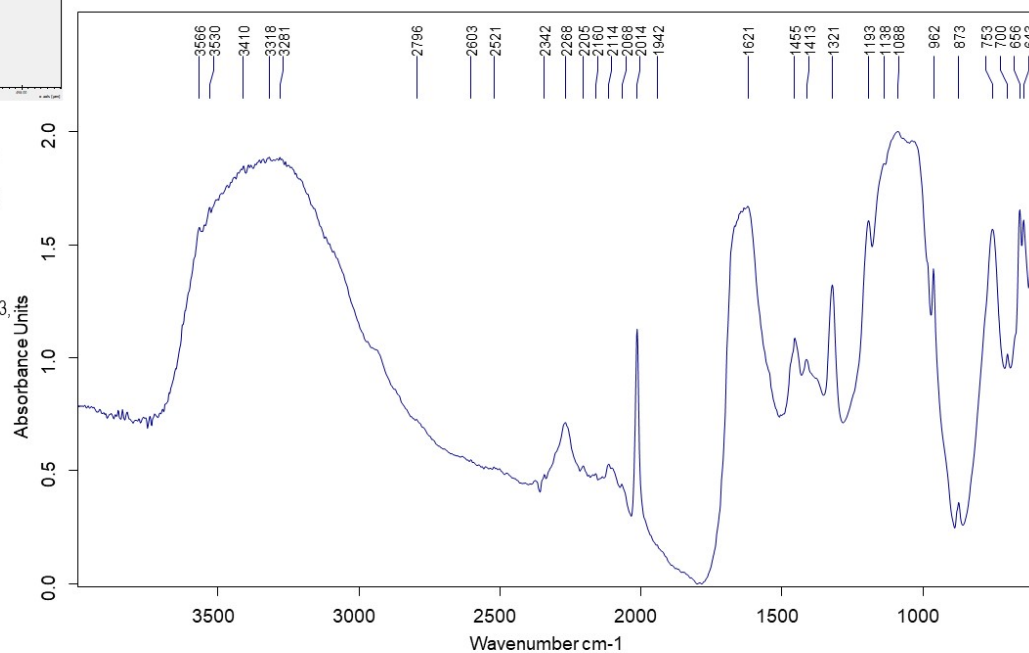




P2_black

(area of dark blue pigment)

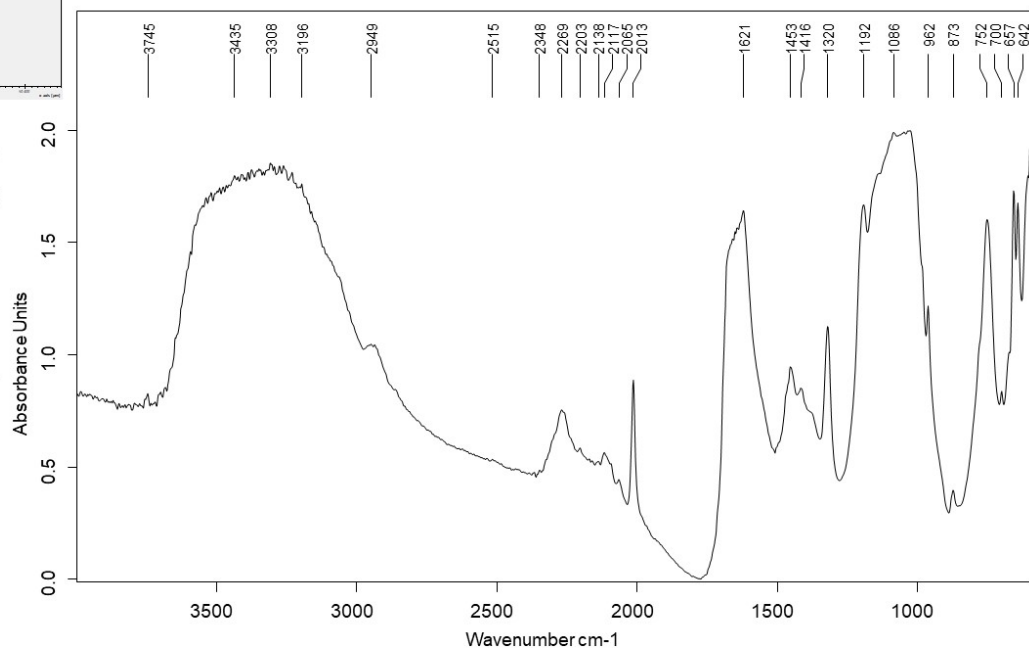
- Bone black (2014 cm^{-1})
- Barium sulphate
- Calcium oxalate
- Identify the inorganic compound with other technique. Peaks at 753 , 656 and 643 cm^{-1} .

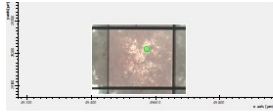


P2_black_rep

(area of dark blue pigment)

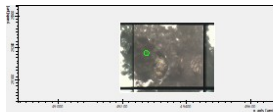
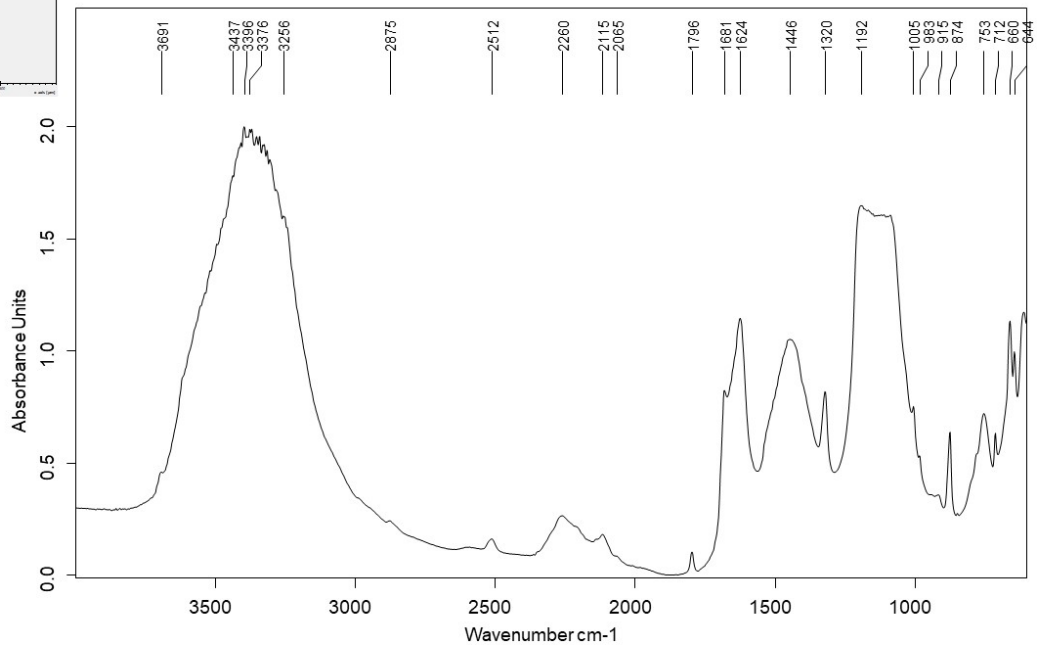
- Bone black (2013 cm^{-1})
- Barium sulphate
- Calcium oxalate
- No presence of anything organic
- Identify the inorganic compound with other technique. Peaks at 752 , 657 and 642 cm^{-1} .



**P6A_6**

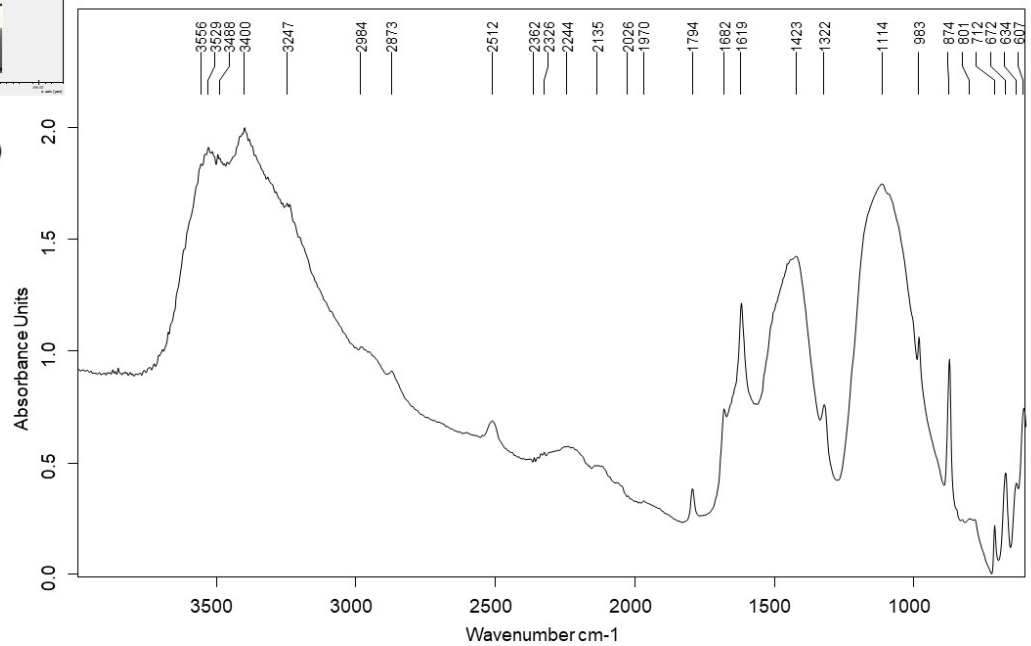
(red shoulder sleeve)

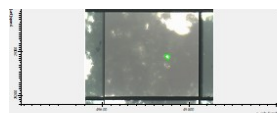
- Aluminium silicates, probably indicating an ochre (peak around 3691, 3620, 915 cm^{-1})
- Nothing related to binder (organic)
- Calcite
- Gypsum
- Calcium oxalate
- Barium sulphate
- Identify the inorganic compound with other technique (753, 660 and 644 cm^{-1}).

**P6A_10**

(greenish blue background)

- Gypsum
- Calcite
- Peak around 801 cm^{-1} might be connected to iron oxide
- Calcium oxalate
- Barium sulphate

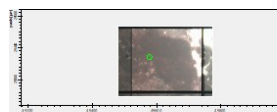
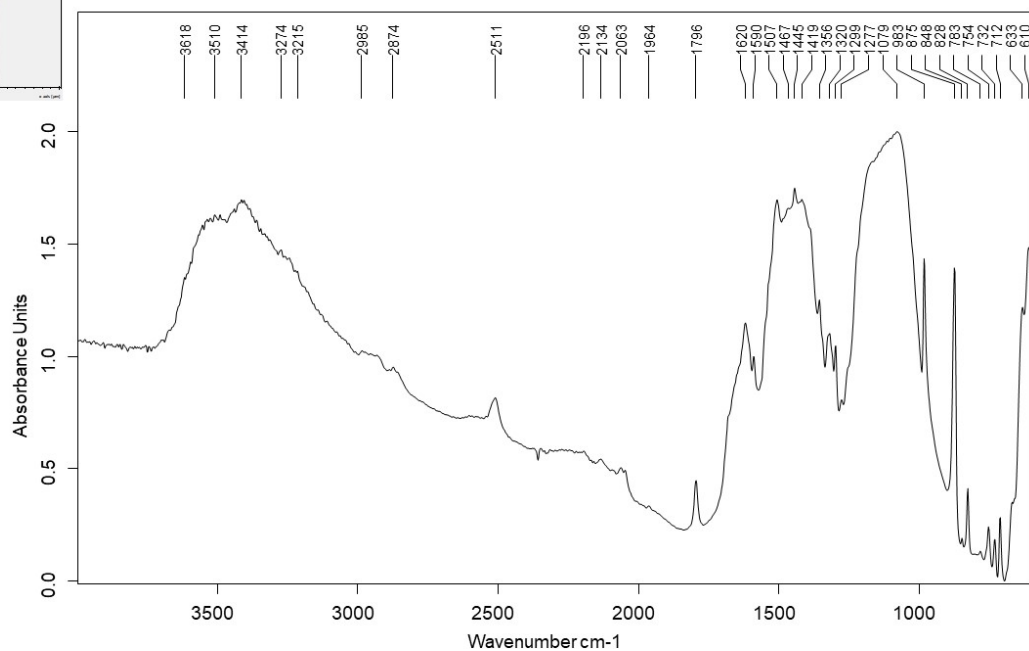




P6A_14

(green boat)

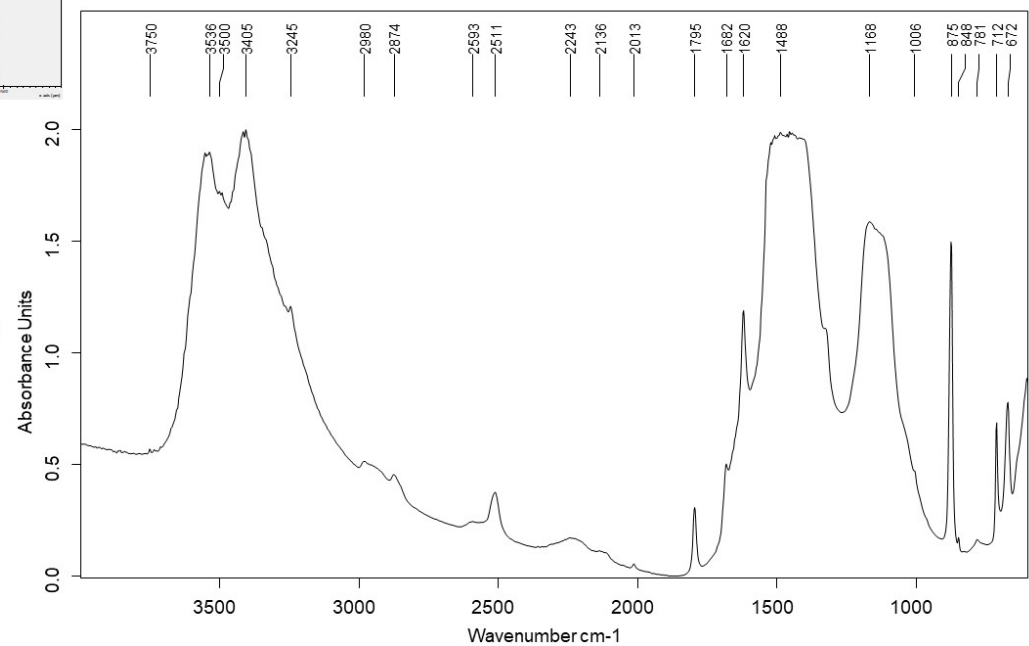
- Gypsum
- Calcite
- Nothing organic was identified
- Calcium oxalate
- Barium sulphate

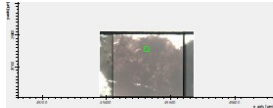


P6A_17rep

(dark red sleeve)

- Gypsum
- Calcite
- Peak around 780 cm⁻¹ indicate the presence of silicates
- Peak at 2013 cm⁻¹ indicates the presence of ivory black

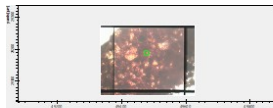
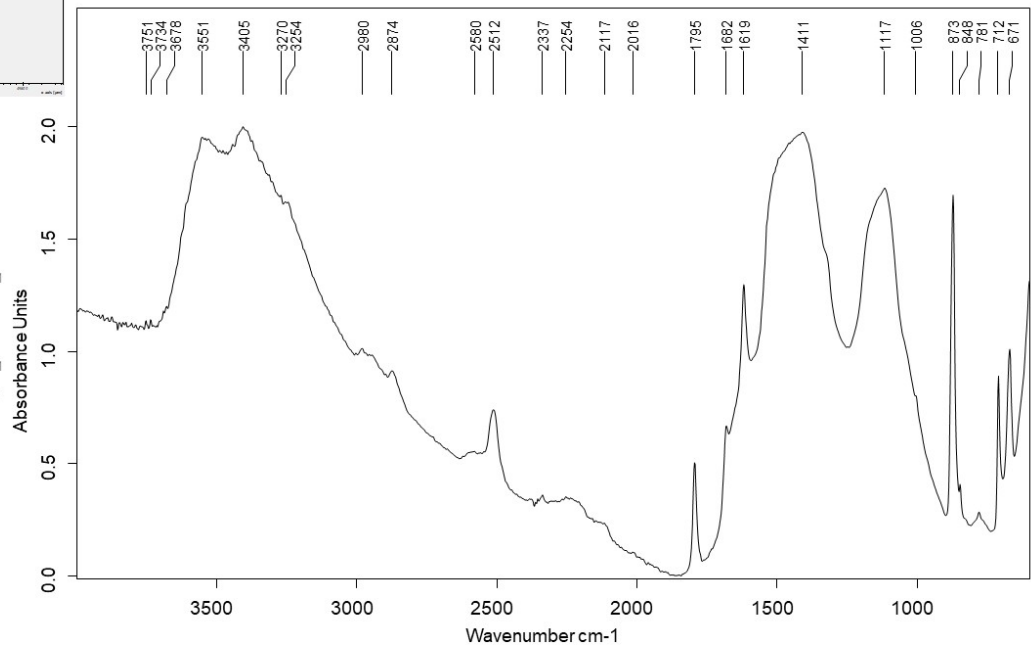




P6A_17

(dark red sleeve)

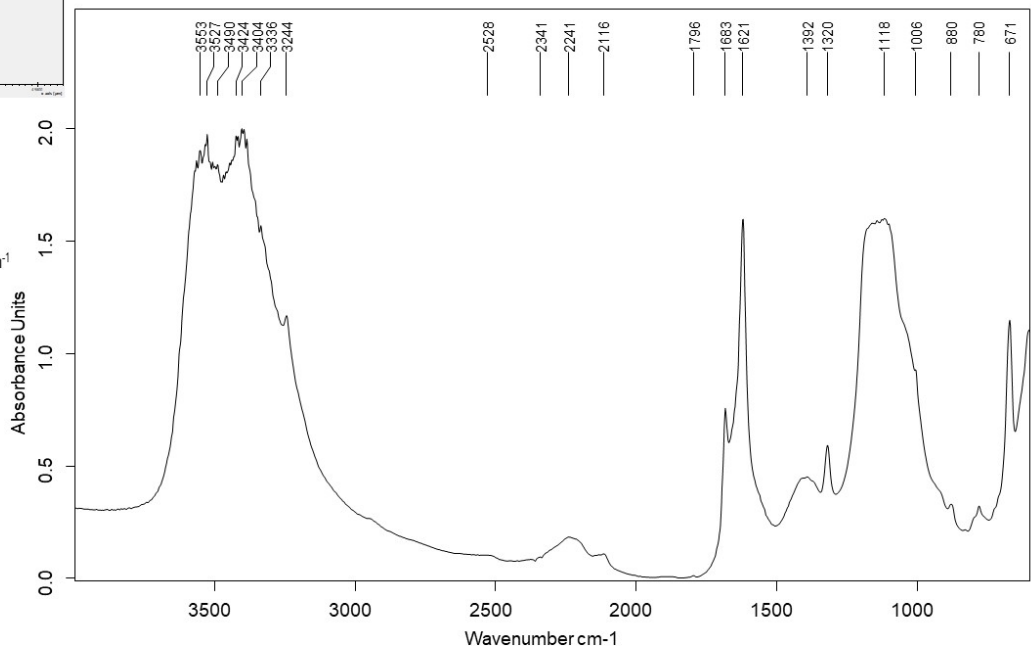
- Gypsum
- Calcite
- Might have something organic due to the peak around 1700 cm^{-1}
- Peak around 780 cm^{-1} indicate the presence of silicates
- Peak around 2014 cm^{-1} indicates the presence of ivory black

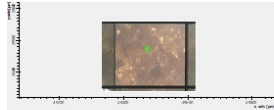


P6A_20

(red part of flaking hand)

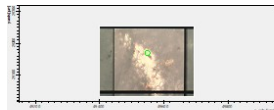
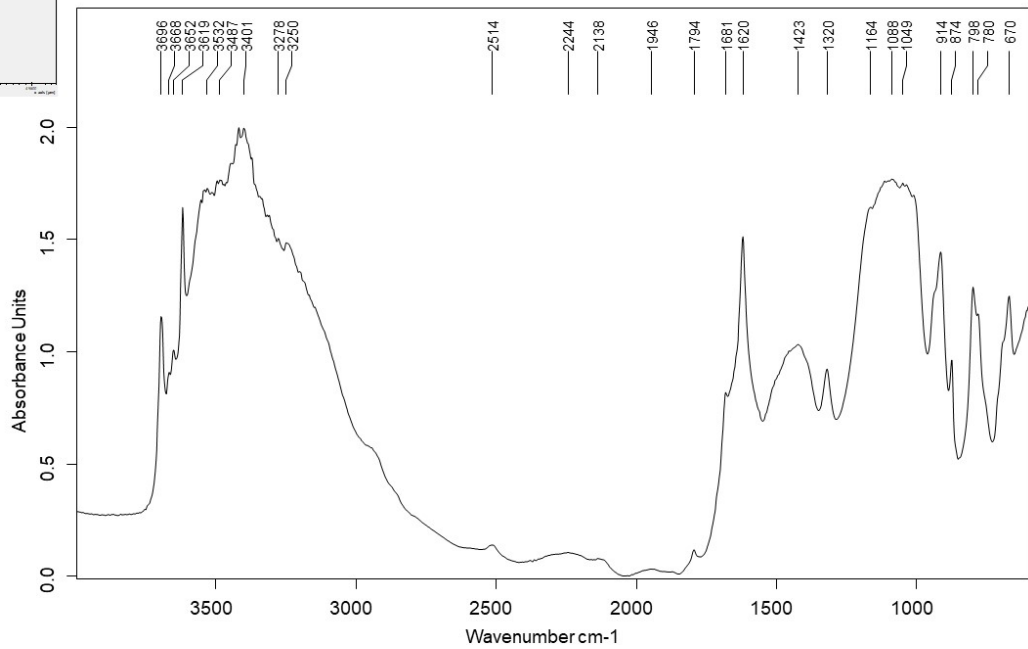
- Gypsum
- Oxalates
- Traces of silicates due to peak around 915 cm^{-1} (fingerprint area)



**P6C_2**

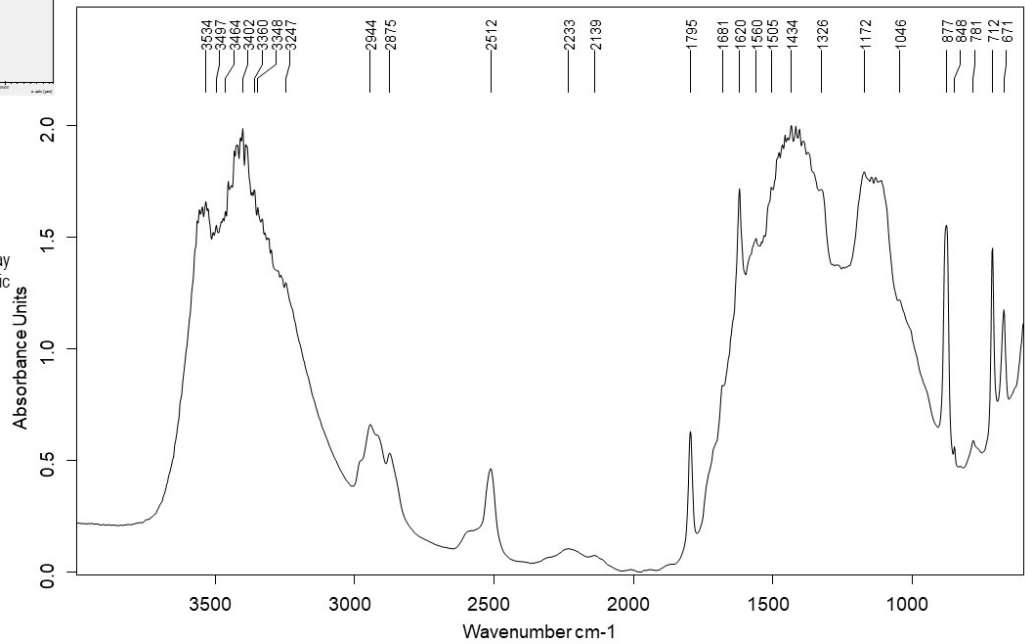
(rope, white spot)

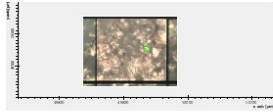
- Aluminium silicates (two sharp peaks on the left)
- Peak related to kaolinite (917 cm^{-1}) indicating ochres
- Gypsum
- Calcite
- Oxalates

**P6C_5**

(greenish blue background)

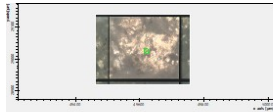
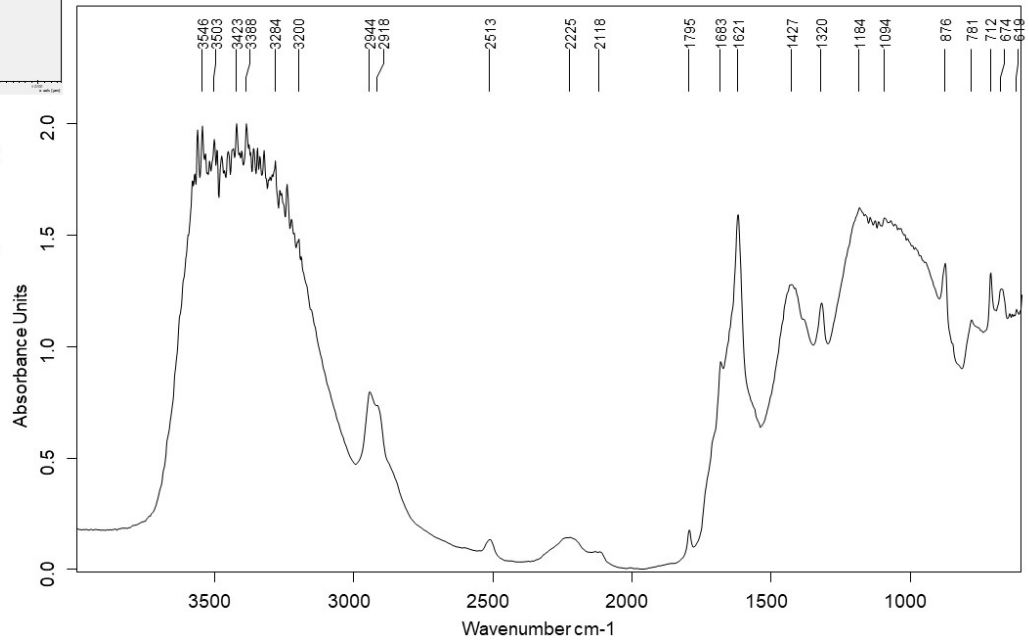
- Gypsum
- Calcite
- Oxalates
- Peak around 1710 cm^{-1} may indicate something organic





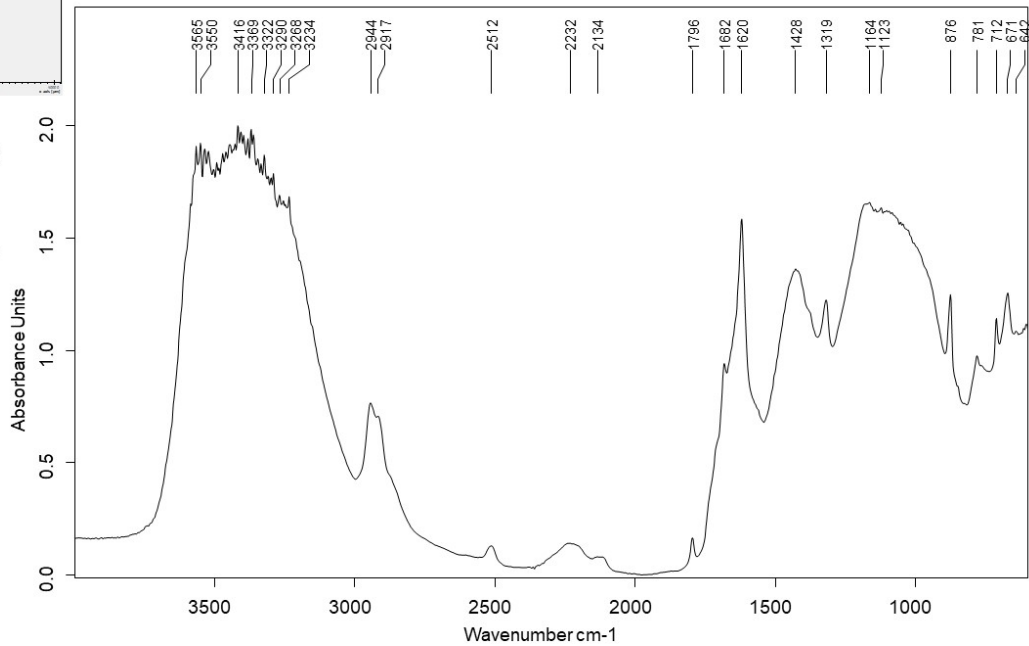
P6C_5 rep1
(greenish blue background)

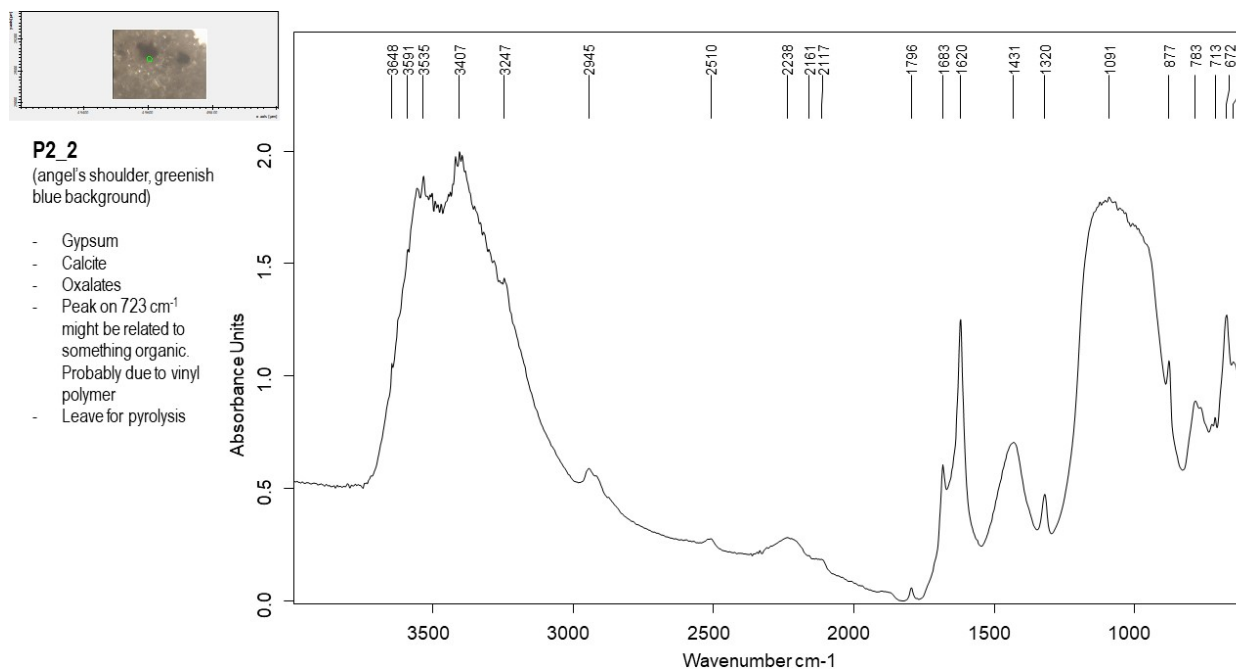
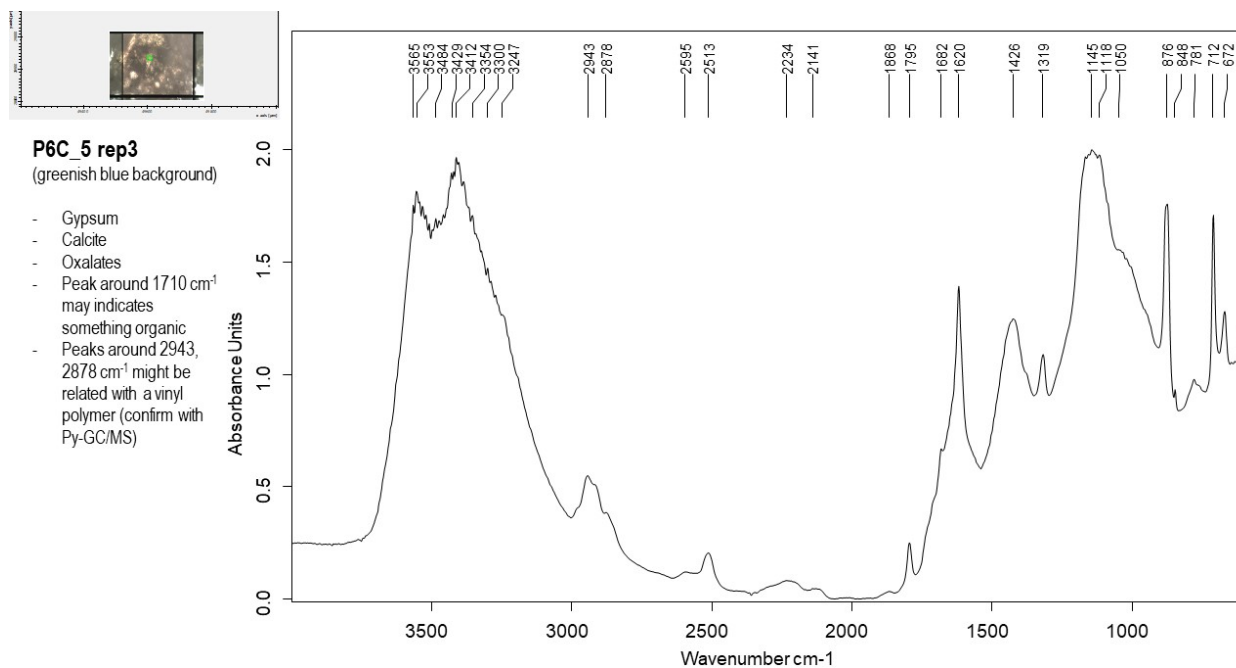
- Gypsum
- Calcite
- Oxalates
- Peak around 1710 cm^{-1} may indicate something organic
- Peaks around 2944 , 2918 cm^{-1} might be related with a vinyl polymer (confirm with Py-GC/MS)

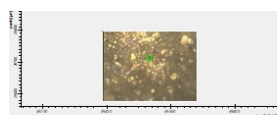


P6C_5 rep2
(greenish blue background)

- Gypsum
- Calcite
- Oxalates
- Peak around 1710 cm^{-1} may indicate something organic
- Peaks around 2944 , 2917 cm^{-1} might be related with a vinyl polymer (confirm with Py-GC/MS)

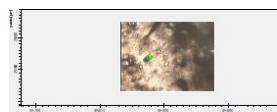
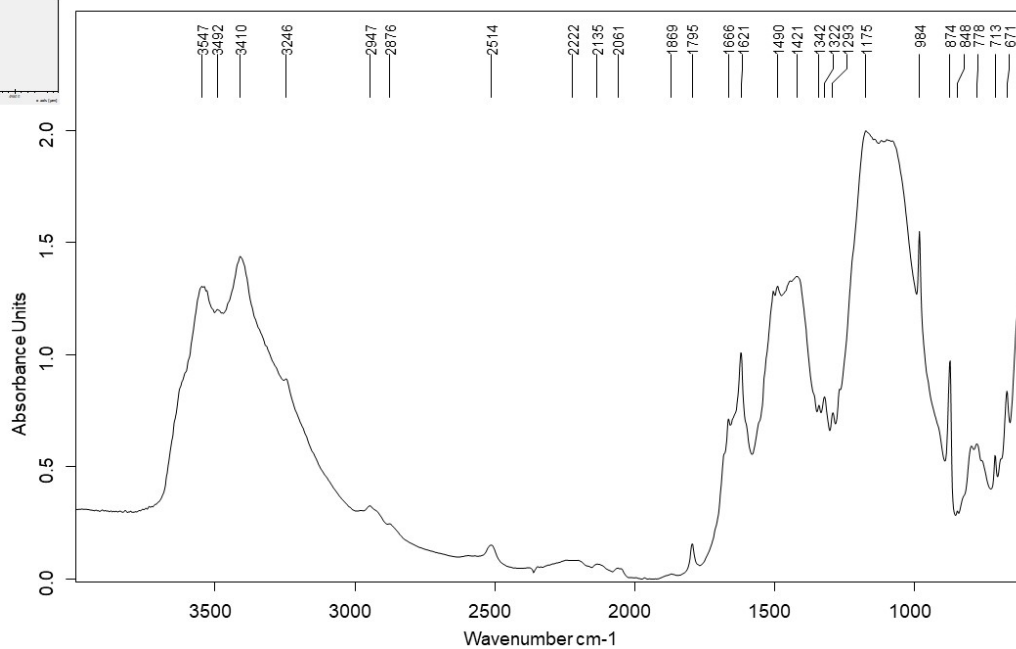




**P2_3**

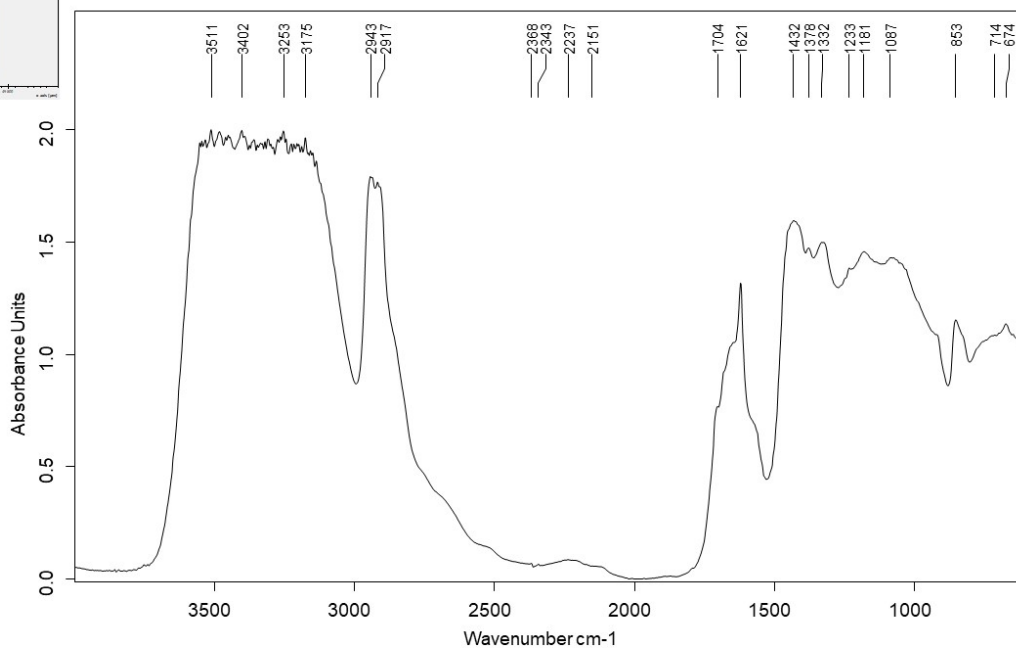
(angel's garment, greenish
blue background)

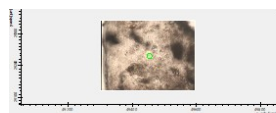
- Gypsum
- Calcite
- Barium sulphate
- Calcium oxalate
- Quartz
- Unidentified vibrations
on 1293 cm^{-1}

**P2_5 rep**

(angel's garment, greenish
blue background, shines
under microscope)

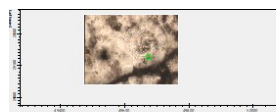
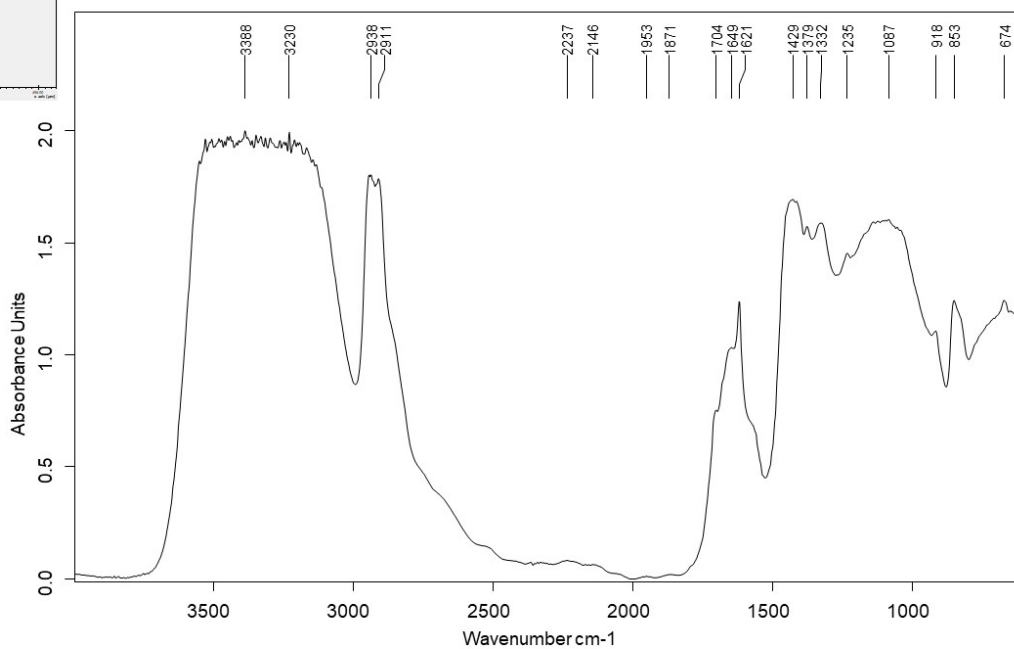
- Peaks on 2943 and 2917 cm^{-1} might
indicate a vinyl polymer
- Gypsum



**P2_5 rep1**

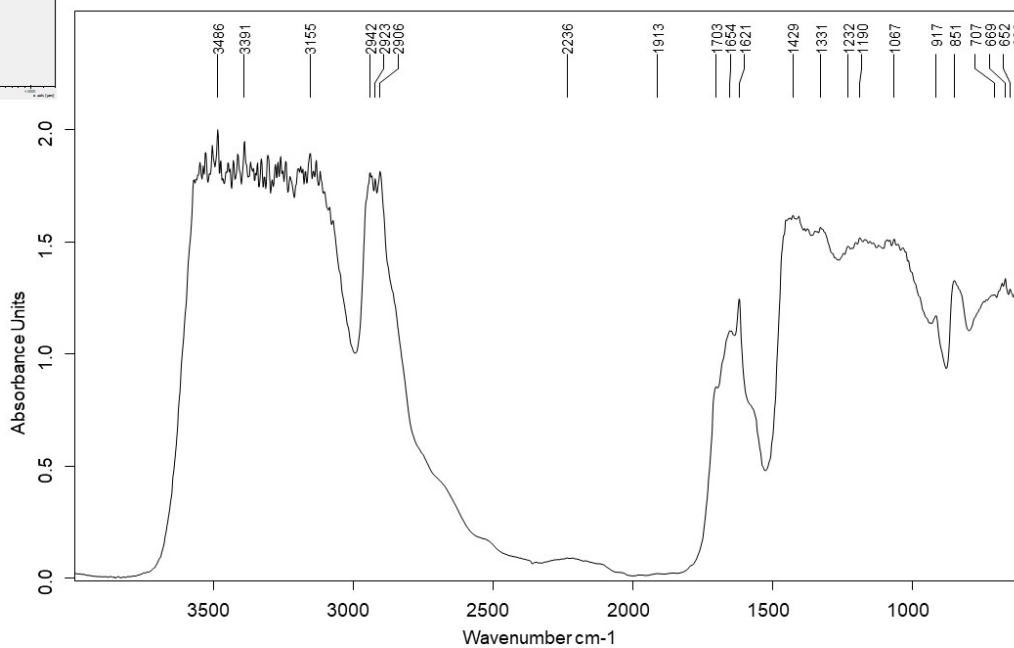
(angel's garment, greenish blue background, shines under microscope)

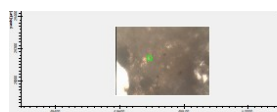
- Peaks on 2938 and 2911 cm^{-1} might indicate a vinyl polymer
- Gypsum

**P2_5**

(angel's garment, greenish blue background, shines under microscope)

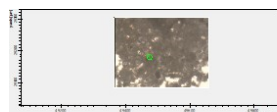
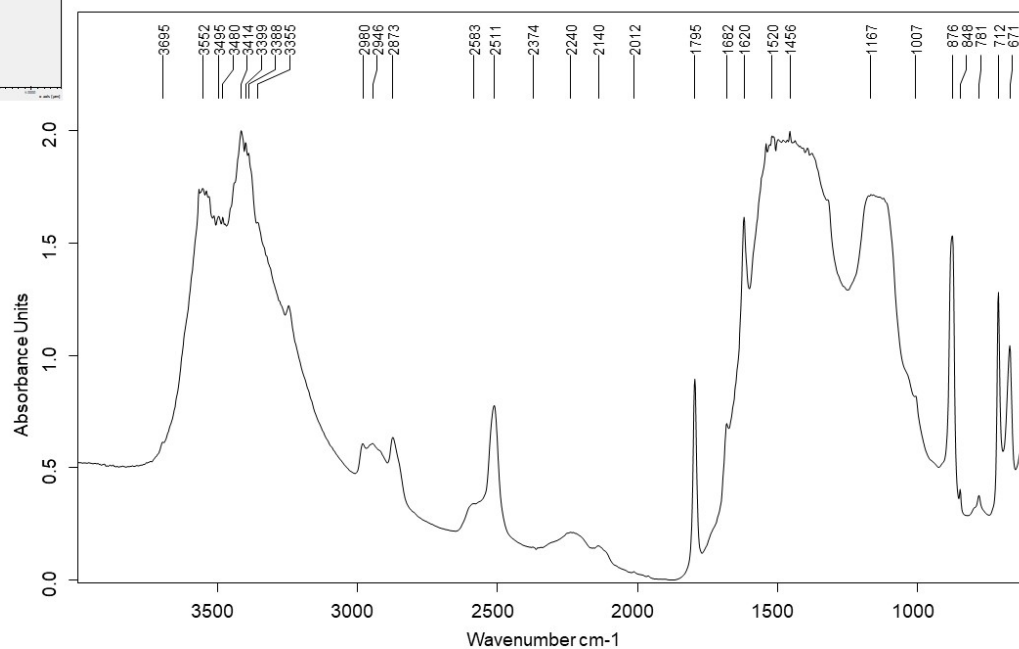
- Peaks on 2942 and 2923 cm^{-1} might indicate a vinyl polymer
- Gypsum



**P2_8**

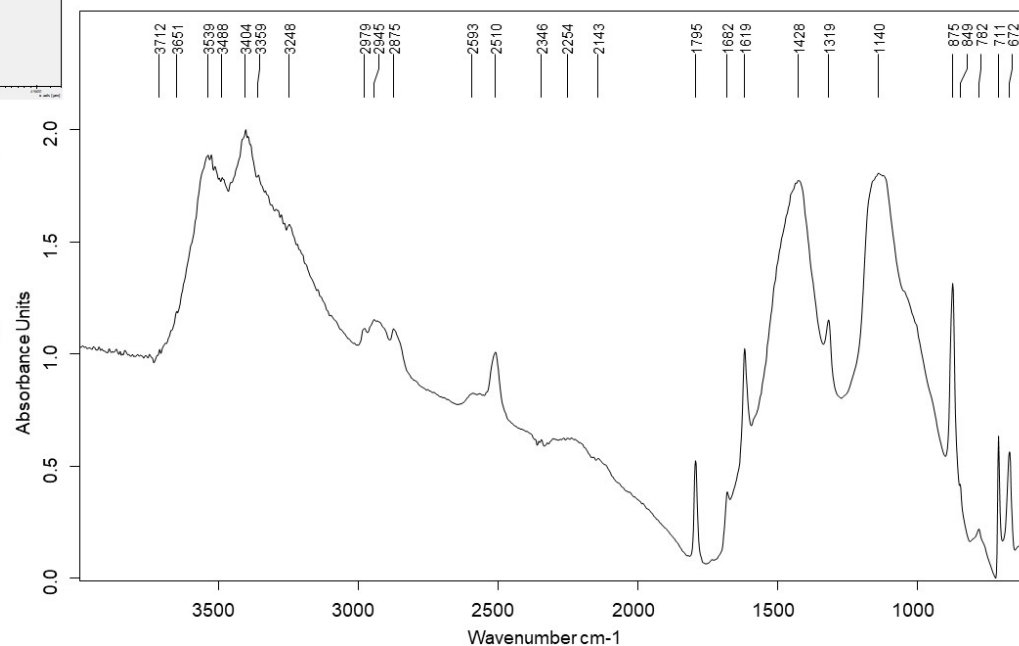
(fragment, green/blue)

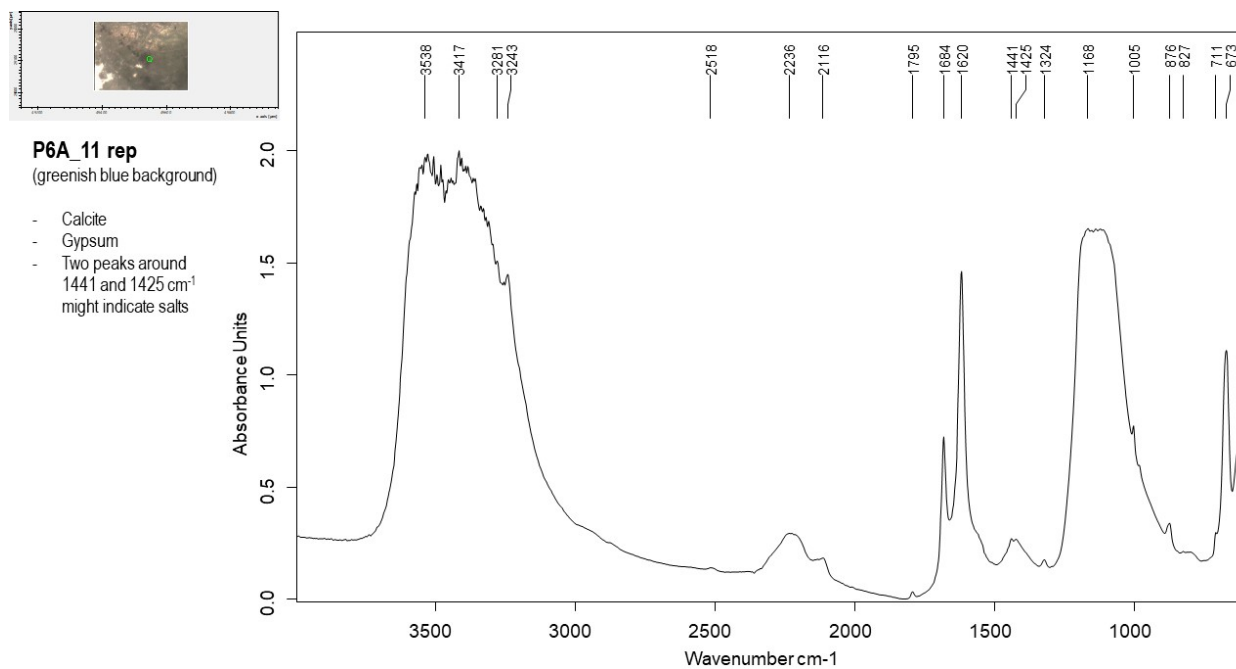
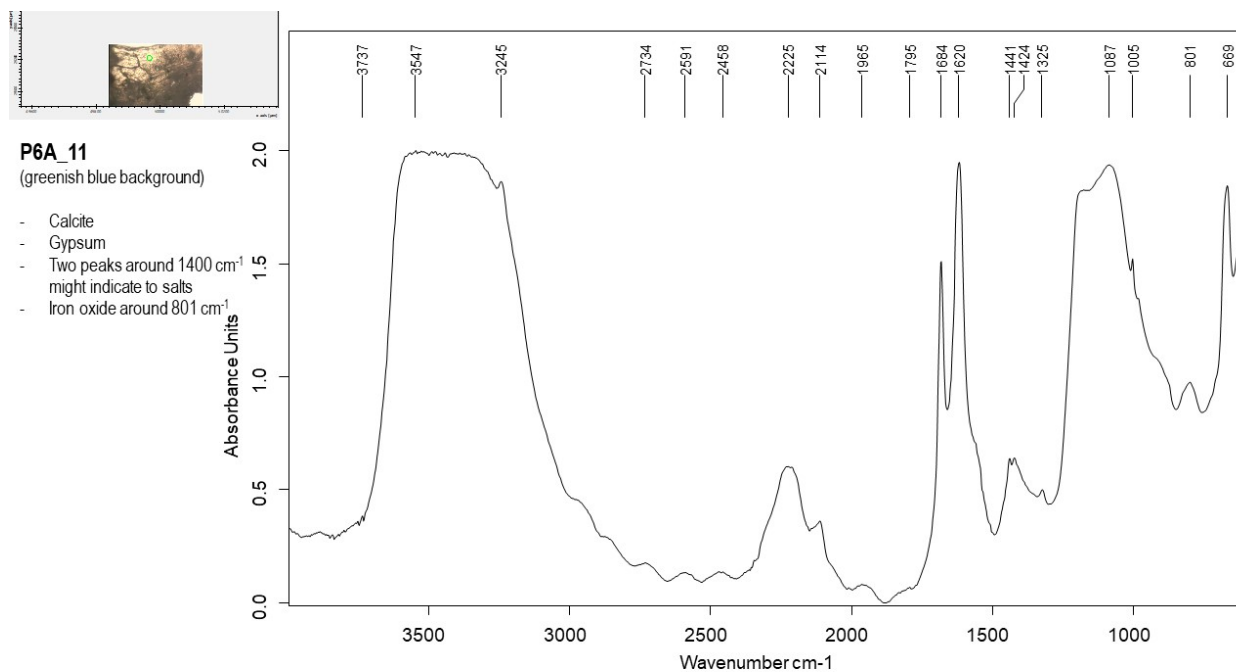
- Calcite
- Gypsum
- Calcium oxalate

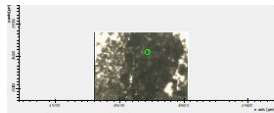
**P2_7**

(angel's garment, greenish blue but shiny under microscope)

- Calcite
- Gypsum
- Calcium oxalate
- Might have something organic present but the peak is very low and broad



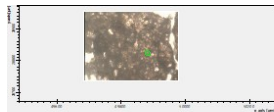
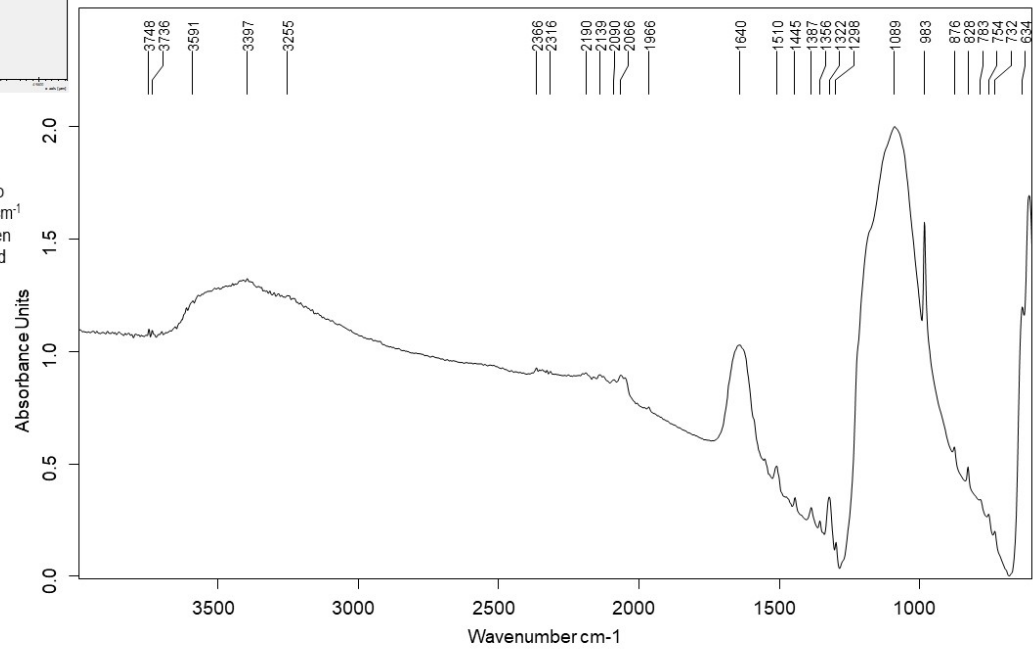




P6A_16

(green boat)

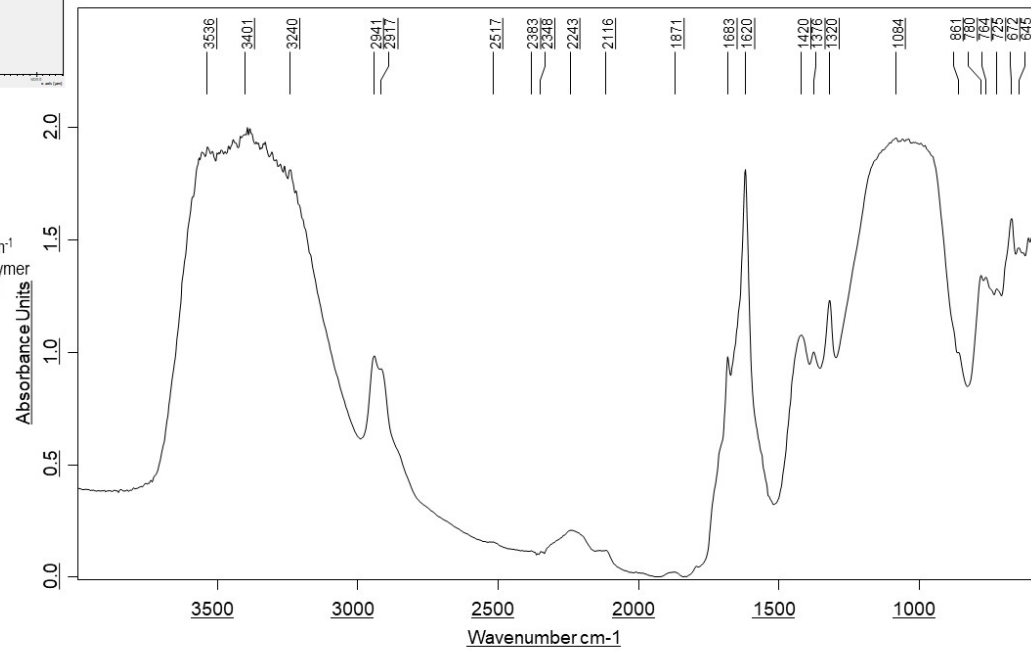
- Barium sulphate due to peaks 1089 and 981 cm^{-1}
- Might be emerald green due to peaks 1552 and 1510 cm^{-1}

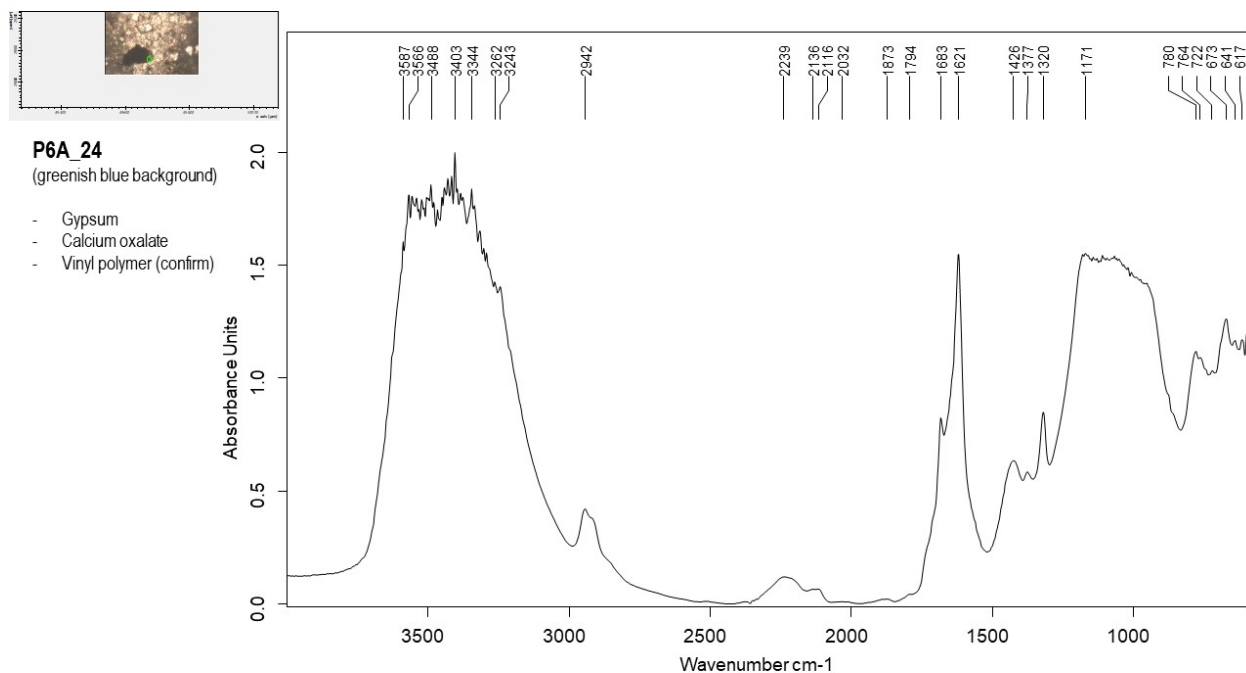
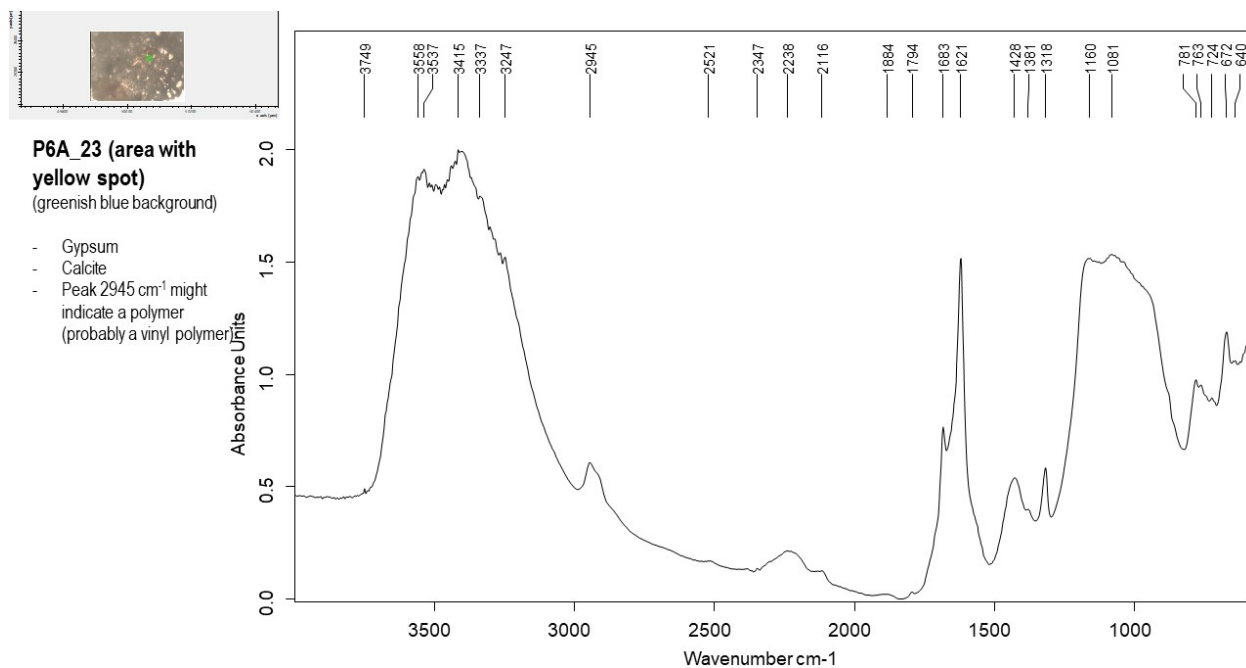


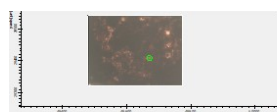
P6A_23 (grey spot)

(greenish blue background)

- Gypsum
- Calcite
- Oxalates
- Peaks 2941 and 2917 cm^{-1} might indicate a vinyl polymer (confirm with Py-GC/MS)



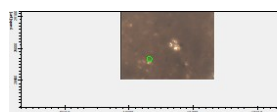
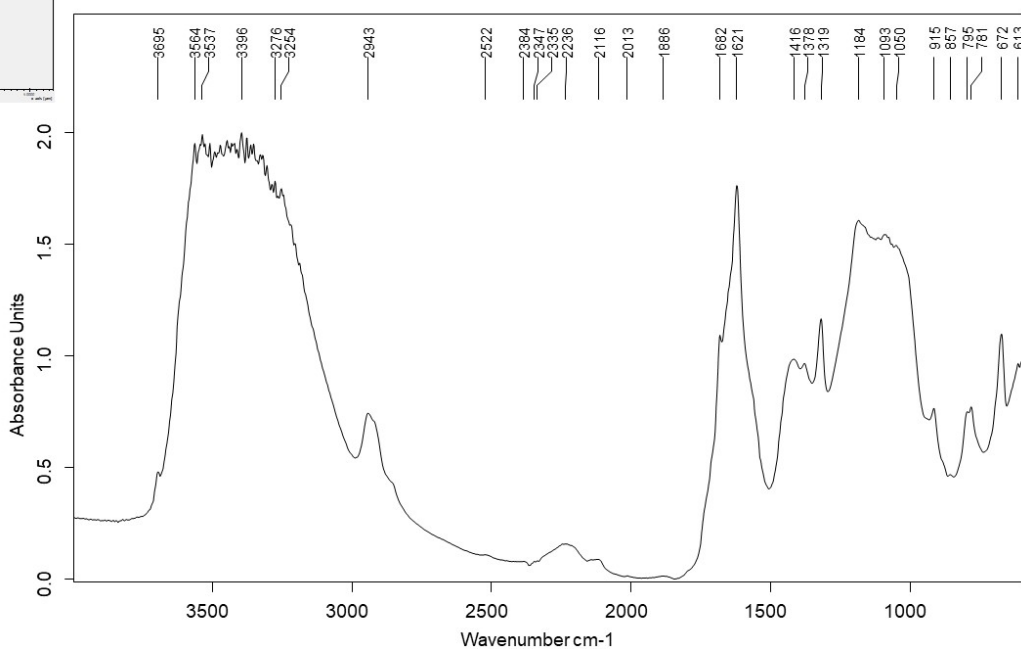




P6C_1a (brown layer)

(rope)

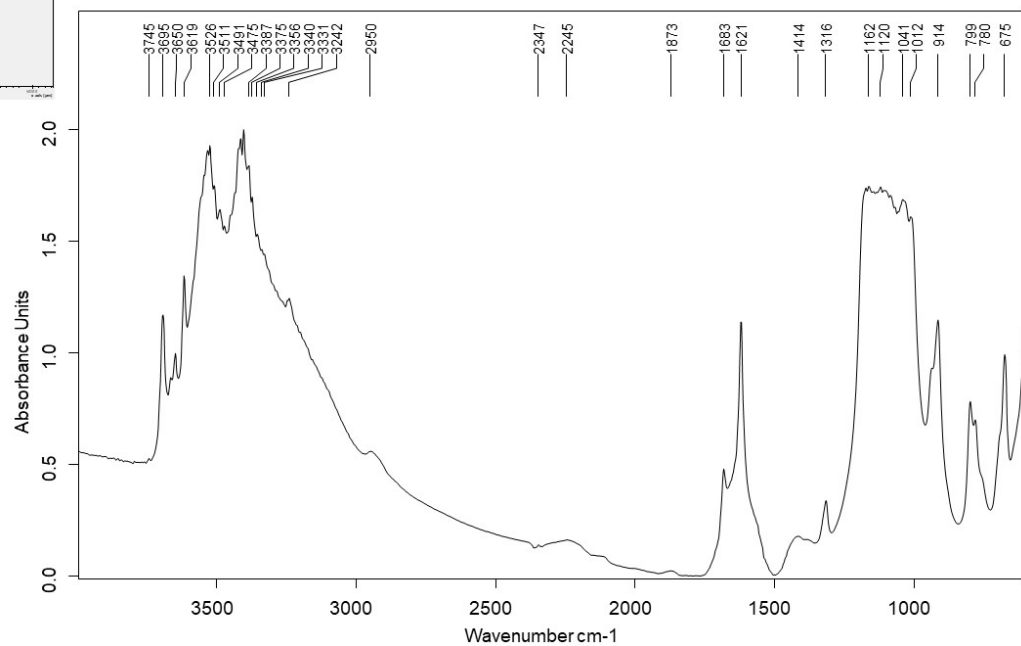
- Gypsum
- Calcite
- Oxalates
- Aluminium silicates (3695 cm^{-1}), connected to kaolinite (ochres)
- Peak at 2943 cm^{-1} due to vinyl polymer (confirm)

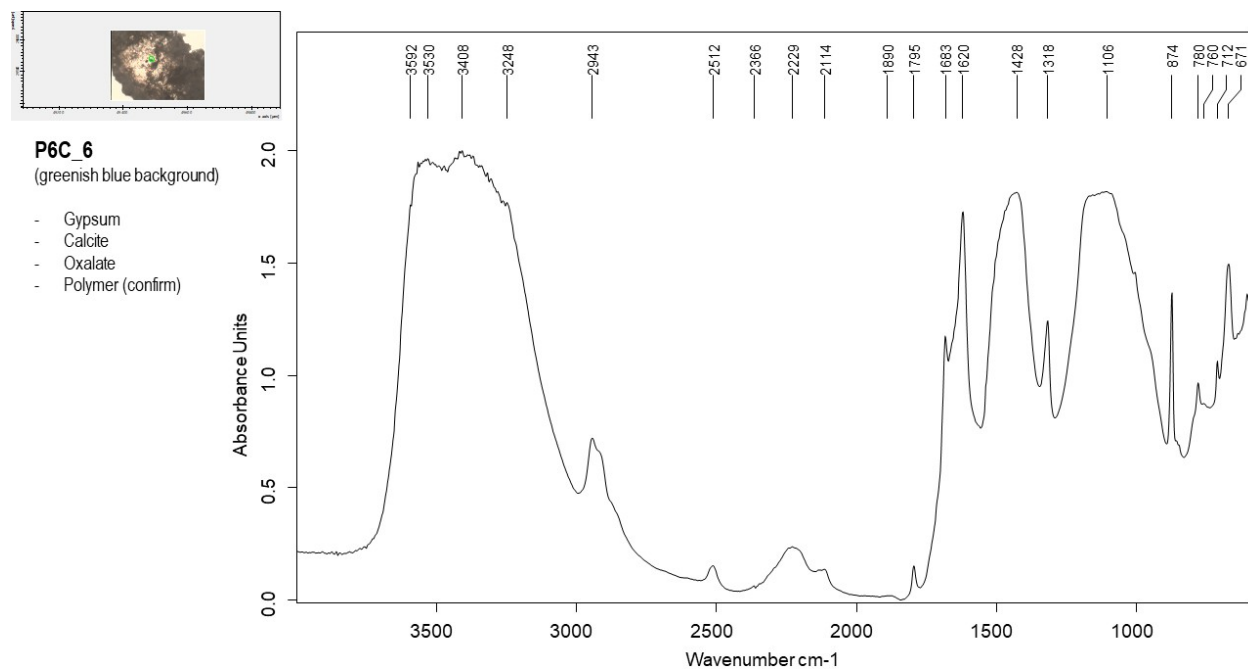
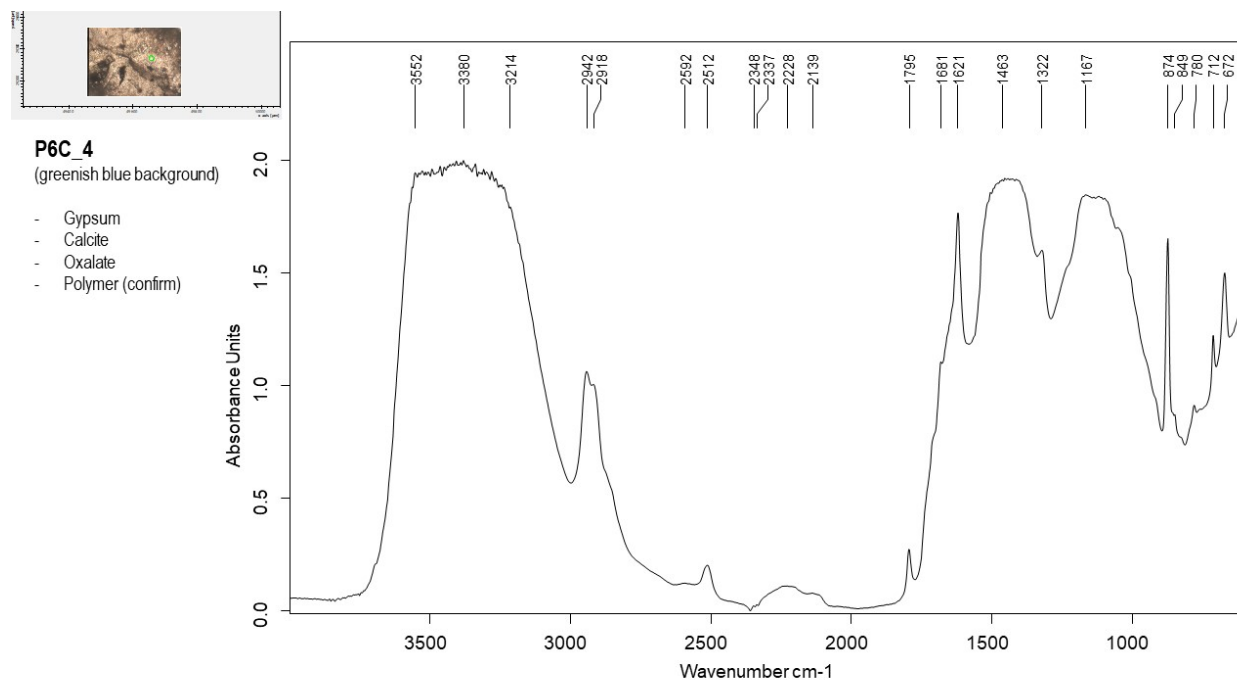


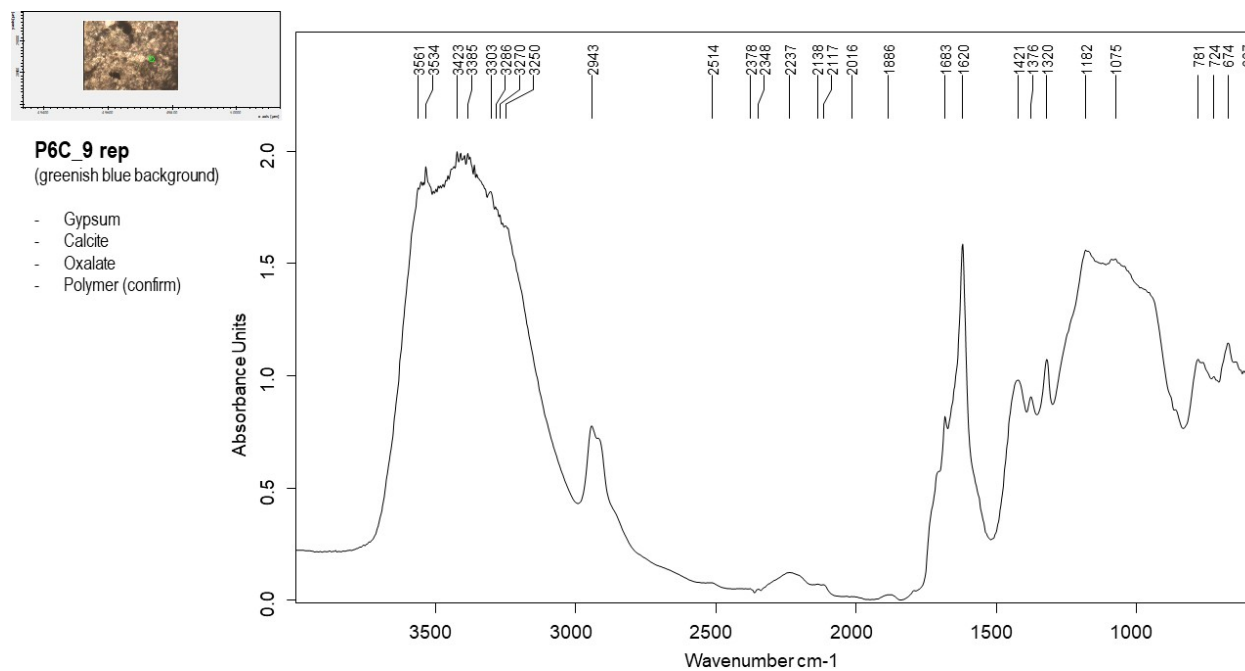
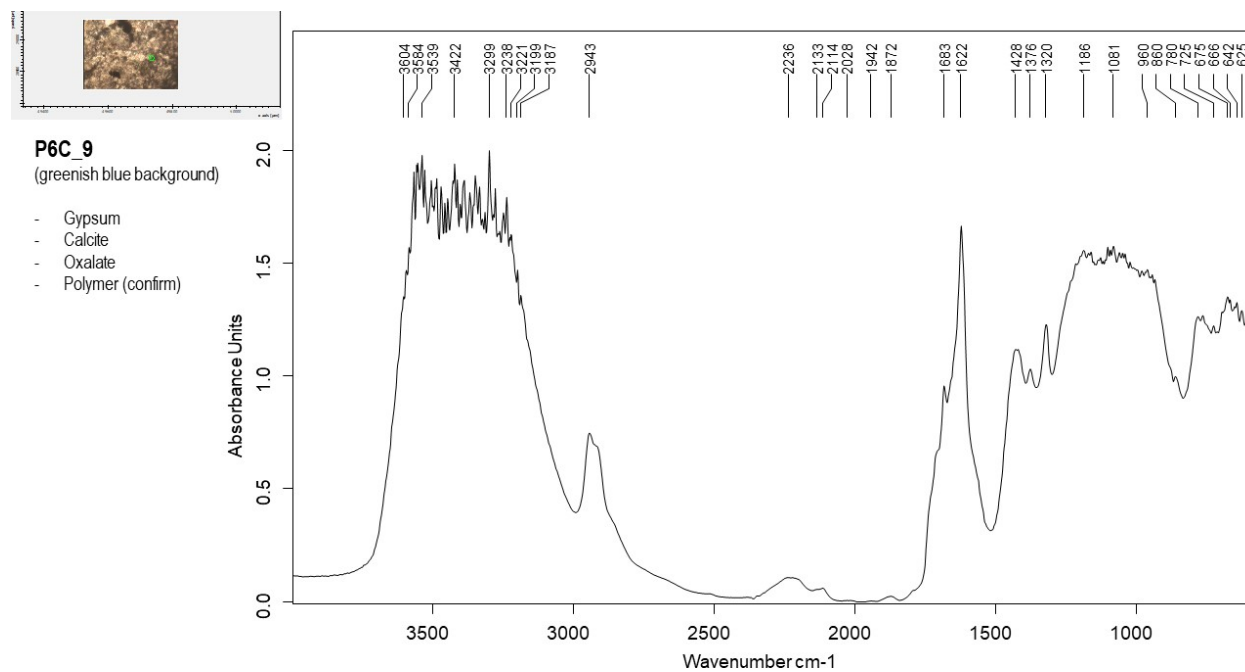
P6C_1a (yellow layer)

(rope)

- Kaolinite (3695, 3650, 3619, 1041, 914 cm^{-1})
- Oxalates
- Aluminium silicates (peak is enhanced by sulphates)
- Nothing organic



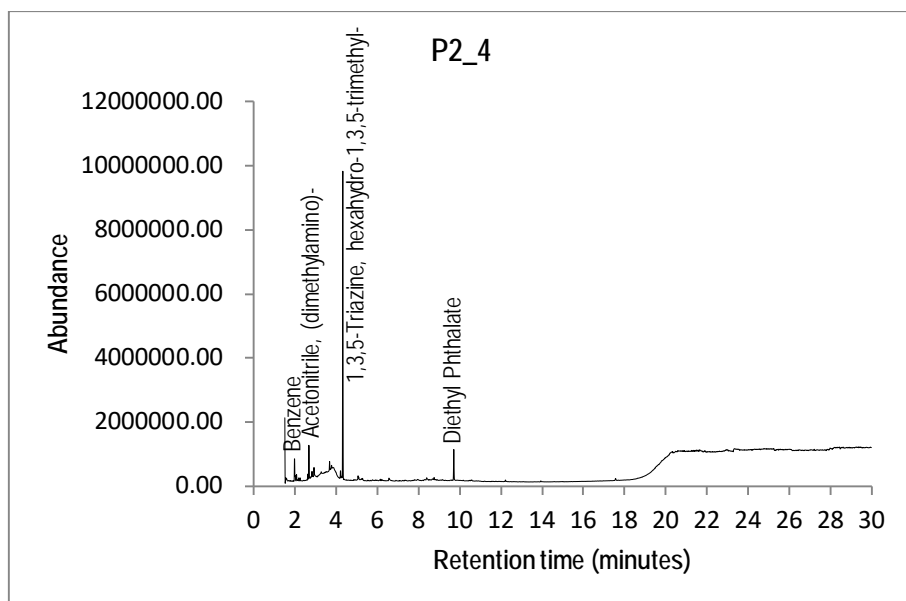




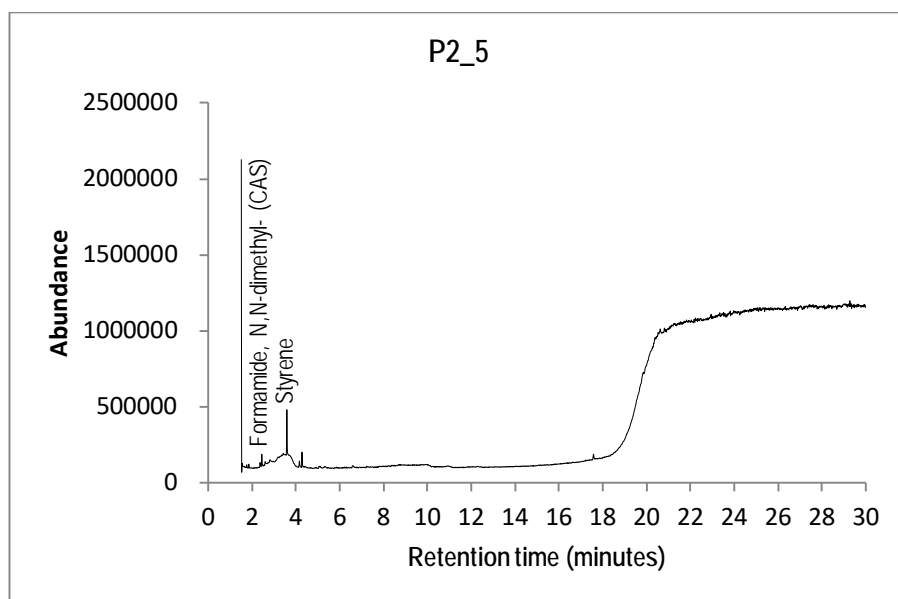
Appendix XII: py-GC-MS Analyses

Analyses of eight samples with Pyrolysis Gas Chromatography coupled with Mass Spectrometry, for identification of organic residues:

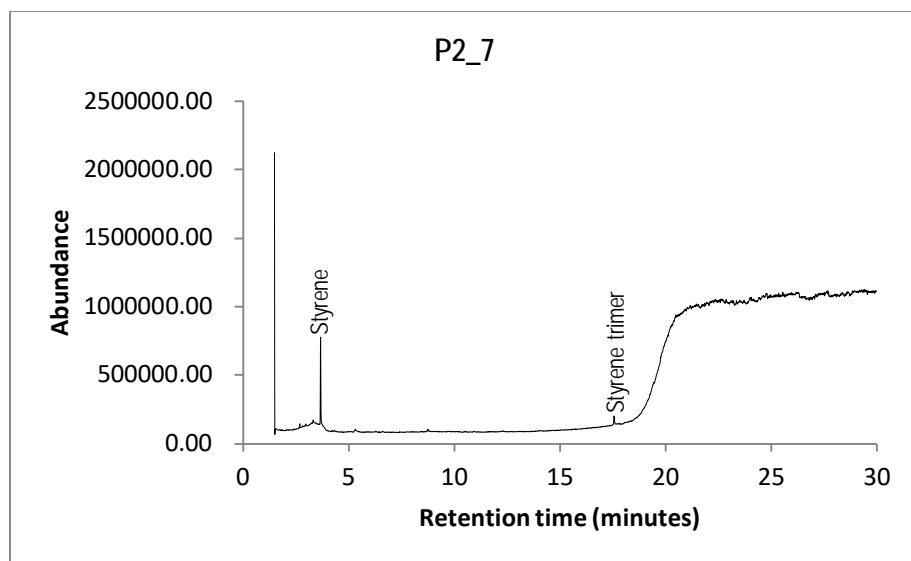
Sample P2_4, Panel 2
greenish background



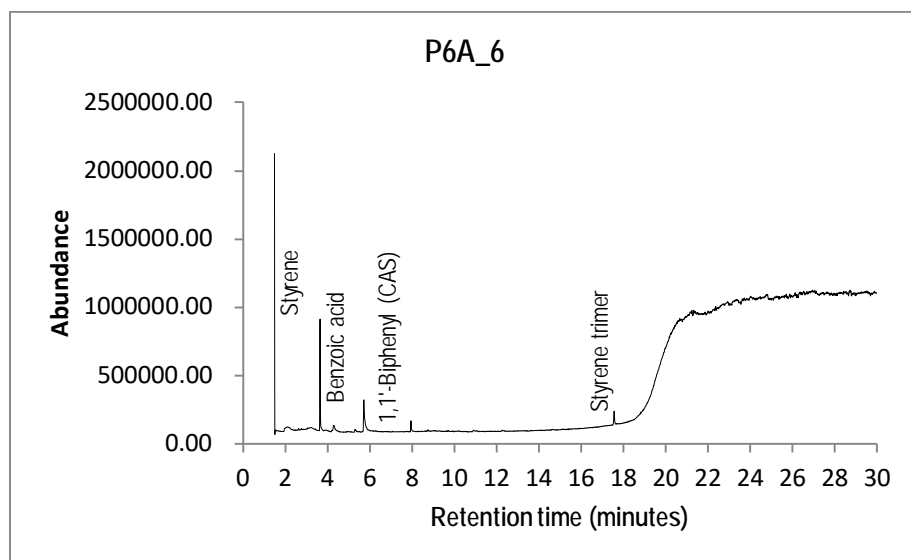
Sample P2_5, Panel 2
greenish background



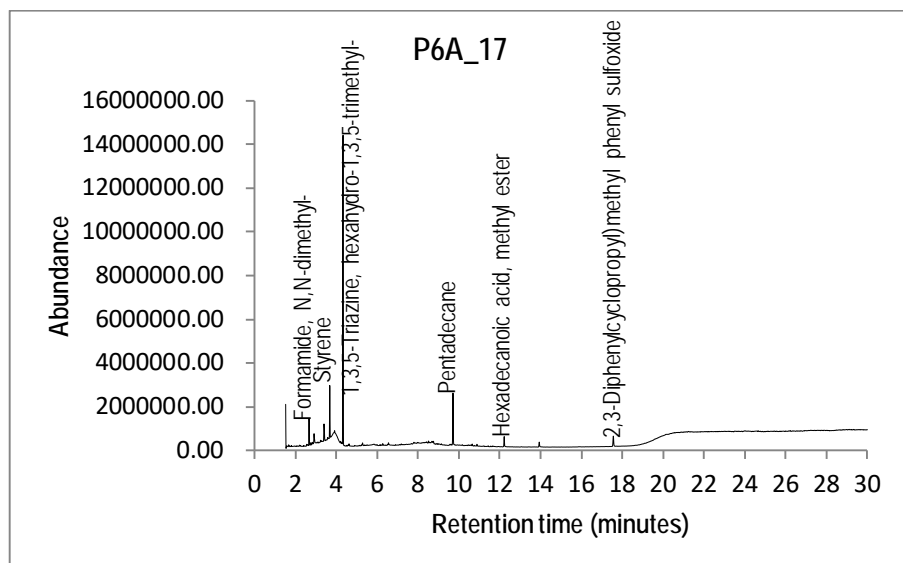
Sample P2_7, Panel 2
greenish background



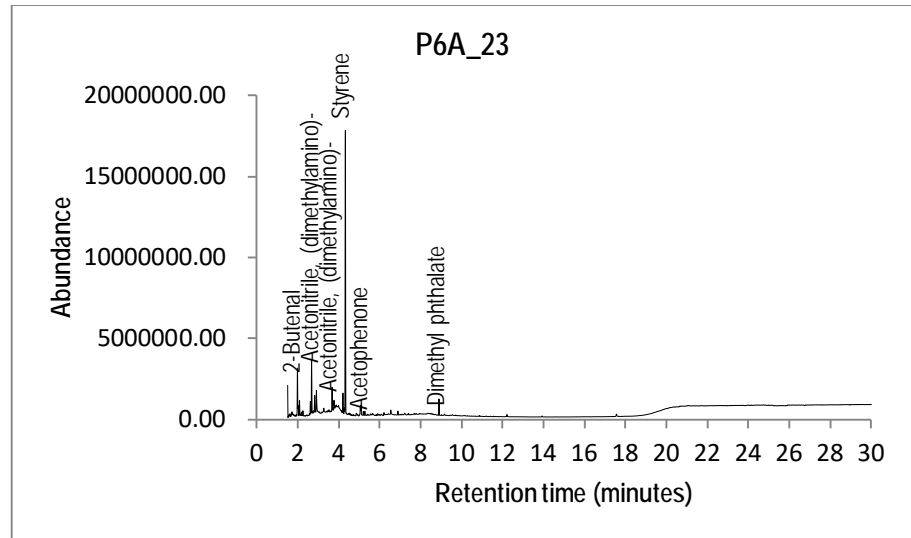
Sample P6A_6
Reddish dress



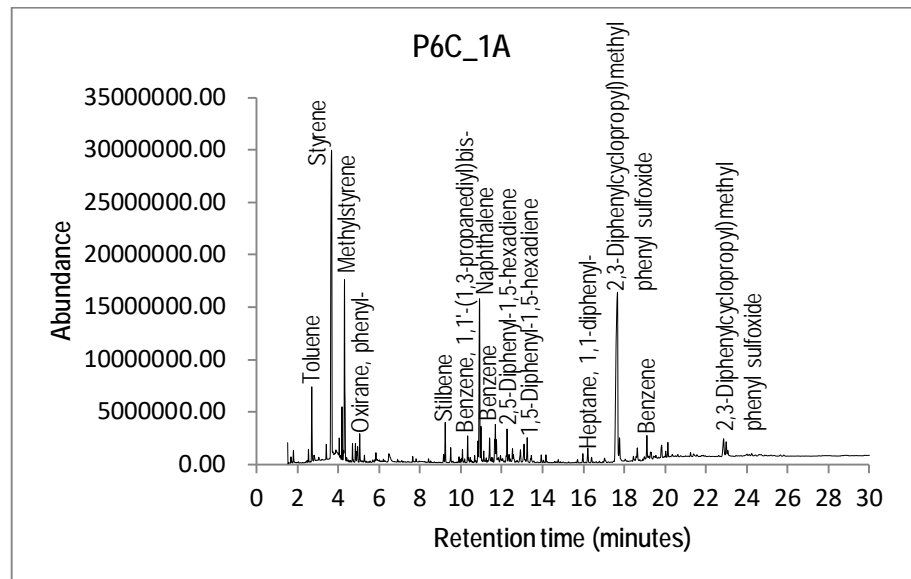
Sample P6A_17
Reddish dress



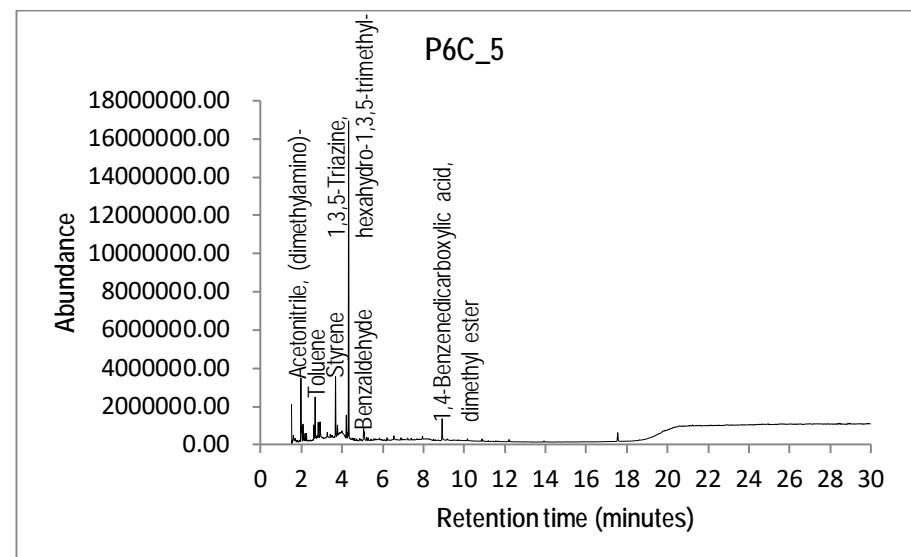
Sample P6A_23
Greenish background



Sample P6C_1a
Brown rope



Sample P6c_5
Greenish background



Appendix XIII: Combined data

Combined data of cross section and powdered samples based their representation regarding painting materials.

Description				Elemental analysis		Chemical analysis
Sample	Location	Colour	Stratigraphy	h-EDXRF main elements	SEM-EDS (at%)	FTIR
<i>Panel 2</i>						
P2_4 cs	Angel's dress (salts)	Area of greenish blue	Layer of white pigment (27-72 μm) over the mortar	E576: Al, Ba, Ca, Cl, Co, Cr, Cu, Fe, K, Mn, Ni, Pb, Rb, S, Si, Sr, Ti, Zn	White pigment: Na (338), Mg (4,51), Al (8,46), Si (14,05), S(10,79), Cl (1,42), Ca (21,81)Ti (30,16), Fe (4,86)	Calcite, Gypsum, Barite, Oxaltes
P2_8 cs	Bottom of the panel	Brownish with blue details	Layer of blue over the layer of brownish pigment (275-375 μm), and mortar underneath	No XRF (fragment collected from the bottom of the panel)	Blue layer: Na (11,08), Al (6,53), Si (7,12), S (3,36), Cl (0,91), K (1,33), Ca (14,89), Ti (38,65), Cr (12,69), Fe (2,15), As (1,29) Brownish pigment: Na (3,77), Mg (2,54), Al (3,15), Si (5,73), S (1,53), Cl (2,64), K (1,11), Ca (76,51), Fe (3,02)	Gypsum, Calcite, Calcium Oxalate
P2_9	Bottom of the panel	Black	/	(fragment collected from the bottom of the panel)	Ca (3,45), Fe (0,78), K (0,39), Cl (0,24), S (1,11), P (0,21), Si (11,04), Al (5,93), Na (4,62), Mg (0,57), Ti (0,51)	/
<i>Panel 3</i>						
P3B_2 cs	Sailor's beret	Dark blue	Dark blue layer (39-104 μm) over mortar	E700: Al, Ba, Ca, Cl, Cr, Cu, Fe, K, Na, Ni, P, Pb, S, Si, Sr, Ti, Zn	Grains: CaCO_3 Layer of pigment: Na (3,96), Al (29,09), Si (25,82), S (3,47), K (2,71), Ca (32,67), Fe (2,27) Mortar: Na (2,01), Mg (0,83), Al (0,73), Si (0,78), S (0,79), Cl (1,40), Ca (93,46)	/
P3B_5	Sailor's hair (salts)	Black	/	Area was too degraded for EDXRF	C (3,74), O (56,84) Na (20,23), Al (0,21), Si (0,19), S (10,59), K (1,67), Ca (0,53)	/
P3B_6	Ribbon (salts)	Black	/	Area was too degraded for EDXRF	C (2,97), O (59,66), Na (22,63), Si (0,13), S (12,02), K (1,27), Ca (1,32)	/
<i>Panel 6</i>						
P6A_2	Background (salts)	Green	/	E361: Al, Ba, Ca, Cl, Co, Cu, Fe, K, Mg, Mn, Ni, Pb, S, Si, Sr, Ti, Zn	C (8,40), O (57,73), Na (17,32), Si (0,25), S (11,21), K (1,24), Ca (3,86)	/
P6A_3	Background (salts)	Green	/	E361: Al, Ba, Ca, Cl, Co, Cu, Fe, K, Mg, Mn, Ni, Pb, S, Si, Sr, Ti, Zn	C (20,80), O (59,66), Na (0,66), Mg (0,43), Al (0,58), Si (0,78), S (2,99), K (0,38), Ca (4,45), Ti (5,98), Fe (3,28)	/

P6A_3 cs	Background	Green	White pigment layer (10 – 23 µm) framing the matrix	E361: Al, Ba, Ca, Cl, Co, Cu, Fe, K, Mg, Mn, Ni, Pb, S, Si, Sr, Ti, Zn	White layer: Na (2,78), Mg (1,87), Al (1,99), Si (2,49), S (1,15), Cl (1,48), K (0,93), Ca (12,51), Ti (71,72), Cr (0,79), Fe (2,28) Matrix: Na (3,00), Mg (14,02), Al (1,68), Si (16,57), S (3,20), Cl (3,00), K (3,11), Ca (55,42)	/
P6A_6rep	Shoulder sleeve	Red	Sample of red pigment	Similar as E433: Al, Ba, Ca, Cd, Cl, Co, Cr, Cu, Fe, K, Ni, P, Po, S, Si, Sr, Ti, Zn	Na (0,43), Al (0,17), Si (0,39), S (6,89), Cl (0,18), K (3,21), Ca (7,99), Ti (0,32), Fe (0,61)	Aluminum silicates, Calcite, Gypsum, Calcium Oxalate, Barite
P6A_7	Shoulder sleeve (salts)	Blue	/	E365/66/67: Al, Ba, Ca, Cl, Cr, Cu, Fe, K, Ni, Pb, S, Si, Sr, Ti, Zn	C (17,16), O (58,87), Na (0,17), Al (0,09), Si (0,23), S (6,79), K (7,23), Ca (9,45)	/
P6A_7 cs	Shoulder sleeve	Blue	Blue pigment layer (10-61 µm), intonaco and arriccio.	E365/66/67: Al, Ba, Ca, Cl, Cr, Cu, Fe, K, Ni, Pb, S, Si, Sr, Ti, Zn	Blue layer: Na (13,30), Mg (0,68), Al (14,36), Si (16,19), P (0,80), S (26,51), K (1,91), Ca (26,25)	/
P6A_10 cs	Grey green with moist	Grey green	Layer of green pigment over mortar	E380: Al, Ba, Ca, Cl, Co, Cu, Fe, K, Mg, Mn, Ni, Pb, S, Si, Sr, Ti, Zn	Mg (0,29), Al (0,77), Si (2,43), S (37,68), K (1,51), Ca (55,96), Fe (1,36)	Calcite, Gypsum, Calcium Oxalate, Barite
P6A_14	Boat (salts)	Green	/	E412: Al, Ba, Ca, Cu, Fe, K, Mn, Ni, Pb, S, Si, Sr, Zn, As	C (33,73), O (40,87), Na (16,32), Si (0,07), S (6,82), Ca (1,00), Ba (1,19)	Gypsum, Calcite, Calcium Oxalate, Barite
P6A_14 cs	Boat	Green	Layer of green pigment (73-277 µm)	E412: Al, Ba, Ca, Cu, Fe, K, Mn, Ni, S, Si, Sr, Zn, As	Na (1,83), Al (2,51), S (36,49), Cl (1,79), K (0,64), Ca (17,35), Fe (3,10), As (2,80), Sr (2,79), Ba (30,68)	Gypsum, Calcite, Calcium Oxalate, Barite
P6A_15	Boat (salts)	Green	/	E415: Al, Ba, Ca, Cu, Fe, K, Mn, Ni, S, Si, Sr, Zn, As	C (24,41), O (50,80), Na (8,30), Mg (0,60), Al (0,68), S (8,33), Ca (0,61), Sr (0,61), Ba (5,65)	/
P6A_17 cs	Sleeve	Brownish red	Layer of red pigment over layer of black pigment	E427: Ba, Ca, Cl, Co, Cr, Cu, Fe, K, Ni, S, Si, Sr, Ti, Zn	Red layer: Na (2,21), Mg (1,17), Al (2,69), Si (2,95), S (30,80), K (1,03), Ca (54,73), Fe (4,43) Black layer: Na (2,34), Mg (0,93), Al (0,93), Si (0,67), P (2,47), S (3,99), Cl (1,57), Ca (87,10)	Gypsum, Calcite, Bone black
P6A_18	Sleeve (salts)	Brownish red	/	E426: Ba, Ca, Cl, Co, Cr, Cu, Fe, K, Ni, S, Si, Sr, Ti, Zn	C (6,41), O (53,98), Na (16,90), Al (0,18), Si (0,38), S (5,49), Ca (6,09), Fe (0,58)	/
P6A_19	Arm	Brown	/	Similar as E433: Al, Ba, Ca, Cd, Cl, Co, Cr, Cu, Fe, K, Ni, P, Po, S, Si, Sr, Ti, Zn	Fragment A: Fragment B: C (13,92), O (65,32), Na (0,56), Mg (0,23), Al (0,63), Si (0,76), S (6,63), Cl (0,08), K (0,28), Ca (9,57), Fe (2,02)	/
P6A_20 cs	Arm	Brown	Layer of red over the layer of black	Similar as E433: Al, Ba, Ca, Cd, Cl, Co, Cr, Cu, Fe, K, Ni, P, Po, S, Si, Sr, Ti, Zn	Red layer: Na (4,73), Mg (2,87), Al (3,95), Si (1,70), S (9,42), Cl (2,87), Ca (64,60), Fe (9,86)	Gypsum, Calcium Oxalate

					Dark layer: Na (1,96), Mg (0,95), Al (0,79), Si (0,68), S (12,74), Cl (2,33), K (0,83), Ca (79,71)	
P6A_21	Dress	Brown	/	E444: Al, Ba, Ca, Cd, Cl, Co, Cr, Cu, Fe, K, Ni, P, Po, S, Si, Sr, Ti, Zn	Ca, Si, Cr, Fe	/
P6A_23 cs	Background	Green	/	E478: Al, Ba, Ca, Cl, Co, Cu, Fe, K, Mg, Mn, Ni, Pb, S, Si, Sr, Ti, Zn	Mg (10,24), Al (8,57), Si (16,87), S (5,16), Cl (1,16), K (0,59), Ca (4,95), Fe (50,15), Ba (2,31)	Gypsum, Calcite, Calcium Oxalate, Vinyl Polymer
P6C_2 cs	Brownish rope	White/brownish area	Layer of white (19-38 µm) over the layer of orange	E527: Ba, Ca, Cl, Co, Cr, Cu, Fe, K, Mn, I, Pb, S, Si, Sr, Ti, Zn	White layer: Na (3,14), Mg (2,18), Al (3,19), Si (3,07), P (0,75), S (2,46), Cl (0,94), Ca (7,95), Ti (71,72), Fe (2,59), Cd (2,00) Layer of orange: Na (3,65), Mg (3,27), Al (15,47), Si (27,52), P (1,68), S (4,34), Cl (1,62), Ca (16,83), Fe (20,93), Cd (2,62), Te (2,09)	Aluminum Silicates, Kaolinite, Gypsum, Calcite, Calcium Oxalate
P6C_4	Greenish blue/yellow	Greenish blue/yellow	/	E527: Ba, Ca, Cl, Co, Cr, Cu, Fe, K, Mn, I, Pb, S, Si, Sr, Ti, Zn	C (38,63), O (51,95), Na (0,40), Mg (0,38), Al (0,32), S (1,74), Cl (0,08), Ca (6,26), Fe (0,25)	Gypsum, Calcite, Oxalate, Vinyl Polymer
P6C_5	Greenish blue	Greenish blue	/	E527: Ba, Ca, Cl, Co, Cr, Cu, Fe, K, Mn, I, Pb, S, Si, Sr, Ti, Zn	C (22,2), O (57,57), Na (0,43), Al (0,17), Si (0,39), S (6,69), K (3,21), Ca (7,99), Ti (0,32), Fe (0,6)	Gypsum, Calcite, Calcium Oxalate, Vinyl Polymer
P6C_5 cs	Greenish blue	Greenish blue	Layer of greenish bleu pigment	E527: Ba, Ca, Cl, Co, Cr, Cu, Fe, K, Mn, I, Pb, S, Si, Sr, Ti, Zn	Mg (2,55), Al (2,12), Si (4,83), S (32,02), Ca (55,79), Fe (2,69)	Gypsum, Calcite, Calcium Oxalate, Vinyl Polymer

Appendix XIV: Presentation for the third ICP congress

Poster and presented for the III Congreso Ibero-Americano ICP. 2020.



Almada Negreiros, self-portrait
source: astron.iag.edu.ciencias.ulisboa.pt

EXPERIMENTAL RESULTS



Unveiling the mural art of Almada Negreiros at the Maritime Stations of Lisbon: diagnosis research of paint layers as a guide for its future conservation

M. Cvetković¹
M. Costa²
C. Bottani³
A. Cardoso⁴
A. Manhita⁵
A.E. Candéias⁶
C.B. Dias⁷
M. Gil⁸*

¹Hercules Laboratory, Évora University
Portugal, cvetkovic.mila93@gmail.com
²corresponding author: mlenegil@uevora.pt





Above: Technical photography: example of the methodology carried out in situ (visible and visible raking light; Ultraviolet fluorescence induced in the visible)

Left: p-OM image of a deteriorated brown paint layer (magnification 20x)

Right: p-OM image of a blue paint layer pigment: ultramarine blue area affected by salts (magnification 434x)

Left: OM-Vis image of a blue paint layer (magnification 100x) identified as fresco painting technique in SEM EDS

Right: OM-Vis image of a flaking green area (magnification 200x) white layer is made with Ti white

Left: OM-Vis image of a brown paint layer (magnification 100x)

Right: OM-Vis image of a green area (magnification 100x) cross sample taken from an area affected by salts

Left: SEM EDS elemental map of Na, Si, Ca, Ba in a green paint layer. Na₂SO₄ (thenardite) was identified by XRD

Right: SEM EDS elemental map of a green paint layer with lack of cohesion




Between 1939 and 1949, Almada Negreiros, one of the leading artists of XX century Portugal, has painted fourteen murals at the main halls of the two Maritime Stations in Lisbon. Since then several conservation surveys have been conducting revealing some detachments, spots and lack of cohesion of paint layers. In June 2020, a diagnostic research was conducted to identify the main decay phenomena of three murals in Alcântara Station with respect to future conservation works. There are three research questions:

- 1) Which paint layers are more deteriorated and do they are link to a specific pigment or not?
- 2) Which are the main decay phenomena and their dynamic?
- 3) What is the role of the painting techniques when it comes to stability and deterioration of the pigments?

Methodological approach includes literature survey, in situ non invasive analysis of paint layers with technical photography, portable optical microscopy, spectrophotometry and EDXRF followed by micro-sampling and a more profound analysis at the laboratory with optical microscopy in visible and UV mode; SEM-EDS, FT-IR and Py-GC-MS.

All the questions stated will help understand the current state of conservation of the murals, the decay occurring and the painting techniques since there is no certainty if they are frescos paintings. Further, the results will help set the guidelines for the future treatments.

Acknowledgements
The research has been conducted within the Erasmus Mundus Joint Master Program in Archaeological Materials Science (edition 2019-2020). The authors also acknowledge PCT Contratos 5/2016/ICP/398 for funding Milene Gil, The Strategic Project funding UIDB/04449/2018 (POCH-01-015-FEDER-007649) and APL Administração dos Portos de Lisboa for allowing this study.



Unveiling the mural art of Almada Negreiros at the Maritime Stations of Lisbon: diagnosis research of paint layers as a guide for its future conservation

M. Cvetković¹
M. Costa²
C. Bortone³
A. Cardoso⁴
A. Mandiluf⁵
A.E. Gendries⁶
C.B. Dias⁷
M. Gil^{8*}

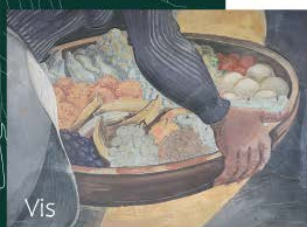


Research questions

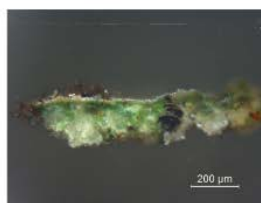
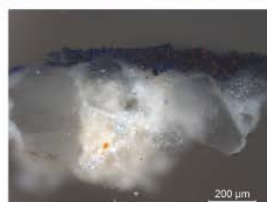
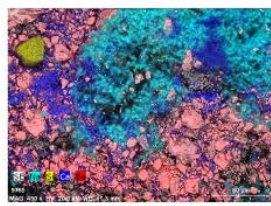
*Which paint layers
are more deteriorated
(do they link to a specific pigment)*

*Which are the main decay
phenomena
(and their dynamics)*

*What is the role of the
painting techniques
(regarding the stability
and deterioration
of the pigments)*



Methodology

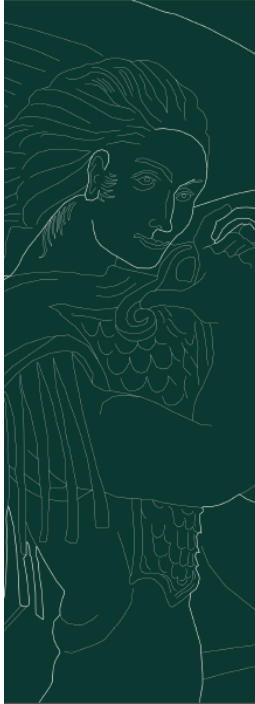


In-situ analysis

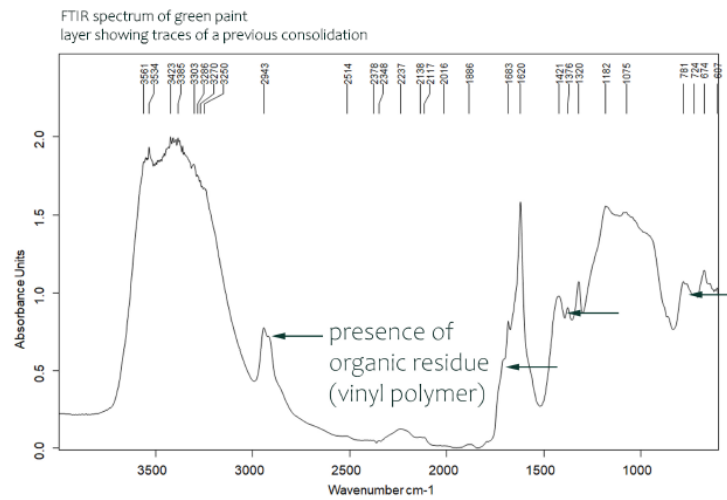
Photo documentation
Portable optical microscopy
(Dino lite)
Spectro - colorimetry
Portable X-ray Spectroscopy
(EDXRF)

Laboratory analysis

Optical Microscopy
Scanning Electron Microscopy
(coupled with Energy Dispersive
Spectroscopy SEM-EDS)
Fourier Transformed
Infrared Spectroscopy
(μ -FT-IR)
 μ -Raman Spectroscopy
Pyrolysis Gas
Chromatography
(coupled with Mass Spectrometry
Py-GS-MS)



Results



Most deteriorated pigment

Light green area
(area shows presence of vinyl polymer)

Main decay phenomena

Salts
(efflorescence/crystallization)
Flaking and lacuna
Lack of cohesion
Mold spots

Painting technique

identified as fresco
some areas show possible presence of a binder
(this is yet to be examined)